N7473338

041053

NASA CR-72321
GE-NMP 67-505

STUDY OF GAS COOLED FAST REACTOR TECHNOLOGY

Final Report

prepared for

NATIONAL AERONAUTICS and SPACE ADMINISTRATION

Contract No. NAS 3-7997

NUCLEAR MATERIALS and PROPULSION OPERATION
NUCLEAR TECHNOLOGY DEPARTMENT
NUCLEAR ENERGY DIVISION

GENERAL ELECTRIC

Cincinnati, Ohio 45215

FF No. 6C

NOTICE

This report was prepared as an account of Government sponsored work. Neither the United States, nor the National Aeronautics and Space Administration (NASA), nor any person acting on behalf of NASA:

A. Makes any warranty or representation, expressed or implied, with respect to the accuracy, completeness, or usefulness of the information contained in this report, or that the use of any information, apparatus, method, or process disclosed in this report may not infringe privately owned rights; or

B. Assumes any liabilities with respect to the use of, or for damages resulting from the use of any information, apparatus, method, or process disclosed in this report.

As used above, "person acting on behalf of NASA" includes any employee or contractor of NASA, or employee of such contractor, to the extent that such employee or contractor of NASA, or employee of such contractor prepares, disseminates, or provides access to, any information pursuant to his employment or contract with NASA, or his employment with such contractor.

GENERAL DISCLAIMER

This document may have problems that one or more of the following disclaimer statements refer to:

- This document has been reproduced from the best copy furnished by the sponsoring agency. It is being released in the interest of making available as much information as possible.
- This document may contain data which exceeds the sheet parameters. It was furnished in this condition by the sponsoring agency and is the best copy available.
- This document may contain tone-on-tone or color graphs, charts and/or pictures which have been reproduced in black and white.
- The document is paginated as submitted by the original source.
- Portions of this document are not fully legible due to the historical nature of some of the material. However, it is the best reproduction available from the original submission.

C67-83978

NASA CR-72321

GE-NMP 67-505

FINAL REPORT

STUDY OF GAS COOLED FAST REACTOR TECHNOLOGY (U)

Prepared for

NATIONAL AERONAUTICS AND SPACE ADMINISTRATION

October 20, 1967

CONTRACT NAS3-7997

Technical Management
NASA Lewis Research Center
Cleveland, Ohio
Nuclear Systems Division
Robert E. Hyland, Project Manager
Advanced Systems Division
John C. Liwosz

NUCLEAR MATERIALS and PROPULSION OPERATION
NUCLEAR TECHNOLOGY DEPARTMENT
NUCLEAR ENERGY DIVISION

GENERAL ELECTRIC

Cincinnati, Ohio 45215

CONFIDENTIAL

[redacted]

PRECEDING PAGE BLANK NOT FILMED.

Preceding page blank [redacted]

CONTENTS

		Page
1.	Introduction	5
	1.1 Purpose and Scope of Study	5
	1.2 Operational Constraints	5
	1.3 Overall System Assumptions	6
	1.4 Design-Point Conditions Imposed	6
2.	Summary	7
	2.1 Overall Description, Major Components, Arrangement, and Operation	7
	2.2 Reactor Design, Problems, and Assessment	7
	2.3 Coolant Loop Circulating System Design, Problems, and Assessment	18
	2.4 Weight Breakdown	20
3.	Materials	23
	3.1 General	23
	3.2 Nuclear Materials Survey, Selection, and Assessment	24
	3.2.1 Fuel and Fuel Element	24
	3.2.2 Reflector Materials	37
	3.3 Non-Nuclear Materials Survey, Selection, and Assessment	63
	3.3.1 Pressure Vessel Materials	63
	3.3.2 Structural Materials	67
	3.4 Assessment of Coolant Impurity Effects	72
4.	Gas Circulator System	81
	4.1 General	81
	4.2 Cycle Studies	81
	4.2.1 Possible Methods	81
	4.2.2 Parametric Data	82
	4.2.3 Aftercooling Considerations	86
	4.2.4 Design Point Selection	90
	4.2.5 Material Requirements for Circulator Design	94
	4.3 Assessment of Problems, Current State-of-the-Art, and Applicable Work Underway	96
	4.3.1 Helium Circulators	96
	4.3.2 Bearings and Seals	99
	4.3.3 Valves	99
	4.3.4 Gas Makeup Supply	100

[redacted]

Page

5. Reactor 109
5.1 General 109
5.2 Mechanical Design and Assessment 109
5.2.1 Reactor Assembly Conceptual Design and Assessment.. 109
5.2.2 Fuel Element Conceptual Design and Assessment 116
5.2.3 Reactivity Control Conceptual Design and Assessment 125
5.3 Nuclear Design and Analysis 159
5.3.1 Design Criteria 159
5.3.2 Parametric Data 159
5.3.3 Reactivity, Power Distribution, and Burnup Control 161
5.3.4 Secondary Heat Generation Rates 167
5.3.5 Afterheat Generation Rates 167
5.3.6 Assessment of Problem Areas and Current State-of-the-Art 167
5.3.7 Parametric Data - Figures 168
5.4 Thermal Design and Analysis 168
5.4.1 Thermal Design Criteria 168
5.4.2 Parametric Data 168
5.4.3 Evaluation of Design 185
5.4.4 Assessment of Problems 196
5.5 Summary Tabulation of Reactor Data 201
5.6 Overall Assessment and Discussion 205
5.6.1 Materials 205
5.6.2 Reactor Assembly and Reactivity Control 206
5.6.3 Fuel Elements 207
5.6.4 Multiplication Constant of Worst Configuration After Crash 208

Appendix A - Materials Design Data Compilation 213

Appendix B - Other Arrangement Concepts 229

[redacted]

1. INTRODUCTION

1.1 PURPOSE AND SCOPE OF STUDY

High-temperature, gas-cooled, fast-spectrum reactor technology is reviewed with reference to possible application for aircraft propulsion. A conceptual design is given for the reactor and associated components to:

1. Determine current state-of-the-art capability
2. Identify problems or areas in which the current state-of-the-art is not yet sufficiently advanced to meet the requirements of the application.
3. Identify the research and development work necessary to achieve the desired levels of performance and reliability, and identify such work currently underway.

The scope includes the reactor assembly and the gas-circulation system components (excluding heat exchangers), and the materials used therein. Parametric data are included for reactor sizing and for estimated fuel growth due to fuel burnup and fission product accumulation. Longitudinal and radial power distributions for the reactor core are presented.

1.2 OPERATIONAL CONSTRAINTS

The operational constraints imposed by aircraft application, as set forth by the contracting agency, are summarized below:

1. Chemical power is used for any flight requirement below an altitude of 20,000 feet. If the aircraft descends below 20,000 feet, transfer must be made from nuclear to chemical power. Aftercooling power is supplied by chemical fuel or other external energy source.
2. Fission product release to the atmosphere is not permitted. Should the aircraft crash, the reactor assembly must be completely contained within a vessel capable of withstanding the crash loads and consequences of reactor shutdown without benefit of active aftercooling. Conditions for the containment shell given by NASA Technical Direction are that it be capable of containing pressures of 1500 psi with a maximum wall temperature of 3000°F for 1000 minutes.
3. Penetrations through the containment vessel (e.g., for gas ducts) must be closed by valves that must operate and seal in not more than 50 milliseconds if a crash is experienced. Reopening of the valves is not required, but they must be capable of remaining pressure-tight for 1000 minutes at 3000°F and for an indefinite period during and after subsequent cooling.

[redacted]

4. Emergency shutdown of the reactor shall be completed within 20 seconds. This time shall include the removal of liquids such as shield water and/or high pressure gas which may cause internal pressure at the containment vessel to exceed its 1500-psi design criterion.
5. Unit-shielding of the reactor is presumed. Shielding of gas-duct penetrations requires special attention to achieve optimum design, but is outside the scope of this study. It should be noted that gas-duct shielding and valve closure are closely interrelated and may represent a significant problem area, depending upon dose rate constraints or the degree to which local shield augmentation is used outside the primary shield.

No constraints are imposed upon size, weight, or arrangement except that the containment vessel is 10 feet in diameter and that as much space as possible be made available between the reactor and containment shell for shield material. These factors, plus the identification of the problem areas and development requirements, are the principal results to be determined by this study.

1.3 OVERALL SYSTEM ASSUMPTIONS

As specified in the work statement for this study, the reactor is helium-cooled by means of a gas circuit directly connected to a helium-to-air heat exchanger. The study indicates that the gas can be circulated either by an externally powered blower or by a gas generator; principal attention is given to the blower cycle because of NASA interest for comparison with other comparable studies and because it is a simpler system from an operational viewpoint.

The reactor conceptual design is derived from the design technology of the 710 Reactor Systems Project as developed under AEC Contract AT(40-1)-2847.

1.4 DESIGN-POINT CONDITIONS IMPOSED

The specified nominal reactor operating conditions are as follows:

Power, Mw	250
Coolant	Helium
Pressure at inlet to pressure shell, psi	1500
Helium temperature, °F	
At inlet to pressure shell	900
At reactor exit (average)	1800
Minimum core lifetime, hours	1000
Reactor structure and components lifetime, hours	2000

The design values for coolant pressure loss, maximum fuel element temperature, and fuel burnup fraction are established by the results of this study.

2. SUMMARY

2.1 OVERALL DESCRIPTION, MAJOR COMPONENTS, ARRANGEMENT, AND OPERATION

As specified for this study, powerplant components consist of a refractory-metal, fast-spectrum reactor supplying heat through a closed inert gas circuit to propulsive turbomachinery by means of a heat exchanger, with gas circulation provided by an externally powered blower. The basic elements are:

1. The reactor assembly inside a containment vessel with its associated tungsten - water shield.
2. A gas circulator powered by an air turbine, using a shaft penetration and seal.
3. A heat exchanger.
4. A pressure equalization system to balance the pressure level of the shield water inside the containment vessel with that of the coolant gas.
5. A gas makeup supply.
6. Containment vessel shut-off valves.

These components are required for normal operation of the powerplant. In addition, the need to restrict the maximum pressure level inside the containment vessel in the event the aircraft should crash, imposes the need for draining the shield water from inside the vessel and for reducing the helium gas pressure as quickly as possible after shutdown. Accordingly, a purge system to eliminate the water is required, and since this procedure is followed after each shutdown, gas storage tanks to conserve the helium charge, as well as water storage tanks, may be desirable.

The gas circulator must be arranged so that a separate air turbine can be used to provide the shaft power. The arrangement is dependent upon convenient access to the air stream and upon integration with the primary gas loop so that neither the helium-duct nor the air-duct runs become unnecessarily long. A separate set of air turbomachinery may be desirable so that the aftercooling function after landing can be provided independently of the propulsive function of the primary engines. The shaft-drive turbomachinery can be operated on chemical fuel to provide the aftercooling function.

2.2 REACTOR DESIGN, PROBLEMS, AND ASSESSMENT

The reactor is a fast-spectrum, refractory-metal assembly of hexagonal fuel elements with tubular coolant channels, using radial

reflector removal for reactivity control. The fuel element materials consist of W-60UO_2 (vol.%) fully enriched UO_2 fueled matrix with W-30Re-30Mo (at.%) cladding. Structural materials for the reactor and ducting consist of Inconel 625. The reactor is inside a containment vessel made of a tantalum alloy, either T-111 or T-222. Tungsten - water shielding is included between the reactor assembly and the containment vessel.

The reactor assembly is vertically supported from the top of the containment vessel by a conical structure connected to a cylinder (the structure used to separate the gas from the shield water) to which the front tube sheet for support of the fuel elements is attached. The fuel elements are suspended by a cantilever attachment from the front tube sheet. The radial reflector is immersed in the shield water and is removable by means of a venetian-blind- or shutter-type mechanism. To restrict the thickness of the cylindrical structure between the core and radial reflector so as to provide the largest possible effect of reflector displacement on neutron leakage, the shield water is pressurized to approximately the same level as the coolant gas. The containment vessel acts as the reactor pressure vessel.

Two gas ducts penetrate the vessel, one for the inlet and one for the discharge gas. Quick acting, pneumatically actuated poppet valves are integral with the penetrations for providing absolute containment of the reactor should the aircraft crash. Upon entering the vessel, the gas is distributed by a scroll to multiple cylindrical ducts, each passing through the shield in a serpentine path to reduce the radiation streaming due to lumped voids. These ducts are connected to the inlet plenum of the reactor; twelve ducts are used in the present conceptual design, and the control actuators for the twelve shutter segments of the radial reflector are nested between the ducts. The gas passes through the reactor and out of the containment vessel by a duct arrangement essentially identical to that for the inward path. This once-through arrangement is possible because the thermal expansion of the gas ducts is restricted in magnitude by keeping the metal temperatures relatively low. This is done by insulating and actively water-cooling the exit gas ducts and the flow divider between the core and radial reflector.

The performance levels achievable with available technology, bases for these conclusions, factors limiting performance, fundamental problems, and areas requiring development are summarized in the following paragraphs for the reactor assembly, fuel elements, and reactivity control system.

2.2.1 Reactor Assembly

A summary of pertinent design values for the reactor assembly is given in Table 2.2.1. The range shown for loop pressure loss represents the uncertainty associated primarily with non-reactor losses; accordingly, the blower horsepower covers a corresponding range. Other values are those either specified by the design requirements or derived during the course of the study. The reactor dimensions are such that a calculated value of excess reactivity, based on experimentally correlated methods,

TABLE 2.2.1

DESIGN VALUES FOR REACTOR ASSEMBLY

Loop pressure loss ($\Delta P/P$)	0.045 – 0.080
Blower power, hp	11,000 – 20,000
Reactor pressure loss, ($\Delta P/P$)	0.015
Total loss in containment vessel ($\Delta P/P$)	0.030 – 0.038
Thermal power, Mw	250
Maximum pressure level, psia	1500
Temperature, °F	
Helium, reactor inlet	900
reactor outlet	1800
Maximum fuel surface (avg.)	2180
Maximum fuel internal (avg.)	2298
Maximum internal rise (avg.)	127
Helium flow rate, lb/sec	212.4
Active core dimensions, in.	
Envelope diameter	31.2
Equivalent circular diameter	29.9
Length, active core	30.0
Total including front tube sheet	36.7
Radial reflector thickness	5.0
Core volume fractions	
Structure	0.103
Free flow and voids	0.478
Fueled matrix (95% of theor. density)	0.419
Total	1.000
Active core volume, $in.^3$	21,068
Free flow area (hot), $in.^2$	267.8
Coolant channels per element	37
Elements per reactor	241
Fuel element pitch, in.	1.834
Fuel element across-flats width, in.	1.730
Coolant channel pitch, in.	0.2821
Coolant channel diameter (cold), in.	0.192
Fuel cladding thickness, in.	0.010
Average Burnup in 1000 hours, fissions/cm^3	1.922×10^{20}

of 9.8 percent is obtained. This is believed to be adequate for providing the necessary nuclear lifetime. However, a critical experiment with the actual geometry will be required to substantiate that sufficient excess reactivity is available.

State-of-the-art values are compared with design values separately in Table 2.2.2 for items of particular interest or which may ultimately establish design criteria. This tabulation shows that the state-of-the-art values are equal to or better than the design values for all items listed except for system circulator pressure level and temperature of the containment vessel under emergency conditions. The state-of-the-art pressure level is shown (in section 4) to be less than 500 psia for blowers which have been or are currently under development. The containment vessel temperature capability is limited by the conditions imposed after a crash in which a pressure of 1500 psi must be contained for 1000 minutes with the vessel at 3000°F and in an oxidizing atmosphere.

The demonstrated fission density in the fueled matrix, while equaling the average value imposed in the current application, requires some engineering interpretation by application of refined analysis techniques to account for shape factors (because of the geometry of the specimen used in the test) and for the trade-off in time-versus-temperature effects. The only significant uncertainty is the effect of irradiation on the creep properties and ductility of the tungsten matrix material. Thus, while it is believed that the design value of fission density is well within current state-of-the-art capability, the test results available do not duplicate the exact conditions expected in the design; proof testing is required to eliminate the need for any interpretive extensions or interpolations of the available data.

Inconel 625 has been found to meet the design requirements of the structural components of the reactor assembly. Experimental irradiation effects data show that for design life dose rates of approximately 1×10^{21} nvt at the core - reflector interface, a design stress intensity of 55,000 psi is available up to 1100°F. Elongation of approximately 17 percent can be accommodated after exposure. The containment vessel can be either T-111 or T-222, approximately 6 inches thick to meet the post-crash design requirements.

Because the concept for the reactor assembly has been uniquely derived for the present application, there are no specific engineering test results to support the design. Accordingly, while the feasibility is not questioned, tests are required to demonstrate that components can perform the required functions. The principal areas requiring further study and development are summarized below:

1. The containment vessel assembly must be tested under the anticipated conditions after crash to demonstrate its ability as an assembly to meet the necessary requirements. Specific items requiring additional attention are:
   a. Material property data must be obtained for the selected tantalum alloy in the required thicknesses (approximately

TABLE 2.2.2

COMPARISON OF STATE-OF-THE-ART AND DESIGN VALUES
(State-Of-The-Art for Individual Items Only)

	State-of-the-Art Value*	Design Value
Circulator discharge pressure level, psia	500[a]	1500
Reactor inlet temperature, °F	~1100[b]	900
Maximum fuel surface temperature (avg.), °F	>3000[c]	2180
Maximum fuel internal temperature (avg.), °F	>2700[d]	2300
Fuel element lifetime, hr	>2000[e]	>1000
Structure lifetime, hr	>2000[f]	2000
Containment vessel temperature, °F	<3000[g]	3000
Equivalent circular diameter of core, in.	30-35[h]	30
Length of fuel element	i	30
UO_2 concentration in cermet, vol %	60[j]	60
Cladding thickness, in.	0.010[k]	0.010
Coolant channel diameter, in.	>0.035 in.[ℓ]	0.168-0.209
Flat width of fuel element, in.	i	1.73
Burnup in 1000 hours (avg.), fissions/cm^3	m	1.922×10^{20}
Number of reactor fuel-power cycles	n	200

*Demonstrated or deduced from related data. Values apply individually, not necessarily in combination.

a. Value from circulating system component limit assuming sealed, oil-lubricated bearing.
b. Based on nonrefractory (Inconel 625) front tube sheet; higher value possible with refractory material.
c. Higher values possible for shorter times. Limit set by metallurgical effects involving the cladding.
d. Set by arbitrary limit of 1% calculated growth due to fission product pressure at design value of power density for 1000 hours.
e. Estimated based upon limit from growth due to fission gas pressure. Presumes good design to limit hot channel effects so that perturbation is less than 200°F.
f. Value subject to details of final design.
g. Conventional oxidation-resistant structural materials melt at temperatures below 3000°F; thickness of shell acting as strength member may be larger than desired in order to meet the specified conditions to be imposed after crash.
h. Feasibility of reflector control uncertain for core sizes above this value. Different control method would significantly affect the structural arrangement and design.
i. Limiting value has not been identified; have been fabricated to 14.77 in. length, 1.426 in. across-flats.
j. Higher concentration (to 70 vol %) may be possible dependent upon ability to maintain continuity of W matrix in the cermet.
k. Thinner claddings may be possible in future designs depending upon quality of available sheet and tube stock.
ℓ. Range demonstrated by actual fabrication and non-nuclear testing.
m. Value subject to operating temperature; see Figure 3.2.13 for available test results. These results, being from test samples as part of the NMPO High-Temperature Materials Program, are considered to be indicative of the minimum capability to be expected when the appropriate fuel element geometry and design is used. Effects of temperature and power distribution are such that use of average burnup at maximum temperature (2468°F) is more life-limiting than where maximum burnup at 2360°F occurs.
n. Test results on a similar geometry have demonstrated ability to cycle from 3000°F to 500°F for 50 plus cycles without deleterious results; test is still in progress. Metallurgical samples have been subjected to up to 400 cycles.

6 inches); also, fabrication procedures must be developed because of this thickness. (See section 3.3.)

b. An oxidation-resistant coating or cladding must be developed for the containment vessel that can withstand crash impact loading and subsequent exposure at 3000°F and 1000 minutes.

c. The valves for closing and sealing the containment vessel penetrations for gas ducts and water lines require engineering development to demonstrate that the necessary rate of closure, leak-tightness of the valve seat, and strength to withstand crash loads and after-crash conditions of pressure, temperature, and lifetime can be achieved.

d. Leak-free closures capable of meeting the required conditions must be designed and developed for the penetrations for instrumentation and control actuator electrical connections.

2. Methods must be identified to prevent the reactor from assuming a critical assembly as a result of an aircraft crash.
3. A pressure-balancing system is required to equalize the pressure of the coolant gas and shield water.
4. Excitation frequencies of the aircraft may necessitate an additional lateral support at the rear of the fuel elements.
5. Additional aftercooling studies of the reactor structure should be performed after operating procedures for normal shutdown are specified.
6. The insulation to be used on the gas-side of the ducts cooled by shield water must be designed and tested.

2.2.2 Fuel Elements

Both experimental and analytical results indicate that the fuel element will meet or exceed the required performance characteristics. Its lifetime may be significantly longer than specified. To verify its capability, in-pile tests should be performed on elements of the specific geometry (porosity and coolant channel size) of the aircraft application under the proper conditions of power density, burnup level, neutron spectrum, and pressure and temperature levels.

Performance - The fuel element temperature levels required in the proposed design are appreciably lower than the levels at which most of the research and development tests have been and currently are being conducted at GE-NMPO. Retention of fuel and fission products has been demonstrated at 2900°F for over 3000 hours and at 3600°F for at least 1000 hours whereas, in the aircraft application, the maximum surface temperature is less than 2200°F for the average element, with hot channels reaching no more than 2400° to 2600°F (depending upon the degree of design sophistication incorporated to control the magnitude of perturbations).

The burnup level required in the design, an average of $< 2 \times 10^{20}$ fissions/cm^3 in 1000 hours, is greater than that of the current fuel element development program for the space power application of the 710 Reactor, but is in the range of burnup levels successfully tested under the High-Temperature Materials Program at GE-NMPO. Since higher burnup can be achieved at the lower temperatures of the aircraft application,

the data accumulated to date (see section 3.2), together with the analysis of growth of the fueled material due to fission product gases (see section 5.2.2), provide a high degree of assurance of achieving at least 1000 hours lifetime and, with careful design to restrict the magnitude of temperature perturbations, reasonable expectation of 2000 hours or more.

State of Technology - The excellent stability of the fuel, as demonstrated by the W-Re-Mo-clad W-UO_2 fuel elements, depends, among other factors, upon maintaining stoichiometric UO_2. Procedures have been developed at GE-NMPO for controlling the stoichiometry of UO_2 during fabrication within the limits of measurement capability. Tests have shown that the diffusion rate of oxygen through claddings of W or Re or their alloys, including Mo, is sufficiently low at high temperatures that stoichiometry can be maintained during operation.

Procedures have been developed at GE-NMPO for fabricating the recommended fuel into the fuel element geometry for this application. Sheet and plate forms of the W-30Re-30Mo (at.%) alloy are available in the required sizes for this fuel element. While not commercially available, tubing has been made at GE-NMPO to the necessary quality level in 19-inch lengths. Achieving the 31-inch-long tubing for this fuel element will be an extension of this work.

Current development effort on the 710 Reactor fuel element is guided by the requirements for space power application, and is comparable with the aircraft requirements as summarized below:

	Space Power Application	Aircraft Application
Lifetime, hours	10,000	>1000
Temperature, °F	2600	<2500
Reactor power, MW_t	1.05	250
Power density in fueled core, MW/ft^3	0.75	49.3
Total average burnup for design life, fissions/cm^3	3.2×10^{19}	1.92×10^{20}
Fuel core material, vol.%	W-60UO_2	W-60UO_2
Cladding material, at.%	W-30Re-30Mo (Ta-8W-2Hf, Mo-50Re)*	W-30Re-30Mo

Test Program - The scope of the development effort in the 710 Reactor Program is based on the results of an evaluation of potential causes of fuel element failure, (see section 5.2.2), for the space powerplant. Because it is subjected to a rocket boost in the space application, consideration must be given to vibration and acceleration forces which prevail before the reactor is brought to operating conditions. The results of these studies are not applicable to the aircraft application.

*Alternative materials.

However, most of the program concerned with non-nuclear and nuclear tests is directly applicable. The non-nuclear testing consists of thermal cycling to temperatures of 3000°F in static gas at both atmospheric and elevated pressure (up to 1000 psig) and in dynamic gas at elevated pressure. The nuclear testing involves thermal cycling at high temperatures in static gas. This program covers all identified potential causes of fuel element failures except for vibration and g-load effects, interference effects in the event that adjacent fuel element contact each other, and the effect of the precise irradiation environment on materials properties. An in-pile dynamic test program has been developed and preliminary design of the in-pile components completed to test fuel elements at the conditions of the space power application, including the proper flux. Results of this effort will more precisely determine the radiation influence.

All non-nuclear test results derived from this program are pertinent and applicable to the present design except for the influence of geometry factors arising from the higher porosity required in the aircraft application. The fuel element design which establishes reference values for the 710 Reactor development program is listed in Table 2.2.3 with the corresponding data for the average element from the present study shown for comparison. To date, 66,803 hours of non-nuclear specimen test time have been accumulated: 44,905 hours of 3000°F static tests of multichannel and single-channel test specimens; 4990 hours of dynamic testing; and 16,908 hours of testing process development specimens of simple geometry at 3000°F.

To some extent, the in-pile work to date is applicable, i.e., insofar as the results are correlatable with analysis methods which can then be used for predicting capability for the lower-temperature, higher-power-density conditions of the aircraft application. In-pile test specimen LT-710-1 has completed 3000 hours of testing in the LITR at a temperature of 2750° to 2800°F. In-pile test specimen LT-710-2 has completed 2130 hours of a scheduled 5000-hour test at a peak temperature of 2800°F in the LITR. Also, the range of burnup levels achieved in tests under the AEC High-Temperature Materials Program at GE-NMPO have reached those required in the aircraft application (see section 3.2).

Design and Development Required - The fuel element design for the aircraft application introduces no new features and is a relatively straightforward application of design concepts that have evolved during previous work on the 710 Reactor concept. To achieve the lifetime requirement, hydraulic diameter variation between fuel elements is required, depending upon the radial position of the element in the reactor. Because of the requirement of high flow volume, the minimum ligament thickness on the fuel (0.015 inch) is reached before temperature flattening is achieved and thus fuel concentration augmentation will be required.

Hydraulic diameter variation within individual fuel elements may also be desirable. This will be determined following a more detailed evaluation of the amount of fuel element bowing to be expected as a result of temperature differentials across a single fuel element and also the differential growth due to radial power density gradients.

TABLE 2.2.3

710 REACTOR FUEL ELEMENT DIMENSIONS

	Space Power Application	Aircraft Application
Matrix (across-flats), in.	1.426	1.73
Number of coolant channels	19	37
Coolant channel hydraulic diameter, in.	0.135	0.192
Coolant channel pitch, in.	0.329	0.282
Coolant channel cladding thickness, in.		
W-Re-Mo	0.010	0.010
Ta – 8W – 2Hf and Mo-Re	0.015	–
Outer cladding thickness, in.		
W-Re-Mo	0.010	0.010
Ta – 8W – 2Hf and Mo-Re	0.015	–
Active fuel length, in.	14.264	30.0

Fabrication procedures have already been developed that can be adapted to accomplish either type of hydraulic diameter variation.

The adequacy of the proposed cantilever support for the fuel element should be determined on the basis of a detailed evaluation of the vibration of the reactor structure as supported in the aircraft, and should be verified by experimental tests. The natural frequency of the fuel element can be increased by the use of a rear restraint.

2.2.3 Reactivity Control System

Various reflector control methods were evolved in earlier studies of the 710 Reactor applied to a nuclear rocket and to a space powerplant. Based on this work, reflector removal control also appears to be promising in the aircraft application, even though the reactor is larger in this application. Several methods were investigated for achieving reflector displacement (see section 5.2.2); rotation of reflector segments, the feasibility of which has been demonstrated* in a reactor design, was selected.

Performance - Nuclear analyses were performed to assess the reactivity worth of two radial reflector materials, Be and Mo, with the reflector immersed (1) in borated water and (2) in the same gas as the primary coolant. The calculated reactivity worths of complete reflector removal are given in this tabulation:

	Total Radial Reflector Worth, % Δk	
Reflector Environment	Beryllium	Molybdenum
Gas	10.7	13.0
Borated water	9.0	11.2

The purpose of these analyses was to determine if all combinations of reflector material and environment would provide sufficient control margin. From a nuclear standpoint, all combinations appear feasible: the worth of total reflector removal is large enough for the aircraft application (see section 5.3.1). Beryllium causes a power spike at the core - reflector interface; however, even Mo causes a power spike when immersed in borated water. Although Mo is a better gamma shield than Be, it is also a source of gamma energy due to neutron capture so that neither material has a particular advantage from a shielding standpoint.

Arrangement studies were made with the reflector immersed in borated water or in primary coolant gas (see section 5.2.1). In the latter case, the coolant is the primary gas both during operation and in the aftercooling mode. In the former, the coolant is water; while forced circulation of the shield water becomes necessary specifically for this purpose, the pumping power required is much less than if the coolant were gas.

The need to maintain aftercooling flow to the reflector led to the concept of including a flow path within the shaft on which the reflector

*"Reactor and Shield Design Status - SNAP-50," PWAC-471 (CRD), Pratt & Whitney Aircraft Division, United Aircraft Corporation.

is mounted, with suitable coolant channels bleeding the flow from the shaft through the reflector. During normal operation, the coolant is recirculated shield water requiring a water-to-air heat exchanger. After the reactor is shut down and the shield water is drained, the coolant must be a gas. The amount of aftercooling required by the reflector (and hence the quantity of gas supply required for this purpose) depends upon the permissible temperature levels in the reflector and its support structure. Higher operating temperatures are permitted by the use of Mo than if the reflector were Be. This higher temperature capability will permit radiation to become the predominant heat transfer mechanism much sooner, thereby significantly reducing the required quantity of inert coolant gas. The preferred arrangement, therefore, is the Mo reflector immersed in borated shield water.

It should be noted that no criterion was established for the rate of reactivity removal because a nonmoderating reflector such as Mo produces no identified positive reactivity effects, either instantaneous or delayed, with increase in reactor temperature. Instead, all identified temperature effects are negative with increasing temperature. Should the reflector be moderating, e.g., Be, a delayed positive temperature coefficient would be present, and the rate of reactivity removal by means of the active control system would have to be specified.

State of Technology - The actuator considered in this study is the Bendix Nutator* stepping motor. It consists of a stationary external bevel gear and eight radial segments each consisting of an electromagnetic solenoid. The electrical components, solenoids, and an optional position feedback potentiometer are contained in a hermetically sealed gas environment. Leak free closures must be provided through the containment vessel for electrical connections. Although scram requirements are not explicitly defined, the highest possible scram rate should be achieved with a minimum of scram torque. Results of analysis (see section 5.2.3) indicate that the Nutator motor's torque capabilities yield 0.2 percent $\Delta k/k$ withdrawal in 0.15 second and, therefore, can meet the control requirements.

The actuator is not an off-the-shelf item; however, according to the manufacturer, models have been built and operated, and its operating characteristics are reasonably firm. Early tests of an actuator built to the design requirements would be desirable to firmly establish the drive rate - torque characteristics and to evaluate bearing and gear operation using borated water as a lubricant.

In summary, the reflector removal reactivity control system has the following advantages:

1. A reflector control based on neutron leakage variation is possible for the size of reactor required for aircraft application.

---

*Registered tradename of the Bendix Corporation.

[redacted]

2. The reflector control segments can operate while immersed in the borated shield water. For this reason, there is no need for waste void to allow for displacement of the reflector segments. This, in turn, reduces the shield weight.

Design and Development Required - The following developmental efforts are required to verify the adequacy of this type of control method:

1. A critical experiment to determine the reflector control worth as a function of angular displacement and to measure the effect of immersing the radial reflector in borated water.
2. Development of the control actuator for the specific environment and to attain the necessary reliability of operation for the design to be used.

2.3 CIRCULATOR SYSTEM

Performance - Parametric data for a range of reactor sizes (see section 4.2.2) meeting the specified design point conditions show that the circulator conditions to be expected are in the following range:

	Nominal	High	Low
Circulator power, hp	13,600	20,000	11,000
Circulator power, % of Q_{th}	4.06	5.96	3.28
Circulator pressure ratio	1.055	1.08	1.045

State of Technology - The required range of circulator power is beyond current state-of-the-art for electric motor drives and gas bearings. Electric motors operating on a 60-cycle power supply weigh about 5 lb/hp; by following aircraft practice of using higher frequency, the specific weight can be reduced to as low as 1 lb/hp. The power for the drive motor must be generated by onboard equipment, resulting in additional weight. Gas bearings have been used in motor-driven circulators up to 200 hp and have been considered for use in turbine drives up to 1000 hp. Under these current limitations, the only possibility for aircraft application would be multiple small-size blowers. Accordingly, an air turbine drive with oil bearings is necessary, using a shaft penetration through the primary loop ducting and dynamic seals.

For helium circulators, the current practice can be summarized as follows:

1. Single-stage radial circulators are used if the pressure rise is 3 percent or less; multistage, axial-flow circulators are used with greater increases.
2. Rotor tip speed is usually limited to 900 ft/sec or less; an exception is the compressor for the Maritime Gas-Cooled Reactor (MGCR) turbomachinery.
3. Inlet temperature and pressure to the circulator are 700°F or less and 500 psia or less, respectively.
4. No axial flow circulators have yet been operated in a nuclear power unit.

5. Current seals consist of sleeve-type bearings, an intermediate buffer gas at pressure above the process gas, a viscous fluid (either oil or water) as a final seal, a static seal to prevent leakage during shutdown, and a separator to permit re-use of the buffer gas and sealing fluid.

Existing hardware that most closely approaches the present design requirement is the radial circulator used in the High-Temperature Gas-Cooled Reactor (HTGR). This circulator is a single-stage, radial overhung type generating a pressure rise of 2.9 percent in a 5-ft rotor diameter at 3460 rpm. The differences between this design and the requirements of the present application are as follows:

	HTGR	Required
Number of stages[a]	1	2
Pressure, psia	450	1500
Inlet temperature, °F	700	900
Driver	Motor	Turbine

[a]At 900 ft/sec tip speed.

To achieve 5 percent pressure rise in a single stage, the circulator must be of the pure radial type (specific speed of 60 or less); the tip speed must be about 1220 ft/sec. The corresponding rotational speed is 5500 rpm and the rotor diameter is 4.25 feet. Data show that a tip speed of 900 ft/sec is achievable at 900°F with titanium alloys, Inconel X, or a high-strength, low-alloy steel such as Super Tricent. At 1220 ft/sec, however, only the Super Tricent alloy would meet even the minimum requirements. Therefore, if no more than a 5-percent rise is required, careful mechanical design of the impeller and use of the best available materials may permit achieving the required 2000-hour lifetime with only one radial stage.

No axial-flow circulator has yet been operated in a nuclear powerplant. Probably the most advanced is the 10-stage axial flow circulator for the Experimental Gas-Cooled Reactor (EGCR), previously under development by the Oak Ridge National Laboratory. This circulator operates at the same volume flow (516 ft^3/sec) as required for the aircraft application, but at a temperature less than 500°F and a pressure below 300 psia; consequently, its power output is only 3100 hp. Therefore, modifications to this design would be required.

In any redesign effort, attention should be given to the aerodynamic design of helium circulator blading. Design practices for air turbomachinery are conventionally used which unduly penalize helium compressors from the standpoint of size and weight.

A modified poppet valve called a cone labyrinth valve developed by the Smirra Development Company, Los Angeles California is recommended to perform the quick-closing gas shut-off. Valves of this type have been operated to 16,000 psi in sizes of 2.00 inch diameter and studies of valves to 11.00 inch diameter are in progress.*

*Private Communication, J. R. Smirra, Santa Monica California, August 14, 1967.

DISCLAIMED

Design and Development Required - In summary, the following problem areas have been identified for the helium circulator system in the aircraft application:

1. There are no existing designs that can be applied without modification. Principal modifications required are those necessary to increase the pressure and temperature capability to 1500 psia and 900°F, respectively.
2. Further study is needed to determine whether to use a single-stage radial-flow circulator at relatively high peripheral speed (>1200 ft/sec), a two-stage radial-flow circulator at moderate speed (∿900 ft/sec), or a multistage axial-flow circulator. Some research in this area to advance the state-of-the-art of axial-flow compressor design for helium may result in significant reduction in the number of stages required for any given pressure rise.
3. Existing circulators were developed for central station power-plant application in which weight is of less concern than cost. A manufacturer experienced in designing components for aircraft application should be included in further study efforts, such as in item 2, above.

The status of shaft seals is similar to that of the circulator in that no existing design can be applied without additional engineering and development effort. The following problem areas have been identified:

1. Three general types of seals - labyrinth, visco, and dynamic head (pump) - are candidates for the application and should be further investigated for the high pressure requirements.
2. Seal leakage and back diffusion of the sealant liquid (if used) must be determined. Seal leakage will determine makeup requirements and back diffusion may cause the release of excess contaminants into the reactor.
3. If a buffered seal is used and recirculation of sealant liquid and buffer gas is desired, the weight and operating complexity of the associated equipment must be evaluated.

The shaft power required by the circulator amounts to 3.3 to 6 percent of the reactor thermal power, depending upon the pressure loss of non-core components. Assuming a drive efficiency of 25 percent, the corresponding parasitic power penalty is 13 to 24 percent of the thermal power output. The thrust penalty associated with this parasitic loss is such that the use of a gas generator to provide the circulation should be considered; this alternative is discussed in section 4.

2.4 WEIGHT SUMMARY

The estimated weights of the reactor components and containment vessel, excluding the shield material, are itemized below:

Reactor Assembly Component	Estimated Weight, lb
Fuel elements and fasteners	6,210
Front tube sheet	470
Radial Mo reflector	8,200
Actuators and drive	830
Reflector structure	650
Core shell and structure	2,560
Inlet - exit gas plenums	2,380
Gas ducting inside vessel	1,080
Miscellaneous	1,000
Total reactor assembly	23,380
Spherical containment vessel (6 inches of T-111 10.0 ft. OD)	148,000
Total	171,380

A major amount of weight is involved in the containment vessel in order to meet the post-crash conditions of 1500 psia at 3000°F for 1000 minutes. Additional conceptual design to integrate the shield arrangement and design with that of the reactor and containment vessel may not significantly increase the total reactor - shield-containment vessel weight while still achieving complete containment.

CONFIDENTIAL

[redacted]

Preceding page blank

3. MATERIALS

3.1 GENERAL

This section presents the results of a survey, assessment, and selection of candidate materials for use in the fuel element, reactor, and structural components. Test data, selection criteria, and an assessment of the completeness of available information and applicable work underway are discussed.

Materials considered for the various components in the survey included:

Fuel Element	Structure	Reflector
Fueled Core	Non-refractory	Moderating
$W-UO_2$ $Mo-UO_2$	Stainless Steel Types 304, 316, 347 Hastelloy C,X Inconel 600, 625 Incoloy 800	Be BeO
Cladding	Refractory	Nonmoderating
W - 30Re - 30Mo* Mo - 50Re Ta - 8W - 2Hf (T-111) Ta	Niobium 752 Ta - 10W, T-111, T-222	Mo

*In atom percent; the same alloy in weight percent is W - 35Re - 18Mo. All other compositions are weight percent.

The fuel element materials are either currently or were previously under development for the 710 Reactor Systems Project, and are those for which the most experimental test data are available. The structural materials are those which are available commercially, for which a relatively large amount of materials property data are available, and for which fabrication procedures have been established. The reflector materials are those that were found best during previous 710 Reactor studies from three standpoints: (1) nuclear worth, (2) the choice between neutron moderation or no moderation, and (3) adaptability to the arrangement under consideration (see sections 5.2.3 and 5.3.3).

The ultimate choice of materials for various components depends upon the power cycle chosen for a particular application (see section 4.2) and the final arrangement selected for the reactivity control system, ducting,

[redacted]

and shielding. Materials considerations which are primarily design-oriented are treated in the appropriate sections of this report, and the overall assessment of materials is included in section 5.6.

3.2 NUCLEAR MATERIALS SURVEY, SELECTION, AND ASSESSMENT

3.2.1 Fuel and Fuel Element

SURVEY OF CANDIDATE MATERIALS

In reviewing the materials property and engineering test data available for each of the candidate fueled-core and cladding materials, singly and as fuel element combinations, the advantages and disadvantages of each material for the design conditions required in this application were evaluated. The result was the selection of W-UO_2 as the fueled core and W - 30Re - 30Mo (at. %) as the cladding material.

Fueled Core

By virtue of several of its physical properties, UO_2 is well suited for reactor applications:

1. It is the most refractory nuclear fuel known
2. It is nonreactive with the refractory metals of interest (necessary condition for the retention of both fuel and fission products)
3. It has good irradiation stability
4. It can be manufactured and chemically reprocessed with relative ease after irradiation.

Its major disadvantages, low thermal conductivity, poor thermal shock resistance, and poor mechanical strength, can be minimized by dispersing UO_2 particles throughout a metallic matrix. In addition, since cermets can be metallurgically bonded to metallic claddings, thermal conductance can be further improved.

In making the selection between W and Mo as the matrix material, primary consideration was given to the effect of fission gas pressure on fuel element growth under the burnup and temperature conditions of the current design. Because of its superior high-temperature strength, W offers the longer lifetime for a growth limit acceptable from a design viewpoint. This criterion was judged important enough to outweigh the advantages offered by Mo; i.e., a smaller thermal expansion differential between the Mo-UO_2 fueled core and the Mo - 50Re cladding alloy.

The elimination of Mo-UO_2 as the fueled core material also eliminated the Mo - 50Re alloy from the list of candidate cladding materials, restricting the choice of the cladding to Ta, Ta - 8W - 2Hf, and W - 30Re - 30Mo.

Cladding

W - 30Re - 30Mo - The W - 30Re - 30Mo alloy is preferred as the fuel element cladding because it has the highest performance potential of the

candidate cladding materials based on the following characteristics:

1. It has high strength, adequate ductility, and a high melting point.
2. Its permeability to oxygen is negligible at the maximum fuel element operating temperature, thus ensuring maintenance of stoichiometric UO_2 within the fueled materials.
3. Its susceptibility to gaseous impurity absorption is low.
4. Void formation at the cladding - fueled core interface caused by interdiffusion is negligible at the maximum fuel element operating temperature.

These characteristics were judged to outweigh the possible disadvantages of W - 30Re - 30Mo:

1. The differential expansion between cladding and fueled core can impart relatively high bond stresses during temperature cycling.
2. Tubing of the necessary quality level is not yet available commercially. However, encouraging progress has recently been made in the fabrication of high-quality tubing.

Mo - 50Re - As indicated previously, interest in the Mo - 50Re alloy is primarily for its application as a cladding for a Mo-UO_2 core; the low differential expansion between cladding and fueled core would result in a significant reduction in bond stresses at the interface. As a cladding for a W-UO_2 fueled core, however, this advantage is lost. In comparison to the W - 30Re - 30Mo alloy, Mo - 50Re is subject to greater grain growth, both in fabrication and operation, and to greater core - cladding interdiffusion. It is, however, commercially available in all required shapes and forms.

Ta and Ta - 8W - 2Hf - The chief advantages of Ta and Ta - 8W - 2Hf (T-111) as cladding materials are their commercial availability in all required forms and their fabricability into the fuel element configuration. The T-111 alloy also maintains a finer grain structure under equivalent temperature conditions than any of the other cladding materials considered. Pure Ta, on the other hand, is most subject to grain growth of the four candidate materials. Both materials, however, are sensitive to gas stream impurities and are more permeable to oxygen than the W-Re-Mo alloy. In addition, both Ta and T-111 are subject to void formation as a result of core - cladding interdiffusion. In this respect, T-111 appears superior in that a much finer void network is formed than in pure Ta.

FUEL ELEMENT FABRICATION

The fuel element design selected for this application is similar to that being developed for the 710 Reactor Systems Project under AEC Contract AT(40-1)-2847. It is a hexagonal element whose support structure is supported in the reactor's tube sheet. The fueled section consists of a fueled matrix within a hexagonal metal cladding bonded to the matrix. The ends are sealed with header plates. Coolant tubes through which the heated gas passes extend from the front to the rear header plate. The interstices between the tubes and between tubes and the outer claddings are filled with fuel-bearing material. An exploded view of a 19-channel,

partial-length fuel element of the type used in static environment testing in the 710 Fuel Element Development program is shown in Figure 3.2.1. The fueled section shown consists of five stacked compacts penetrated by coolant tubes.

Fabrication of Fueled Compacts

Fabrication of the fueled compacts containing a dispersion of UO_2 particles throughout a W metal matrix uses powder metallurgy techniques. In the compact fabrication the fuel is first agglomerated by isostatic pressing into cakes, crushing, sieving out the desired particle size and firing these particles in helium. The agglomerated fuel is then blended with the tungsten, pressed in a hexagonal die, pre-sintered and then sintered at 4000°F in hydrogen. The fuel agglomeration process converts the submicron as-received UO_2 powder into low-density spherical particles, as shown in Figure 3.2.2, without reducing the activity or sinterability of the UO_2 powder. A low-temperature (1100°F) firing operation in helium imparts additional strength to the particles for the subsequent roller blending operation. The W and UO_2 agglomerates are blended without the addition of binders, thereby eliminating the problem of binder contamination and removal in subsequent sintering.

Each fueled compact is processed individually through the pressing operation to insure uniformity of fuel loading. The "green" fuel compacts are pre-sintered in batches using a slow, cam-controlled heating rate to prevent cracking of the relatively delicate pieces. Rapid heating rates are used during the final sintering to reach the sintering temperature of 4000°F without damage to the compacts. A photomicrograph of a section through a fueled compact sintered to 95 percent of theoretical density is shown in Figure 3.2.3, illustrating the random distribution of the fuel particles in the W metal matrix.

Densification of the "green" fuel compacts by sintering alone requires that both the W and UO_2 powders be active or sinterable. Consequently, the use of high-fired, fully dense, inactive UO_2 microspheres is inapplicable to this process, as is the use of W-coated spherical UO_2. Densification of such materials requires techniques other than sintering alone, such as hot pressing, hot extrusion, Dynapak* consolidation, and hot-gas isostatic pressure bonding.

Two of these techniques, i.e., hot pressing and hot-gas isostatic pressure bonding, have been evaluated briefly with both fully dense UO_2 and W-coated UO_2 microspheres. Fueled compacts prepared by hot-gas isostatic pressurization were superior both to hot-pressed compacts and to compacts prepared by the current fabrication process in the degree of densification, uniformity of interparticle spacing, and freedom from contamination. However, thermal cyclic testing results of hot-gas isostatically densified compacts encapsulated in T-111 alloy showed higher volumetric growths and susceptibility to cladding leakage than in compacts prepared by the current fabrication process. These results indicate the need for further study and characterization of W-coated UO_2 microspheres to make full use of their advantageous characteristics.

*Tradename of a process of the General Dynamics Corporation.

The principal advantages of the current process for fabricating fueled compacts are:

1. Compacts of high theoretical density (>95 percent of theoretical) are routinely obtained, with tolerances of ± 1 percent.
2. Different density levels can be obtained by adjusting the sintering schedule and/or the hot-gas pressure bonding cycle.
3. Fuel particles are randomly distributed throughout the W matrix with no stringering or fuel breakup.
4. The fuel particle size range can be easily adjusted by selective screening in the fuel agglomeration process.
5. Individual processing of each compact ensures uniformity of fuel loading.
6. Very low impurity levels can be maintained due to binder-free blending and high sintering temperatures.
7. Excellent control of individual compact quality can be maintained.

Principal disadvantages of the current fabricating process are:

1. Uniform interparticle fuel spacing cannot be maintained.
2. Attrition of low-density UO_2 agglomerates in the blending operation leads to formation of some fuel fines in the W matrix.

Fabrication of Fuel Elements

The sequence for machining the as-sintered compact is as follows: the compact is face-ground to provide flat and parallel surfaces, drilled for coolant tubes, and finish-ground on the hexagonal surfaces. After the final machining operation, the segments are treated in hydrogen (-20° to -50°F dewpoint) to re-oxidize the fuel and produce stoichiometric UO_2. The refractory-metal cladding components, as shown in Figure 3.2.1, are the header plates, outer cladding, and coolant tubes. The header plates are face-ground and drilled, and then embossed to provide weld preps for joining to the coolant tubes and outer cladding. The outer hexagonal cladding is formed in two halves and joined by electron beam welding.

The fuel element is assembled by first stacking the fueled segments and inserting the coolant tubes. This assembly is then slipped into the outer cladding. Next, header plates are added and, finally, all joints are electron-beam welded in an evacuated chamber.

After helium leak checking in a mass spectrometer, the assembly is hot-gas pressure bonded at 3180°F for 1.5 to 3 hours in helium at 10,000 psig. Final inspection operations include a leak-check by helium mass spectrometer techniques, outer cladding - matrix bond check by pulse echo and resonance frequency methods, and inner cladding - matrix bond check by through-transmission techniques. A photomicrograph of the core - cladding interface after bonding is shown in Figure 3.2.4.

The principal advantages of this portion of the current fabrication process are:

1. Close dimensional tolerances of the fuel segment and cladding components can be maintained.

2. The stoichiometry of the fuel in each individual segment can be controlled within a measurement uncertainty of 0.003.
3. High quality levels can be maintained by suitable inspection techniques applied to the individual fuel segments and cladding components.
4. Excellent dimensional control of the bonded fuel element assembly can be maintained.
5. Stacking compacts in series along the length of the fuel elements alleviates hot channel factors by randomizing tolerance effects.

Disadvantages are:

1. The machining and drilling operations presently performed on the fueled segments involve a significant loss of material.
2. The machining operations can introduce contaminants into the fueled segments.

With continued development of techniques for fabricating reactor-size quantities, these disadvantages can be minimized by several possible approaches. Drilling losses may be reduced by pressing and sintering fueled compacts with coolant holes which would require only a cleanup operation to size the holes. Other material losses may be further reduced by development effort currently in process, i.e., by making longer segments and by using finer grit grinding wheels which would eliminate a lapping operation and also reduce the possibility of contamination.

COMPILATION AND REVIEW OF MATERIALS AND ENGINEERING TEST DATA

Materials test data of interest to the aircraft reactor application are discussed below with respect to four key characteristics.

1. The chemical, metallurgical, and mechanical stability of fuel element materials.
2. The fission product retention capabilities of fuel element cladding.
3. The burnup capabilities of the fuel element materials.
4. Radiation effects on materials properties.

Supplementary materials property data for the candidate fuel element materials are summarized in Appendix B.

In the GE-NMPO High Temperature Materials Program, each combination of refractory-metal fuel element materials is subjected to a 10,000-hour non-nuclear evaluation test program at the temperatures of interest as shown in Figure 3.2.5. A fuel element's performance is measured by the integrity of the cladding, quality of the bond between the core and the cladding, nonreactivity between fuel and metallic components, and fuel form stability.

T-111-Clad W-UO_2 Fuel Element Materials

The first series of photomicrographs, Figure 3.2.6, show the results obtained from the 10,000-hour test program evaluation of the T-111-clad W-UO_2 fuel element system.

[redacted]

The microstructures at the core - cladding interface are shown after 500,2500, 5500, and 10,000 hours of testing in high-purity helium at slightly above atmospheric pressure. Testing of the cladding showed an increase in the T-111 cladding hardness by atmospheric impurities from 191 DPH initially to 432 DPH. Although not apparent in the photomicrographs, some of the Hf content of the T-111 cladding has been converted into a fine dispersion of HfO_2. Because of the fine oxide precipitation, the cladding showed very little grain growth after 10,000 hours at 2900°F. Post-test analyses revealed no significant reaction between fuel and matrix nor between fuel and cladding. No significant quantity of free U was produced in the core as a result of loss of oxygen through the cladding. No measurable change in physical dimensions was detected. Although the very fine band of voids in the cladding adjacent to the fuel interface has moved with time into the cladding away from the interface, the cladding integrity is excellent.

W-Re-Mo-Clad W-UO_2 Fuel Element Materials

Under equilibrium conditions, the NMP-306 alloy (W - 30Re - 30Mo, at. %) composition is in a two-phase region of Re-rich sigma phase dispersed throughout the W-Re-Mo solid solution. Figure 3.2.7 shows four NMP-306-clad W-UO_2 fuel system specimens which were fabricated to evaluate the thermal cycle stability of this system. The upper left photograph shows the core - cladding interface after autoclaving at 3180°F. After 10 thermal cycles to 3000°F, the structure shown at the upper right was obtained. This test showed good maintenance of core - cladding interface bond and little change in the disposition of the sigma phase in the cladding. It should be noted that the sigma precipitate minimizes grain growth below solutioning temperatures. The photomicrograph at the bottom left shows the microstructure after a heat treatment at 4530°F. Noteworthy is the solution of the sigma phase. Microprobe analyses at the core - cladding interface showed a diffusion of Re and Mo into the W matrix to a depth of 18 to 20 mils and a concomitant movement of W into the cladding. The photomicrograph at the lower right shows the core - cladding interface after 10 thermal cycles to 3000°F following the 4530°F treatment. Some slight precipitation of sigma phase at the grain boundaries of the recrystallized cladding is apparent.

Figure 3.2.8 shows the core - cladding interface after 1900 hours at 2910°F. The cladding is clean and dense but contains some sigma phase in the grain boundaries in the outer part of the cladding. The freedom from sigma phase in the cladding near the core resulted from depletion of rhenium by diffusion into the core matrix. Since the sigma phase is a hard inclusion, it was originally anticipated that cladding ruptures would be likely to appear in these regions; however, this has not been evident as demonstrated by test results. In addition, the sigma phase is depleted near the matrix - cladding interface, the high stress region, by diffusion of rhenium into the matrix. Therefore, the presence of sigma phase dispersion in the NMP-306 alloy is not considered objectionable and may be advantageous in preventing grain growth.

Mo - 50Re-Clad Mo-UO_2 Fuel Element Materials

Figure 3.2.9 shows the interface of a Mo - 50Re-clad Mo-UO_2-ThO_2

[redacted]

fuel element after 2000 hours at 2910°F. There are some voids slightly below the interface in the Mo matrix structure. These may be diffusion voids, indicating that the diffusion of Mo into the Mo-Re cladding alloy is faster than the diffusion of Re into the Mo. At very high temperatures where diffusion voids have been noted in the W-Re-Mo system, movement of the void band appears to be from the interface into the core rather than into the cladding as is the case in the Ta-clad systems.

HIGH-TEMPERATURE MATERIALS IN-PILE TEST PROGRAM

Most of the in-pile testing on fueled specimens up to the present time has been done under the High-Temperature Materials program. Table 3.2.1 lists the tests, operating conditions, burnups achieved, and release rates observed. The first in-pile test cartridge prepared under the 710 Reactor Program is also listed in this table. Representative photomicrographs from some of the tests are shown in Figures 3.2.10 through 3.2.12. The results of in-pile testing during 1963, 1964, and 1965 indicate that, if exact stoichiometry of the fuel form is maintained, no significant diffusion of fuel nor fission products is to be expected through claddings of interest under aircraft reactor conditions. In effect, these experiments showed the capability of the W-Re-Mo alloy cladding to retain fuel and fission products at 3630°F for at least 1000 hours and at 2910°F for over 3000 hours.

Since essentially all fission products are retained within the fuel element matrix structure which has an average void fraction of less than 4 percent, the next important consideration is the burnup which may be achieved as a function of materials, temperatures, and time. Fission gas pressure may produce blistering of the cladding and leakage from the cladding structure. In-pile results obtained to date have already demonstrated fission product burnup capabilities of approximately 2.0×10^{20} fissions/cm^3 of fueled matrix.* Using the release of fission products as a criterion, Figure 3.2.13 indicates current burnup capability of refractory-metal in-pile test specimens.

The photomicrographs in Figure 3.2.11 show an interface area of Ta-clad and Ta - 10W-clad $W-UO_2-ThO_2$ fuel elements in the as-fabricated condition, after static testing, and after exposure in the ETR at elevated temperatures for 345 hours in a helium - argon atmosphere. The burnup obtained as a result of this exposure was 1.3×10^{20} fissions/cm^3. These specimens were leak-tight at the completion of the test and a good bond between core and cladding was maintained. Void formation in the Ta-clad specimen was insignificant. In the case of the Ta - 10W alloy, a noticeable void formation was apparent. The irradiated fuel form shows some cracking and fission gas bubbles were detected at higher magnification.

The photomicrographs in Figure 3.2.12 show the condition of the W-Re-Mo-clad $W-UO_2-ThO_2$ fuel element as-fabricated, after static testing, and after in-pile testing in the ETR for 285 hours at 2910°F in a helium - argon - hydrogen atmosphere. The burnup obtained was 7×10^{19} fissions/cm^3 and, once again, the condition of the specimen was excellent.

Figure 3.2.14 shows the microstructure of a W-Re-Mo-clad $W-UO_2-ThO_2$ specimen as-fabricated, after static testing, and after in-pile testing

*All burnups quoted are based on fueled matrix.

TABLE 3.2.1

SUMMARY OF TEST CONDITIONS AND RESULTS OF REFRACTORY METAL FUEL ELEMENTS SPECIMENS IN-PILE TESTED DURING CY 1965 AND 1966

	Specimen Composition			Test Conditions					Test Results							
Test Number[a]	Cladding[i,j]	Core, vol %	U^{235}/(total)[i], %	Time at Temp.[i], hours	Temperature, °C	Cycles[c]	Test Atmosphere[h]	Burnup, fissions/cm³	Maximum Power Density, kw/cm³	Max. Dia. Growth, %	Fission Gas Release Fraction of Xe-133 N/F[d]	Results of Visual Inspection	Interface Bond[e]	Core Cracking[e,f]	Diffusion Voids[g]
LTFF-9	W-Re-Mo	W – ($54UO_2$ + $6ThO_2$)	33	1015	2000	15	He	2.2×10^{19}	0.15	0.9	NR	No deform.	Good	CC	None
LTFF-11	W-Re-Mo	W – ($54UO_2$ + $6ThO_2$)	32.3	3085	1650	24	He + $5H_2$	3.6×10^{19}	0.20	0.8	NR	No deform.	Parted	CC	Sigma inter.
GEFP2-6(1)	W-Re-Mo	W – ($54UO_2$ + $6ThO_2$)	31.9	537	2015	16	He + 50Ar + $5H_2$	1.4×10^{20}	2.1	1.3[g]	8×10^{-4} at 208 hrs	Swelled	ID Parted	CC-S	Minor
(2)	W-Re-Mo	W – ($54UO_2$ + $6ThO_2$)	31.9	537	1910	16	He + 50Ar + $5H_2$	1.3×10^{20}	1.8	1.6[g]		Swelled	ENP	ENP	ENP
(3)	W-Re-Mo	W – ($54UO_2$ + $6ThO_2$)	31.9	537	1755	16	He + 50Ar + $5H_2$	0.9×10^{20}	1.2	1.9[g]		Swelled	ID Parted	CC-S	Minor
(4)	W-Re-Mo	W – ($54UO_2$ + $6ThO_2$)	31.9	537	1600	16	He + 50Ar + $5H_2$	0.7×10^{20}	1.0	0.6	NR	No deform.	Good	CC-S	Minor
ORRF-1(1)	W-Re-Mo*	W – 10Re – ($60UO_2$)	8.76	873	1590	12	He + $5H_2$	0.7×10^{20}	0.63	0.42	NR	No deform.	Good	No	None
(2)	W-Re-Mo*	W – 10Re – ($60UO_2$)	8.76	873	1590	12	He + $5H_2$	0.7×10^{20}	0.63	0.38	NR	No deform.	Good	No	None
(3)	W-Re-Mo*	W – 10Re – ($60UO_2$)	8.76	873	1590	12	He + $5H_2$	0.7×10^{20}	0.63	0.36	NR	No deform.	Good	No	None
LT-710-1	W-Re-Mo*	W – ($54UO_2$ + $6ThO_2$)	26.6	3000	1640	38	He + $5H_2$	3.6×10^{19}	0.09	0.31	NR	No deform.	Good	No	None
ORRF-2(1)	W-Re-Mo*	W – 10Re – ($60UO_2$)	8.76	233/370	1365/1640	2	He	5.2×10^{19}	0.67	0.22	NR	No deform.	EI	EI	EI
(2)	W-Re-Mo*	W – 10Re – ($60UO_2$)	8.76	233/370	1635/1735	2	He	5.7×10^{19}	0.76	0.18g	RMA	Swelled	EI	EI	EI
(3)	W-Re-Mo*	W – 10Re – ($60UO_2$)	8.76	233/370	1520/1590	2	He	4.8×10^{19}	0.62	0.18	NR	No deform.	ENP	ENP	ENP
(4)	W-Re-Mo*	W – 10Re – ($60UO_2$)	8.76	233/370	1400/1470	2	He	4.1×10^{19}	0.52	0.15	NR	No deform.	ENP	ENP	ENP
LTFF-14	W-Re-Mo*	W – ($54UO_2$ + $6ThO_2$)	27.5	751	1650	14	He	0.9×10^{19}	0.1	1.1	3.20×10^{-4} at 720 hr	No deform. specimen pitting	Good	No	No
LTFF-13	Mo - 50Re	Mo - $60UO_2$	23.9	1146	1650	14	He	1.2×10^{19}	0.1	~0.14	2×10^{-5} at 929 hr	No deform. specimen pitting	Good	No	No
GEFP2-4(1)	Ta	W + $0.8ThO_2$ – ($55.4UO_2$ + $3.8ThO_2$)	32.1	984	1930	26	He + 20Ar	3.9×10^{20}	2.8	2.2[g]	1×10^{-4} at 413 hr	Swelled	Good	CCR	Yes
(2)	Ta	W + $0.8ThO_2$ – ($55.4UO_2$ + $3.8ThO_2$)	32.1	984	1800	26	He + 20Ar	3.7×10^{20}	2.7	2.4[g]		Swelled	ENP	ENP	ENP
(3)	Ta	W + $0.8ThO_2$ – ($55.4UO_2$ + $3.8ThO_2$)	32.1	984	1590	26	He + 20Ar	2.5×10^{20}	1.8	2.5[g]		Swelled	ENP	ENP	ENP
(4)	Ta	W + $0.8ThO_2$ – ($55.4UO_2$ + $3.8ThO_2$)	32.1	984	1434	26	He + 20Ar	2.1×10^{20}	1.6	0.6	NR	No deform.	Good	No	Nil
GEFP2-7(1)	Ta – 10W	W – ($54UO_2$ + $6ThO_2$)	32.3	512	1650	8	He + $5H_2$	1.3×10^{20}	1.3	0.37	NR	No deform.	Good	No	Yes
(2)	Ta	W – ($54UO_2$ + $6ThO_2$)	32.3	512	1580	8	He + $5H_2$	1.1×10^{20}	1.2	0.29	NR	No deform.	Good	No	Minor
(3)	Ta	W – ($54UO_2$ + $6ThO_2$)	32.3	512	1530	8	He + $5H_2$	0.9×10^{20}	0.8	0.17	NR	No deform.	ENP	ENP	ENP
(4)	Ta – 10W	W – ($54UO_2$ + $6ThO_2$)	32.3	512	1430	8	He + $5H_2$	0.8×10^{20}	0.7	Nil	NR	No deform.	ENP	ENP	ENP

[a] Tests designated as successful (based on absence of deformation and leaks) shown in large type.
[b] ETR Testing Time expressed in Equivalent Full Power Operation hours.
[c] Reduction in operating temperature of 50% of test temperature (±10%).
[d] Release attributed to those specimens which showed leaks during post-test leak checks. NR = No release above recoil. RMA - Radiation Monitor Alarm.
[e] EI - Evaluation Incomplete. ENP - Evaluation Not Performed.
[f] CC - Core Cracked. CC-S - Core crack associated with separation. CC-R - Core crack associated with rupture due to forces caused by lack of separation.
[g] Measurements influenced by specimen swelling.
[h] Test pressure 35 - 45 psi unless otherwise specified.
[i] W-Re-Mo cladding is W - 30Re - 30Mo at. %.
[j] Cladding thickness 0.015 inch, * indicates 0.010 inch cladding.

[redacted]

at 3630°F for 1015 hours in a helium atmosphere. The burnup obtained was 2.0×10^{19} fissions/cm^3. The condition of the specimen at the end of this exposure was excellent; no faulting of the core structure nor the core - cladding interface was noted. The fuel form was somewhat friable and difficult to polish without pullout. No microporosity was apparent at the core - cladding interface. Because of the higher operating temperature of 3630°F, no sigma phase precipitation had occurred. The excellent stability of this system after 2000 hours in a laboratory test at 4000°F is shown in the two center photomicrographs.

The photomicrographs in Figure 3.2.15 show a W-Re-Mo-clad W-UO_2-ThO_2 specimen as-fabricated, after static testing, and after 3085 hours of in-pile testing at 3000°F in a helium atmosphere. The burnup obtained was 4.0×10^{19} fissions/cm^3. The irradiated microstructure shows that precipitation of sigma phase occurred during the test. In this particular case, an extensive void formation weakened the structure at the core - cladding interface and some faulting of the structure was evident. Post-test evaluation of this specimen is still in progress and the cause of this void formation has not yet been fully identified. It is noteworthy in this particular experiment that blistering of the cladding, as a result of fission gas pressure, did not occur. This result lends credence to the premise that a significant fraction of the gaseous fission products at these burnup levels and temperatures is held in the crystal lattice of the fueled core matrix.

710 REACTOR PROGRAM THERMAL TEST DATA

With the exception of in-pile test cartridge LT-710-1 listed in Table 3.2.1, all the data derived to date under the 710 Reactor Program have been generated from non-nuclear static and dynamic testing. The current status of these programs is shown in Figure 3.2.16.

Current failure-free tests on single-channel W-Re-Mo-clad specimens have reached 7800 hours in an unpressurized static environment. Diametral expansion is about 2.3 percent after 61 thermal cycles. W-Re-Mo-clad 19-channel element P1W-1D has accumulated 4560 failure-free hours in a static furnace pressurized to 200 psig. A slight reduction in across-flats dimensions was noted after 48 cycles. The T-111-clad 19-channel elements are also being tested in a pressurized atmosphere. Volumetric changes of the specimens currently on test are shown in Figure 3.2.17. The effect of the 200 psig ambient pressure is quite apparent. The visual appearance of all specimens on test is excellent. All specimens are leak-tight and ultrasonic bond inspection shows they are still well bonded.

Two W-Re-Mo-clad specimens were removed from test and sectioned for metallographic and electron microprobe analysis to determine core - cladding interdiffusion and degree of bond retention. The diffusion of Re and Mo from the cladding into the pure W matrix is expected to improve bond retention under thermal cycling conditions by increasing the low temperature ductility of the W matrix. Specimen ASL-6, which contained inner and outer cladding of NMP-306, was cycled 51 times between 3900°F and 500°F, with a total of 500 hours at 3900°F. Specimen A7C-2, containing an outer cladding of NMP-256* and NMP-306 inner cladding, was cycled

*NMP-256 is W - 25Re - 30Mo (at. %).

40 times between 3000°F and 500°F with 300 hours at 3000°F. Neither specimen showed any significant physical changes at test termination and both were leak-tight and well bonded. Metallographic examination of both specimens showed excellent core - cladding bonding as illustrated in Figures 3.2.18, 3.2.19, and 3.2.20. Sigma phase precipitation occurred in the NMP-306 inner cladding of specimen A7C-2, as shown in Figure 3.2.18. Because of its higher W and lower Re content, the NMP-256 alloy remained single phase well below 3000°F, and sigma phase precipitation was not observed in the outer cladding of specimen A7C-2 (Figure 3.2.19). At 3900°F, the NMP-306 alloy is also single phase as indicated by the cladding of ASH-6 shown in Figure 3.2.20.

Electron microprobe scans across the core - cladding interfaces of both specimens, Figures 3.2.21 and 3.2.22, show that the extent of the interdiffusion zone is approximately equal on both sides of the original core - cladding interface; therefore, no significant development of diffusion voids in either the cladding or the core would be expected. These plots also show that, as diffusion proceeds, the changes in Re, Mo, and W content in the interdiffusion zone become more gradual. Figure 3.2.21 also indicates that the NMP-306 alloy maintains a higher Re content at the core - cladding interface than the NMP-256 alloy, which is expected to result in improved bond retention. Depletion of the Re in the cladding adjacent to the original interface, as shown in Figure 3.2.21, is reflected in the absence of sigma precipitation in the cladding next to the core, Figure 3.2.19.

Data from these two specimens together with microprobe data on three other NMP-306-clad specimens, obtained under the High-Temperature Materials Program, were used to prepare an isochronal plot of the extent of Re and Mo diffusion into W-UO_2 cores as a function of temperature, Figure 3.2.23. In all samples analyzed to date, the respective depths of Re and Mo diffusion into the matrix have not been significantly different. These preliminary data, representing only five specimens, permit a rough estimation of the extent of interdiffusion between NMP-256 and NMP-306 alloy cladding and W-UO_2 cores at various times and temperatures.

RADIATION EFFECTS ON MATERIAL PROPERTIES

Irradiation effects studies are being performed on the refractory metals and their alloys under the High-Temperature Materials program. The objective of these studies is to determine:

1. Temperatures at which irradiation-induced defects are removed in these materials
2. Neutron dose and spectrum dependency
3. Influence of elevated temperature irradiations on the hot-hardness, tensile, and creep-rupture properties.

An example of the defect removal temperature is shown in Figure 3.2.24 for Mo and several Mo alloys. The parameter "ratio of the irradiated to the unirradiated mechanical property" is presented as a function of the test temperature for the case of hardness measurements and as a function of annealing temperature for the case of tensile properties. This family of curves shows that Mo and [redacted] dilute alloy (Mo-TZM) recover at a temper-

ature slightly below 1100°C (2000°F). On the other hand, the binary alloy, Mo - 50Re, shows almost complete recovery at temperatures slightly above 600°C (1100°F). The irradiated Mo-TZM was too brittle to tensile-test at the low temperature.

A similar plot is shown in Figure 3.2.25 of W and several alloys of W. Based on the present experimental data for low and intermediate fluence values, i.e., less than 5 x 10^{19} neutron/cm^2, it appears that, as a general rule, the alloys show recovery at temperatures above 0.22 Tm and the unalloyed metals show recovery above 0.35 Tm. Experiments are in progress to complete the determination of the recovery properties of those alloys for which the data are not shown. Supplementary radiation effects testing will be done under the 710 fuel element development program.

SUMMARY OF STATE-OF-ART OF SELECTED MATERIAL PERFORMANCE

1. Stoichiometric UO_2 is compatible with the refractory metals W, Re, Mo, and their alloys.
2. Stoichiometric UO_2 clad with W, Re, Mo or their alloys does not lose oxygen significantly at high temperatures in inert atmospheres because of the low diffusion of oxygen through these metals and alloys.
3. W-Re-Mo-clad W-UO_2 fuel elements which contain nonstoichiometric fuel are unstable and subject to failure due to uranium metal penetration of the cladding, deterioration of the metallic matrix, and core - cladding separation.
4. Retention of fuel and fission products at 2900°F for over 3000 hours and at 3600°F for at least 1000 hours has been demonstrated experimentally by W-Re-Mo-clad W-UO_2 test specimens containing stoichiometric fuel. Corresponding burnups were 3.6 and 2.2 x 10^{19} fission/cm^3, respectively.
5. The W-Re-Mo-clad W-UO_2 fuel materials have demonstrated burnup capability over 1 x 10^{20} fissions/cm^3 at 3000°F for cores containing 60 volume percent fuel and less than 3 percent porosity. Complete retention of fuel and fission products was obtained without significant growth or distortion of the matrix structure.
6. W-Re-Mo-clad UO_2 test specimens do not grow significantly in nonnuclear testing. A 19-channel test specimen, tested in a helium atmosphere at 200 psig, sustained negligible changes in dimensions after 4564 hours at 3000°F with 48 thermal cycles.
7. Irradiation-induced defects are removed at lower temperatures in alloys of W, Re, and Mo than in the unalloyed metals.
8. The W-Re-Mo cladding material is available commercially in the form of sheet and plate. Fabrication procedures have been developed at GE-NMPO for making high-quality, thin-wall tubing.
9. Procedures have been developed for fabricating the W-Re-Mo materials into the geometries required for fuel element fabrication and for metallurgically bonding the cladding to the fueled matrix.
10. Procedures have been developed for precisely controlling the stoichiometry of W-UO_2 matrices containing 60 volume percent fuel.

RESEARCH PROBLEMS

A review of the current status of refractory-metal fuel element tech-

nology indicates that effort is needed to establish the burnup capability and dimensional stability of the W-Re-Mo-clad W-UO_2 matrix for the conditions imposed by the aircraft application.* While in-pile test results have shown the W-Re-Mo cladding capable of fission product retention for over 3000 hours at 3000°F, no specimens have been tested to the burnups of this particular reactor application. Such testing is required to establish the capability of the fuel element materials to meet the requirements of ANP. In decreasing order of importance, data are needed on the effects of irradiation on the mechanical and physical properties of cladding, matrix metal, and fuel agglomerates; the optimum matrix material compositions; and the degree of mobility of fission gases within the matrix.

Research on these problems is currently being conducted by GE-NMPO under both the High-Temperature Materials Program and the 710 Reactor Systems Project. In-pile test cartridges now being tested or scheduled for testing in the near future are listed in Table 3.2.2 which summarizes pertinent test data. The OPRF-2 and LTFF-14 test cartridges were prepared under the High-Temperature Materials Program; the other test cartridges are part of the 710 Reactor Systems Project fuel element development program. In addition to the in-pile test program, out-of-pile tests are being performed under both tasks to evaluate refractory-metal fuel element performance under various non-nuclear conditions. The following are the High-Temperature Materials Program work plans:

1. Thermal stability test program
   a. 10,000-hour tests to investigate various cladding and matrix material combinations between 2550° and 3630°F.
   b. 1,000-hour tests to investigate fuel additives and cladding - matrix compositions above 4500°F.
2. Thermal cycling growth study
   a. Evaluate better fuel dispersions and coated fuel particles
   b. Evaluate W-alloy-clad specimens with stoichiometric fuel plus diffusion treatment at high temperatures
   c. Establish an understanding of the mechanism of growth
3. Core optimization
   a. Study coated spheroidized fuel particles
   b. Determine the optimum uniform fuel particle size

The 710 non-nuclear static tests now in progress have been described previously in the engineering test data section. Two additional 19-channel, partial-length, W-Re-Mo-clad W-UO_2 fuel elements are scheduled for static testing early in CY-67. Four 19-channel, full-length, W-Re-Mo-clad W-UO_2 fuel elements and two single-channel, full-length, W-Re-Mo-clad W-UO_2 specimens are scheduled to begin dynamic testing during CY-67. These specimens will be resistively heated to simulate the internal heat generation of an actual fuel element.

In summary, test results and post-test evaluation of current and planned test specimens described above should yield part of the data required to demonstrate the required fuel material performance for aircraft application.

*Per Table 5.5.2.

[redacted]

CONFIDENTIAL

TABLE 3.2.2

SUMMARY OF CURRENT AND SCHEDULED IN-PILE TESTS OF W-Re-Mo-CLAD SPECIMENS

Test Number	Core	Test Conditions: Time at Temperature, hr	Test Conditions: Temperature, °F	Test Conditions: Test Atmosphere	Burnup, fissions/cm^3	Test Status and Remarks
ORRF-2	W-Re-UO_2	1500	2680-3000	He + 5 H_2	1.1×10^{20}	In progress – four test specimens
LTFF-14	W-UO_2-ThO_2	3000	3000	He + 5 H_2	3.6×10^{19}	In progress
LT710-1	W-UO_2-ThO_2	3000	2800	He + 5 H_2, 200 psi	3.5×10^{19}	Complete – post-test evaluation in progress
LT710-3	W-UO_2-ThO_2	5000	2800	He, 200 psi	6.0×10^{19}	In progress – 9 inch-long specimen
LT710-4	W-UO_2 W-UO_2-ThO_2	5000	2800	He, 200 psi	6.0×10^{19}	Cartridge in assembly – six test specimens
LT710-5	W-UO_2 W-Re-UO_2	5000	2800	He, 200 psi	6.0×10^{19}	Planned – six test specimens

3.2.2 Reflector Materials

The three candidate materials considered for the reflector are Be, BeO, and Mo. Although the two metals, Be and Mo, have reasonably good ductility in the unirradiated condition, the design can probably be made so that ductility is not an important consideration for any of the reflector materials since the reflector is not a structural element.

REFLECTOR MATERIAL REQUIREMENTS

The specific requirements for the reflector materials include:

1. A minimum design life of 2000 hours
2. A design-point temperature level of 400°F
3. An integrated neutron flux (> 1 Mev) of about 2×10^{21} nvt
4. Adequate corrosion resistance in a water environment at the design temperature or capable of being canned or clad with a suitable corrosion-resistant material
5. Sufficient strength to support itself or capable of being canned or clad with a structural material to provide the required support.
6. Meet nuclear requirements

CANDIDATE REFLECTOR MATERIALS

Primarily due to the neutronic requirements of a reflector material, the three candidate materials selected were Be, BeO, and Mo. Although fabrication procedures are well established for all these materials, special precautions are required in handling and fabricating Be and BeO due to their toxic nature. They are all readily available commercially and can be fabricated in the shapes and sizes that would be required for the reflector. However, it is assumed that, in the case of BeO, it would be necessary to provide a structural can to support the reflector pieces. The properties of the candidate reflector materials are summarized in Table A3.1 and Figures A3.1 through A3.7 of Appendix A. With the concurrence of NASA, Mo was selected as the reference reflector material.

MOLYBDENUM PROPERTIES AND FABRICATION PROCESSES

Physical Properties

Molybdenum has a density of 0.369 lb/in.^{3}, a melting temperature of approximately 4750°F, and is normally available commercially with a purity of 99.9 percent (the principal impurity being carbon which is normally less than 0.04 percent).

Thermal Properties

The effects of temperature on the thermal conductivity, specific heat, and mean coefficient of thermal expansion are shown in Figures A3.1, A3.7, and A3.2, respectively.

Mechanical Properties

The effect of temperature on the modulus of elasticity is shown in

CONFIDENT

Figure A3.6. The value of Poisson's ratio at room temperature and for arc-cast material is approximately 0.32 and for the powder-metallurgy material about 0.31 and there is little variance in these values from room temperature to 1100°F. Figures A3.3, A3.4, and A3.5 show the effect of temperature on the ultimate tensile strength, yield strength, and elongation, respectively. The properties should only be considered as "a typical set" of mechanical properties for Mo since the strength and ductility properties of a material normally are dependent upon its complete processing history.

Effects of Irradiation

Since the reflector material is not required to perform a structural role other than supporting its own weight and since it was assumed that the design could be made on the basis of a "semi-brittle" material, the effects of radiation are not considered to be of great importance for the reflector material. The rather limited amount of irradiation data available[1] does indicate that this assumption of a semi-brittle material is, in fact, required since the elongation at fracture was zero in a room-temperature test after irradiation to 5.1×10^{19} nvt (> 1 Mev) at 200°F, while the tensile strength increased by 50 percent. Additional data on the effects of irradiation on the properties of Mo obtained under the GE-NMPO High-Temperature Materials Program are shown in Figure 3.2.24.

Fabrication

Molybdenum is readily formable by forging, using established practices.[2] Reference 2 also gives a brief summary of recommended machining practices. It can be welded by arc, electrical resistance, percussion, flash, or electron-beam techniques. Properly welded material has good ductility at room temperature. Riveting can also be used successfully for sheet material. Stress relief of all welded joints is recommended.

MECHANICAL AND THERMAL TEST DATA

While considerable engineering experience is available on the use of Mo, no directly applicable engineering-type mechanical and thermal test data were found.

CORROSION - EROSION DATA

Corrosion

Available data indicate[3] no corrosion problems in degassed water at the design point conditions. However, Mo does oxidize rapidly at temperatures above 1000°F and therefore no aftercooling method employing air as a coolant could be considered unless the reflector temperature is well below 1000°F throughout the period of aftercooling.

[1] M. J. Makin and E. Gillies, "The Effect of Neutron Irradiation on the Mechanical Properties of Molybdenum and Tungsten," J. Inst. of Metals, 86, 1958.

[2] Aerospace Structural Metals Handbook, ASD-TDR-63-741, Volume II.

[3] LaQue and Copson, "Corrosion Resistance of Metals and Alloys," Second Edition, Reinhold Publishing Company, New York, N. Y.

[redacted]

Erosion

No specific erosion data were found for Mo.

SUMMARY OF MOLYBDENUM STATE-OF-THE-ART MATERIAL PERFORMANCE

The available data indicate that Mo can meet the requirements for the reflector material on a state-of-the-art basis assuming the design could be made on the basis of a semi-brittle material. In addition, it appears that the life capability could be extended well beyond 2000 hours on a state-of-the-art basis.

RESEARCH PROBLEMS

On the basis of the available data, there does not appear to be need for any basic materials research and development effort in order to use Mo as the reflector material.

CONFIDENTIAL

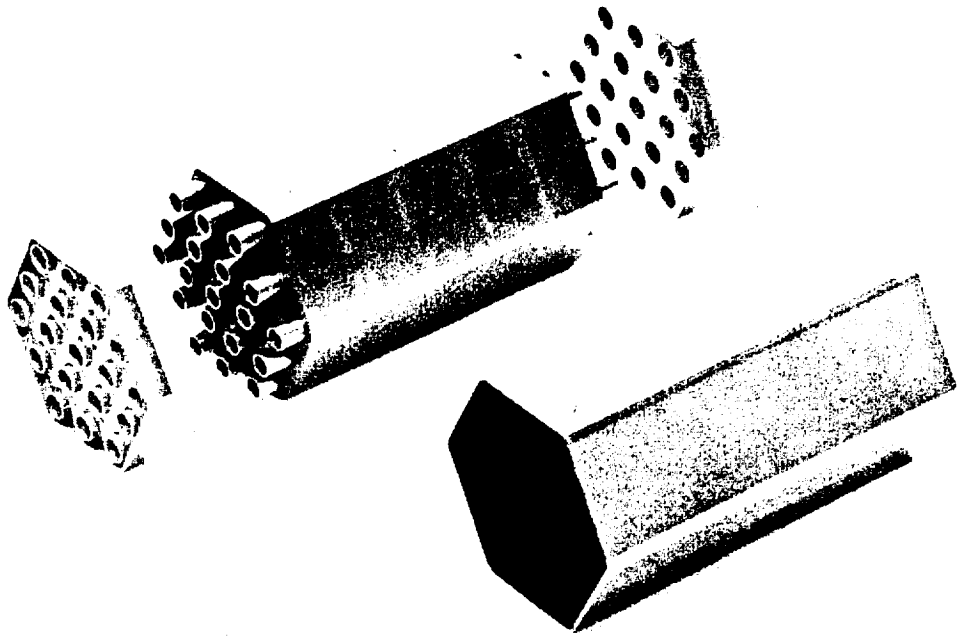

Fig. 3.2.1 – Exploded view of 19-channel partial-length fuel element

[redacted]

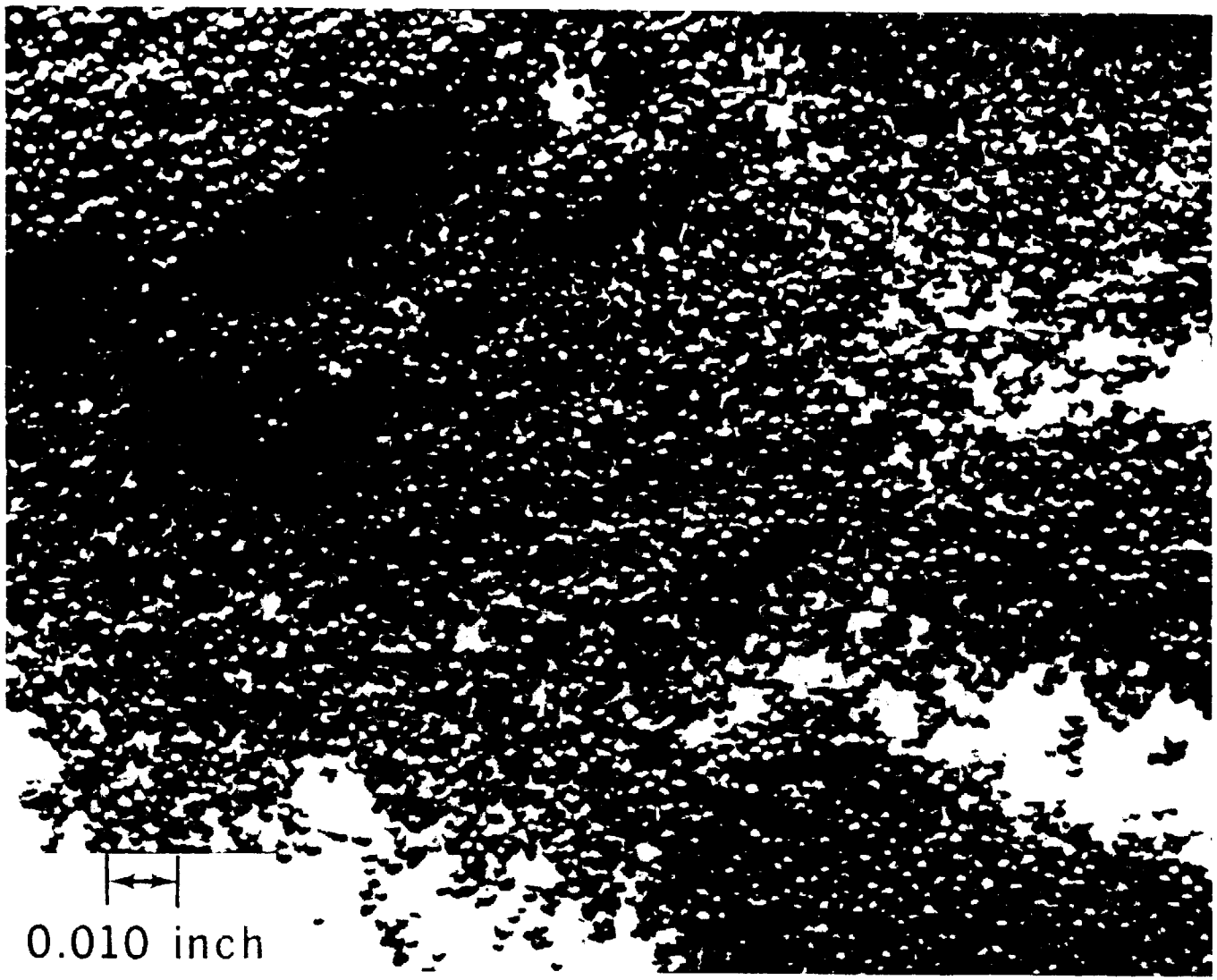

PARTICLE SIZE:

Range-approx. 0.005–0.0017 inch (long axis);

Average-approx. 0.003 inch (long axis)

Fig. 3.2.2 – Agglomerated fuel particles, –200/+325 mesh size (AS-513)

CONFIDENTIAL

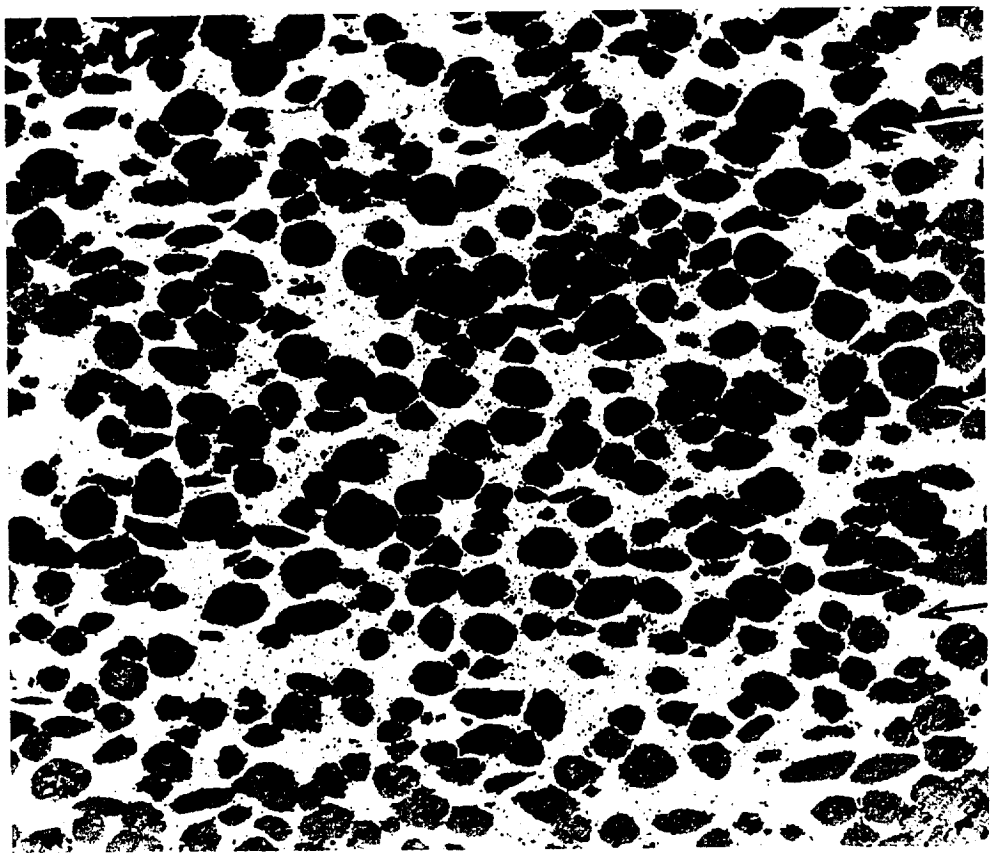

Fig. 3.2.3 – Photomicrograph of 40W – 60(UO_2 + additive), volume percent; sintered to 95 percent of theoretical density
(Neg. 6389, as-polished, 200X)

[redacted]

W-Re-Mo
cladding

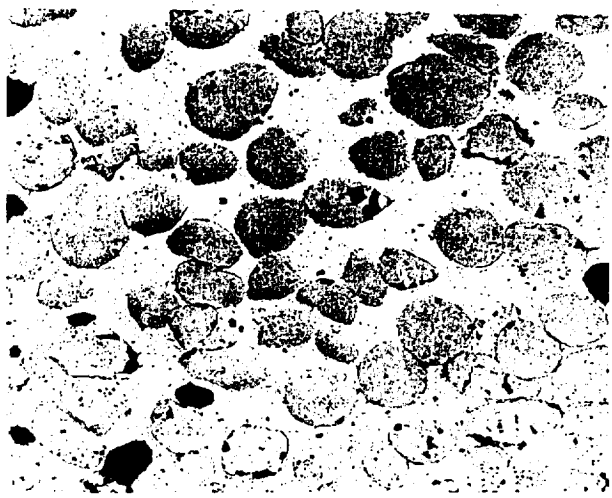

Fig. 3.2.4 – W-Re-Mo cladding bonded to W – 60UO_2 fueled matrix, as bonded at 3180°F and 10,000 psi for 3 hours *(AS-517)*

CONFIDENTIAL

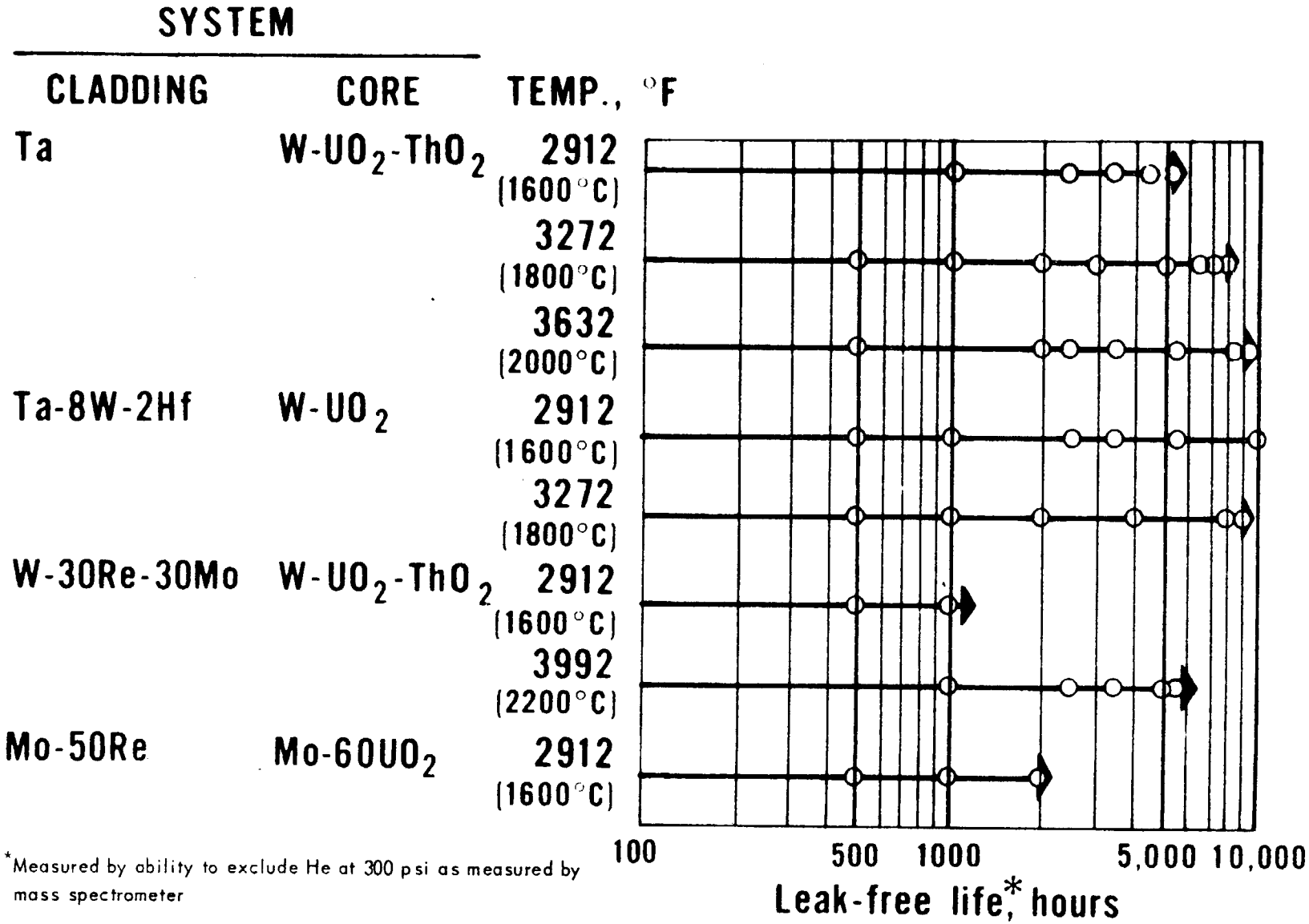

*Measured by ability to exclude He at 300 psi as measured by mass spectrometer

Fig. 3.2.5 – Excerpts from high-temperature materials program non-nuclear life tests

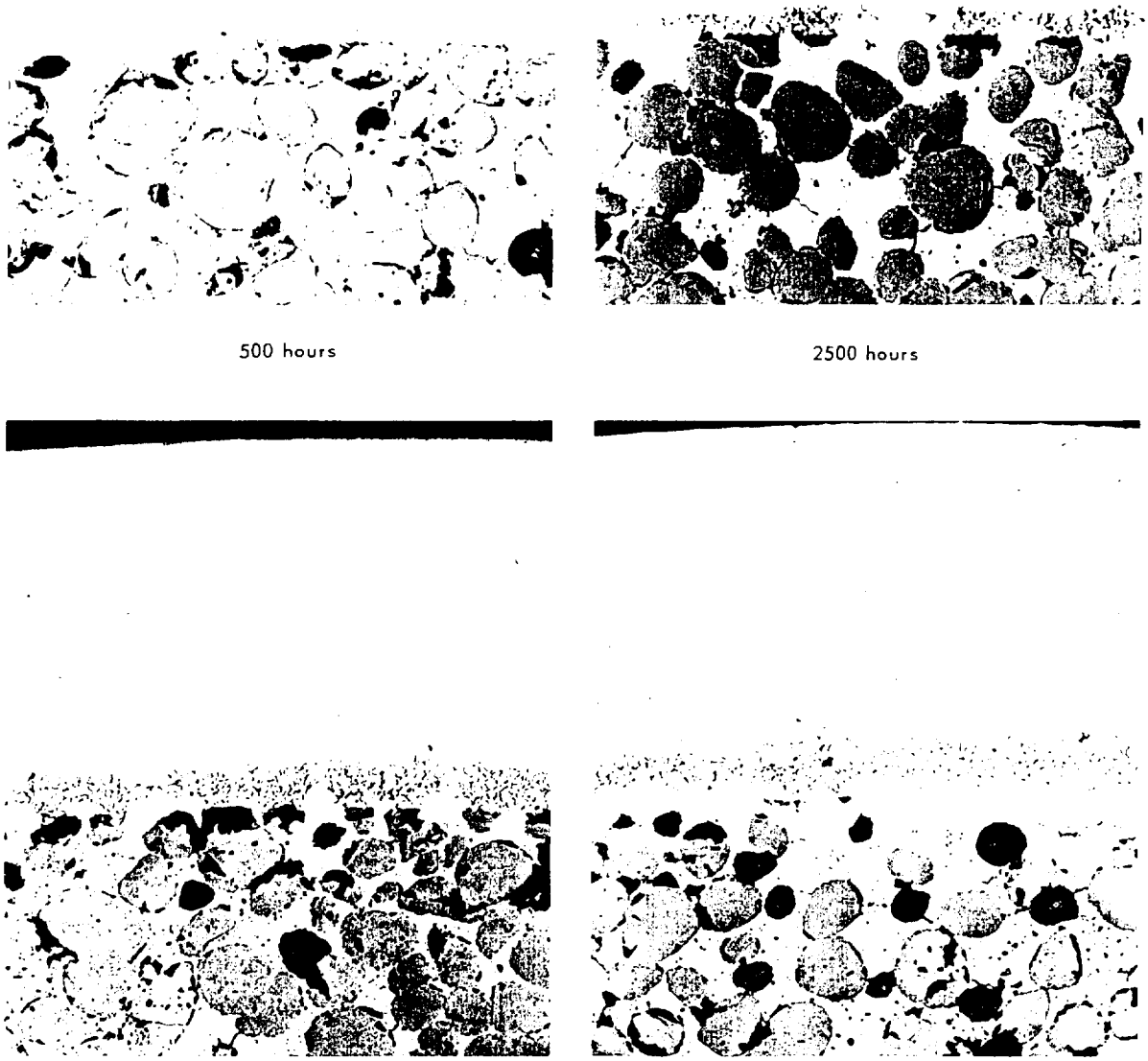

Fig. 3.2.6 – T-111-clad W-UO_2 specimens after 1600°C tests up to 10,000 hours

(AS-510, 100X)

CONFIDENTIAL

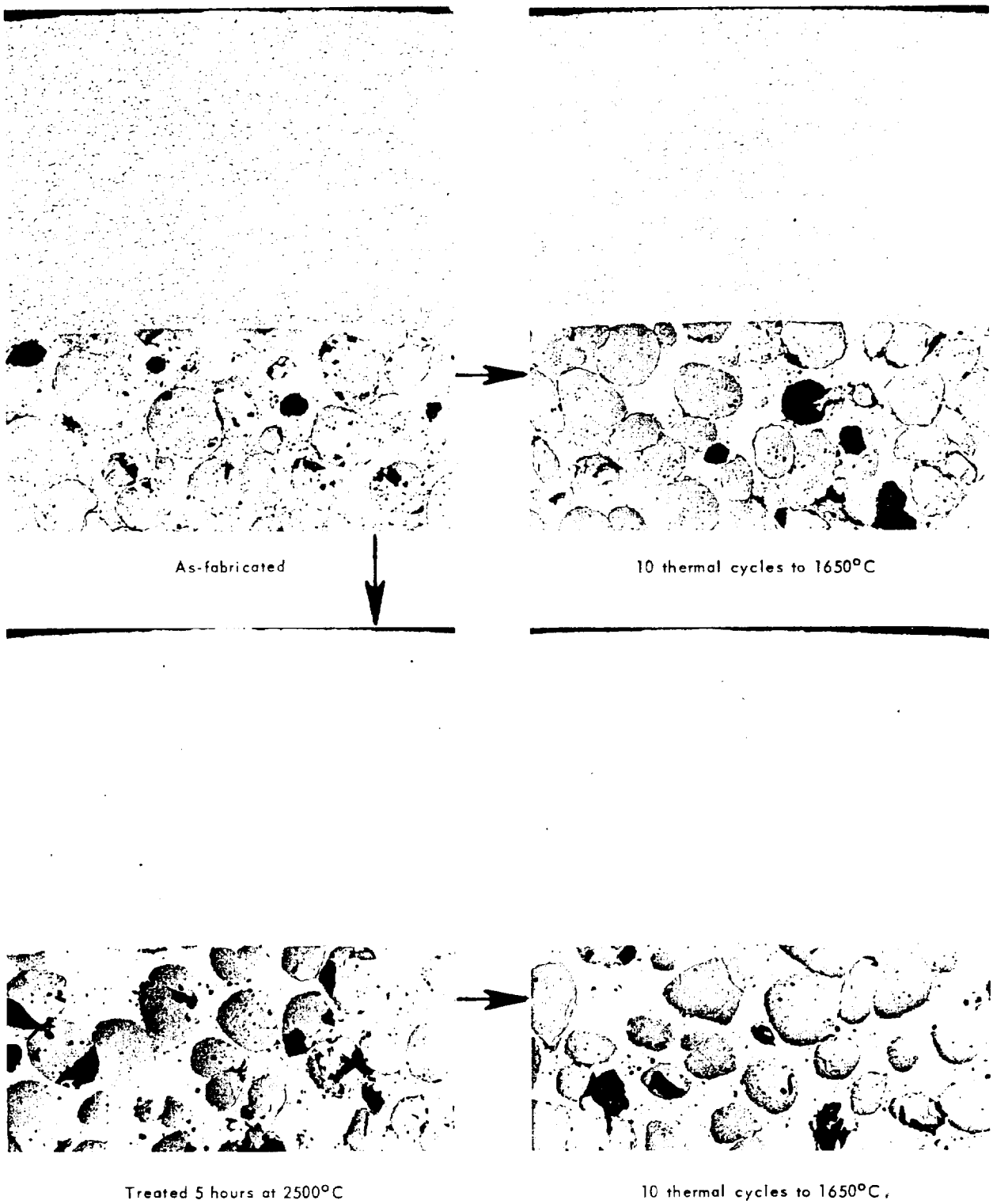

Fig. 3.2.7 – W – 30Re – 30Mo-clad W-UO_2 thermal cycled to 1650°C *(AS-511, 100X)*

CONFIDENTIAL

[redacted]

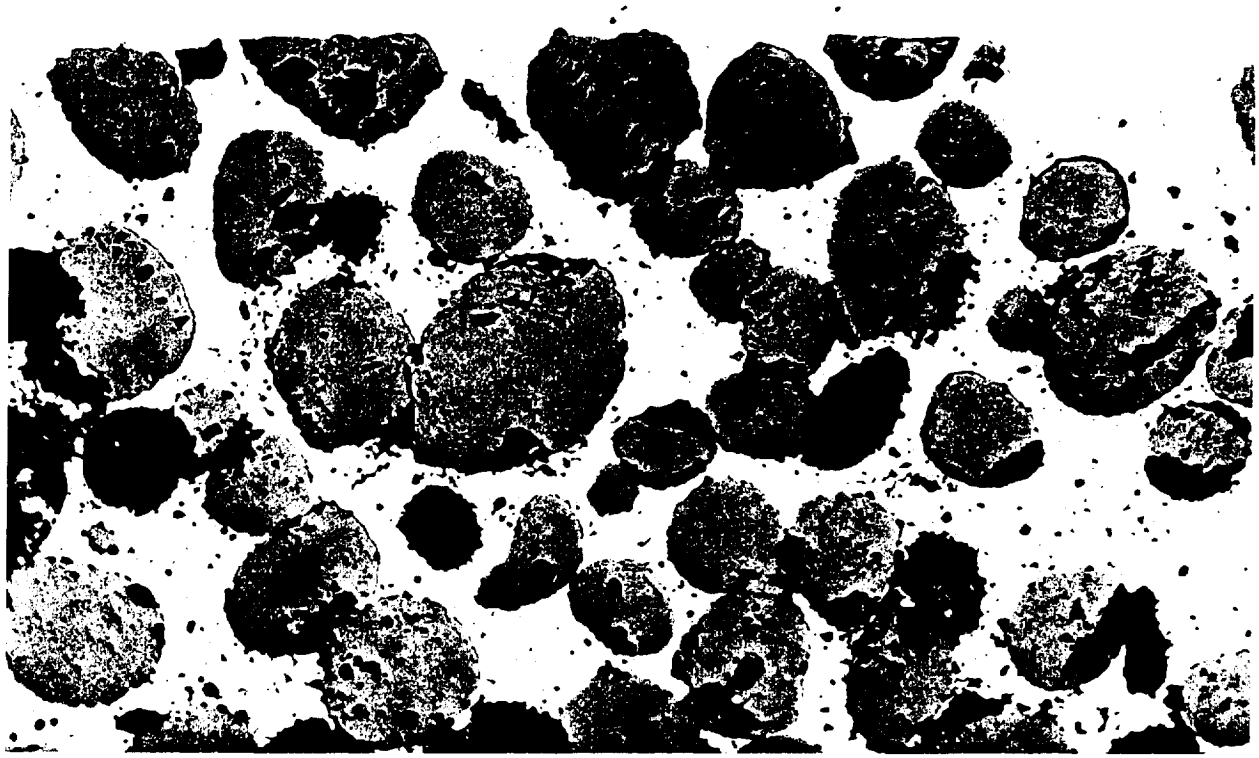

Fig. 3.2.8 – W – 30Re – 30Mo-clad W – 60UO_2 after 1900 hours at 1600°C *(AS-502, 200X)*

CONFIDENTIAL

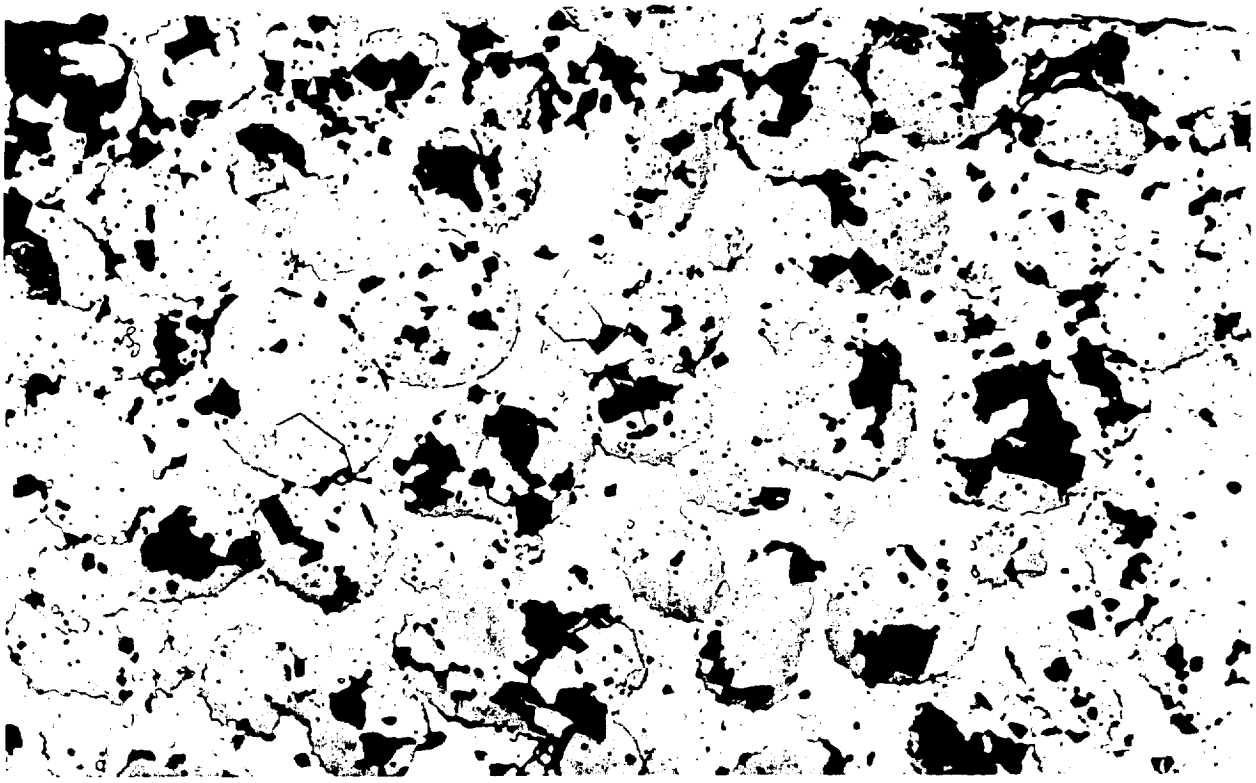

Fig. 3.2.9 – Mo – 50Re-clad Mo-UO_2-ThO_2 after 2000 hours at 1600°C *(AS-503, 200X)*

[redacted]

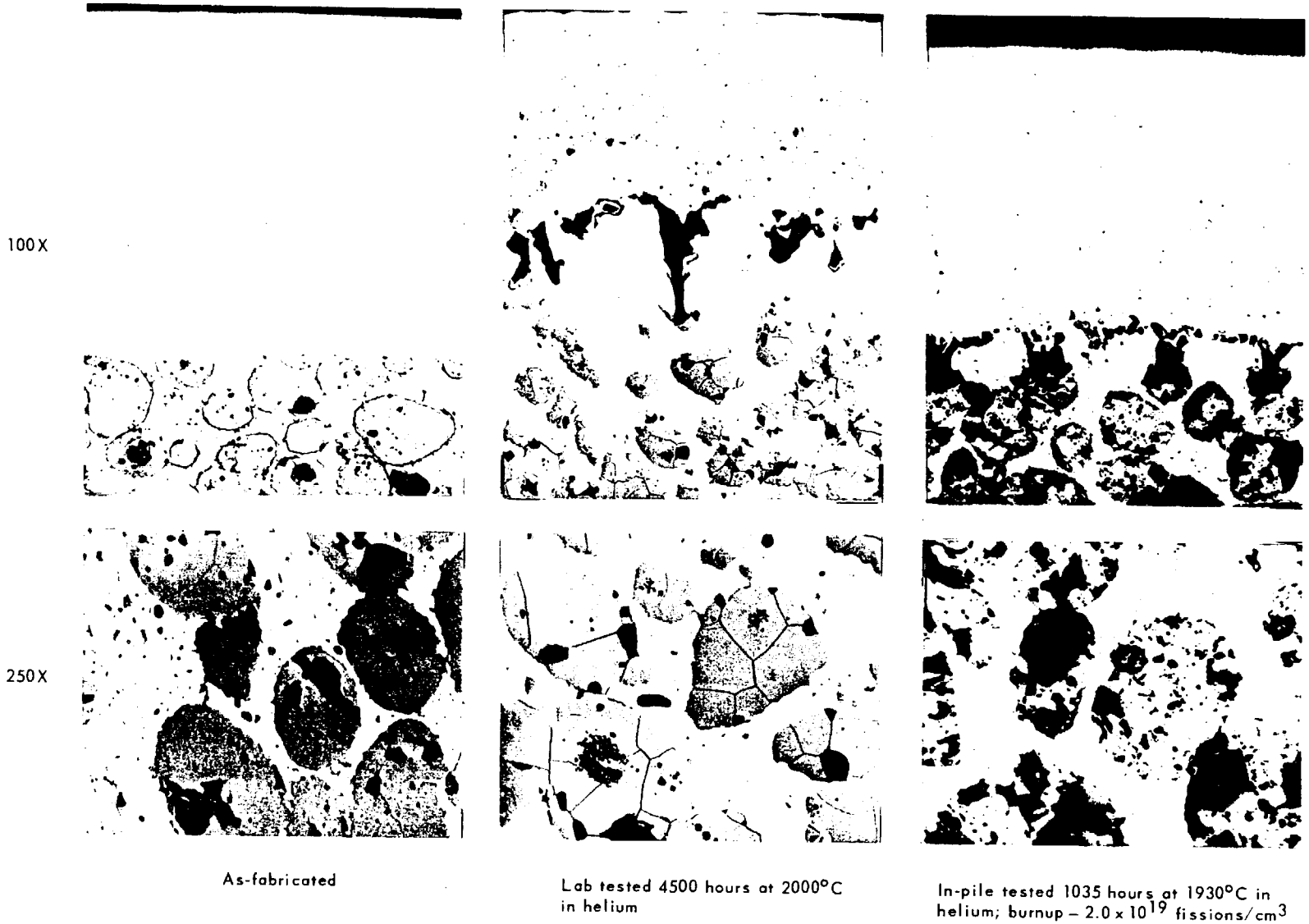

Fig. 3.2.10 – Ta-clad (W + 0.8ThO_2) – (55.4UO_2 + 3.8ThO_2) vol % LTFF-8 specimens *(AS-505)*

CONFIDENTIAL

[redacted]

Ta-clad

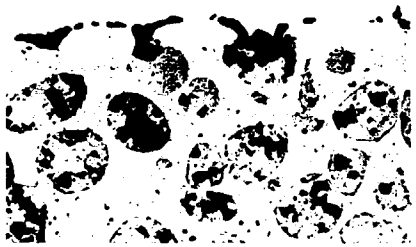

1000 hours at 1930°C in helium

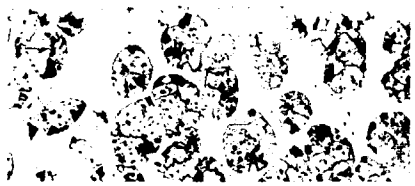

345 hours at 1580°C in He + Ar; burnup – 1.1×10^{20} fissions/cm^3

Ta – 10W-clad

As-fabricated

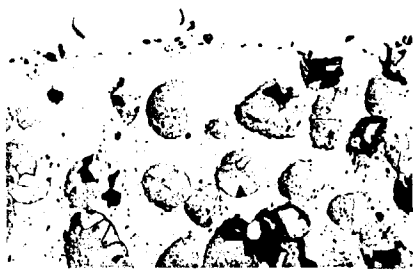

Lab tested 511 hours at 2000°C in helium

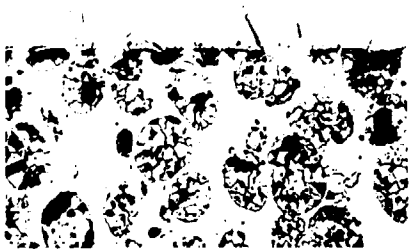

In-pile tested 345 hours at 1650°C in He + Ar; burnup – 1.3×10^{20} fissions/cm^3

Fig. 3.2.11 – Ta and Ta – 10W-clad W – ($54UO_2 + 6ThO_2$) vol % fuel element system GEFP2-7 *(AS-507, 100X)*

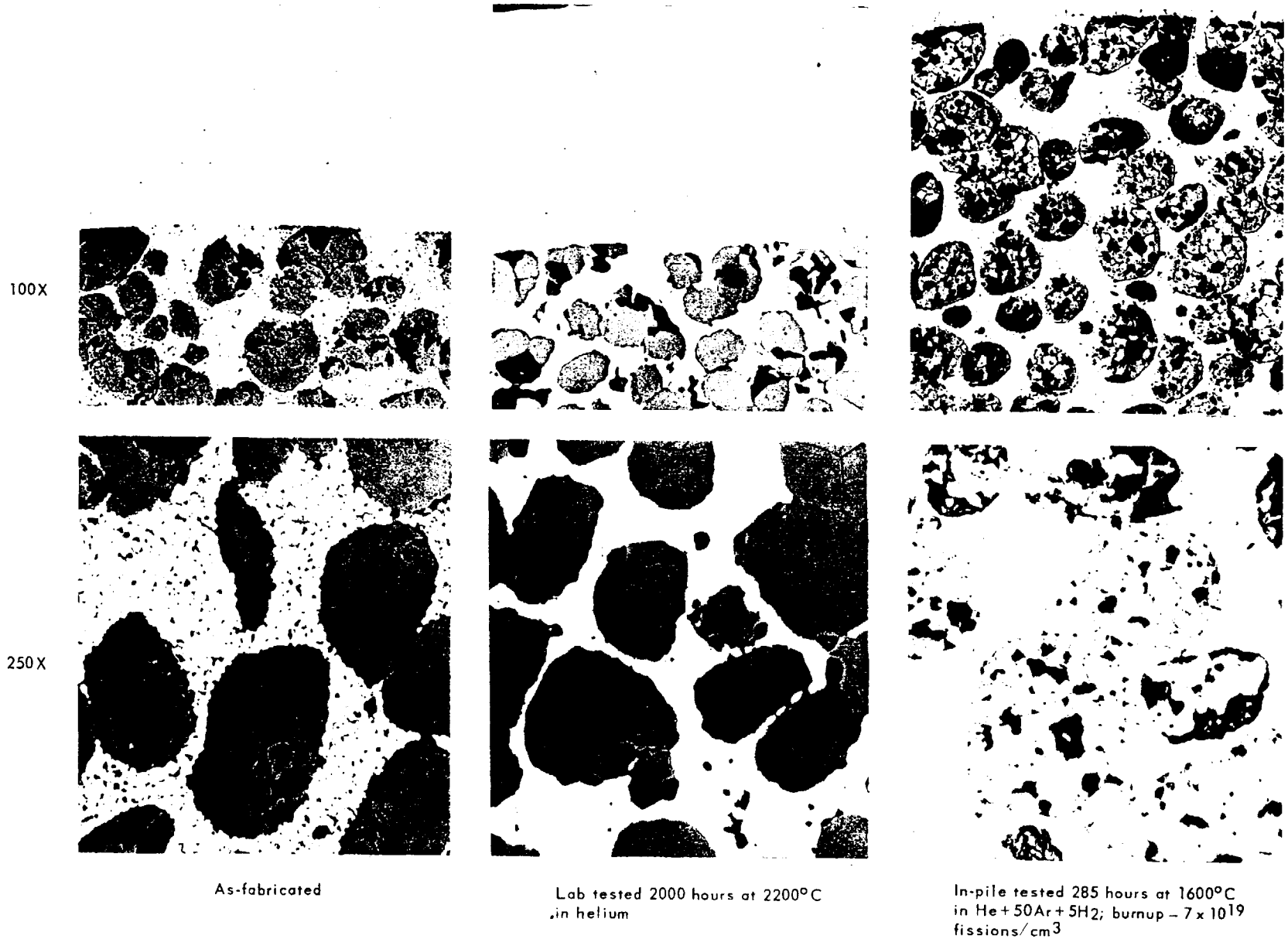

Fig. 3.2.12 – W – 30Re – 30Mo (at. %)-clad W – ($54UO_2 + 6ThO_2$) vol % fuel element system GEFP2-6 *(AS-509)*

CONFIDENTIAL

Fig. 3.2.13 – Summary of results from refractory-metal in-pile test specimens

NOTE: Burnup rates (fissions/cm^3-hr): 1.5 – 4 x 10^{17}, 8 x 10^{16}, 1 – 2 x 10^{16}; cladding materials: Ta, Ta – 10W, W – 30Re – 30Mo; different core porosities; different geometries; and variations in fabrication procedure are represented by the data.

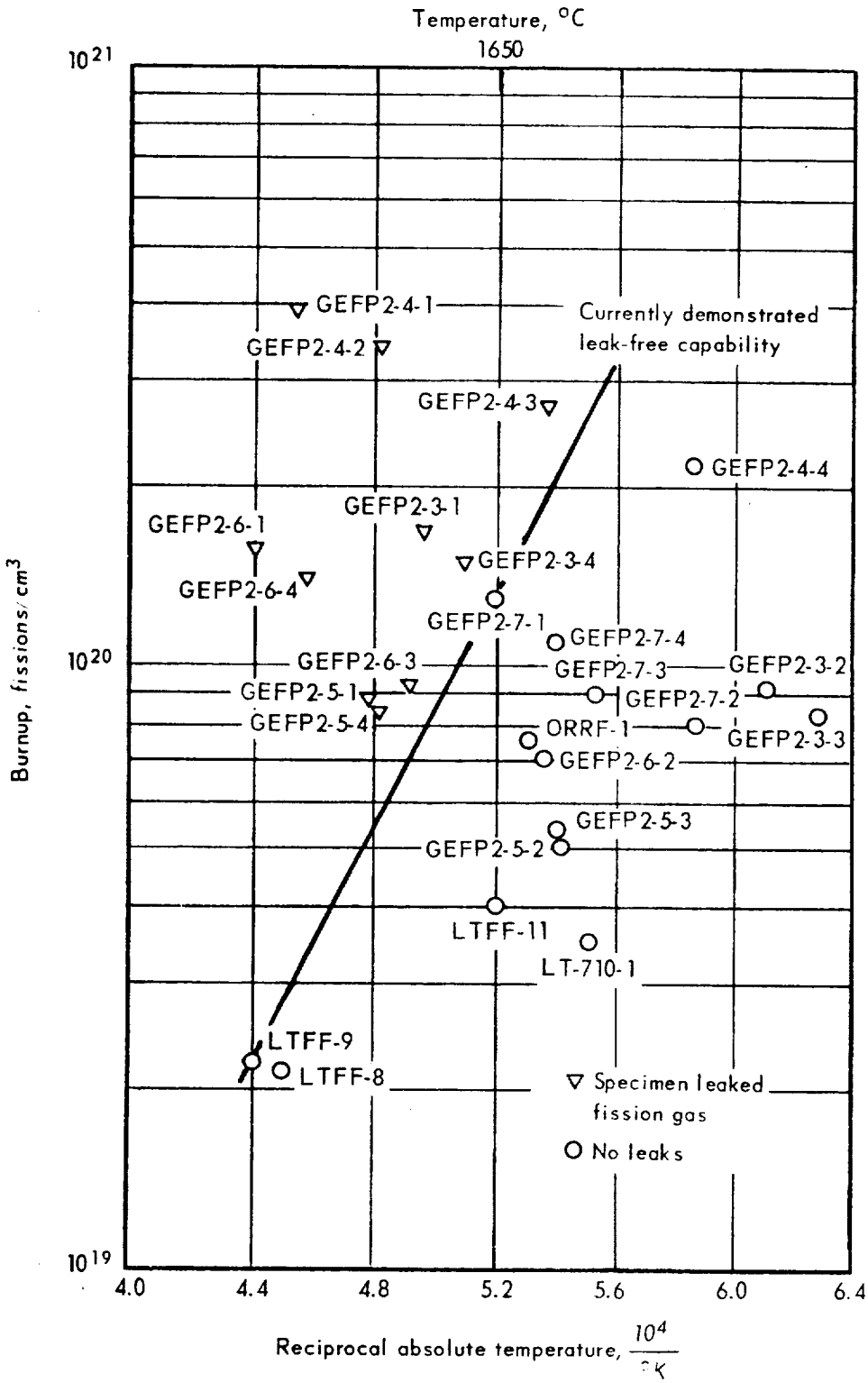

[redacted]

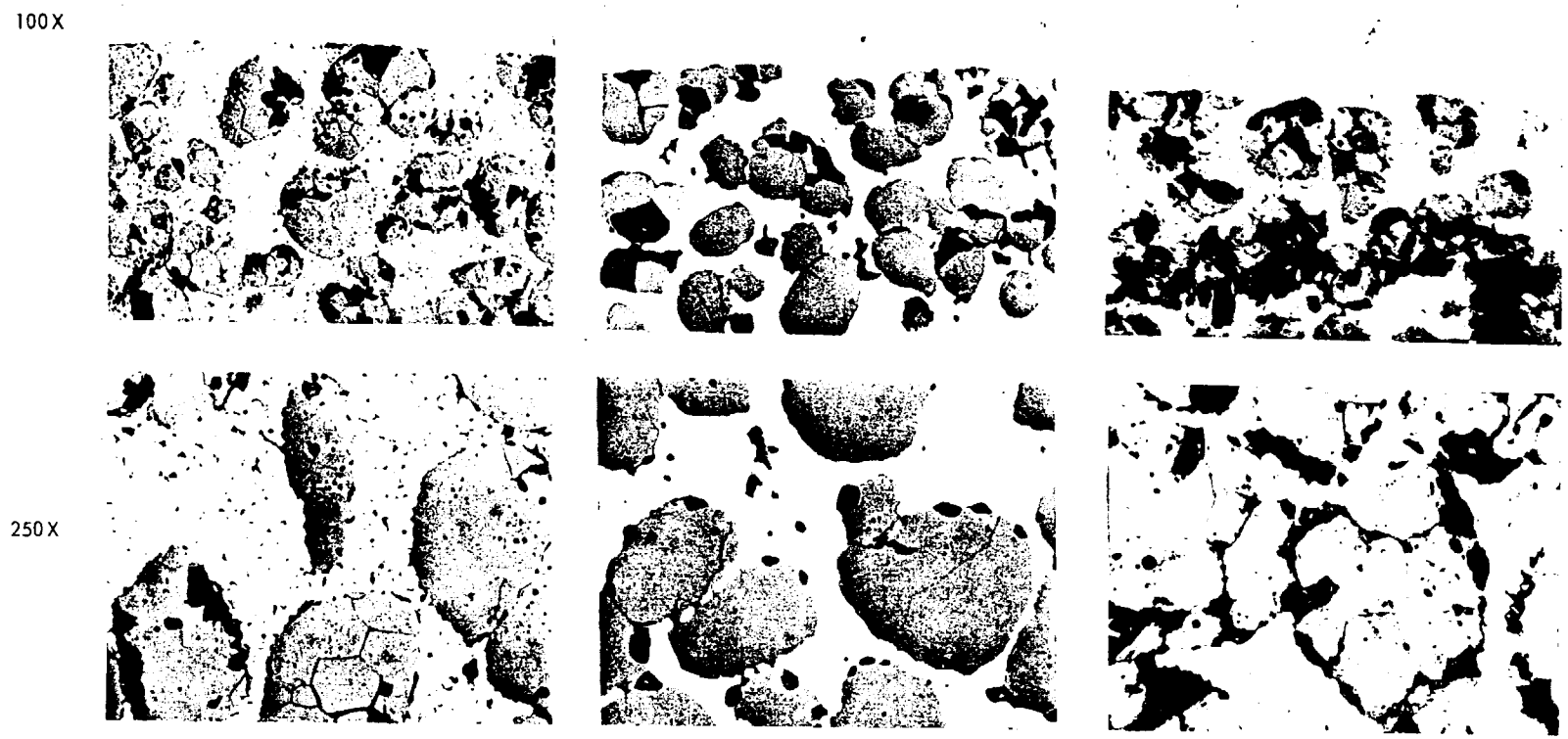

As-fabricated

Lab tested 2000 hours at 2200°C in helium

In-pile tested 1015 hours at 2000°C in helium; burnup – 2.0 x 10^{19} fissions/cm^3

Fig. 3.2.14 – W – 30Re – 30Mo (at. %)-clad W – ($54UO_2 + 6ThO_2$) vol % LTFF-9 specimens *(AS-506)*

CONFIDENTIAL

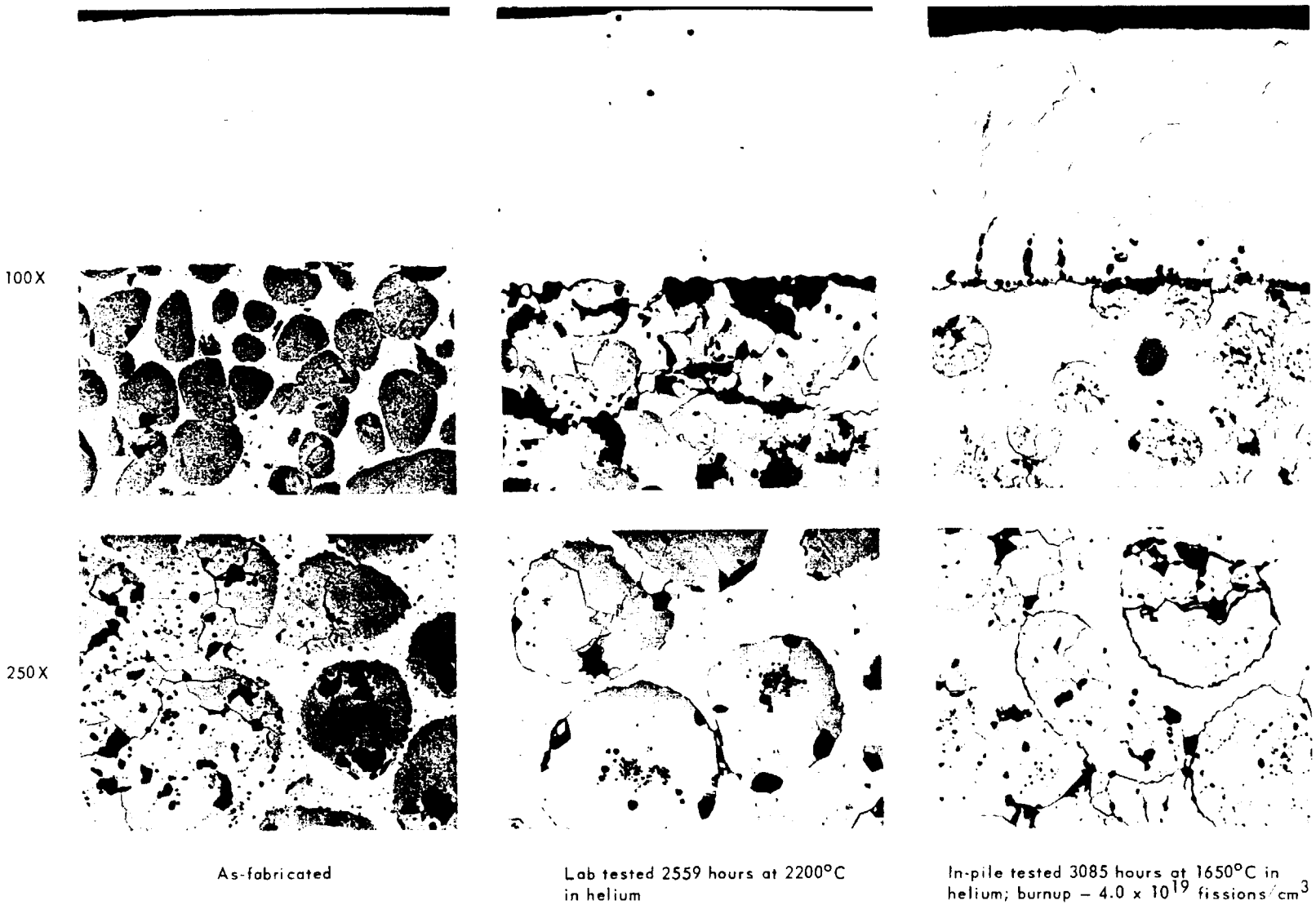

Fig. 3.2.15 – W – 30Re – 30Mo (at. %)-clad W – ($54UO_2 + 6ThO_2$) (vol %) LTFF-11 specimens *(AS-504)*

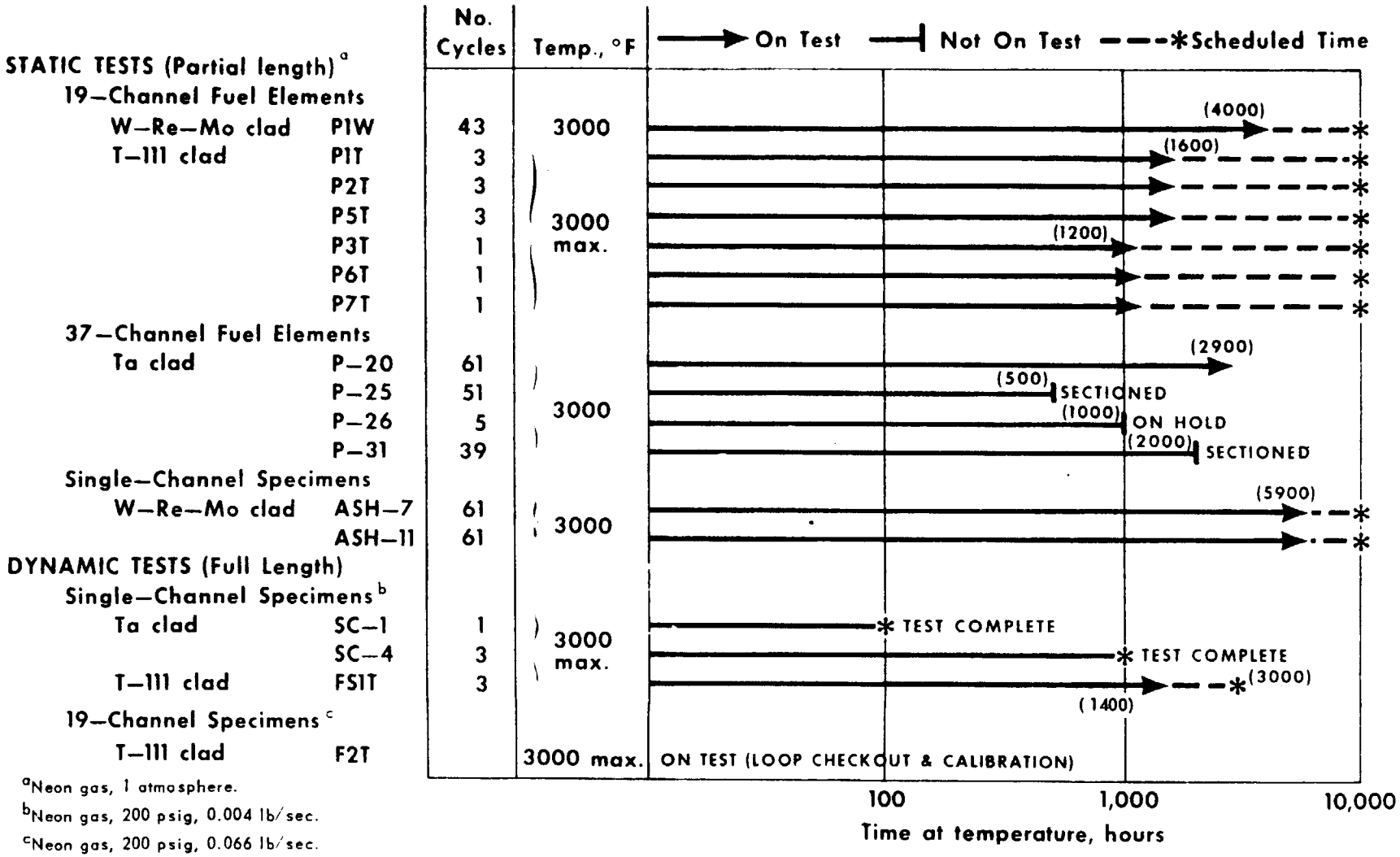

[a]Neon gas, 1 atmosphere.

[b]Neon gas, 200 psig, 0.004 lb/sec.

[c]Neon gas, 200 psig, 0.066 lb/sec.

Fig. 3.2.16 – Current status of non-nuclear static and dynamic test programs

CONFIDENTIAL

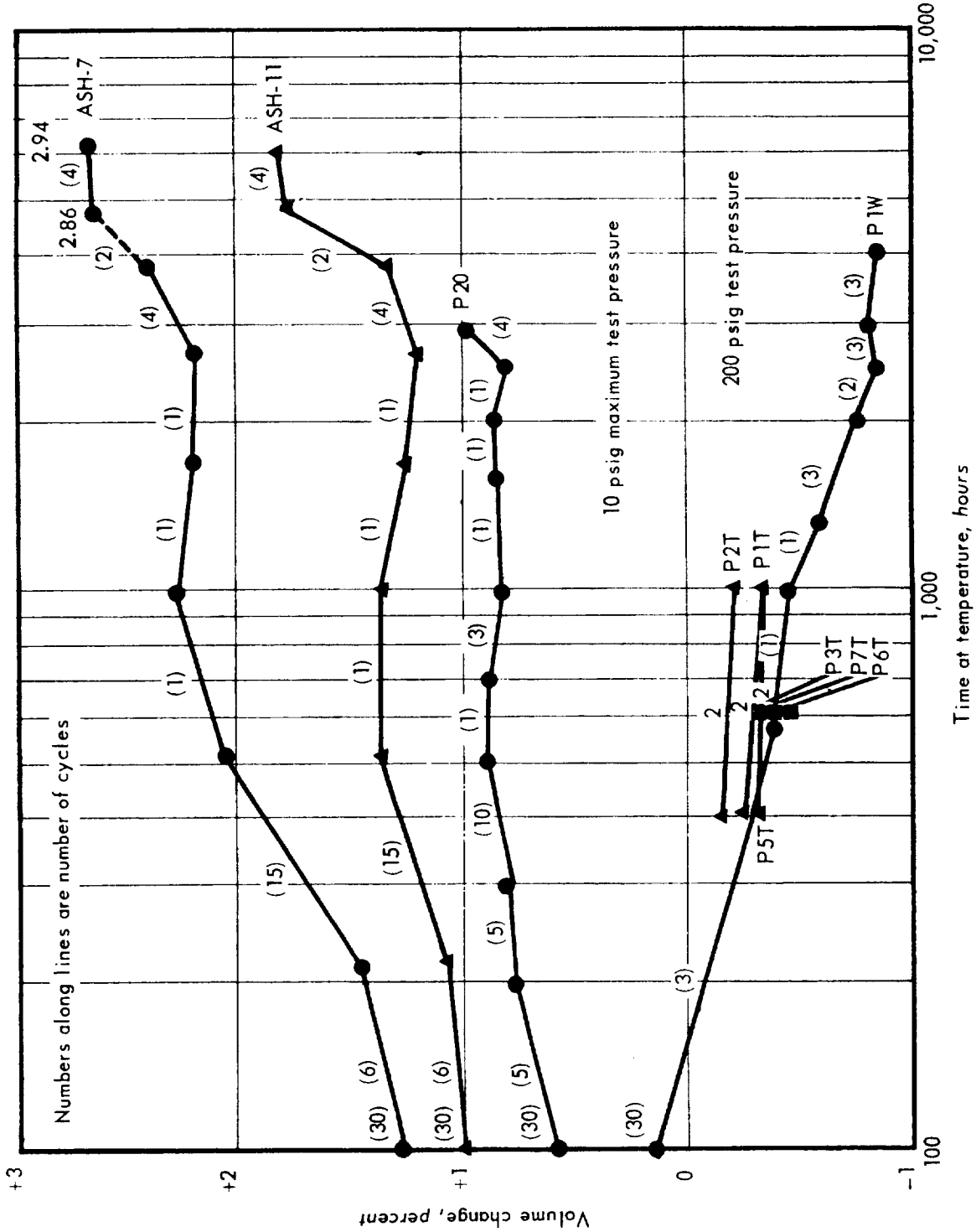

Fig. 3.2.17 – Volume change of 710 test specimens as a function of time at 3000°F in static helium

[redacted]

Fig. 3.2.18 – Photomicrograph of transverse section of specimen A7C-2 after 300 hours at 3000°F showing condition of matrix bond with 306 alloy inner cladding and sigma phase precipitation in cladding grain boundaries *(Neg. 7388, as-polished, 100X)*

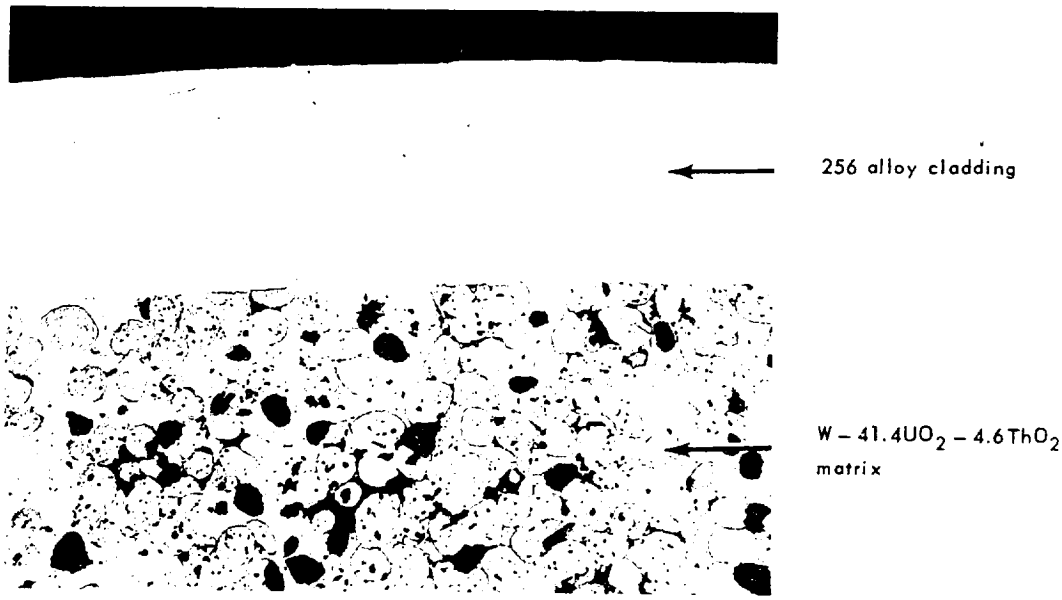

Fig. 3.2.19 – Photomicrograph of transverse section of specimen A7C-2 after 300 hours at 3000°F showing condition of matrix bond with 256 alloy outer cladding *(Neg. 7387, as-polished, 100X)*

CONFIDENTIAL

[redacted]

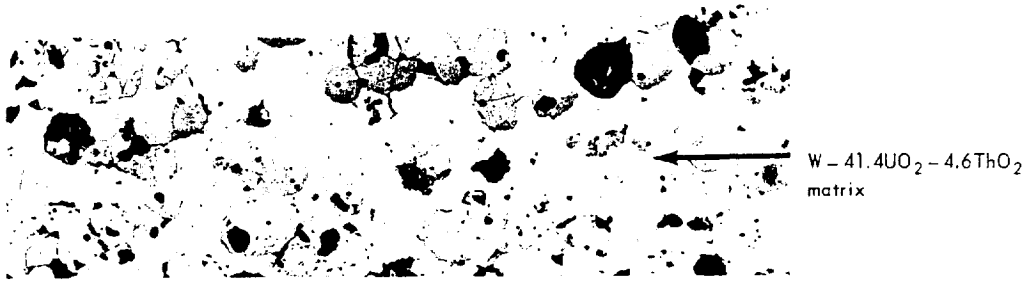

Fig. 3.2.20 – Photomicrograph of transverse section through specimen ASH-6 after 500 hours at 3900°F showing bond of matrix with inner 306 alloy cladding *(Neg. 7389, as-polished, 100X)*

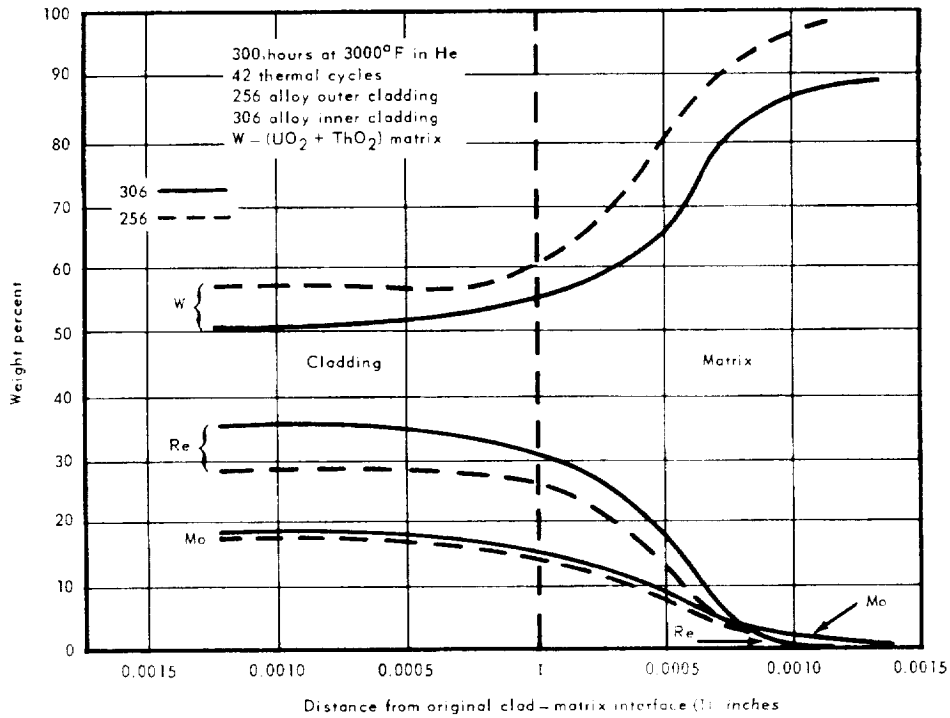

Fig. 3.2.21 – Plot of electron microprobe scan showing cladding – matrix interdiffusion in specimen A7C-2

[redacted]

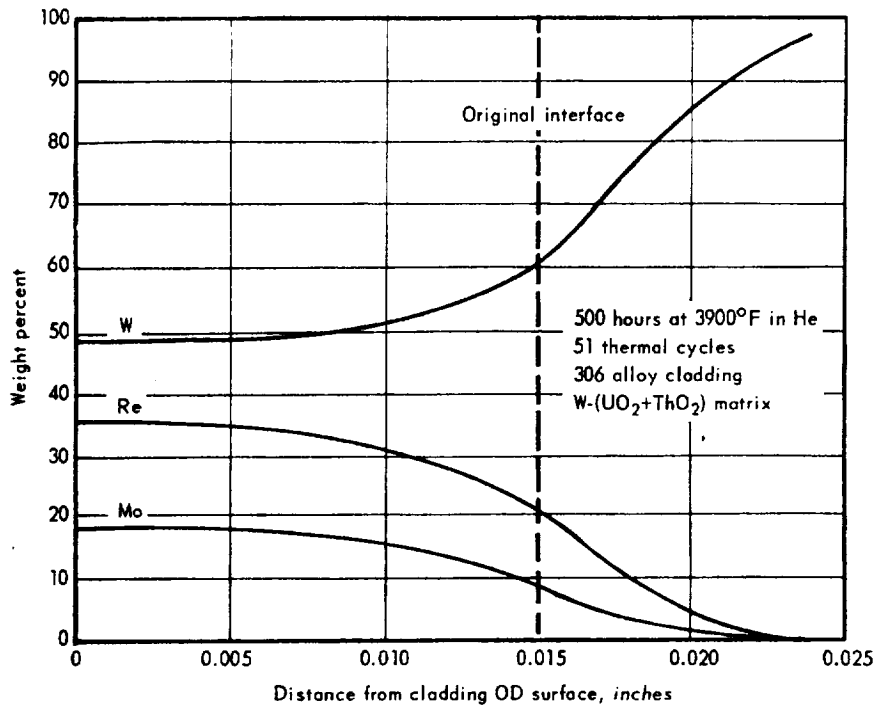

Fig. 3.2.22 – Plot of electron microprobe scan showing cladding – matrix interdiffusion in specimen ASH-6

CONFIDENTIAL

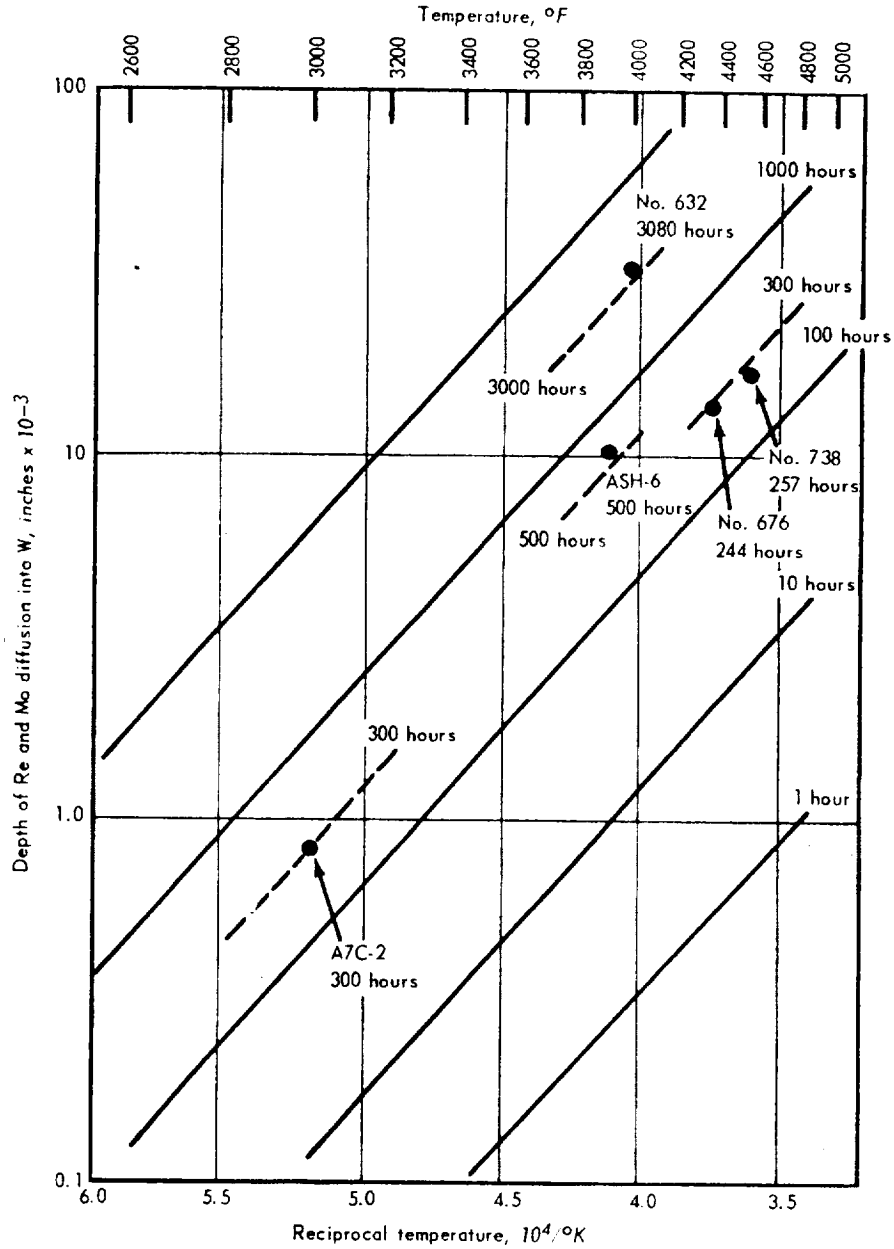

Fig. 3.2.23 – Re and Mo diffusion into W as a function of temperature

[redacted]

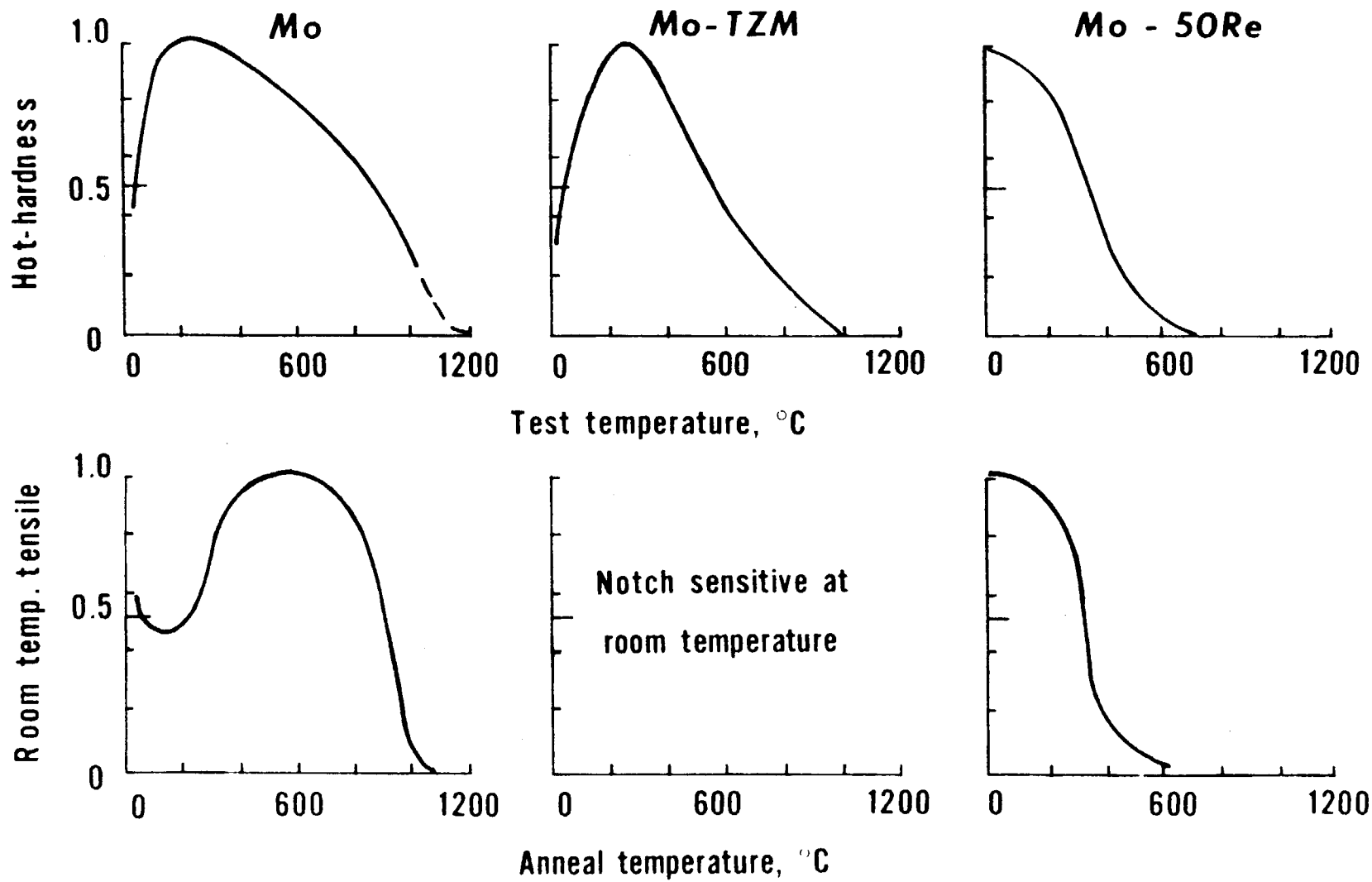

Fig. 3.2.24 – Normalized irradiation induced defect recovery parameter versus temperature

CONFIDENTIAL

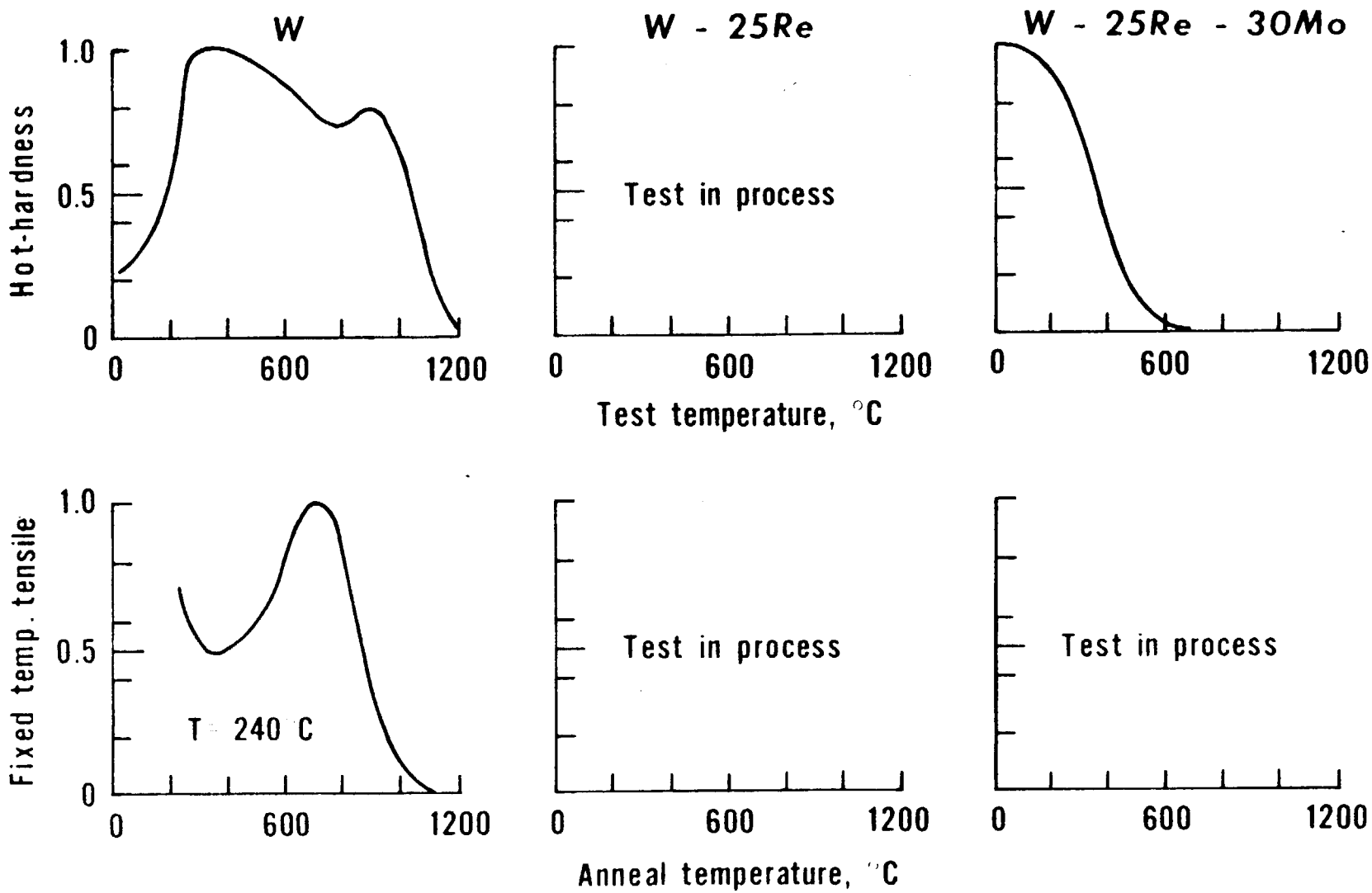

Fig. 3.2.25 – Normalized irradiation induced defect recovery parameter versus temperature

3.3 NON-NUCLEAR MATERIALS SURVEY, SELECTION, AND ASSESSMENT

The term "non-nuclear materials" as used herein refers to all the materials for use in the reactor system other than those which are an integral part of the fuel elements or reflector. Specifically, this section summarizes the evaluation of candidate materials for the pressure vessel, ducting, supporting structures, and the valves and seals as applicable.

3.3.1 Pressure Vessel Materials

MATERIAL REQUIREMENTS

The system design concept, described in section 2, utilizes the outer spherical shell as the primary pressure-containing member for the system. The principal requirements for the pressure shell material are:

1. Sufficient tensile strength at the design temperature (approximately 400°F) to contain the design internal pressure of 1500 psi without any permanent gross distortion
2. Sufficient tensile creep- and short-time strengths to limit any off-design-point permanent gross deformations (e.g., the after-cooling condition) to a maximum of 0.2 percent over the design lifetime
3. Sufficient strain (low-cycle) fatigue strength to accommodate the local plastic deformations associated with stress risers and local thermal stresses
4. Sufficient tensile creep strength to prevent rupture of the vessel for the specified post-crash core meltdown accident condition (see section 5.3.6)
5. Adequate resistance to corrosion by water at the design temperature for the design life
6. Suitable formability and weldability properties to permit fabrication of a vessel in the size and thickness required
7. A nil-ductility temperature which is at least 60°F below the lowest temperature at which the vessel will be pressurized or be subject to shock loading as in the crash condition
8. Either adequate oxidation resistance or compatibility with a suitable cladding material to provide the required oxidation resistance for the external surface of the vessel for the specified post-crash core meltdown accident conditions
9. Retain adequate strength and ductility properties throughout the design life under the combined action of the thermal, fluid, and neutron flux environments.

CANDIDATE PRESSURE VESSEL MATERIALS

The specified post-crash condition of a pressure shell capable of containing 1500 psi at 3000°F for 1000 minutes immediately eliminates all the normal high-temperature oxidation-resistant alloys as potential pressure vessel materials. Accordingly, only the refractory metals and their alloys can be considered. Many of these, e.g., W and some W alloys, must be eliminated since they lack adequate ductility or have too high a nil-ductility temperature. Others (e.g., Ta, Nb, and Mo) were eliminated

on the basis of low creep strength at 3000°F. On the basis of the information available in the literature, the Ta alloys, Ta - 10W, T-111, and T-222 appear to offer the most promise and are selected as the candidate materials for the pressure vessel. Since these alloys are only slightly different in composition, many of their properties (see Appendix A) and procedures for fabrication are quite similar.

Although fabrication and welding procedures are quite well established for thin sheet material,[1] no data are available on fabrication and welding of these materials in the thicknesses required for the pressure shell.

MATERIALS DATA FOR THE PRESSURE VESSEL MATERIALS

Materials Properties and Fabrication Processes

Physical Properties - These alloys all have a density of approximately 0.6 lb/in.^{3}, estimated melting temperatures between 5400°F and 5500°F, and nominal chemical compositions as follows:

Element	Composition, wt %		
	Ta - 10W	T-111	T-222
W	10	7 - 9	10
Hf	-	2 - 2.8	2.5
Ta	Bal.	Bal.	Bal.

Thermal Properties - The effect of temperature on the thermal conductivity of Ta is shown in Figure A1.1. It is assumed that, due to the small alloying additions involved in the three alloys of Ta, they will have essentially the same thermal conductivity as pure Ta. A similar assumption was made (and in some cases substantiated by limited available data) with regard to the enthalpy which is shown in Figure A1.6 The variation of thermal expansion with temperature for T-111 is shown in Figure B1.2; the other two alloys are assumed to have essentially the same expansion properties. A similar assumption was made with respect to the electrical resistivity which is shown in Figure A1.7.

Mechanical Properties - The effect of temperature on the modulus of elasticity of the three alloys (based on Ta - 10W and Ta data) is shown in Figure A1.5. No value of Poisson's ratio was found for these materials other than a room-temperature value of 0.35 for commercially pure Ta. Figures A1.3 and A1.4 give typical ranges of ultimate tensile strength, yield strength, and elongation as functions of temperature. These strength properties are primarily based upon data from thin sheet and rod stock. A substantial development program would be required to establish strength properties for these materials in the thicknesses required for the pressure vessel.

[1] "The Engineering Properties of Tantalum and Tantalum Alloys," BMI, DMIC 189, September 1963.

The same is true of the creep rupture properties of thin sheet stock,[1] shown in Figure 3.3.1 in a Larson-Miller plot. For the specified post-crash accident conditions on the vessel of 3000°F with 1500 psi internal pressure for 1000 minutes and using 80 percent of the 1000-minute creep-rupture strength as the design allowable, the required thickness of the containment vessel is determined from

$$S = \frac{P}{(2 \times 0.8)} \left[(R/t) + 1\right]$$

to be approximately 6 inches

Effects of Irradiation - A limited number of Ta - 10W tensile test specimens have been irradiated to approximately 2×10^{19} nvt (> 1 Mev) under the GE-NMPO High-Temperature Materials Program; however, the tensile testing of these specimens has not yet been accomplished. No other data were found in the literature on irradiation effects on any of the three candidate pressure vessel materials. Limited data do exist[2] for Ta irradiated at -150°F and tested at room temperature. These data indicate significant losses of ductility at 7.8×10^{19} nvt and 1.6×10^{20} nvt (> 1 Mev).

It should be noted that irradiation-induced defects can be eliminated by annealing or by operating at sufficiently high temperature so that defect removal rates are higher than production rates, and that the required temperature for recovery is lower for alloys than for the pure metal (see section 3.2).

Fabrication - As reported elsewhere,[3,4] all three of these alloys appear to have good fabricability. However, this information is based on results for thin sheet and small diameter rod and tubing material. Considerable development work would be required to demonstrate fabricability in the thicknesses required for the pressure vessel. The same situation exists with regard to machining and welding of these alloys. No particular difficulty has been encountered in the small sizes, but considerable development work is required to establish the feasibility of using these materials in the thicknesses required for the pressure vessel.

Mechanical and Thermal Test Data

No directly applicable data on engineering type mechanical and thermal tests were found for any of these alloys in the thicknesses required for the pressure vessel.

---

[2] S. H. Bush, "Irradiation Effects on Structural Materials," HW-81334 - Part 2, October 1964.

[3] DMIC 189, Ibid.

[4] "Pilot Production and Evaluation of Tantalum Alloy Sheet," Westinghouse Astronuclear Laboratories, WANL-PR-M-014, October 1965.

CONFIDENTIAL

Corrosion - Erosion Data

Corrosion - Available data on the corrosion of Ta alloys do not indicate any potential corrosion problem at the design temperature (400°F) in either an air or water environment. However, since Ta is known[5] to oxidize rapidly in air at temperatures above 2552°F and tarnishes in 24 hours at 572°F, this would place limitations on any aftercooling method involving the use of air as the coolant unless an appropriate oxidation-resistant cladding material could be used.

However, the specified post-crash accident condition appears to be the most severe condition from a corrosion standpoint since nickel based oxidation-resistant cladding materials have melting temperatures in the range from 2300° to 2800°F, and would not, therefore, be suitable as a cladding in the usual sense. If this specified condition cannot be relaxed, development effort would be required to establish a suitable means for providing oxidation protection such as iridium-base coating for the pressure vessel during the specified accident condition.

Erosion - No applicable data were found.

State-Of-The-Art Material Performance

Available data on these materials indicate that any of the three candidate materials can potentially satisfy the design-point conditions. Data are lacking for strength properties or for fabrication procedures in the thicknesses required; hence, development work is required both from the fabricability and the strength standpoints. In addition, the specified post-crash accident conditions cannot be met on a state-of-the-art basis from a corrosion standpoint, assuming the existing data to be valid for the thicker material required.

Primary Research Problems

Three major areas of research and development are evident for the pressure vessel material:

1. Development of fabrication procedures for the thicknesses required for the pressure vessel
2. Determination of the mechanical properties attainable in the thicknesses required for the pressure vessel
3. Development of a suitable means for providing oxidation protection for the pressure vessel for the specified post-crash accident condition.

Another area which may require development work is in the determination of irradiation effects on the pressure vessel material. This will depend on the neutron flux at the pressure vessel.

[5] C. A. Hampel, "Rare Metals Handbook," Second Edition, Chapman and Hall, London, 1961.

CONFIDENTIAL

3.3.2 Structural Materials

As used herein, the term "structural materials" includes the materials for the tube sheet, the inner shell, ducting, and all supporting structures for components within the primary pressure vessel.

STRUCTURAL MATERIAL REQUIREMENTS

The specific requirements for these materials include the following:

1. A minimum design life of 2000 hours
2. A design temperature level of 1100°F for the tube sheet and 350°F for all other structures
3. Strength properties sufficient to insure no permanent distortion at limit load conditions and no failures at the ultimate load conditions
4. Retention of adequate strength and ductility properties with integrated neutron fluxes (> 1 Mev) of the order of 2×10^{21} nvt
5. Adequate corrosion resistance for 2000 hours at 350°F in a water environment
6. An endurance limit sufficient to assure no failure due to vibration-induced stresses
7. Low-cycle or strain-fatigue strength properties sufficient to accommodate localized plastic strains due to stress risers or local thermal stresses.

CANDIDATE STRUCTURAL MATERIALS

To minimize development requirements, only well-known alloys were considered as candidate materials for the structures. These include stainless steel types 304, 316, and 347; Inconel 600 and 625 and Incoloy 800; and Hastelloy C and X. These are all materials which are available commercially, for which a relatively large amount of materials property data are available, and for which the fabrication procedures (including welding) have been established. The unirradiated material properties for these materials are summarized in Table A2.1 and Figures A2.1 through A2.7 of Appendix A. In the case of the ultimate tensile strength, yield strength, and elongation at fracture, the data are presented as a range for each of the three basic groups of materials (i.e., the stainless steels, the Inconel/Incoloys, and the Hastelloys) since specific mechanical properties for a given material will, in general, be a function of the heat treatment, amount and type of cold work, specific chemical composition, and the supplying vendor.

On the basis of these data together with data on irradiation effects (discussed in following paragraphs) on the strength and ductility properties for these materials, Inconel 625 was selected as the structural material. The principal reasons for this selection are (1) its high strength at the design temperature (see Figure 3.3.2), (2) its excellent ductility, and (3) it suffers relatively little degradation of the mechanical properties due to irradiation up to integrated neutron fluxes of 1.5×10^{21} nvt (> 1 Mev) and for irradiation temperatures as high as 1364°F (see Figures 3.3.3 and 3.3.4, from Claudson.[6]) The other materials are not

[6] T. T. Claudson, "Effects of Neutron Irradiation Upon the Mechanical Properties of Inconel 625," Battelle-Northwest Labs, BNWL-153, October 1965.

CONFIDENTIAL

preferred because: (1) The austenitic stainless steels are known to be susceptible to chloride stress corrosion at temperatures above 250°F with relatively small concentrations of chlorides (a few ppm) and suffer substantial losses in ductility due to irradiation at levels of the order of 10^{21} nvt and greater;[7] (2) the Hastelloys suffer severe losses of ductility at irradiation levels as low as 10^{20} when irradiated at 1200°F and, in general, much less is known about the effects of irradiation on these alloys;[7] and (3) substantially less information was found in the literature on irradiation effects on Inconel 600 and Incoloy 800 than on the Inconel 625.

MATERIALS DATA FOR INCONEL 625

Material Properties and Fabrication Processes

Physical Properties - Inconel 625 has a density of 0.305 lb/in.^{3} and a melting range of 2350° to 2460°F. Its chemical composition is:

Element	Percent
Chromium	20.0 - 23.0
Iron	5.0 max.
Niobium + Tantalum	3.15 - 4.15
Manganese	0.50 max.
Silicon	0.50 max.
Carbon	0.10 max.
Sulfur	0.015 max.
Aluminum	0.40 max.
Titanium	0.40 max.
Molybdenum	8.0 - 10.0
Cobalt	1.00 max.
Nickel	Remainder

Thermal Properties - The effect of temperature on the thermal conductivity and specific heat of Inconel 625 is shown in Figures A2.1 and A2.7, respectively. The temperature dependence of the mean coefficient of thermal expansion is shown in Figure A2.2.

Mechanical Properties - The effect of temperature on the modulus of elasticity is shown in Figure A2.5. The value of Poisson's ratio for Inconel 625 at room temperature is approximately 0.31 and increases with increasing temperature to a value of approximately 0.33 at 1400°F. Figure 3.3.2 gives a typical set of short-time tensile and creep properties for Inconel 625. As previously discussed, these can only be considered as "a typical set" of mechanical properties for this material since strength properties are usually a strong function of the processing history of the material.

Effects of Irradiation - Claudson[6] gives a rather comprehensive evaluation of the effects of irradiation on the mechanical properties of Inconel 625. The data presented by Claudson cover the test temperature

[7] Bush, op. cit.

range from room temperature to 1200°F, an irradiation temperature range from reactor ambient (∿ 120°F) to ∿ 1360°F, and an integrated neutron dose from 4×10^{19} to 1.46×10^{21} nvt (> 1 Mev). Claudson's data as plotted in Figure 3.3.3 show the effect of neutron exposure (at 540°F) on the tensile strength properties of Inconel 625 at room temperature and 1200°F. From this, it is evident that, for the temperatures and exposures covered, the radiation effects are quite small. Figure 3.3.4 shows the effect of irradiation temperature on the room-temperature tensile properties. Claudson notes that the control specimens were exposed to the same thermal history as the irradiated specimens to eliminate thermal aging effects from the results. As Claudson points out, the thermal aging effects are of the same order of magnitude as the irradiation effects.

Fabrication[8] - Inconel 625 can be both hot- and cold-formed by standard processes; due to its higher strength, however, somewhat higher forces are required. Hot working should be done in the temperature range from 1850° to 2150°F.

Inconel 625 may be inert gas welded with either a W electrode or a consumable electrode of Inconel Filler Metal 625. Excellent welds have been made in 0.5-inch-thick annealed plate.[8] The tensile strength of the weld is about 80 percent of that of the parent metal while the yield strength is slightly greater than that of the parent metal.

Mechanical and Thermal Test Data

No directly applicable data on engineering type mechanical and thermal tests were found for the Inconel 625 Alloy.

Corrosion - Erosion Data[8]

Corrosion - Inconel 625 exhibits excellent resistance to oxidation at temperatures up to 1800°F; a weight change of -0.081 percent after a 1000-hour cyclic test to 1800°F is reported.[8] Also reported is an essentially zero corrosion rate in fresh water. Data on attack by various acid and salt solutions are also given. Of particular interest is a stress-corrosion cracking test of a bar specimen exposed to a boiling 42 percent Mg-Cl solution for 90 days; no evidence of cracking was found.

Erosion - No applicable data were found.

State-Of-The-Art Material Performance

The available data indicate that the Inconel 625 material should be satisfactory for the structural components within the main pressure vessel. This alloy has excellent strength and ductility at temperatures as high as 1200°F and usable strength as high as about 1500°F for 1000 hours. Claudson's data indicate that it retains adequate strength and ductility to satisfy the strength requirements set forth in section 3.3.2. The available corrosion data do not indicate any potential corrosion problems with Inconel 625 unless an off-design condition should require the introduction of air at structural temperatures above 1800°F.

---

[8] "Preliminary Data of Inconel Alloy 625," Huntington Alloy Products Div., Technical Bulletin S-16.

[redacted]

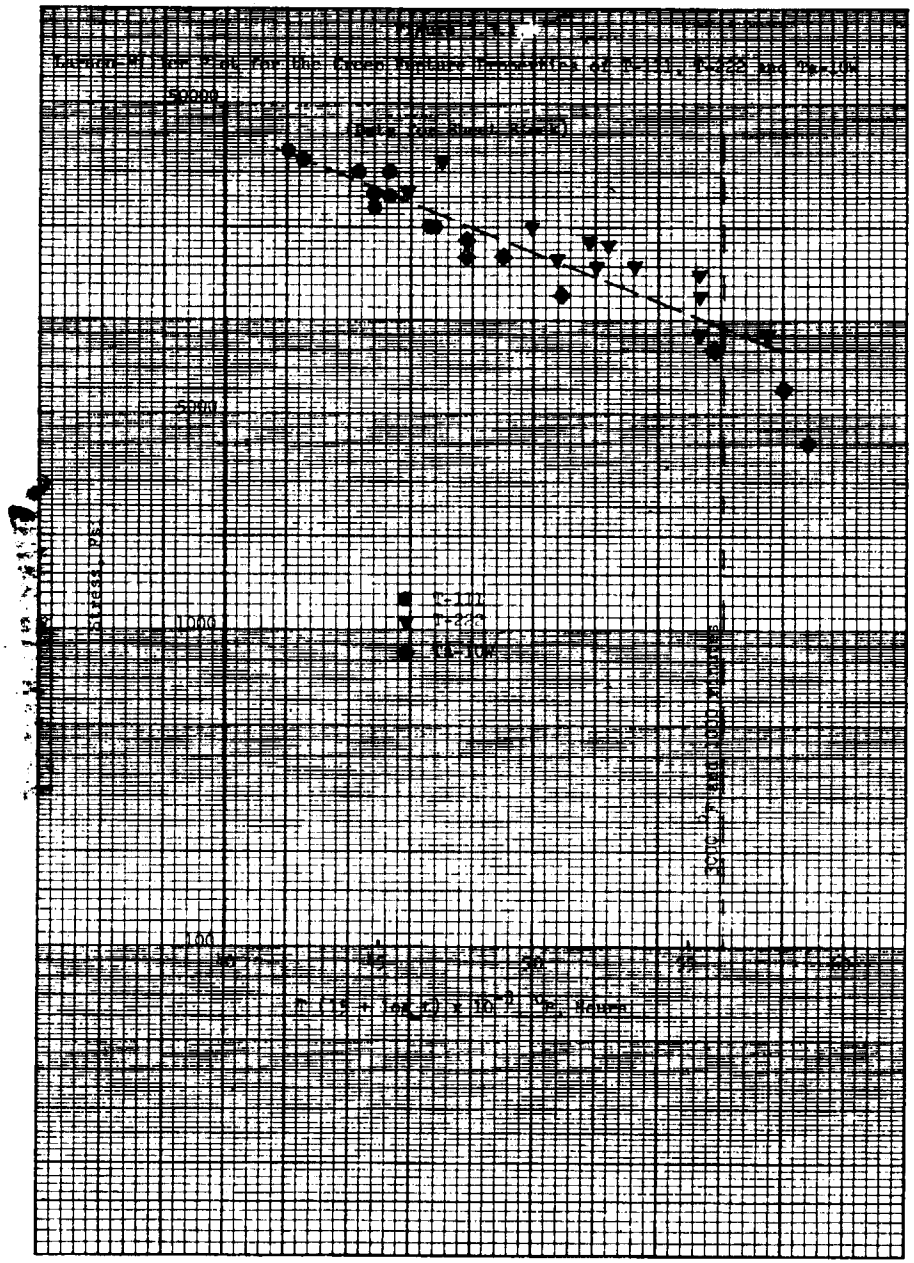

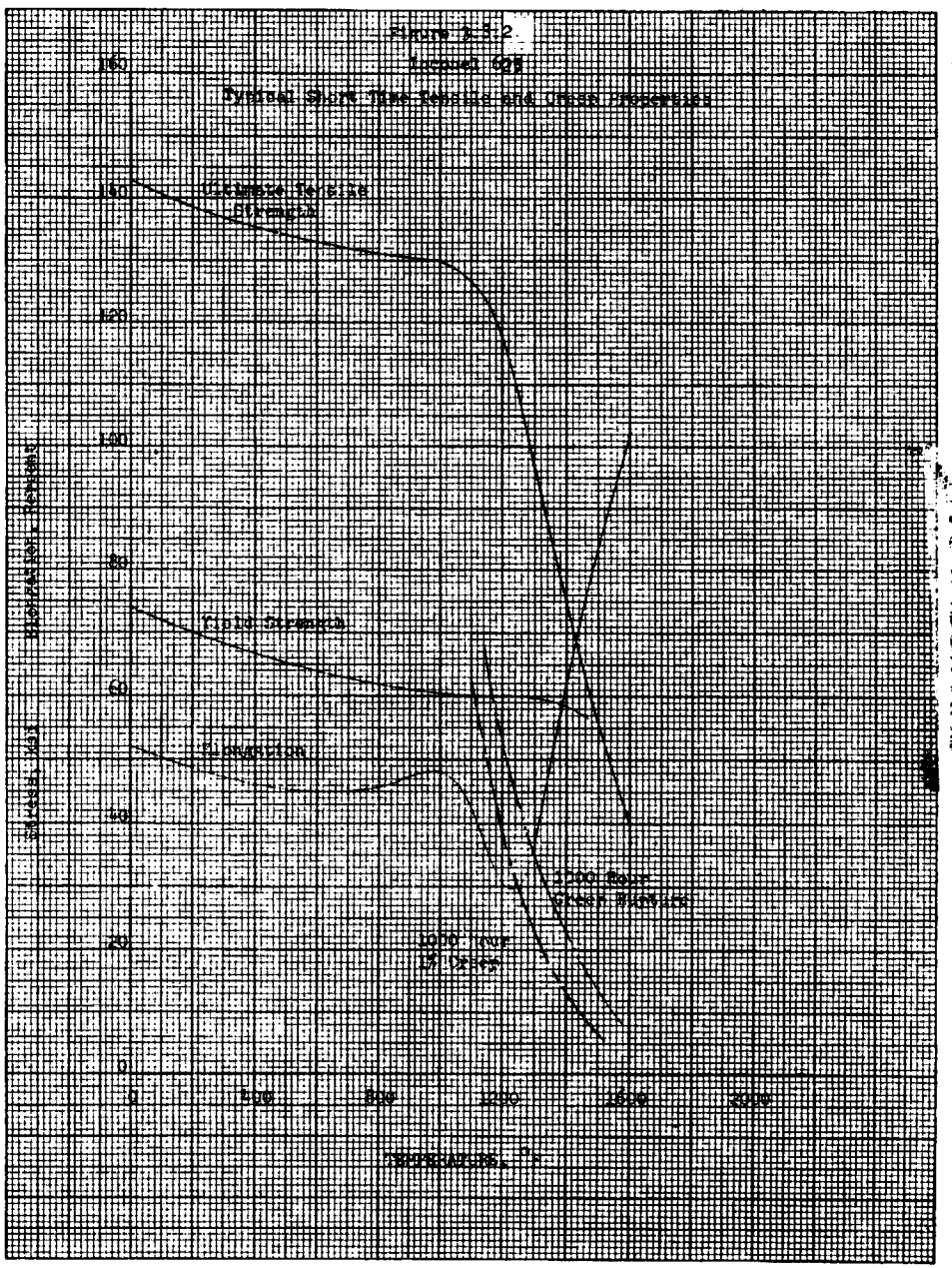

PROPRIETARY

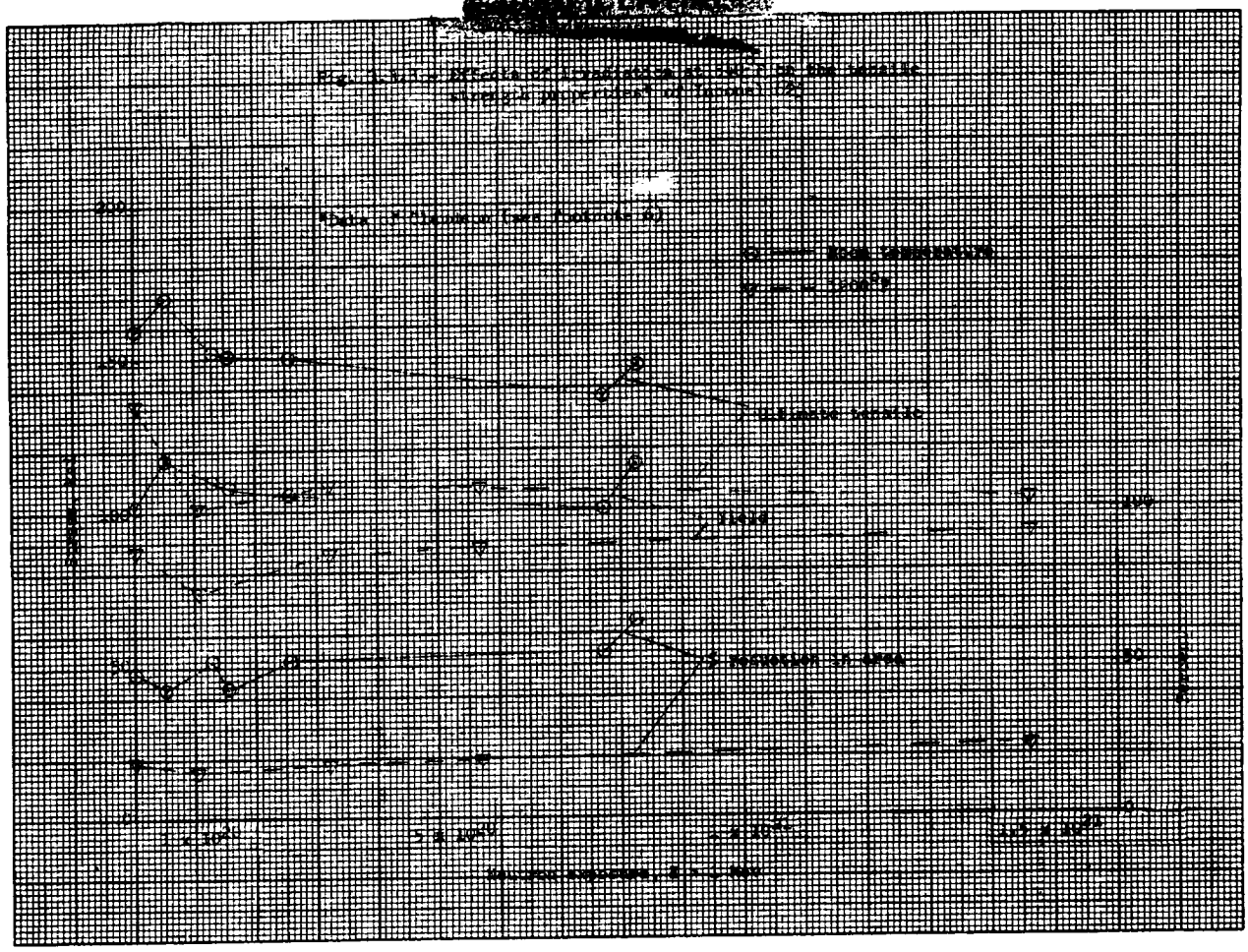
Ultimate tensile
Yield
% reduction in area

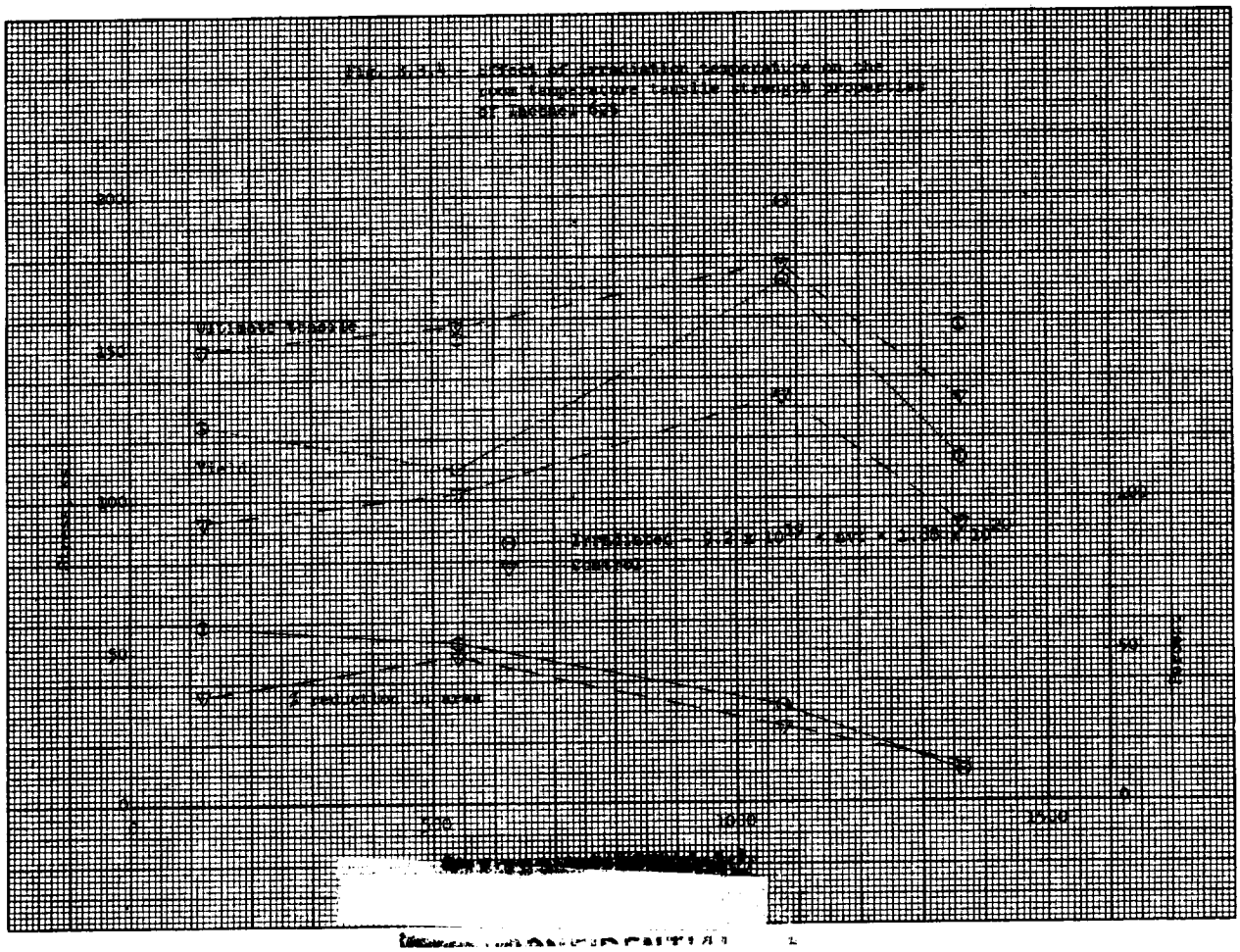
Ultimate tensile
Yield
% reduction in area
500
1000
1500

The endurance limit of about 90,000 psi at 10^8 cycles should be adequate for vibration-induced stresses.

Although no low-cycle nor strain-fatigue data were found, the combination of high ductility and high strength exhibited by this material (even after irradiation) would lead one to expect adequate strain fatigue strength. This is based on the relationships proposed by Coffin, Manson and others, together with the extensive strain fatigue data available for this general class of materials, i.e., the Inconels and the austenitic stainless steels.

Primary Research Problems

Although Inconel 625 is currently available commercially in many standard sizes of sheet, bar, tubing, and plate, the 4.00 inch thickness required for the tube sheet supporting the fuel elements at the inlet end is appreciably greater than is currently available commercially. Accordingly, a development program would be required to demonstrate that such a plate can be successfully manufactured with strength and ductility properties approaching those of the rod and sheet material typified by the data of Figure 3.3.2.

3.4 ASSESSMENT OF COOLANT IMPURITY EFFECTS

A major effort underway in the 710 Reactor Program is the design, construction, and operation of dynamic facilities for testing both single- and multi-channel fuel elements with inert gas coolant. One single- and one multi-channel test loop are now in operation; a schematic of these loops is shown in Figure 3.4.1. Design parameters for the loops are given in Tables 3.4.1 and 3.4.2. Major components of the loops are (1) test sections, (2) gas purification system, (3) gas pre-heater, (4) gas supply system, (5) gas recovery systems, and (6) gas circulator (gas-bearing circulator in the multi-channel loop and diaphragm pumps in the single-channel loop). These loops are interconnected at the vacuum system and at the gas supply and recovery systems. An additional test section is being installed in the multi-channel fuel element test loop; a schematic of this installation is shown in Figure 3.4.2. Figure 3.4.3 is a photograph of the multi-channel fuel element test loop; the second test section will be installed immediately to the right of the test section shown. Another test loop having two additional multi-channel fuel element test sections is in the design and fabrication stage and will be installed in a new test facility. A schematic of this loop is shown in Figure 3.4.4.

Experience gained in the design, construction, and operation of the dynamic test facilities indicates that the major gas impurity problems to be encountered in a circulating gas loop arise from seal leakage and out-gassing of components. These potential problems were recognized in the design of the circulating system, and a concentrated effort was made to minimize them. Cleaning and out-gassing procedures and specifications were established for all loop components and were rigidly adhered to in the fabrication and assembly. Joints were welded whenever possible; however, when separable joints were necessary, Conoseal* tube and pipe

*Aeroquip Corp., Indianapolis, Indiana.

joints were used. Flanges on the test sections were also machined to the Conoseal geometry. These seals have proved to be exceptionally leak-tight and stable under both vacuum and pressure conditions.

Valves are another potential source of impurities or leaks in the system. All valves used in the primary gas system are of the bellows-sealed type and have proved to be adequate.

The mechanical and thermodynamic performance of the gas-bearing circulator met performance specifications; however, the rate at which the circulator released contaminants to the loop gas did not,[9] and it was necessary to install a separate gas purification loop to the circulator motor cavity to maintain an impurity level of 5 ppm total impurity as specified for the multi-channel fuel element test loop.

Operation of the dynamic test loops has been exceptionally stable. A 3000-hour test has been completed in the single-channel test loop with an 80-percent utilization factor, and a 1000-hour test is nearing completion in the multi-channel test loop. Operating parameters for the multi-channel, full-length fuel element dynamic test loop are shown in Table 3.4.3. Gaseous impurities in the loops during operation have remained at or below the detection limits of the gas chromatograph.

The gas chromatograph is an integral part of the loops. It was designed to use helium as a carrier gas to analyze helium, neon, and hydrogen, or a mixture of these three gases. Krypton can also be determined. Limits of detection for trace impurities in neon or helium are given in Table 3.4.4.

In summary, the dynamic gas test experience has shown that by careful design of the closed gas circuit and by monitoring the impurity content of the circulating gas, sources of difficulty can be identified and corrected to the extent that impurity effects are of negligible concern.

---

[9] H. E. Wagner and R. E. Tallman, "Evaluation of a Mechanical Technology, Inc. Gas-Bearing Circulator," GE-NMPO, GEMP-479,

CONFIDENTIAL

TABLE 3.4.1

SINGLE-CHANNEL FUEL ELEMENT DYNAMIC LOOP

Design pressure, test section, psig	1100
Design pressure, gas supply and recovery systems, psig	1650
Maximum flow rate at design conditions (neon), ft^3/min	0.36 (0.01944 lb/sec)
Test section inlet gas temperature, °F	650
Test element outlet gas temperature, °F	3500
Heat exchanger gas outlet temperature, °F	120
Preheater design temperature, °F	1000
Test section pressure vessel design temperature, °F	300
Purifier maximum flow rate, ft^3/hr	10
Recovery system volume, $in.^3$	6000

TABLE 3.4.2

MULTI-CHANNEL FUEL ELEMENT DYNAMIC LOOP DESIGN PARAMETERS

Test section design pressure, psig	1100
Gas bearing circulator design pressure, psia	1000
Maximum flow rate at loop operating conditions (neon), ft^3/min	14.8 (0.426 lb/sec)
Test section inlet gas temperature, °F	650
Test section outlet gas temperature, °F	3500
Gas bearing circulator inlet gas temperature (max), °F	400

[redacted]

TABLE 3.4.3

OPERATING PARAMETERS OF THE MULTI-CHANNEL FULL-LENGTH FUEL ELEMENT DYNAMIC TEST LOOP

Test atmosphere	Neon
Operating pressure, psig	200
Flow rate, lb/sec	0.066
Maximum specimen temperature, °F	3000
Inlet gas temperature, °F	465
Outlet gas temperature, °F	2200

TABLE 3.4.4

LIMITS OF DETECTION FOR GAS CHROMATOGRAPH

	Limit of Detection, ppb	
Impurity	Ionization Detector[a]	Thermal Conductivity Detector[b]
H_2[c]	300	800
O_2[d]	100	50
Ar	300	50
N_2	300	50
Kr	200	50
CH_4	100	50
CO	500	200
CO_2	50	50

[a]Flow rate: 100 ml/min.
[b]Flow rate: 18 ml/min.
[c]Can be determined in He only.
[d]O_2 and Ar are not separated during the analysis. Relative amounts present can be obtained by comparison of the response of both detectors.

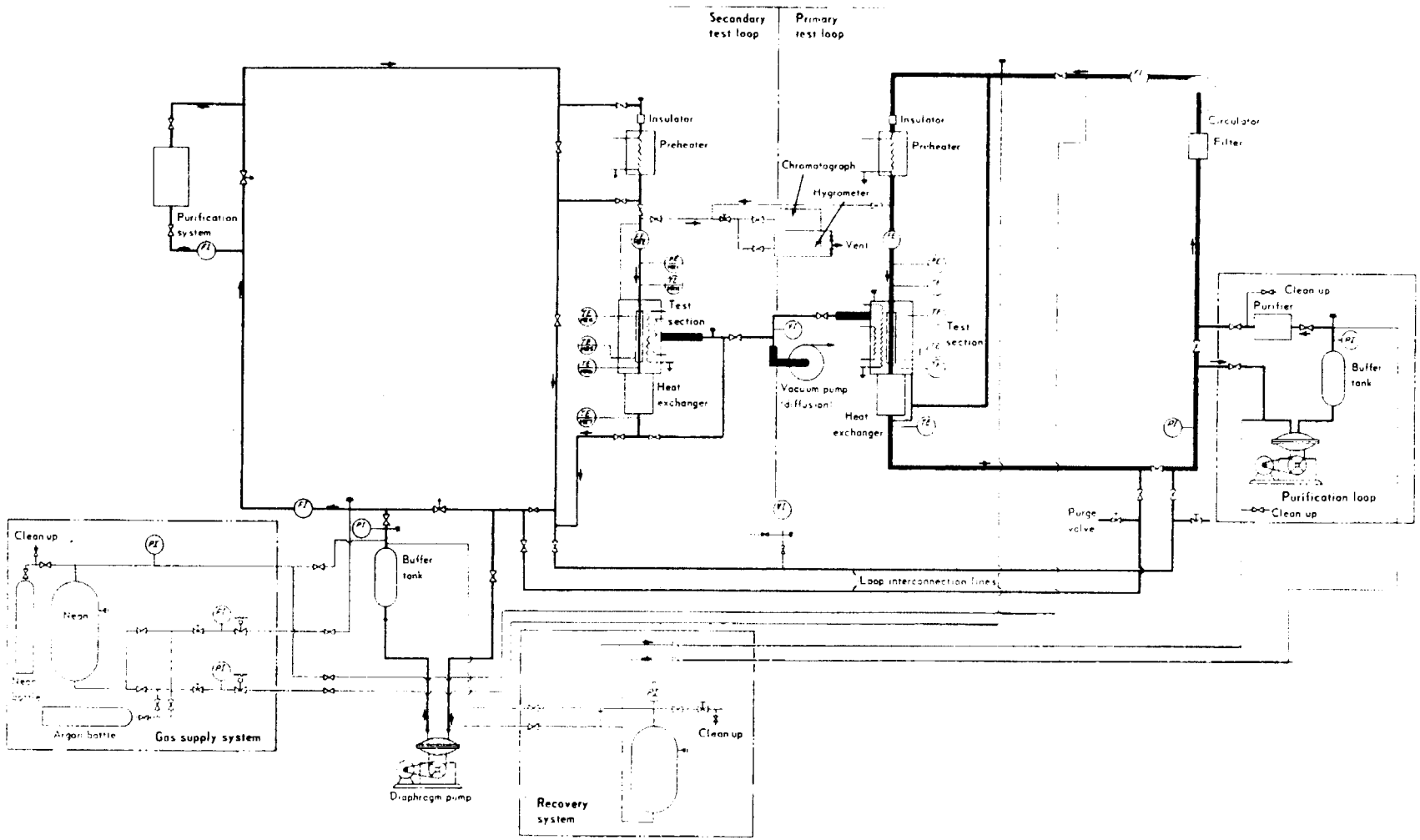

Fig. 3.4.1 – Schematic flow diagram of the fuel element dynamic test loop *(Dwg. 692E816)*

Fig. 3.4.2 – Schematic diagram of primary loop, two-test-section configuration *(Dwg. 221R502)*

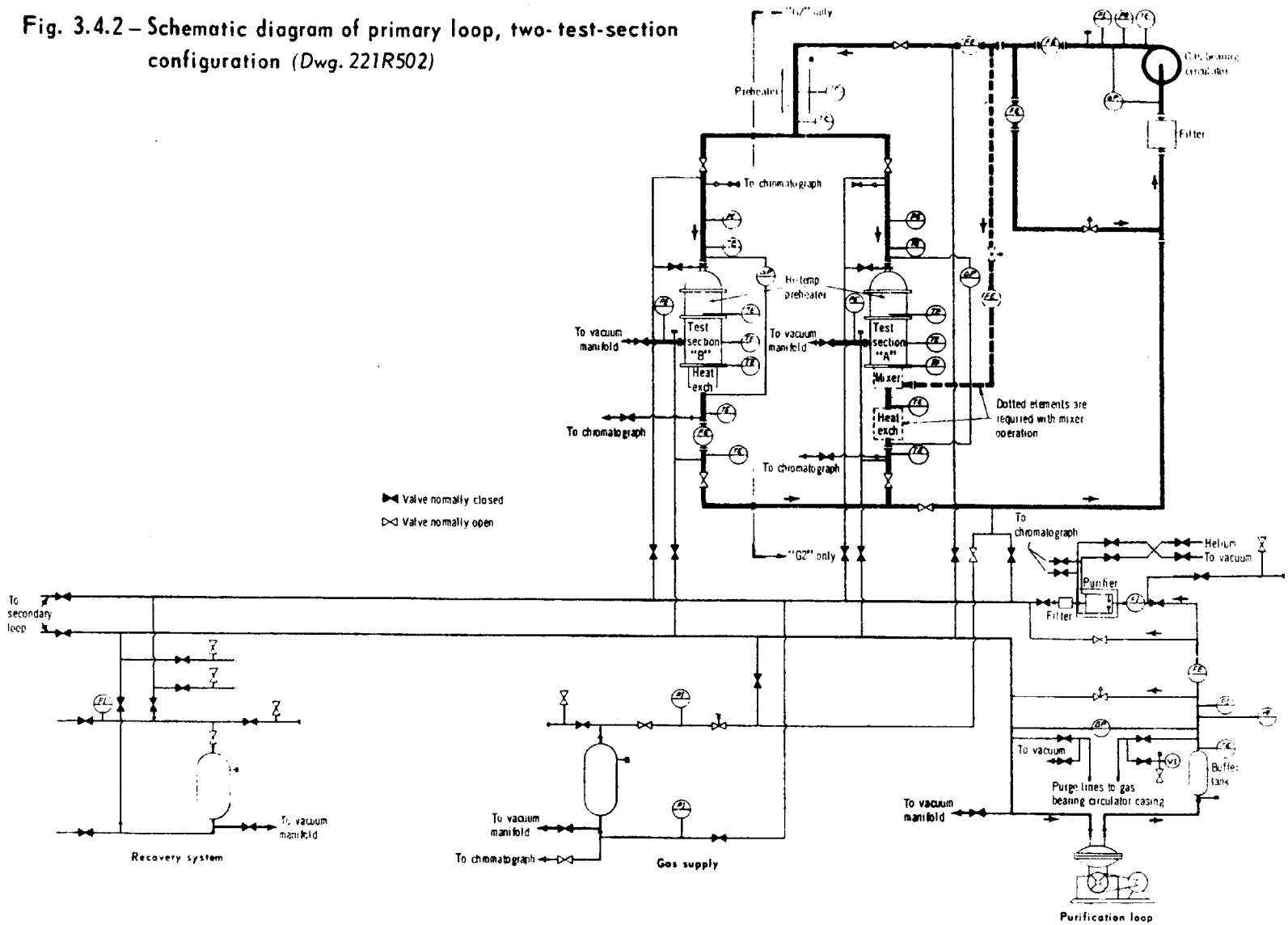

CONFIDENTIAL

CONFIDENTIAL

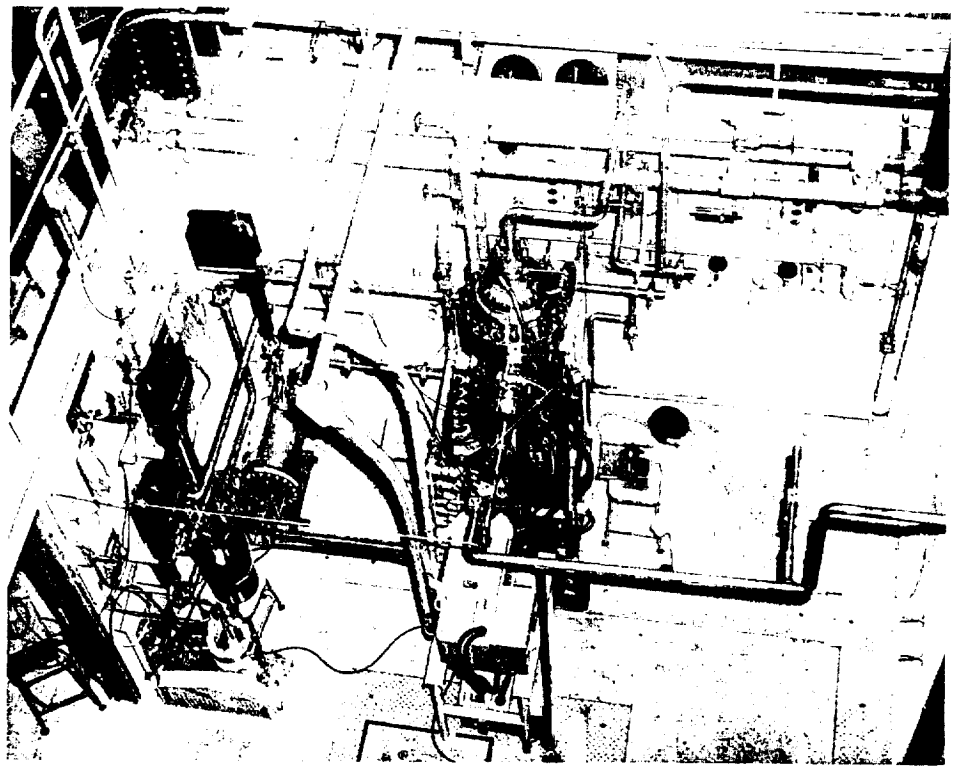

Fig. 3.4.3. – Multi-channel fuel element dynamic loop No. 1 behind test area barrier *(Neg. P66-8-15A)*

[redacted]

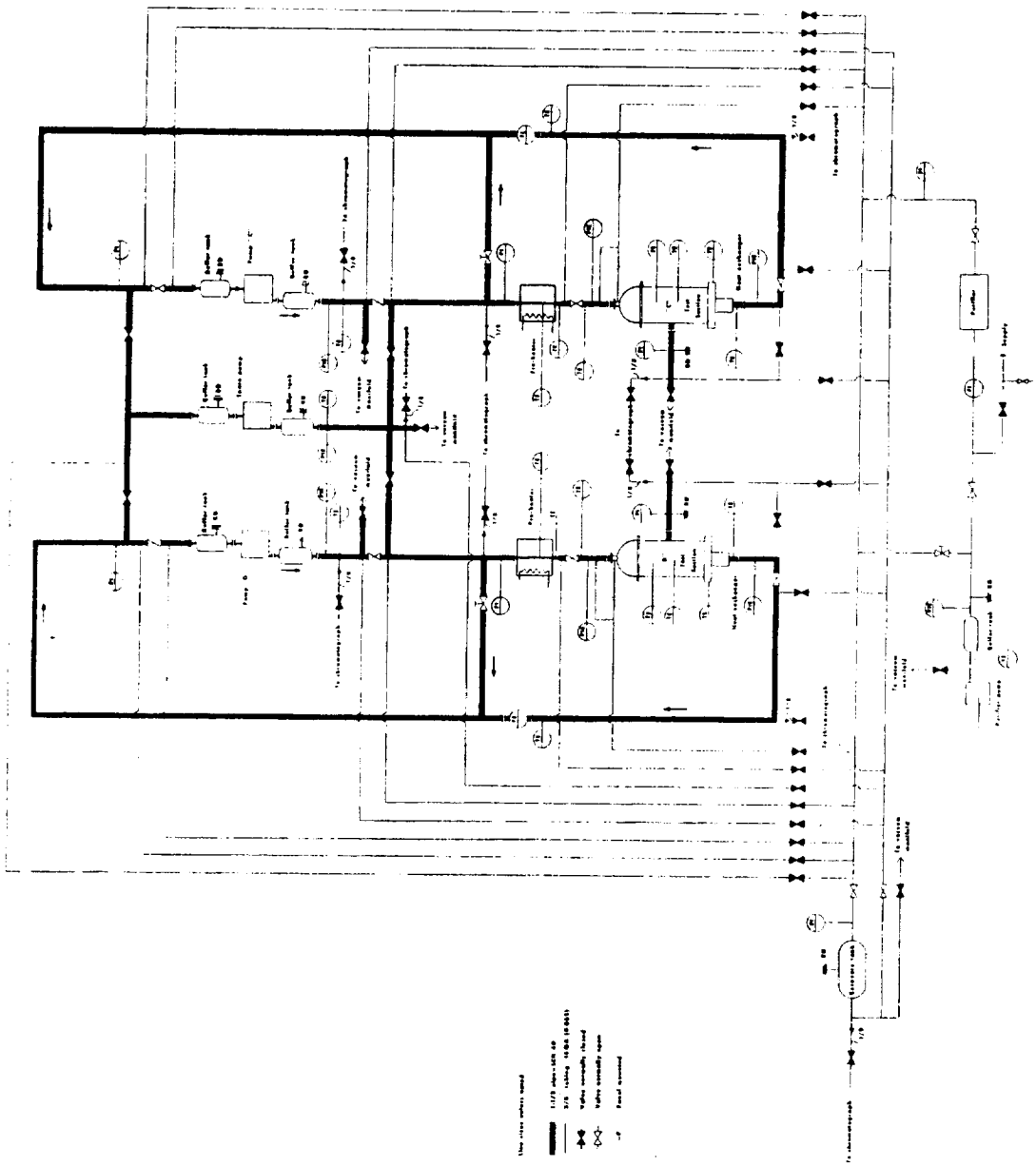

Fig. 3.4.4 – Preliminary schematic of Primary Loop No. 2 *(Dwg. 707E100)*

CONFIDENTIAL

[redacted]

PRECEDING PAGE BLANK NOT FILMED

4. GAS CIRCULATOR SYSTEM

4.1 GENERAL

The results of analysis and assessment of the blower cycle and gas-generator cycle methods of circulating helium through the reactor - heat-exchanger primary loop are presented. Schematic diagrams of the two cycles are shown, including the auxiliary components required. Parametric data showing the required reactor size and temperature levels are given for both, as well as the selected reference design points. Differences in materials requirements and in operational modes are listed and discussed.

Assessments of problem areas and of the current state-of-the-art are given for the rotating equipment, bearings and seals, and valves. Applicable work underway is identified.

4.2 CYCLE STUDIES

4.2.1 Possible Methods

Of the many possible cycles, three are of particular interest for use in aircraft application. Common to each is a closed inert-gas circuit which heats air by means of a heat exchanger. These alternatives, shown schematically in Figure 4.1,* consist of:

1. An externally powered blower for the closed helium loop in which the temperature levels across the reactor are essentially the same as those across the heat exchanger.
2. A completely contained set of turbomachinery used as a gas generator for the closed inert-gas loop, in which temperature levels across the reactor are higher than those across the heat exchanger, and essentially all the power generated by the reactor is useful for propulsive thrust.
3. A gas generator and power turbine contained within the closed inert-gas loop, using the shaft power to drive a fan or low-pressure-ratio compressor to pass air over the heat exchanger prior to exhausting it out a nozzle for propulsive thrust. This alternative imposes the lowest temperature and pressure levels on the heat exchanger for any fixed jet velocity from the propulsive engines.

---

*A bleed turbine, using air from the compressor of the propulsive engine, is indicated for the blower cycle. Aftercooling considerations indicate the desirability of an auxiliary air compresor-turbine set for this function.

CONFIDENTIAL

The same types of major components are required within the closed inert-gas loop for all these cycles except for the following differences:

1. Blower cycle
   a. Relatively low-temperature blower
   b. Shaft penetration and seal
   c. Gas makeup supply
2. Gas-generator cycle
   a. Additional low-pressure-ratio turbomachinery in the reactor loop
   b. Lubrication system inside reactor loop, but no shaft penetration
   c. Startup system for in-loop turbomachinery
   d. Provision for aftercooling either separately or in combination with the startup system.
3. Gas-generator and power turbine cycle
   a. Power turbine in reactor loop for driving air compressor or fan
   b. Shaft penetration and seal
   c. Lubrication system inside reactor loop
   d. Higher-pressure-ratio turbomachinery than for gas-generator cycle
   e. Startup system for in-loop turbomachinery
   f. Provision for aftercooling either separately or in combination with the startup system
   g. Gas makeup supply

These differences only appear outside the reactor containment vessel and, in the present concept, affect the reactor assembly design and performance only to the extent that different temperature levels are required. The inert gas in cycles 2 and 3 could be a mixture of helium and xenon if desired to reduce the number of stages in the turbomachinery.

The blower cycle provides the primary reference in this study because of NASA interest in it for comparative purposes with other systems. However, the gas generator was also studied to a minor extent because of its potential advantages. The third cycle, sometimes called the compressor-jet cycle, was not analyzed because systems optimization studies, outside the scope of the contract, are required to establish conditions to be imposed upon the reactor assembly.

4.2.2 Parametric Data

BLOWER CYCLE

The results of preliminary core sizing studies for the blower cycle are shown in Figure 4.2. Active-core pressure loss is plotted versus maximum fuel temperature of the average fuel element, with active core diameter and fuel surface temperature as parameters. The corresponding average fission density in the fueled matrix material (excluding cladding) is shown as a function of active-core diameter (length equal to diameter) in Figure 4.3.

[redacted]

Required pumping power can be derived only after determining the pressure loss for the entire closed circuit, including not only the reactor and the ducting between the reactor and containment shell, but also the heat exchanger and the ducting connecting the containment shell, heat exchanger, and blower. The losses for the ducting inside the containment shell are estimated to be within a range of 1.5 to 2.3 percent as shown in Table 4.1, with a probable value of 2 percent being reasonably achievable. If another 2 percent may be assumed for those portions of the circuit outside the containment shell, then 4 percent pressure loss should be added to the reactor pressure loss shown in Figure 4.2. Under these assumptions, the pump power required for various pressure losses is shown by the solid line in Figure 4.4. In view of the uncertainty in actual losses to be encountered, values of non-reactor pressure losses of 3 percent and 5 percent are also shown in Figure 4.4 to bracket the power and pressure ratios required for assessing the blower state-of-the-art.

A design reference point is indicated in Figures 4.2 to 4.4: reactor pressure loss of 1.5 percent; core diameter of 30 inches; maximum fuel temperature for the average element of almost 2300°F (for a surface temperature of 2200°F); and required blower power of 13,600 hp, or more than 4 percent of the thermal power* of the reactor. It should be noted that a thermodynamic engine must be used to supply the shaft power for the blower. If this engine operates at 25 percent efficiency, then the parasitic penalty is more than 16 percent of the reactor's gross thermal power. Unless the reactor thermal power is increased to compensate for this penalty, the thrust of the propulsion engine will be reduced in direct proportion to the reduction in net power. Thus, there is a strong incentive for restricting the pressure loss in the primary loop.

The possibility of reducing the reference core size by increasing the fuel temperature may be of interest. To answer this question, the effect of increased temperature on the potential fuel element lifetime capability was determined for the selected reference fuel element material, as shown in Figure 4.5. This figure also shows the permissible temperature perturbations from average conditions. The maximum internal fuel temperature for the average fuel element is plotted versus core size together with lines of constant reactor pressure loss; calculated times for 1 percent linear growth of the fuel element due to gaseous fission product pressure are also shown. Again, the selected design reference point is indicated. These data permit the following observations:

1. The reference design can operate for well over 1000 hours before reaching the 1 percent calculated growth.
2. The amount of time over 1000 hours that may be possible depends upon the magnitude of the temperature perturbation to be actually experienced within the fuel element. Since the maximum fuel temperature shown is for the average channel, the curve shows that the reference design, which has a nominal maximum of 2300°F, could tolerate 100°F perturbation (to 2400°F) for 2000 hours, 280°F (to 2580°F) for 1500 hours, or 420°F for

---

*250 Mw = 335,200 hp

CONFIDENTIAL

TABLE 4.1

ESTIMATED PRESSURE LOSS FOR REACTOR CONTAINMENT SHELL DUCTING

Item	Assumed Loss Coefficient (q/P)	Pressure Loss ($\Delta P/P$)[a]
Inlet distribution scroll and turning into duct	1 to 2[b]	0.0042 – 0.0084
Duct loss and dump into front plenum	1	0.0042
Entrance to discharge duct and duct loss	0.5	0.0021
Discharge distribution scroll	1 to 2[b]	0.0042 – 0.0084
Totals	3.5 – 5.5	0.015 – 0.023

[a]For gas Mach number of 0.0707, consistent with flow areas per Figure 5.2.2.

[b]Refined design and flow tests required to achieve the range assumed for loss coefficients.

[redacted]

1000 hours (to 2720°F). The estimate of temperature perturbations due to fabrication tolerances (see Table 5.4.3) shows that less than 80°F is expected from tolerance effects. Other factors dependent upon design approach must also be considered, as discussed in section 5.4.3. In particular, radial control of the fuel temperature by hydraulic diameter variation is required to compensate for the radial variation in power density; the number of other refinements to be incorporated in the design will be determined by the incentive to increase the expected lifetime from 1000 hours to 2000 hours (or more). There is extensive analytical and design experience available to achieve the refinements which may be desired.

3. The potential reduction of the core diameter by increasing the design value of the maximum fuel temperature, amounts to less than 2 inches. If a full 2-inch reduction were attempted for the 1.5 percent reactor pressure loss case, achievement of the 1000-hour lifetime in the fuel element would be unlikely. A better approach would be to increase the reactor pressure loss; e.g., a reduction in diameter of 3 inches would be possible if the reactor pressure loss were increased from 1.5 to 3.0 percent; this would increase the required blower power from about 4 to about 5 percent of the reactor thermal power (for the nominal conditions shown in Figure 4.4).

In summary, the parametric data for the blower cycle show that, for the design point conditions of interest (see section 1.4), the blower conditions to be expected are as shown in Table 4.2.

Table 4.2: Blower Power Requirement

	Nominal	High	Low
Blower power, hp	13,600	20,000	11,000
Blower power, % of Q_{th}	4.06	5.96	3.28
Blower pressure ratio	1.055	1.08	1.045
Possible thrust penalty[a], %	16	24	13

[a]For a reactor power of 250 Mw_{th} without compensation and 25% conversion efficiency

GAS-GENERATOR CYCLE

In view of the thrust penalty associated with the blower cycle, preliminary core sizing studies were also performed for the gas-generator cycle; the results are shown in Figure 4.6. Maximum fuel temperature is plotted versus turbine inlet temperature required to yield the same heat exchanger temperature conditions as for the blower cycle; lines of constant core diameter and constant fuel surface temperature are also shown. The same pressure level (1500 psi) was held on the reactor side

as for the blower cycle, so the pressure level on the heat exchanger side is lower and varies depending upon the turbine inlet temperature. The simplifying assumption was made that the reactor pressure loss is 40 percent of the total loop loss; other necessary assumptions are noted on the graph.

The data show that the same size core as for the blower cycle (30-inch diameter) is possible with less than 100°F increase in the required maximum fuel temperature even though the reactor discharge temperature is 200° to 300°F higher than for the blower cycle. This is possible because of the higher core pressure loss which the gas-generator permits while remaining self-sustaining. There are relatively narrow bands of permissible turbine inlet temperature, for any given reactor diameter, because of the inherent characteristics of turbomachinery. That is, when the turbine inlet temperature is decreased, less pressure loss is allowable and less heat transfer area is permissible; while, when it is increased, the reactor must produce hotter gas, more than the increased allowable heat transfer area can compensate.

The potential fuel element lifetime capability for the selected reference fuel element material in the gas-generator cycle is shown in Figure 4.7. The loci of minimum fuel temperatures for the various turbine inlet temperatures of Figure 4.6 have been plotted, thereby presuming that the best choice of turbine inlet temperature has been made for any particular core diameter. Again, the selected reference point indicates a fuel element lifetime of more than 1000 hours, based on the fuel growth criterion, may be expected. As in the case of the blower cycle, more than 2000 hours may be possible, depending upon the magnitude of temperature perturbations.

Characteristics of the reactor core are summarized in Table 4.3 for both cycles. Identical assumptions were made for both reactors with regard to entrance and exit losses in the fuel element, nuclear parametric data, etc.; the results, therefore, are directly comparable. (It should be noted however, that the blower cycle data are not the final estimates derived in this study.) The principal difference between the two core configurations is that the gas-generator cycle permits higher reactor pressure loss, has higher reactor inlet and outlet temperatures, has 100°F higher maximum fuel temperature but lower internal fuel temperature rise, and has smaller coolant channels. The latter fact makes it desirable to increase the number of coolant channels per fuel element from 37 to 61. The most significant item is the higher reactor inlet temperature, and the influence this may have upon the front tube sheet structural design. Ducts connecting the reactor outlet to the turbine might have to be made of refractory metal because of the higher outlet temperature.

4.2.3 Aftercooling Considerations

BLOWER CYCLE

Aftercooling of the blower cycle can be accomplished by driving the blower by means of a chemical energy source; no other additional equipment is required. If the blower is driven by a set of air turbomachinery independent of the propulsive engines, continued operation for aftercooling will be possible without interruption even after landing.

TABLE 4.3

REACTOR CORE CHARACTERISTICS FOR BLOWER VERSUS GAS GENERATOR CYCLES

	Blower	Gas Generator
Reactor pressure loss, $\Delta P/P$	0.015	0.025
Thermal power, Mw	250	250
Reactor pressure, psia	1500	1500
Temperatures, °F		
Reactor inlet	900	1193
Reactor outlet	1800	2100
Maximum fuel surface (avg)	2200	2342
Maximum fuel internal (avg)	2291	2391
Maximum internal rise (avg)	106	68
Helium flow rate, lb/sec	212.4	210.6
Active core dimensions, in.		
Envelope diameter	31.2	31.2
Equivalent circular diameter	29.9	29.9
Length	30.0	30.0
Active core volume, in.^{3}	21,068	21,068
Core volume fractions		
Structure	0.106	0.128
Free flow and voids	0.520	0.491
Fueled matrix (95% of theoretical density)	0.374	0.381
	1.000	1.000
Free flow area (hot), in.^{2}	296.7	275.2
Coolant channels per element	37	61
Elements per reactor	241	241
Channel diameter (cold), avg.	0.2028	0.1521
Burnup in 1000 hours, fissions/cm^3	2.254×10^{20}	2.225×10^{20}

At some point in time, special internal aftercooling equipment may be desirable in the interest of economy.

The efficiency of a helium blower can be maintained at reduced mass flow rates during aftercooling by decreasing the pressure level of the helium and keeping the blower speed constant, so that the volume flow remains constant. This can be seen from an analysis of the terms involved in the definitions of specific speed and specific diameter, both of which determine the efficiency of blowers:

$$\text{Specific speed } (N_S) = \frac{N\sqrt{V}}{h_{ad}^{3/4}}$$

$$\text{Specific diameter } (D_S) = \frac{D\, h_{ad}^{1/4}}{\sqrt{V}}$$

where: N = speed of rotation, rpm
V = volume flow rate of gas at blower inlet, ft^3/sec
D = diameter of blower, ft
h_{ad} = adiabatic head imparted to the gas by the blower, ft-lb/lb

The adiabatic head term required of the blower is given by:

$$h_{ad} \sim \Delta P/\rho \sim f\,\frac{(G^2T/P)}{\rho}$$

$$\sim f\,(W\,T/P)^2$$

where: f = friction factor, dependent upon Reynold's number
W = weight flow rate of the gas, lb/sec
T = temperature of the gas, ^oR
P = pressure of the gas, lb/ft^2
ρ = gas density, lb/ft^3
ΔP = pressure rise across blower, lb/ft^2

The volume flow rate term is given by

$$V = W/\rho \sim WT/P$$

Therefore, the adiabatic head required of the blower can be expressed in terms of the volume flow rate:

$$h_{ad} \sim f\,V^2$$

Thus, when the volume flow rate is held constant, the adiabatic head (ft-lb/lb) required of the blower is constant. Consequently, when the rotational speed is held constant, the specific speed is constant. Likewise, all the terms involved in the specific diameter are constant; hence, the blower efficiency is constant.

The Reynold's number effect upon friction factor introduces an uncertainty in the simplified treatment given above. The pseudo-friction factor will be insensitive to Reynold's number if a large portion of the loop pressure loss arises from non-frictional resistances such as contractions and expansions, turning losses in bends, or other such factors which cause turbulence. Should the Reynold's number effect be significant, which can be determined only after the entire primary loop design has been established, then a minimum pressure level at which the main blower can be used economically for aftercooling will be established.

[redacted]

Of immediate concern in this respect is the desire to reduce the pressure level of the helium loop to about 200 psia within 20 seconds after shutdown* so as to reduce the pressure level that must be contained should the aircraft crash. Since the normal operating pressure is 1500 psi, this amounts to a reduction of about one decade. Since the Reynold's number in the fuel element is about 50,000, a factor of 10 reduction yields a value above the 2000 to 4000 Reynolds number range at which the transition to laminar flow occurs. The Reynold's number in other flow passages, excluding the heat exchanger, is about 2×10^6 or about 50 times that in the fuel element; a pressure reduction even by a factor of 500 in these passages would still not produce laminar flow in the ducts. It is possible that flow conditions may be reasonable for a pressure level as low as 1 atmosphere, or about 1 percent of the operating pressure, which is the minimum level required 2.8 hours after shutdown (following 1000 hours of full-power operation) in order to prevent over-temperaturing the fuel elements. After this time, special aftercooling equipment could be used to reduce operating costs.

If a bleed air turbine were used to drive the helium blower, constant speed control would be a feasible approach for the aftercooling mode provided the same quantity of air is passed through the turbine as during normal operation. The power output of the turbine can be reduced by reducing the turbine inlet temperature. If a separate set of air turbomachinery is used to drive the blower, consideration should also be given to reduced speed operation during aftercooling. Several methods of operation are possible, but this illustrates the relative simplicity of aftercooling the reactor when the blower cycle is used.

GAS-GENERATOR CYCLE

Aftercooling of the gas-generator cycle requires an external power source and equipment in the closed loop that is not otherwise needed during normal operation. The size, weight, and power requirements for this auxiliary equipment depend upon the operational mode to be used for reactor shutdown. The need for special startup equipment and the operational procedure during this phase are of equal importance. The helium flow vector diagrams of the compressor and turbine can be maintained at their design point values by keeping the volume flows constant; in this manner, the helium weight flow is fixed by the pressure level and by operating the turbomachinery at its design point value. Again, as for the blower cycle, this will yield compressor and turbine efficiencies equal to their design point values throughout both the startup and aftercooling phases, except for the Reynold's number effect. Conceivably, therefore, the gas generator could be self-sustaining on the afterheat energy available from the reactor for some time after shutdown. Some power output from the gas-generator turbine is desirable since, at full-power operation (for the conditions listed in Table 4.2 and 6.25 percent loop loss) the gross power output of the turbine is 113,000 hp (see Table 4.4). The afterheat generation rate, following 1000 hours of full-power operation, declines to 10 percent of operating power within 25 seconds and to 1 percent within 2.8 hours after shutdown. If the pressure level were reduced in accordance

*Afterheat generation rates indicate this is possible on a scheduled basis.

with this schedule, the gas generator would continue to provide power for circulation, but some auxiliary power would be required to compensate for increased frictional effects due to the decrease in Reynolds number.

Since the gas generator can be self-sustaining only if the turbine inlet temperature is maintained at or near the design point value, a control system is required to assure that the rate of reduction of pressure level is closely matched to the rate of afterheat decay. In addition, since the reactor structural arrangement in the present concept is dependent upon water cooling to restrict thermal expansion strains, continued water cooling flow will be required in the gas-generator cycle. Since a design objective is that no water be present in the containment shell after reactor shutdown, an exception would be required in this case. The volume of water inside the shell can be minimized by using a closed-circuit coolant path into and out of the shell without intermixing the coolant water with the shield water. Although this concept was not incorporated into the design evolved in this study because principal interest was centered on the blower cycle, the necessary modifications appear to be minimal. This may be an attractive feature, in fact, for providing the necessary aftercooling for the long-time-after-shutdown case, not only for the gas generator cycle but also for the blower cycle.

4.2.4 Design Point Selection

BLOWER CYCLE

The blower power requirement, being in the range of 11,000 to 20,000 hp, excludes the possibility of an electric motor drive or gas bearings based upon current state-of-the-art. Electric motors operating on a 60-cycle power supply weigh about 5 lb/hp; by following aircraft practice using higher frequency, the specific weight can be reduced to as low as 1 lb/hp. The power for the drive motor must be generated by onboard equipment, resulting in additional weight. Further discussion of the problems of motor drives for circulators is available elsewhere.[1] Gas bearings in motor-driven circulators, are limited to 200 hp although consideration has been given to their use with turbine drives up to 1000 hp.[*2] These capabilities are far below that required in the present application, excluding the possibility of multiple small-size blowers. Hence, an air turbine drive with oil bearings is necessary, using a shaft penetration through the primary loop ducting and using a dynamic seal.

The type of circulator to be used must be selected from three possibilities: radial-flow, axial-flow, or some intermediate type. For any given pressure rise and volume flow requirement, a circulator designer

---

[1] G. Novickis, "Survey of Component Requirements and Availability for Gas-Cooled Nuclear Reactor Power Plants - Circulators" NYO-9790, August 1961, p. 63, Franklin Institute Laboratories.

[2] "Rotating Machinery for Gas-Cooled Reactor Application" Proceedings of Meeting at Mountain View Hotel, Gatlinburg, Tenn., November 4-6, 1963, p. 353, TID-7690.

*Gross power output; if the drive is by shaft power extraction from a turbine - compressor set, the power for driving the compressor must be subtracted.

[redacted]

has the option of using large diameter and relatively slow rotational speed or a small diameter with high rotational speed. Experience shows that, among all the various types of blower designs which can be purchased from various manufacturers, there is a unique relationship between the diameter of the machine and its speed of operation. A plot of specific diameter versus specific speed, using a conventional parametric grouping for these terms such as defined in section 4.2.3, shows the unique relationship; it is known as the Cordier - curve.[1] Selection of a particular specific speed fixes the type of circulator, i.e., radial, axial, or mixed flow.

Balje[3] has improved upon the simple Cordier correlation by showing not only the speed - diameter relationship and the type of circulator inherent for any preferred values of speed or diameter, but also the efficiency that can conservately be expected. Balje's correlation for low-pressure-ratio compressors is reproduced in Figure 4.8. The graph shows the regimes for radial flow, mixed flow, and axial flow; these types apply for intermediate- to high-specific-speed designs. At low specific speeds, other types of machinery such as rotary displacement pumps, drag pumps, and pitot pumps are indicated as being inherently preferred. In the present case, attention is restricted to the conventional machinery because of the need to maintain purity of the gas, to avoid metal-to-metal contact, and to stay within the current state-of-the-art for the relatively large volumetric flow rate required in the aircraft application.

The data in Figure 4.8 have been used to determine the single-stage pressure rise as a function of the rotor tip speed and rotational speed for the gas conditions of the present study. The specific speed considered in this evaluation ranged from 60 to 300, covering pure radial- and mixed-flow types, with the corresponding specific diameter that yields an expected blower efficiency of 80 percent. Balje's assumptions for preparing this particular illustration result in indicated efficiencies for axial flow circulators of 70 percent or less; however there is wide experience showing multistage axial compressors with efficiencies approaching 90 percent. Therefore, the data in Figure 4.8 can be interpreted only as a guide, with higher efficiencies or higher pressure ratios to be normally expected through the application of good state-of-the-art design practice. With this qualification, the results of this evaluation are representative of the rotor tip speeds and rotational speeds to be expected for various required values of pressure rise in a single stage.

The results are shown in Figure 4.9. To achieve 5 percent pressure rise in a single stage, the circulator must be of the pure radial type (specific speed of 60 or less); the tip speed must be about 1220 ft/sec; the corresponding rotational speed is 5500 rpm, and the rotor diameter is 4.25 feet. Figure 4.9 also shows the design point for the HTGR blower for comparison (as discussed in Section 4.3.1).

Alternatively, two stages can be used in series to achieve a 5 percent pressure rise. If desired in this case, either a pure radial- or

---

[3] O. E. Balje, "A Study on Design Criteria and Matching of Turbomachines," J. of Energy for Power, AIME, January 1962, pp. 103-114.

a mixed-flow-type circulator can be used. The tip speed can be reduced to less than 865 ft/sec and the rotational speed to less than 3260 rpm for a rotor diameter of about 5 feet.

GAS GENERATOR CYCLE

In view of the possible interest in the gas-generator cycle, the sizes of the compressor and turbine were estimated. The assumptions made were that the design temperatures on the helium-to-air heat exchanger must be the same as for the blower cycle (i.e., 900° and 1800°F helium temperature) and that the maximum pressure level of 1500 psia would be maintained at the compressor discharge. The reference point given in Figure 4.6, which shows the core parametric sizing data as a function of the cycle variables, was used for this study; this point is consistent with the tabulation of core characteristic data in Table 4.3. The size estimates were made not only for pure helium but also for a mixture of helium and xenon, with an average molecular weight of 40, to show this effect upon the number of compressor and turbine stages required.

Conventional design practice was used in the selection of blade angles and stage loading. (This practice does not exploit the relatively high sonic speed of helium. In a system requiring high performance, as for aircraft application, the possibility that the high sonic speed might be used to advantage is of sufficient interest to warrant further consideration as part of other studies.) A nominal allowance of 2.5 percent compressor bleed flow was made for cooling the turbine rotor; cooling for the turbine blades is considered to be unnecessary.

The results are given in Table 4.4. The compressor pressure ratio is 1.55, which yields the 6.25 percent loop pressure loss as required for this particular design point. Figure 4.6 shows that a lower turbine inlet temperature can be used, which results in lower allowable loop pressure losses and lower compressor pressure ratios, but of the 6.25 percent available for the entire loop, the reactor core requires 2.5 percent. This leaves only 3.75 percent for the remainder of the primary loop; this is comparable with 4 percent as the nominal allowance for the non-core components in the blower cycle (see Figure 4.4). Hence, any reduction in the turbine inlet temperature and, consequently, in the compressor pressure ratio, would not be a fair comparison of the gas-generator cycle with the blower cycle. As it is, the comparison is fair except that the pressure level on the heat exchanger side has been reduced to 1500/1.55 = 968 psia; this is a feature that may be attractive considering the stress levels in the oxidation-resistant materials required in the helium-to-air heat exchanger.

Twenty stages are required in the helium compressor. The blade tip diameters are 37.4 inches at the inlet and 35.0 inches at the exit. The exit blade height is 0.75 inch. The flow path length is estimated to be 28 inches. The assumed efficiency of 85 percent is believed achievable with state-of-the-art design practice currently in use in General Electric's Flight Propulsion Division. Some stall-prevention mechanism may be required.

TABLE 4.4

TURBOMACHINERY SIZING RESULTS FOR GAS-GENERATOR CYCLE

Coolant	He	He-Xe
Molecular weight	4	40
Compressor discharge pressure, psia	1500	1500
Compressor inlet temperature, °F	900	900
Turbine discharge temperature, °F	1800	1800
Loop pressure loss, %	6.25	6.25
Turbine inlet temperature, °F	2114	2114
Gas flow rate, lb/sec	211	2110
Compressor pressure ratio	1.55	1.55
Turbine shaft power, hp	113,000	113,000
Compressor efficiency, %	85	85
Turbine efficiency, %	88	88
Rotational speed, rpm	5665	3586
Turbine		
No. of stages	8	2
Inlet tip diameter, in.	34.4	36.4
Exit tip diameter, in.	34.5	36.8
Inlet blade height, in.	1.25	4.02
Exit blade height, in.	1.35	4.37
Flow path length, in.	22	10
Compressor		
No. of stages	20	6
Inlet tip diameter, in.	37.4	38.0
Exit tip diameter, in.	35.0	35.9
Inlet blade height, in.	1.95	2.55
Exit blade height, in.	0.75	1.7
Flow path length, in.	28	17

In the helium turbine, eight stages are required with a blade tip diameter of about 34.5 inches and minimum blade height of 1.25 inches. The flow path length is estimated to be 20 inches.

The rotational speed is 5665 rpm for the helium turbomachinery set, which yields a peripheral velocity of 922 ft/sec for the compressor and 852 ft/sec for the turbine.

Corresponding data are tabulated for the mixture of helium and xenon showing that slower machinery with fewer stages are possible. The compressor and turbine lengths are shorter, but slightly larger in diameter. It should be noted that the helium - xenon mixture has poorer heat transport properties and that higher pressure levels would be required to avoid an increase in the reactor sizes (see Figure 4.6).

4.2.5 Material Requirements for Circulator Design

The data in Figure 4.9 show that a 5 percent pressure rise can be achieved in a single radial-flow blower stage provided the rotor can withstand the stresses imposed when the peripheral speed of the rotor is 1220 ft/sec. The operating temperature level is 900°F. The parameter of interest for the rotor material is its strength-to-weight ratio.

A simple analysis shows the relative degree of difficulty to be expected. If the blower rotor is shaped structurally so as to have a constant cross-sectional area with radius such that the stress due to centrifugal force is like that in a rotating rod, the stress in the rotor at the axis is given by

$$S = 12 \frac{\rho V_T^2}{g}$$

where S = stress, lb/in.^{2}
ρ = density of the material, lb/in.^{3}
V_T = peripheral velocity of the rotor at the tip, ft/sec
g = gravitational constant, ft/sec^2

Therefore, the parameter of interest becomes

$$\frac{S}{\rho} = 12 \frac{V_T^2}{g}$$

At V_T = 1220 ft/sec, the required value of S/ρ = 555,000 inches; at V_T = 900 ft/sec, it is about 300,000 inches. For comparison, the strength-to-weight ratios of some aircraft metals are given in Table 4.5; these data are for typical values of short-time yield strength (0.2% offset), and actual design values must be lower than tabulated to achieve useful lifetime. The data show that the tip speed of 900 ft/sec (S/ρ = 300,000 inches) should be achievable at 900°F with titanium alloys, Inconel X, or a high-strength, low-alloy steel such as Super Tricent. At 1220 ft/sec, however, only the Super Tricent alloy would meet even the minimum requirements. Therefore, to achieve the blower pressure ratio requirement, as tabulated in Table 4.2, conservative design would require two stages. However, if no more than 5 percent rise is required, careful mechanical

TABLE 4.5

TYPICAL STRENGTH-TO-WEIGHT RATIOS FOR SOME AIRCRAFT METALS[a]

Material	Average Composition, %											Ratio of Strength-[c] to-Density (S/ρ) at 900°F, inches
	Fe	Ni	C	Mn	Si	Cr	Mo	V	Ti	Co	Other	
Super Tricent	Bal.	3.60	0.55	0.80	2.10	0.90	0.50	–	–	–	–	640,000
Super Hy tuf Tricent	Bal.	–	0.40	1.30	2.30	0.35	0.20	–	–	–	–	550,000
Titanium[b] MST 6Al – 4V	–	–	0.2	–	–	–	–	4	Bal.	–	6 Al	520,000
Inconel X	7.	Bal.	0.05	–	–	15.	–	–	2.5	–	0.7 Al, 1. Nb	400,000
A 110-Ti[b]	–	–	–	–	–	–	–	–	Bal.	–	4 – 6 Al, 2 – 4.5 Sn	390,000
Molybdenum												290,000
Aluminum SAP												150,000
L605	1.	10.	0.12	–	–	20.	–	–	–	Bal.	15. W	110,000
Type 321 SS	Bal.	10.	–	–	–	18.	–	–	0.4	–	–	80,000

[a]"Aerospace Propulsion Data Book" General Electric Co., Flight Propulsion Division, GED-4505.
[b]Impurities (maximum): 0.2 C, 0.1 N, 0.25 O_2, 0.015 H_2.
[c]Strength is the yield stress as measured by the 0.2% offset method.

CONFIDENTIAL

design of the impeller and use of the best available material may permit achieving the required 2000-hour lifetime in a blower with only one stage.

4.3 ASSESSMENT OF PROBLEMS, CURRENT STATE-OF-THE-ART, AND APPLICABLE WORK UNDERWAY

4.3.1 Helium Circulators

The current state-of-the-art for helium circulators is summarized in Table 4.6, which lists the design conditions for the various helium-cooled reactors that have been proposed, designed, and/or built. Although not all items of interest were available, the tabulation shows that current practice can be summarized as follows:

1. Radial blowers are used if the pressure rise is 3 percent or less; multistage axial-flow circulators are used if the pressure rise is greater than 3 percent.
2. Rotor tip speed is limited, in general, to 900 ft/sec or less; a singular exception is the compressor for the Maritime Gas-Cooled Reactor (MGCR)[4] turbomachinery, which was not put into operation.
3. Inlet temperature to the circulator is limited to 700°F or less.
4. Inlet pressure to the circulator is limited to 500 psia or less.

The closest approach to the present design requirement in existing hardware is the radial blower used in the High-Temperature Gas-Cooled Reactor. This point is plotted in Figure 4.9 to show how that design corresponds with the predicted performance using Balje's data; the slight degree of conservatism in Balje's correlation is indicated, although the HTGR blower efficiency is only 78 percent as compared with the 80 percent for which the curves in Figure 4.9 apply. The HTGR blower* consists of a single-stage, radial-overhung type generating a pressure rise of 2.9 percent in a 5-foot rotor diameter at 3460 rpm. The differences between this design and the requirements of the present application are as follows:

	HTGR	Required
Number of Stages[a]	1	2
Pressure, psia	450	1500
Inlet Temp., °F	700	900
Driver	Motor	Turbine

[a] At 900 ft/sec tip speed

Also, a design for minimum weight for aircraft use rather than central station use would be required.

The dynamic seal (to prevent contamination of the primary helium coolant with oil) has been discussed in the literature in considerable depth[5] for the case of the single-stage radial overhung arrangement.

[4] "Maritime Gas-Cooled Reactor Program, MGCR Prototype Preliminary Design, Vol 1" General Atomics Div., General Dynamics Corp., GA-1612, December 9, 1960.

[5] "Rotating Machinery for Gas-Cooled Reactor Application," TID-7031, Proceedings of Meeting at ORNL, April 2-4, 1962.

*Built by the Clark Bros. Co., Olean, N. Y.

CONFIDENTIAL

TABLE 4.6

HELIUM CIRCULATOR APPLICATIONS

Reactor	UTREX[3,9,10]	MGCR[8]	DRAGON[1,2]	AVR[2,3]	GCPR[1]	EGCR[5]	HTGR[6]	PBR[1]	GCR-2[4]	GCR-3[5]	TARGET[7]		HGCR-1[6]
Thermal power, Mw	3	–	20	49	84	85	115	300	687	–	2,337		3,095
Type of circulator	Radial	Axial	Radial	Radial	Axial	Axial	Radial	Radial	Axial	Axial	Gas Generator		Axial
											Compressor	Turbine	
Number of stages	1	41	–	–	–	10	1	–	–	7	5	2	–
Isentropic eff., %	75	88	–	80	–	88	~78	–	80	–	89.4	90.3	–
Power per circulator, hp	65	–	75	83	1,940	3,100	1,900	4,070	5,700	34,300	–	–	9,000
Type of drive	Motor	Turbine	Motor	Motor	–	Motor	Motor	–	Motor	Turbine	Turbine	–	Motor
Type of bearing	Gas	Oil	Gas	Oil	–	Oil	Oil	–	–	Oil	Oil	Oil	–
Number of circulators	1	–	6	2	2	2	2	3	4	4	6	–	8
Speed, rpm	12,000	12,200	10,900	3,500	–	6,130	3,460	–	3,580	3,720	5,120	–	3,600
Peripheral velocity, ft/sec	601	1,060	761	–	–	582	906	–	–	607	840	1,094	–
Rotor tip diameter, ft	0.957[11]	1.66	1.333	–	–	1.813	5.0	–	–	3.12	3.13	4.08	–
Speed range	–	–	10/110	–	–	20/110	10/100	–	Constant	–	–	–	Consta
Inlet temperature, °F	600	85	660	390	510	483	628 (700 design)	~550	450	550	682	1500	506
Inlet pressure, psia	500	442	289	140	303	298	340 (450 design)	–	300	415	394	442	290
Pressure ratio	1.018	2.63	1.0173	1.00716	1.037	1.056	1.029	–	1.022	1.059	1.15	1/1.12	1.04
Flow rate per circulator, lb/sec	2.85	–	3.71	–	59.3	59.7	65.8	124.3	243	634	396	396	300
Type of seal	Canned	See ref. 5, 8	Canned	Canned	–	Water buffer and axial sleeve	Helium buffer and floating bushing	Canned	–	Helium buffer	Buffered labyrinth, floating bushing, and visco seal combination		Canne
Manufacturer	MTI	–	–	–	–	Joy Mfg. Co.	Clark Bros. Co.	–	–	Westinghouse	–		–

[1] G. Novickis, "Survey of Component Requirements and Availability for Gas-Cooled Nuclear Reactor Power Plants – Circulators," NYO-9790, August 1961, p. 63.
[2] R. L. Loftness, "Nuclear Power Plants," D. Van Nostrand Co., Inc., 1964.
[3] "Rotating Machinery for Gas-Cooled Reactor Application," TID-7690, Proceedings of Meeting at Mountain View Hotel, Gatlinburg, Tennessee, November 4-6, 1963, p. 353.
[4] "The ORNL Gas-Cooled Reactor, Parts 1 through 4," Oak Ridge National Laboratory, ORNL-2500, April 1, 1958.
[5] "Rotating Machinery for Gas-Cooled Reactor Application," TID-7631, Proceedings of Meeting at ORNL, April 2-4, 1962.
[6] W. B. Cottrell, "HGCR-1, A Design Study of a Nuclear Power Station Employing a High-Temperature Gas-Cooled Reactor With Graphite – UO_2 Fuel Elements," ORNL-2653, July 28, 1959.
[7] J. Yampolsky, "Investigation of Turbocirculator for TARGET, a 1000-Mw Reactor, Summary Report," General Atomics, GA-5559, September 28, 1964.
[8] "Maritime Gas-Cooled Reactor Program, MGCR Prototype Preliminary Design, Vol. I," General Atomics, GA-1612, December 9, 1960.
[9] "Ultrahigh Temperature Reactor Experiment (UTREX). Quarterly Status Report for Period Ending February 20, 1962," LAMS-2678.
[10] "Ultrahigh Temperature Reactor Experiment (UTREX). Quarterly Status Report for Period Ending September 20, 1963," LAMS-2984.
[11] "Ultrahigh Temperature Reactor Experiment (UTREX). Quarterly Status Report for Period Ending March 20, 1963," LAMS-2894.

In the case of axial-flow circulators, the state-of-the-art has not yet been applied to an existing power plant. The most design study and development effort has probably been spent on the 10-stage axial flow circulator for EGCR[5], the Experimental Gas-Cooled Reactor previously under development by the Oak Ridge National Laboratory, with the circulator being developed by the Joy Mfg. Co., Buffalo, N. Y. The circulator operates at the same volume flow (516 ft^3/sec) as required as for the aircraft application, but at less than 500°F and less than 300 psia; consequently, its power output is only 3100 hp, whereas 13,600 hp is required in the aircraft application.

Therefore, modifications to the design would be required in this case, as for the radial-flow blower for HTGR.

In any redesign effort, attention should be given to the aerodynamic design of the blading. In this regard, there appears to be a carry-over of the design practice for air turbomachinery which unduly penalizes helium compressors from the standpoint of size and weight; this is of particular concern for aircraft application. An indication of the problem can be seen in Figure 4.10, which shows the number of stages used in the compressor to achieve various pressure rise fractions required by the powerplants tabulated in Table 4.6. The compressor design evolved in the present study for the gas-generator cycle is also shown for comparison. Note that the design for TARGET, the most recent design effort from previously published reports, requires only five stages to achieve 15 percent pressure rise across the compressor; in contrast, the EGCR design uses 10 stages to achieve only 5.6 percent pressure rise.

In summary, the following problem areas have been identified for the helium circulator in the aircraft application:

1. The blower cycle method of circulating helium primary coolant imposes a significant parasitic power penalty and, therefore, thrust penalty. The driving power may be provided by an air turbine drive using oil bearings.
2. The gas-generator cycle may be an attractive alternative to eliminate the thrust penalty associated with the blower cycle, but a higher temperature will be required in the reactor.
3. There are no existing designs that can be applied without modification. Principal modifications required are those necessary to increase the pressure and temperature capability to 1500 psia and 900°F, respectively.
4. Further study is needed to determine whether to use a single-stage radial-flow blower at relatively high peripheral speed (> 1200 ft/sec), a two-stage radial-flow blower at moderate speed (∿ 900 ft/sec), or a multistage axial-flow circulator. Some research in this area to advance the state-of-the-art of axial-flow compressor design for helium may result in significant reduction in the number of stages required for any given pressure rise.
5. Existing circulators were developed for central station powerplant application in which weight is of less concern than cost. A manufacturer experienced in designing components for aircraft application should be included in further study efforts, such as in item 4, above.

4.3.2 Bearings and Seals

The subject of bearings and seals for helium circulators has been well treated in existing literature[5-8] and the designs that have been evolved for HTGR, MGCR, and EGCR provide practical experience in development and application of approaches necessary for the present case. The manufacturers who have provided the circulator development for these powerplants have also provided the bearing and seal designs. A discussion of basic seal types, given in Reference 5, pg. 85 et. seq., is recommended as introductory material for basic sealing methods; the same reference shows the shaft seals for the EGCR (Joy Mfg. Co.), the HTGR (Clark Bros. Co.), and the GCR-3 (Westinghouse).

As with the circulator itself, the problem to be expected from the bearing and seal area stems from the relatively high pressure of the aircraft application.

4.3.3 Valves

A summary of advanced valve technology is given in reference 9. Of particular concern in this study was the closure valve for the containment vessel.

Smirra Development Company, Los Angeles, California, has developed a valve concept,[9] the "Cone Labyrinth Valve" (patent pending) which employs a novel means of seat surface contact. This concept promises improvements in contamination-insensitive, leak-tight sealing, for a wide range of fluids. Figure 4.11 illustrates a prototype version of this device.

The flow control element of the Cone Labyrinth Valve accomplishes both throttling and shut-off by the use of two concentric sets of flexible metal blades. Throttling is effected by forcing capillary flow through the labyrinth created in closing the valve; the sealing action results from the engagement of the resilient metallic sliding surfaces. The concentric blades approach each other with an intermeshing action which tends to be self-adjusting and finally provides shearing contact.

Some of the advantages of this type of design are:

1. Maximum possible corrosion resistance is afforded by the material choices possible with an all-metal design.

---

[5] Ibid.

[6] S. B. Malanoski and D. D. Fuller, "Survey of Component Requirements and Availability for Gas-Cooled Nuclear Reactor Power Plants - Bearings and Seals," NYO-9792, June 1961, Franklin Institute Laboratories.

[7] "Shaft Seals for Compressors and Turbines for Gas-Cooled Reactor Application," TID-7604, Proceedings of Meeting at Oak Ridge National Laboratory, Oak Ridge, Tenn., December 16-17, 1959.

[8] "Machine Design," 14, Vol. 36 - Reference Issue on Seals, Penton Publishing Co., Cleveland, Ohio, June 11, 1964.

[9] K. D. May, "Advanced Valve Technology," Midwest Research Institute, NASA SP-5019, February 1965.

2. Extreme service temperature capability resulting from an all-metal design. Radiation and vacuum problems associated with the use of elastomers and plastics are similarly eliminated.
3. Contamination insensitivity, since impurities are scraped away instead of being crushed or imbedded.
4. Sealing redundancy by the use of multiple seats.

4.3.4 Gas Makeup Supply

The problems of providing a clean gas supply and of maintaining purity levels low enough to avoid deterioration of materials' properties are discussed in section 3.4; this was based on experience gained during the 710 Reactor Program.

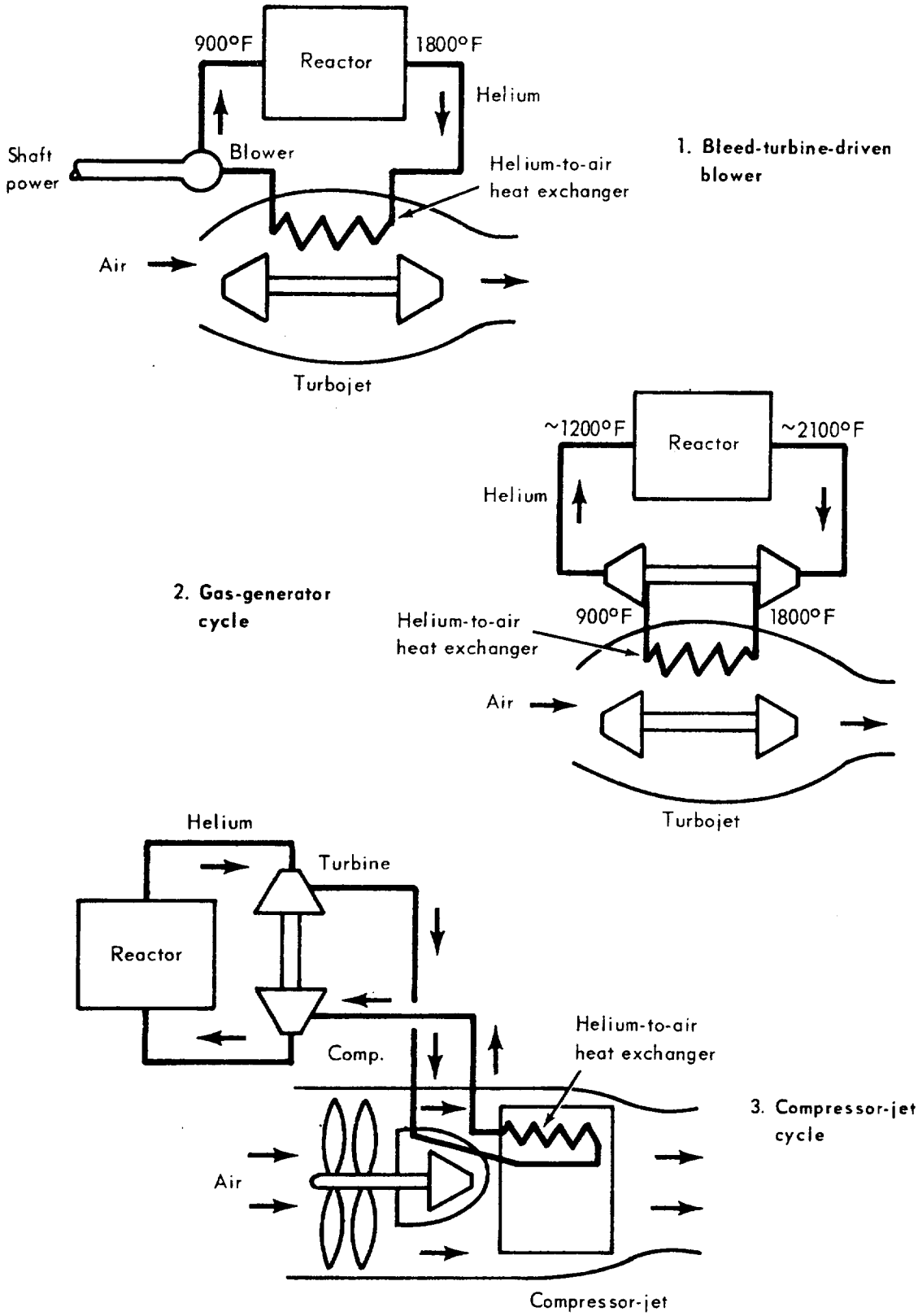

Fig. 4.1 – Typical cycles with gas coolant

[redacted]

CONFIDENTIAL

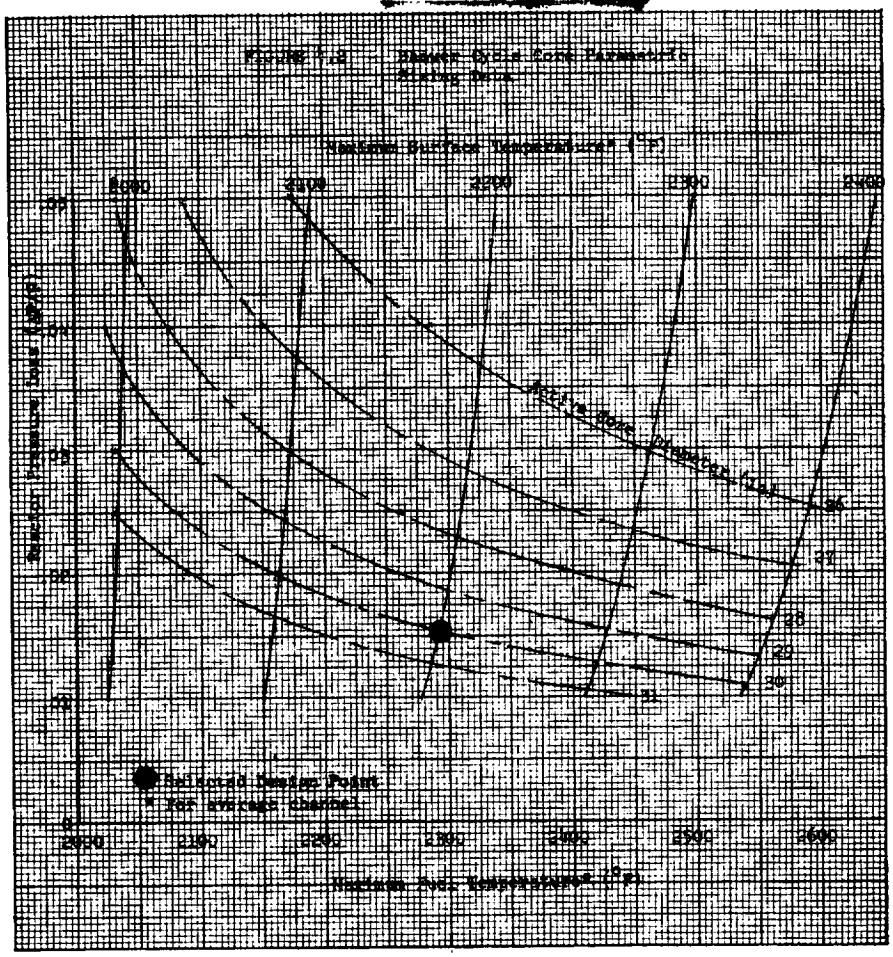

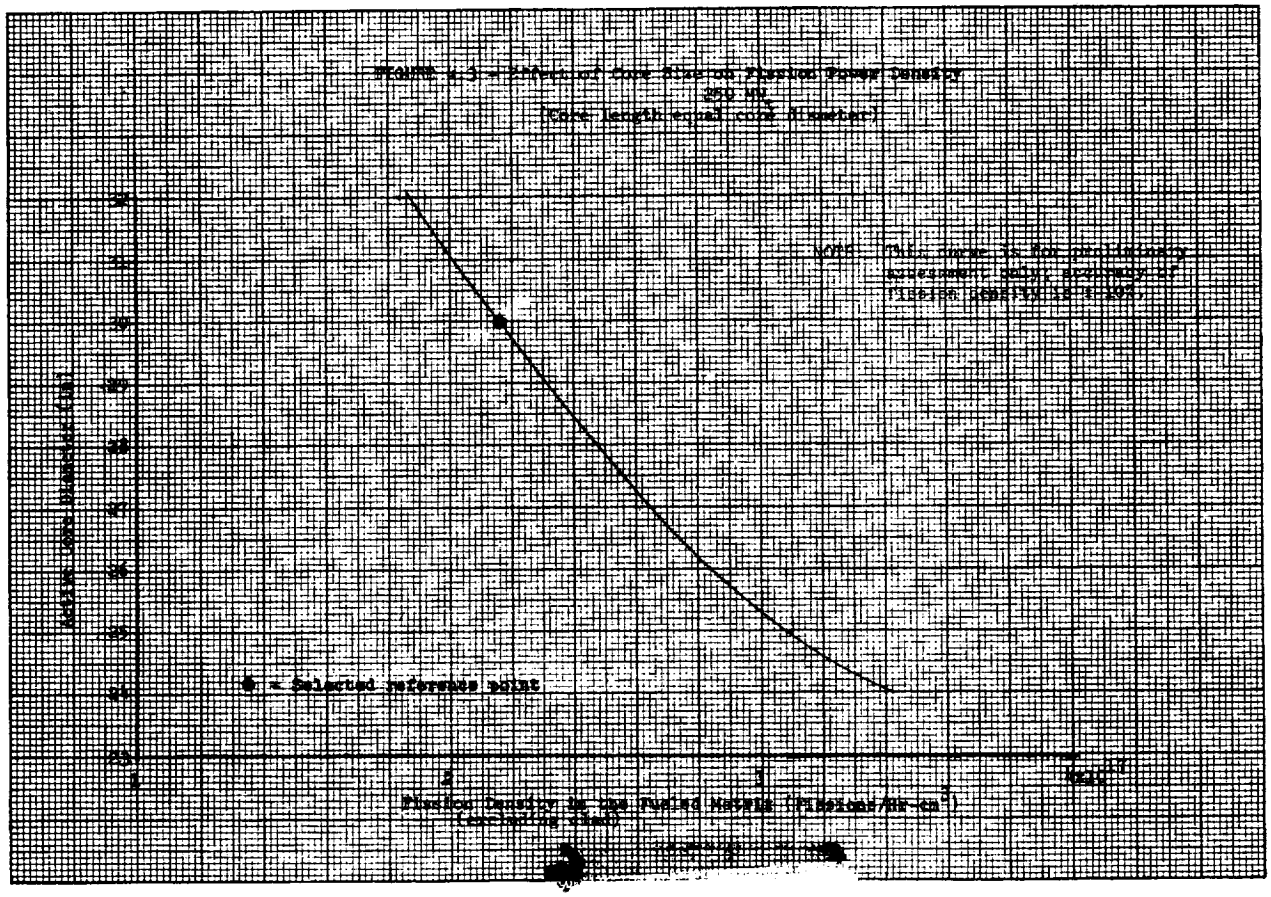

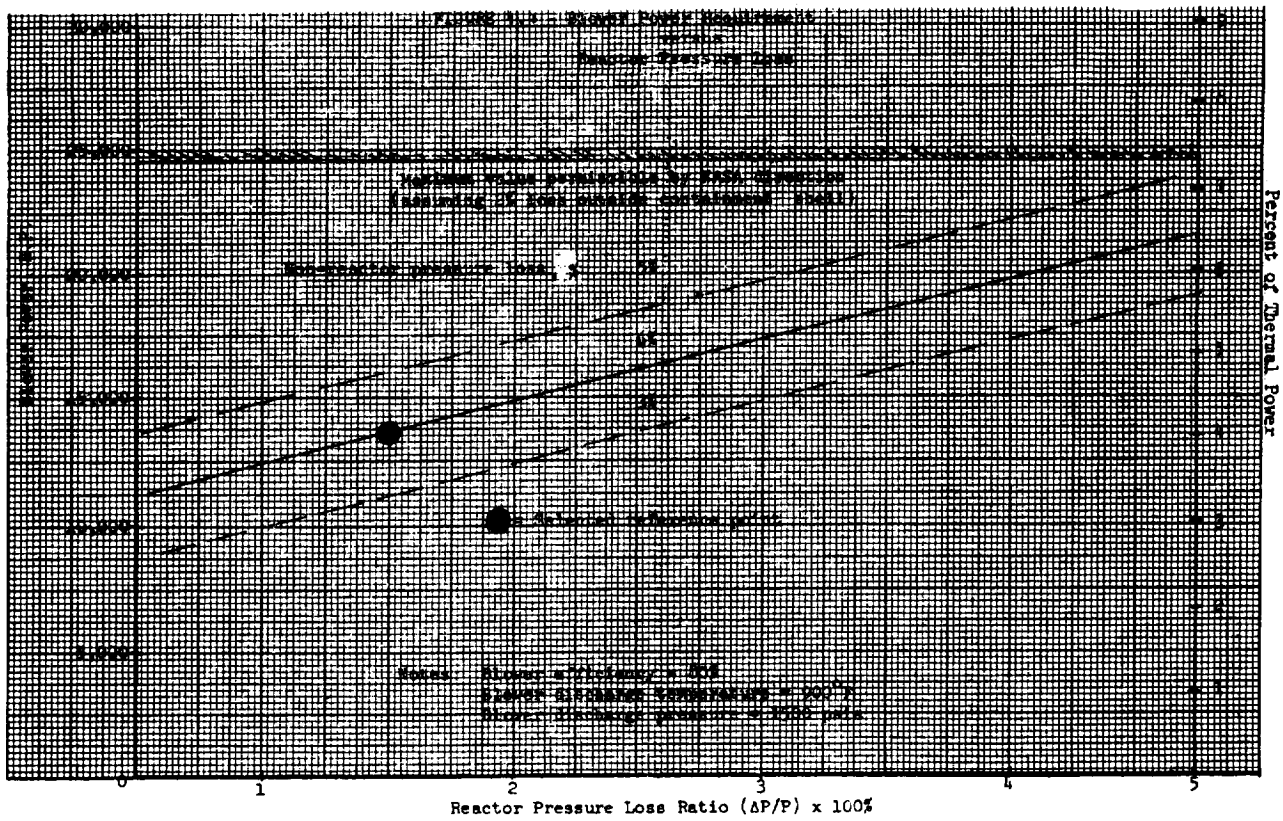
Percent of Thermal Power
Reactor Pressure Loss Ratio (ΔP/P) x 100%
0
1
2
3
4
5

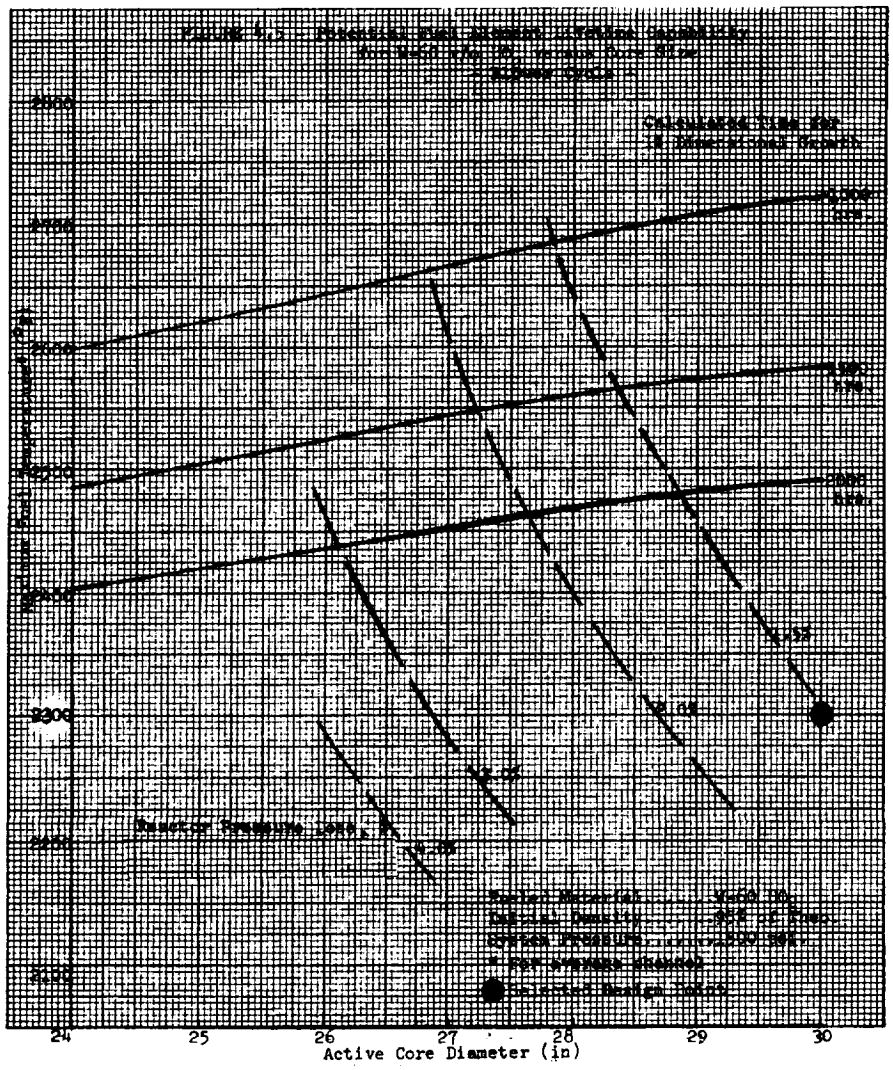
Active Core Diameter (in)
24
25
26
27
28
29
30

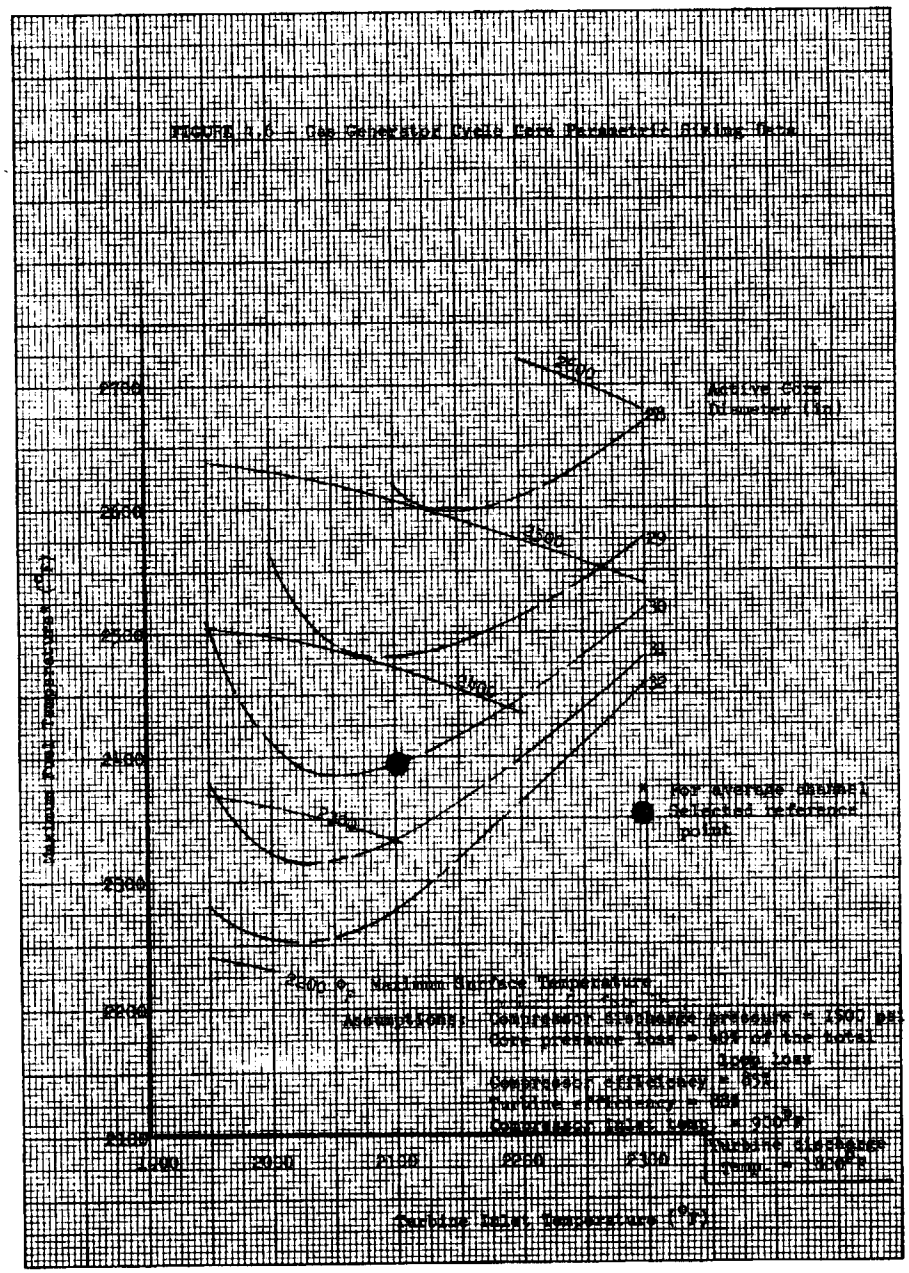

FIGURE 5.6 - Gas Generator Cycle Core Parametric Sizing Data

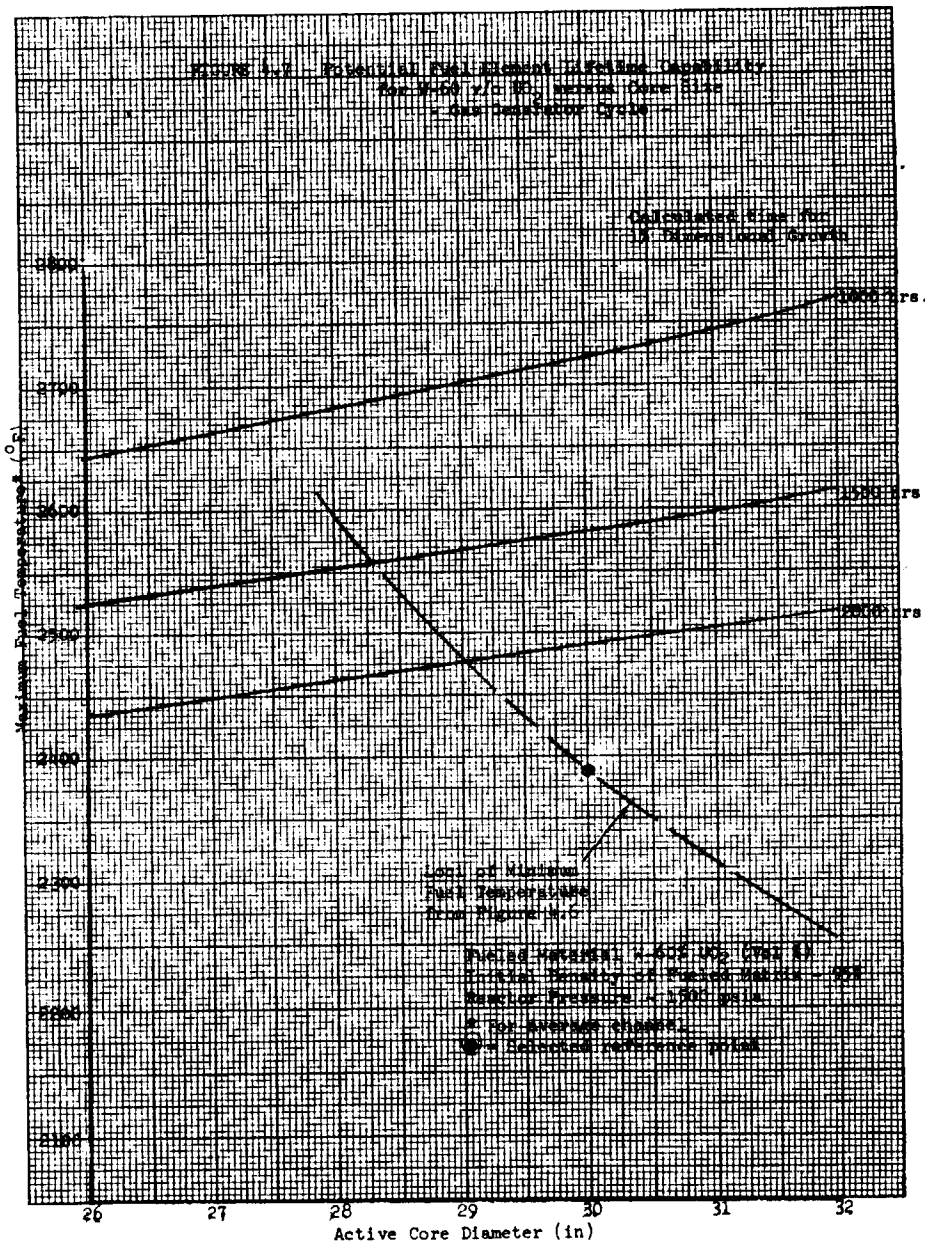

FIGURE 5.7 - Potential Fuel Element Lifetime Capability for W-60 v/o UO_2 Across Core Size - Gas Generator Cycle -

CONFIDENTIAL

UNCLASSIFIED

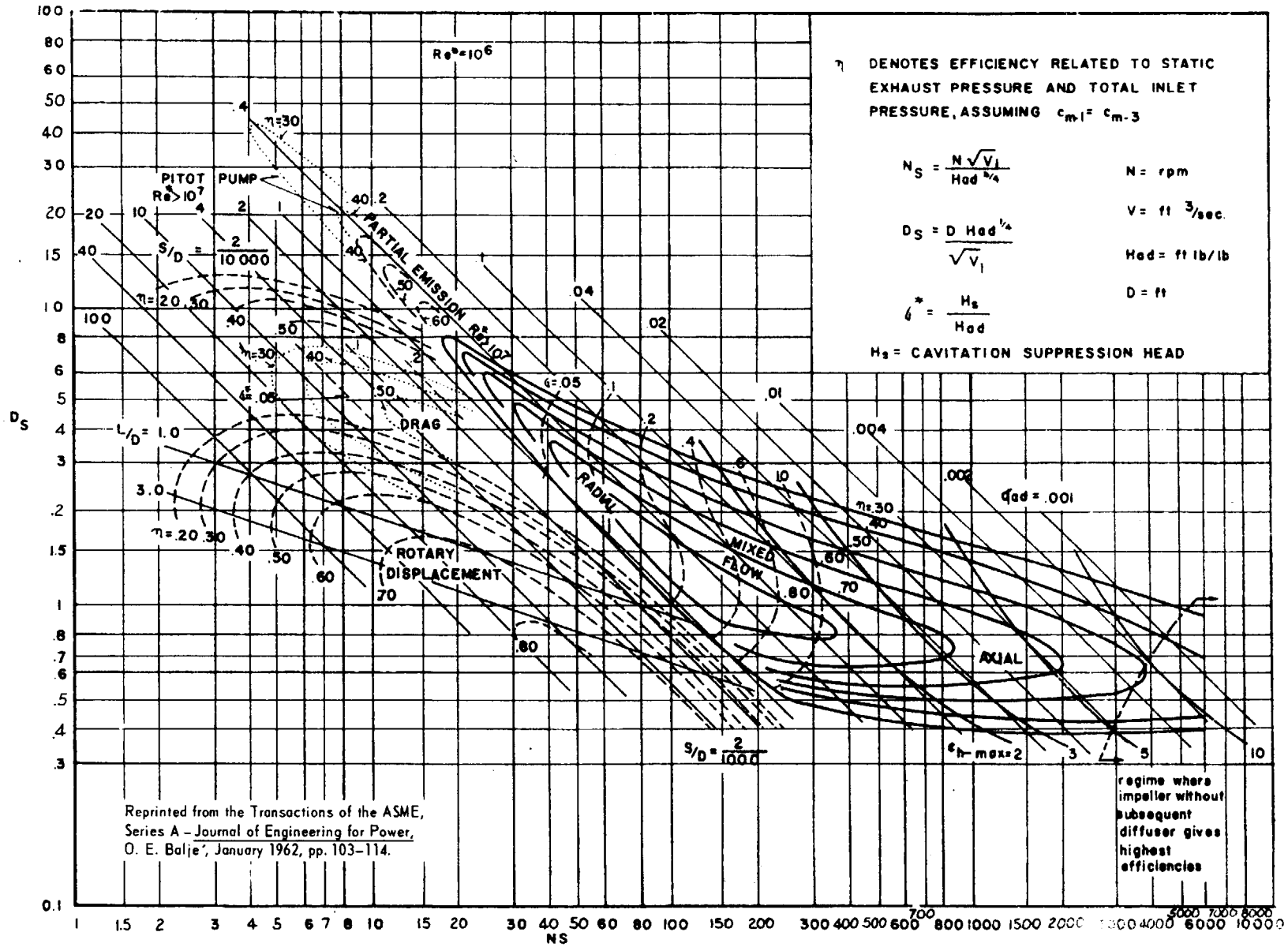

Reprinted from the Transactions of the ASME, Series A – Journal of Engineering for Power, O. E. Balje', January 1962, pp. 103–114.

Fig. 4.8 – **Approximate N_sD_s-diagram for single-disk pumps and low-pressure-ratio compressors**

UNCLASSIFIED

[redacted]

FIGURE 4.9
CIRCULATOR TIP SPEED VERSUS STAGE PRESSURE RISE

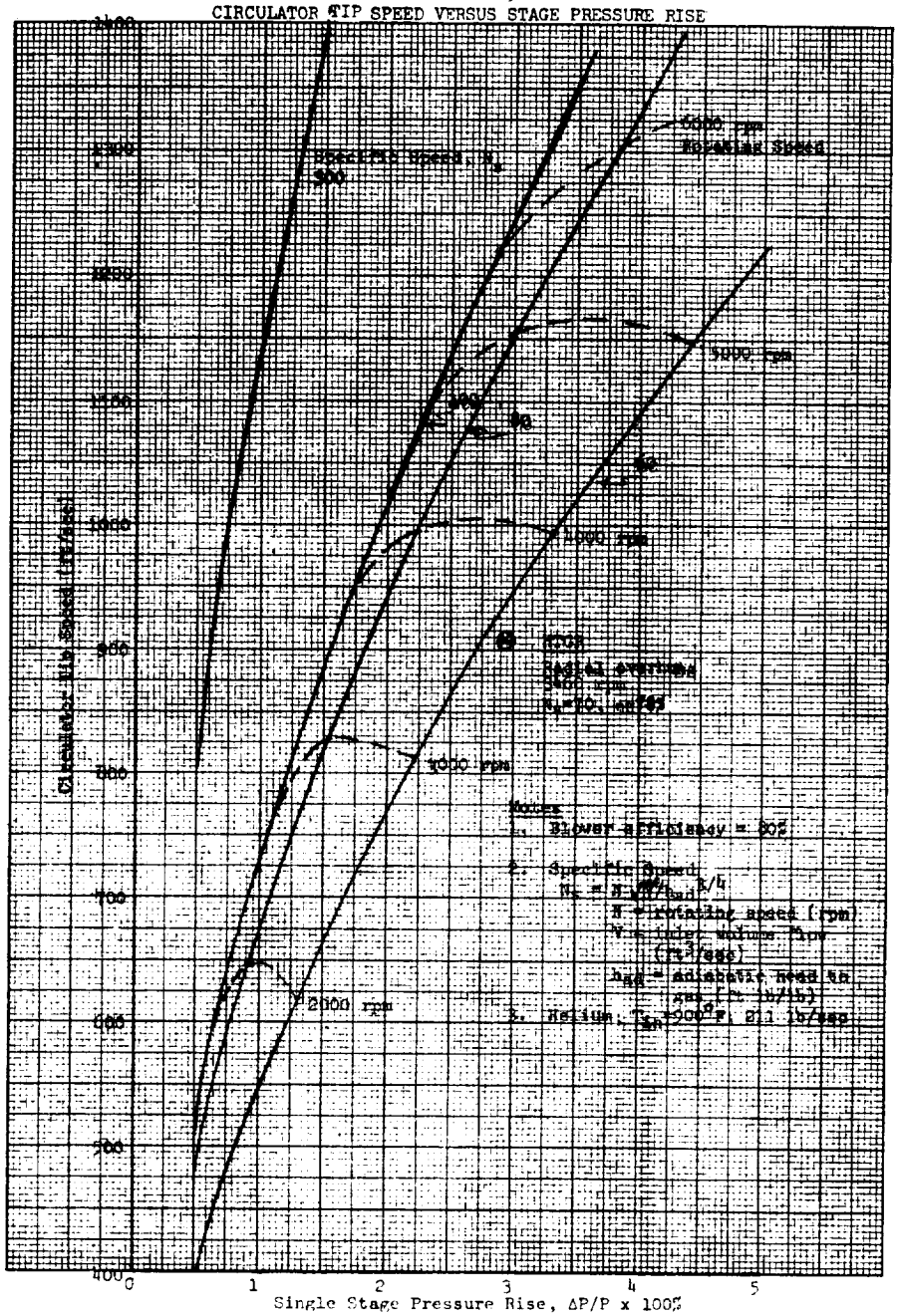

[redacted]

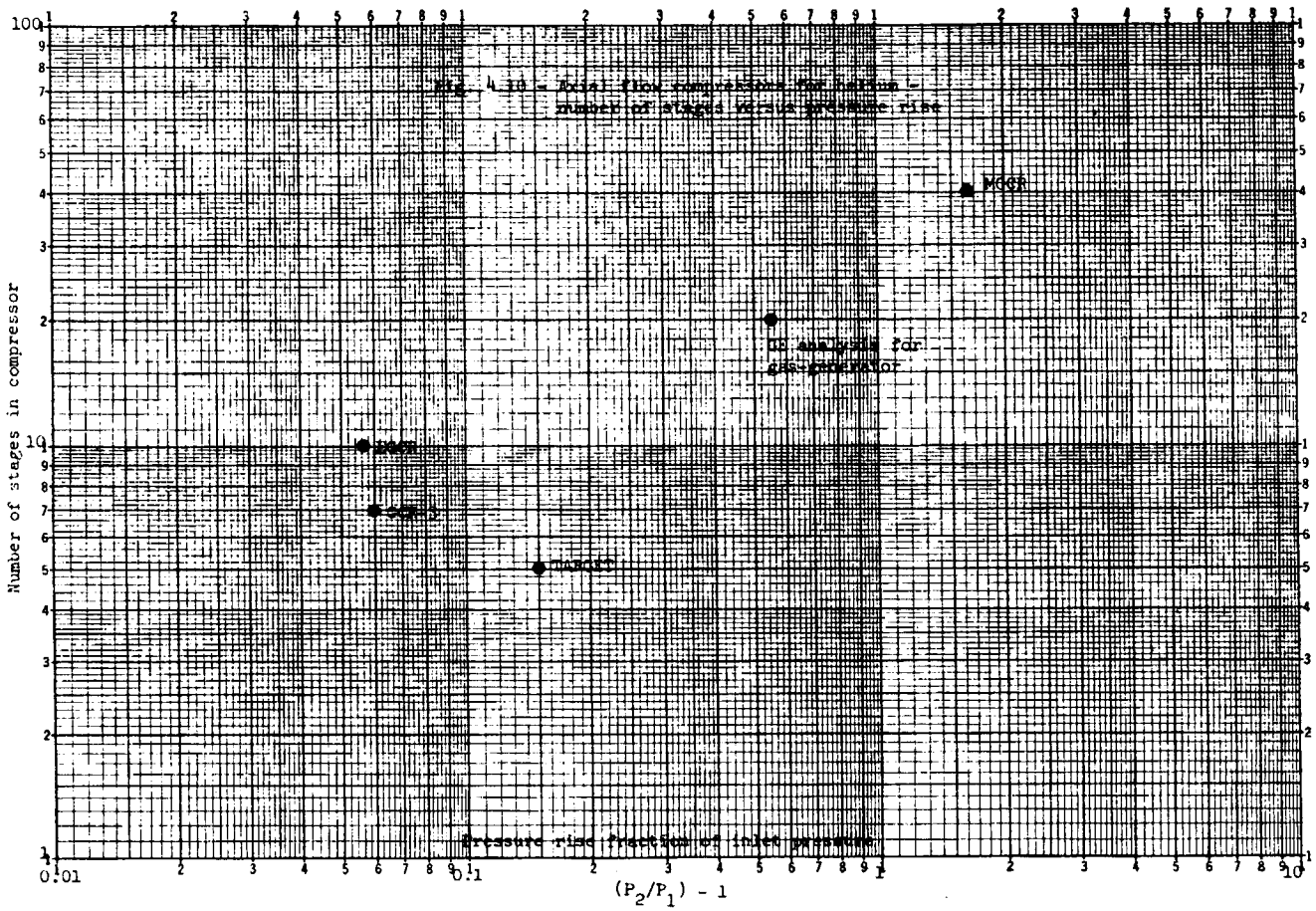

Fig. 4.10 - Axial flow compressors for helium - number of stages versus pressure rise

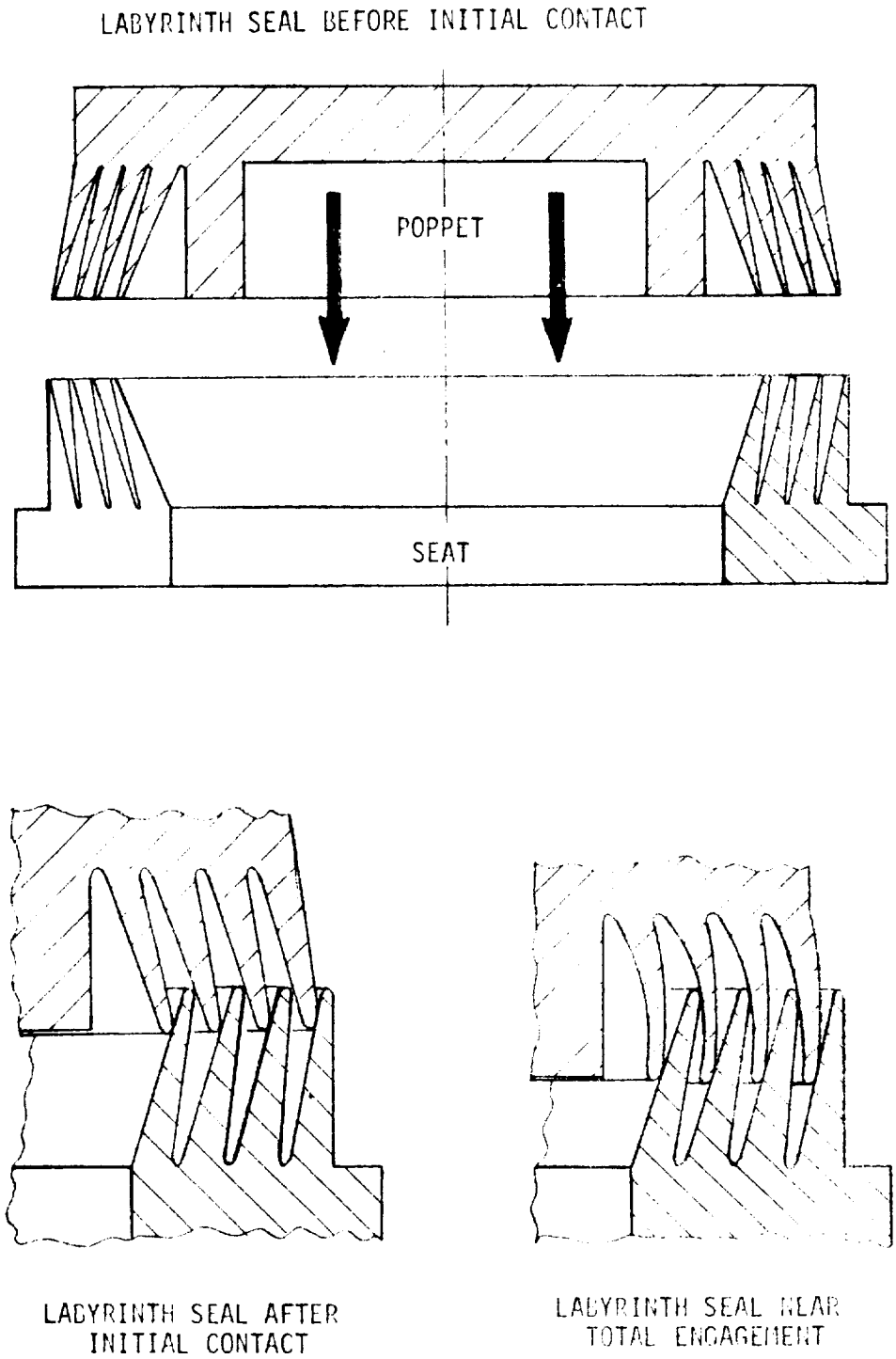

Fig. 4.11- Cone Labyrinth Valve - Prototype Version

5. REACTOR

5.1 GENERAL

This section presents the conceptual design of the reactor assembly evolved for the application of the 710 Reactor technology to aircraft propulsion. Design and analysis, evaluation, and identification and assessment of problems are covered for the mechanical, nuclear, and thermal areas. A summary of design values and state-of-the-art values for reactor design data is given to establish areas in which differences exist and to determine the magnitude of problem areas; applicable development work necessary for solving such problems is identified, and current work underway is discussed. Finally, an overall assessment and discussion of problems and work required for achieving the required design conditions is given for the materials, reactor assembly, fuel elements, and reactivity control system.

5.2 MECHANICAL DESIGN AND ASSESSMENT

The mechanical design and assessment are presented in the following for the reactor assembly, fuel element, and reactivity control system. Design criteria, analysis and parametric data, and design layouts are included. State-of-the-art performance, problem areas, and applicable development work currently underway are identified and discussed for critical individual mechanical components.

5.2.1 Reactor Assembly Conceptual Design and Assessment

DESIGN CRITERIA

In addition to the operational constraints specified in section 1.2, the following design criteria were used for the reactor assembly:

1.* The reactor assembly must be structurally capable of withstanding normal flight loads; i.e., maximum maneuvering load of 2.5 g and gust load of 3.5 g. Operational loss of the reactor is assumed in the event of an aircraft crash although it remains completely contained within the containment vessel.
2.* Required lifetime of structural components at full power and design temperature levels is 2000 hours, with a design goal of 10,000 hours.
3.* Number of temperature cycles from minimum to maximum temperature levels will be 200, maximum. Factors or components that limit rate of change in power or temperature are to be identified.

*Technical direction - R. E. Hyland, NASA, to R. E. Motsinger, GE-NMPO.

4. Structural components within the reactor - shield assembly will be exposed only to inert gas or to water containing a soluble boron compound.
5. Average temperature levels may transiently exceed those for normal operation to the extent determined to be feasible.
6. Clearance gaps between fuel elements will be sufficient to allow for thermal expansion, for tolerances on fuel element straightness and twist, and for a maximum of 1 percent linear growth of the fuel elements due to gaseous fission product buildup.

ARRANGEMENT STUDY

Conceptual arrangement studies were based on the following objectives:

1. Use of multiple, small-diameter, convoluted ducts to reduce the loss of shield effectiveness introduced by duct penetrations, and at the same time maintain low friction and turning losses in the gas stream.
2. Limit the thickness of structural material between the core and radial reflector in order to maintain a high value of reflector swing worth for reactor control.
3. Maintain a series cooling circuit for the primary gas loop, i.e., all gas entering the reactor containment vessel should flow through the fuel element with no bypass or mixing required. This reduces the problems of maintaining proper flow and temperature distribution during off-design operation.
4. Separate the gas and water containment structures so that the loss of pressure in one system would not influence the other. (This objective was subsequently discarded as unnecessary.)
5. Obtain essentially an isothermal structure in order to reduce the magnitude of thermal stresses, stress concentrations, and differential thermal expansions.
6. Restrict the number of valves that require closing during emergency shutdown to reduce or eliminate possible sources of potential leakage.

Several possible approaches for satisfying these objectives were explored, and the arrangement drawings prepared during this phase of the study are illustrated in summary form in Figure 5.2.1. Two of the approaches use a pressure vessel surrounding the reactor and radial reflector (Figure 5.2.1a and b); while the third uses the containment shell as the reactor pressure vessel (Figure 5.2.1c). Figure 5.2.1a and c show the radial reflector bathed in borated shield water and Figure 5.2.1b shows the radial reflector separated from the shield water. Results of a study of the reflector control worth with and without the borated water show that either method can be used without significantly reducing the reactivity worth of the radial reflector, regardless of whether it is beryllium or molybdenum (see Table 5.3.3).

Accordingly, the choice between either approach depends upon other considerations; the decisive factor was believed to be the probable shielding benefit of having the shield water as close to the active core as possible, thereby reducing the amount of radiation from secondary gammas in the reflector and structural components outside the active core. Use of the shutter or venetian blind type mechanism inherently accommodates this scheme, provided the torque requirement for the control actuator is not unduely increased by the drag forces introduced by the water; as discussed in section 5.2.3, this was found to be of no consequence, and the shutter type of reflector removal was adopted. Therefore, the concept shown in Figure 5.2.1b was not considered further.

With the shield water surrounding the reflector, the cylindrical shell between the active core and shield water could become prohibitively thick from a control worth viewpoint unless the shield water pressure were balanced with the gas pressure. However, the gas pressure of 1500 psi is the same as the design requirement of the containment shell, and if the shield water surrounding the reflector must be pressurized, the next logical step is to let the containment shell become the reactor pressure vessel.

Considering the fact that the ducting and the cylindrical shell (flow divider) between core and reflector are bathed in water and can be water-cooled provided insulation is incorporated on the gas side of the ducting, the concentric ducting arrangement into and from the reactor is no longer necessary. Thermal expansion strains can be significantly reduced by maintaining the structural temperatures essentially at water temperature. The pressure losses in the primary coolant gas can be significantly reduced by having the flow pass only once through the reactor, rather than the twice-through path required with the concentric duct scheme.

Accordingly, the duct arrangement of Figure 5.2.1c is preferred. The engineering layout drawings of the two discarded concepts are included in Appendix B.

DESIGN LAYOUT

The drawing of the selected arrangement with the reactor inside the containment shell is given in Figure 5.2.2. The reactor assembly is vertically supported from the top of the containment shell. A conical structure is attached to the cylindrical vessel separating the core and reflector, i.e., the flow divider between the helium coolant and the shield water. The front tube sheet for the reactor fuel elements is attached to this same cylinder. The fuel elements are suspended from the front tube sheet by a cantilever attachment (details of this part of the design are discussed in section 5.2.2).

This arrangement meets all the objectives listed in the preceding section ("Arrangement Study") and has the following additional attractive features:

1. The load path from the containment vessel to the front tube sheet is direct. The gas ducts are not required as structural members and can be designed to accommodate flexure.

2. The reflector control concept excludes the need for any waste space that is normally required for actuation or displacement of the control element. Borated shield water completely surrounds the reflector shutter, with access to the region immediately outside the active core.
3. The relatively small core size inherent from the use of the fast-spectrum 710 Reactor, in conjunction with the reflector control concept of item 2, above, provides a relatively large space between the reactor and containment shell for the inclusion of neutron and gamma shielding materials.
4. The actuators and supports for the reflector control segments are integral with the reactor support structure, providing a good base for maintaining alignment. The number of gas ducts and reflector segments has been chosen so that each segment can be controlled with its own actuator, the drive shafts passing between ducts.

There is no rear support for the fuel elements in the present concept but one may be desirable depending upon the results of detailed design analysis. The two important considerations, in this respect, are: (1) vibration frequency of the fuel element as compared with excitation frequencies to be expected in the aircraft, and (2) direction and magnitude of bowing of the fuel elements to be expected with and without the rear support because of differential thermal expansion and permanent growth due to fission product pressure. In the present design, the direction of the bowing of the fuel element is such that the effect upon the temperature coefficient of reactivity is negative.

Since water is used to cool the ducting, flow divider, and containment shell, the temperature difference between these components is small, minimizing differential thermal strains. Preliminary estimates indicate that, for water temperatures possible at 1500 psia pressure, strains due to expansion of the flow divider and gas ducts should not be a problem. Additional design attention should be given to the attachment of the gas-cooled front tube sheet to the flow dividers, but any potential problem should be solvable by application of current state-of-the-art design practice. Aftercooling with the elimination of water cooling, and concurrent depressurization of the primary coolant* in such a manner that gas temperatures are essentially the same as those during normal operation, could introduce differential thermal expansion strains during the shutdown operation that exceed those for normal operation. Consideration must be given to the actual conditions expected during the shutdown transient. The secondary coolant passages on the flow divider and ducts must be sized to provide sufficient aftercooling flow when gaseous coolant replaces the water.

To control the shield liquid pressure in this system, a gas-to-liquid accumulator must be used to regulate the water pressure, with the amount of gas charge in the accumulator being a function of the reactor core gas pressure. In this concept, the reactor core pressure is applied to the gas side of the accumulator after it has been reduced by some constant

*At a rate not to exceed the decay rate of afterheat generation.

pressure differential (e.g., 150 psi). The gas accumulator then pressurizes the liquid system to that of the gas less the pressure drop across the pressure reducer. The same effect can be obtained by spring loading the liquid side of the accumulator with a spring equivalent to the desired differential pressure load. To allow for volumetric expansions, leaks, or other losses or gains, a makeup liquid system would be required. This system would be operated to maintain the fluid at some desired level in the accumulator. The makeup system would consist of the pump, reservoir, and a flow modulating valve. A three-position valve may be sufficient: no-flow, full-flow, and half-flow. The reservoir might also be pressurized by reduced gas pressure to permit a smaller pumping pressure ratio. Sizes of the reservoir, pump, accumulator, and valves can be determined by liquid makeup requirements, rate of response, and accuracy requirements.

The reactor containment vessel is to be designed to accommodate two operating conditions: normal operation, and an emergency condition involving core meltdown. Because an ultimate capability of containing 1500 psi internal pressure and 3000°F for 1000 minutes is specified, refractory materials were considered for strength with an outer cladding for oxidation protection. Tantalum alloy T-111 (Ta - 8W - 2Hf - 0.01C) was selected because of its high strength and fabricability, and because its physical properties are relatively well known. Using available Larson-Miller creep data, it was determined that approximately 6 inches of T-111 or T-222 (Ta - 9.5W - 0.01C) would be required to meet the specified conditions (see section 3.3).

The following guides were used for selecting the type of valve for the gas duct penetrations of the containment shell:

1. In the open position, the valves should impose the least possible resistance to normal coolant flow.
2. Valves should be located so that no leakage will result even under crash and impact loading conditions.
3. To restrict the number of valves, only one inlet and one exit duct penetration should be included in the containment vessel.
4. Since the valves are to be used only for emergency conditions, only one closure operation is required, and reopening is not necessary.
5. Because of the high-temperature operating requirement, only valves with metal-to-metal contact surfaces should be considered.

A cone-labyrinth valve that conceptually satisfies these objectives is shown in Figure 4.11. For this specific application, the valve could be constructed of a Ta or W alloy with the valve seat of a softer refractory material such as pure Ta to help provide the proper valve-seat deflection required for leak-tight closure. An external high-pressure inert gas supply would energize the valve actuator. Sticking of the piston is not anticipated because internal gas leakage is not objectionable and large clearances can be provided.

[redacted]

CONFIDENTIAL

ASSESSMENT OF PROBLEMS AND CURRENT STATE-OF-THE-ART

In the reactor assembly conceptual design, the problems which have been identified are summarized and discussed below.

1. Use of the containment shell as the reactor pressure vessel - The fundamental reason for this approach is the desire to use radial reflector removal for reactivity control and to bathe the reflector with shield water so as to make the best possible use of available space. The swing worth of the radial reflector is dependent upon having the least possible structural material between core and reflector. This can be accomplished by pressurizing the water, and keeping a balance between helium pressure and water pressure so that the cylinder between core and reflector becomes only a flow divider. A concept for maintaining this pressure balance has been identified and is believed to be possible using conventional equipment, but engineering development of the necessary hardware components will be required to demonstrate capability and reliability.
2. Need for the containment shell to withstand 1500 psia at 3000°F for 1000 minutes - The results of the materials evaluation (section 3.3) show that containment shell thickness should be approximately 6 inches when the best available refractory metal alloy (T-111 or T-222) is used. Also, all conventionally used oxidation-resistant cladding materials have melting temperatures below 3000°F, and development is required to identify and apply suitable oxidation-resistant coatings. Need for additional strength data and fabrication development for the refractory-metal thicknesses of interest is discussed in section 3.3.
3. Need for a rear support for the reactor fuel elements - A lateral support at the rear of the fuel elements may be desirable but the consequences of its use on bowing of the fuel elements have to be evaluated.
4. Aftercooling the reactor structure - Differential thermal expansion problems are not expected if full-flow aftercooling is possible for a sufficient time after shutdown to reduce the reactor discharge gas temperature to such a level that the gas-duct temperature does not significantly exceed its temperature during normal operation with water cooling. Depressurization of the primary coolant is required, however, by operational constraints such that the discharge gas temperature could remain constant or, if the rate of depressurization is not properly controlled to match the rate of afterheat decay, could even increase after shutdown. Aftercooling of the gas ducts is required therefore, after reactor shutdown by a gas coolant separate and apart from the primary gas stream.
5. Containment vessel closure valves - The valves for the gas ducts proposed as a result of this study effort can conceptually meet the requirement of containment as well as the vessel itself, but the conditions imposed are much more severe than previously met by available equipment. Engineering development tests are necessary to demonstrate the ability of the concept to function as required.

CONFIDENTIAL

Valves for the water lines penetrating the shell are also required. The requirement of draining all the shield water within 20 seconds requires additional conceptual design work, with better definition of the shield arrangement between the reactor and containment vessel, in order to determine feasibility of meeting the requirement. No serious obstacle to achieving the design goal is apparent, presuming the same type of valve closure is used for the water lines as for the gas ducts.

APPLICABLE WORK UNDERWAY

The problems with respect to reactor assembly conceptual design are uniquely introduced by the requirements for aircraft application, principally the requirement for absolute containment after aircraft crash. The work done in the 710 Reactor Program has provided a basis for establishing design concepts which are believed to be within the current state-of-the-art of high-temperature refractory metal technology. There are no identified barrier problems, but detailed engineering work is required to apply relatively well-established information, followed by proof-tests to demonstrate the capability of the design to meet the imposed conditions. Further engineering study of the shield configuration and of the transient behavior of the reactor assembly during and after crash of the aircraft may permit sufficient alleviation of the design performance required of the containment vessel that demonstration of its capability may also become a matter of thorough proof-testing. This type of proof-testing is not currently underway, but would be a part of the preliminary and final design effort to meet the specific conditions finally imposed.

CONFIDENTIAL

5.2.2 Fuel Element Conceptual Design and Assessment

DESIGN CRITERIA

1. Fuel elements must meet the same requirements as the reactor assembly except that the required lifetime is 1000 hours. Modifications in the design, if any, required to achieve 2000 hours lifetime are to be noted.
2. Fabrication procedures are to be consistent with those developed for the 710 Reactor under AEC Contract AT(40-1)-2847. The minimum fueled-meat ligament thickness is to be not less than 0.015 inch. Cladding thickness for the coolant channel and outer hexagonal enclosure is to be 0.010 inch.
3. Sufficient clearance is to be provided between adjacent fuel elements to prevent contact during reactor operation. A total gap of 6 percent of the fuel element width is provided in the design, allowing for dimensional tolerances, thermal expansion and deflection of the fuel element, and permanent growth due to fission product accumulation. Of the 6 percent, 1 percent is allowable for growth because of gaseous fission product pressure.
4. The fuel elements are to be supported from a front tube sheet by means of a cantilever attachment designed to meet the load conditions imposed upon the reactor assembly. Provision is to be included for differential thermal expansion between the front tube sheet and the fuel element. A suitable seal is to be provided to prevent leakage of the coolant gas from the path leading to the fuel element coolant channels.

ANALYSIS OF ALLOWABLE FUEL BURNUP

Parametric analyses were made of the allowable fuel burnup based on the criterion of 1 percent permissible linear growth due to gaseous fission product pressure. These analyses were done for both the W-UO_2 and the Mo-UO_2 fueled core compositions, for UO_2 volume fractions of 40, 50, and 60 percent, and for cermet matrix densities of 90, 95, and 100 percent of theoretical. Time of operation elapsed before reaching a permanent growth of 1 percent was calculated as a function of temperature level and power density.

The cladding is excluded from the calculation, since the cladding volume fraction varies from one design to another, depending on the coolant channel size; for the current reference design, the power density can be converted to include the cladding by multiplying the quoted power density by the factor 0.806, which is the ratio of fueled core volume to the total metal volume including cladding. Therefore, the results of the analysis can be applied generally, without the necessity of a correction for cladding volume fraction.

[redacted]

The analytical model and method of analysis used for this study are extensions of the method developed by Foreman[1] and used by Chubb and Paprocki[2] to determine the swelling of fuel only. The Foreman model is simply a sphere with a concentric spherical cavity in which all the fission gases are assumed to collect. The extension of the Foreman model consists of using a composite (two-material) sphere to represent a matrix-type material. The analytical model used in this case is shown in Figure 5.2.3. Growth due to the accumulation of solid fission products is in addition to that of the gaseous products considered in this analysis. The effect of solid fission products was not included in the present analysis since it becomes significant for fission product accumulation levels about one order of magnitude higher than in the reference design.

The basic assumptions underlying the analyses are:

1. The constraint upon swelling due to the cladding is neglected.
2. The only significant deformations caused by the gaseous fission products are those due to second-stage creep.
3. The second-stage creep behavior of the materials can be represented by a power law of the form

$$\dot{\varepsilon} = Ae^{-Q/RT}\sigma^n$$

where $\dot{\varepsilon}$ = creep rate
σ = stress
Q = activation energy
R = gas constant
T = absolute temperature
A, n = material constants

4. The fission gases obey the ideal gas law.
5. The fission gases remain in the fuel particle and nucleate to many small uniformly distributed "bubbles" in a time which is small relative to the time for creep deformations to occur.
6. There is no swelling until the fission gas pressure exceeds the system pressure.
7. There is no change in the creep properties due to the irradiation effects.
8. The gaseous fission product yield is 8.64×10^{-25} gram-moles per fission for the temperature range of interest.

Calculations were performed using methods developed for the 710 Reactor Program. Results of the analysis are presented in Figures 5.2.4 through 5.2.21. The curves show the calculated time to 1 percent growth versus temperature of the cermet element when operating at various power densities (fissions/cm^3-hour). The data in Figure 5.2.11, for W - 60UO_2 (vol. %) of 95 percent of theoretical density were used for estimating the

---

[1] A.J.E. Foreman, "Calculations of the Rate of Swelling of Gas Bubbles in Uranium," AERE-TM-134, March 1956.

[2] W. Chubb and S. Paprocki, "Development of Advanced High-Temperature Nuclear Materials During November 1964 through January 1965," BMI, BMI-1716, February 1965.

burnup capability using the 1 percent growth criterion for the current reference design (section 4.2). The data for the remaining compositions, together with the nuclear parametric data of section 5.3.2,* can be used to estimate reactor size and fuel element lifetime for other designs which may subsequently be of interest.

System pressure was assumed to be 1500 psi; this parameter is of importance since the analysis presumes that no growth can occur until the gaseous fission product pressure exceeds the system pressure. Therefore, the analysis implicitly assumes that there will be no prolonged periods during which the fuel material is at operating temperature in the absence of external pressurization. Therefore, to avoid the possibility of growth after shutdown, i.e., after depressurization of the system, the fuel temperature should be reduced by at least 100°F as soon as possible and then to lower temperatures, as convenient, to take advantage of the higher creep strength of the tungsten matrix.

To check the validity of this analysis, analytical predictions were compared with experimental data obtained from the AEC-funded programs at GE-NMPO. The imposed conditions of temperature, burnup rate, and total burnup, together with the calculated and measured values of the diametral growth, are summarized in Table 5.2.1. The ratio of the experimentally measured-to-calculated diametral growth is plotted in Figures 5.2.22 through 5.2.26 respectively as a function of burnup rate, total burnup, temperature, number of thermal cycles, and total time at the test conditions. These figures show that there is no well defined trend as a function of any of these parameters and that the calculated values are conservative. The calculated growth values for the Mo-UO_2 matrix specimens (LTFF-10 and LTFF-12) are appreciably more conservative than for the W-UO_2 matrix specimens. This result was expected since the creep data used for the Mo is based on data for arc-cast Mo, whereas the Mo in the matrix of the experimental specimen is basically a powder-metallurgy product, which is believed to be more creep-resistant than the arc-cast material. It is not yet clear why the one W-UO_2 specimen (LTFF-8) exhibited such low growth relative to the other W-UO_2 specimens; however, the presence of ThO_2 in the W matrix may have resulted in a dispersion-strengthened effect. The dimensional measurements on the LT-710-1 specimen are not yet complete; however, it is clear from the extremely small magnitude of the calculated growth (0.04%-see Table 5.2.1) that the correlation between the measured and calculated values cannot be expected to be nearly as good in this case since the tolerance of the measured value is ± 0.06 percent.

In summary, this comparison shows that the analysis overpredicts the amount of permanent growth to be expected and is, therefore, conservative.

---

* The nuclear data is for the W-UO_2 system only, but use of Mo-UO_2 would result in cores with slightly higher excess reactivity.

STEADY-STATE AND CYCLIC STRESS ANALYSIS

Stress analysis of the 710 Reactor fuel element has been emphasized in the 710 Reactor program to gain a good understanding of the behavior of the fuel elements during operation. Stress analysis methods[3] have been developed for the matrix-type fuel element including a plane - strain plastic-visco-elastic computer program[4] to carry out the stress analysis. The analyses were designed to:

1. Define the loading conditions
2. Evaluate the relative sensitivity of the stresses and strains associated with the various loads and thermal conditions at the design-point operating conditions
3. Provide a preliminary evaluation of the magnitude and direction, i.e., shrinkage or growth, of possible ratchet mechanisms associated with cyclic operation of the element
4. Further evaluate the mechanical properties data requirements for the final analysis phase
5. Provide information to aid in the evaluation of the current fuel element tests and to further define future fuel element test requirements
6. Define the analytical models to be used in the final fuel element analysis
7. Provide background information to aid in the evaluation of alternative materials, design details, and modes of operation.

The design-point loading conditions evaluated to date have been for static conditions, primarily for correlation with results of static tests without dynamic loading. As only limited mechanical properties data were available for the specific materials used in the fuel elements, it was necessary to extrapolate and interpolate the existing data as well as to use data from the literature, where available. Consequently, the results are viewed as preliminary and primarily qualitative. The magnitude, including direction, of the results are believed to be correct and have been substantiated by experimental testing. Results and conclusions are not presented herein as they are valid only for the specific fuel element geometry and operating conditions analyzed, since the creep properties of the materials are very strong functions of both stress and temperature. However, results and conclusions for the 710 Reactor fuel element are presented in footnote 3.

The loading conditions considered for this analysis are applicable to any matrix-type fuel element and discussed below.

---

[3] J.E. McConnelee, "710 Experimental Reactor Fuel Element - Preliminary Stress/Strain Analysis," GE-NMPO, GEMP-370, June 28, 1965.

[4] J.P. Yalch, "Plane - Strain Plastic-Viscoelastic Deformation of a Composite Tube," GE-NMPO, GEMP-415, June 1966.

Other than the dynamic loads incurred during normal operation of the vehicle, the loading conditions on the fuel element are primarily static in nature. The thermal transients are all much too slow to involve any inertial thermoelastic coupling effects. There should be no flow-induced vibration as there is no back-side flow. Also, a review of Los Alamos data[5] indicates that there should be no Helmholtz or pipe organ type of flow-induced vibration in the fuel element.

The static loads on the element are summarized below.

Steady State Loads

1. Mechanical (see Figure 5.2.27)
   a. Dead weight load of the element - This produces a simple axial tensile load which is proportional to the weight per unit length of element and the distance from the bottom of the element.
   b. Drag load associated with the flow through the coolant channels - This also produces a simple axial tension which is proportional to the pressure drop between a specific axial position and the exit end of the fuel element.
   c. Higher internal pressure in the coolant channels relative to the pressure outside of the element - The separation between inlet and exit pressures is at the inlet end of the fuel element. Therefore, the exterior of the element sees exit gas pressure, whereas the interiors of the coolant channels see some pressure $[P=f(x/L)]$ intermediate between the inlet and exit pressures.
   d. Relatively high isotropic pressure component due to the high overall system pressure and small pressure drop through the element - It is well established experimentally that isotropic states of stress do not produce plastic flow in homogeneous and isotropic media. Since this is a compressive isotropic state of stress, its principal effect should be to retard any volumetric growth mechanisms. Hence, it need not be considered in the analysis.
2. Thermal
   a. Local temperature distribution about a single coolant channel - Removal of heat from the element by the flowing coolant produces local temperature gradients in the vicinity of each of the coolant channels. The typical element is so designed that, exclusive of perturbations, each of the coolant channels of a given element will have essentially the same heat flux and the same local temperature distribution relative to the axis of the individual channel. The magnitude of these local temperature differentials will be a function of local power level, thermal properties of the cladding and matrix, and local heat transfer coefficient and bulk coolant temperature.

[5] R.S. Thurston, "Pressure Osciallations Induced by Forced Convection Heat Transfer in Two Phase and Supercritical Hydrogen," LAMS-3070, May 1964.

b. Cladding - matrix and header-plate - matrix differential thermal expansion - The different thermal expansion properties of the cladding and matrix materials produce thermal stresses which are a function of the local temperature level.

c. Local temperature perturbations - Local variations in tolerances, fuel density, etc., can result in local temperature perturbations and associated local high stresses or strains.

d. Axial temperature distribution - The axial variation of power level and coolant properties result in an axial variation in the mean temperature of the element (gross mean across the complete cross section of a single element).

e. Gross temperature differentials across the element cross section - Variation in core power density with radius produces an essentially linear temperature gradient across a typical element remote from the core periphery. As long as the element is not externally constrained, a linear temperature gradient will only produce a simple bowing of the element without stress. The present design philosophy is to provide sufficient clearance between adjacent elements to avoid contact as a result of this bowing. This eliminates the possibility of external constraint.

   Asymmetries of the thermal environment in the vicinity of a given element (particularily near the periphery of the core) may result in gross temperature differentials across the element which are nonlinear and hence would produce thermal stresses. The analysis of these must await the results of the detailed temperature calculations for the final design.

Transient Loads

1. Mechanical
   Excluding vibration, there are no significant transient mechanical loads on the fuel element during normal operation.
2. Thermal
   Since the thermal stresses are all quasi-static in nature, i.e., sufficiently slow that inertia effects can be neglected, the transient thermal stresses are simply treated as special cases of the steady-state thermal stress analysis.

A summary of the elastic stress analysis is shown in Figure 5.2.28. The analytical model, method of analysis, planned evaluation tests, and required material properties are included in this figure.

A preliminary vibration analysis was performed on two 710 fuel elements. The results, shown in Figure 5.2.29, show good correlation between the calculated natural frequencies and the experimentally measured values, when vibrated in the free - free condition, for the 37-channel and 91-channel 710 fuel element configurations. Values for the bending and

longitudinal modes were calculated from the classical equations and the following assumptions:

1. The UO_2 particles are "loose", i.e., they contribute to the mass but not the stiffness.
2. The cross-sectional properties are constant along the length of the element.

The fact that measured frequencies are generally lower than the calculated values was attributed to the presence of the thick header plates at each end of the element which have a greater mass per unit length than the average cross section.

In addition to the two assumptions used in the longitudinal and bending vibrations, it was assumed that the equation for a circular rod could be used and a value of 0.3 was assumed for Poisson's ratio to calculate the torsional natural frequencies.

For preliminary design purposes, agreement is good between the measured and calculated frequencies in bending, longitudinal, and torsional free - free vibration. However, since the fuel elements are to be used in a cantilevered condition and the method of attachment to the tube sheet has not been tested, additional testing will be required to substantiate the calculated natural frequencies of the fuel elements in the reactor.

LAYOUT OF THE FUEL ELEMENT DESIGN

The layout of the fuel element design and the method of attachment to the upper tube sheet are shown in Figure 5.2.30. The fuel element is affixed to the tube sheet with a threaded fastener. Projections on the rear face of the tube sheet assist in aligning the fuel element with the hole in the tube sheet during assembly and resist the torque when tightening the fastener. There is a seal between the aft face of the tube sheet and the forward face of the fuel element to prevent the coolant from bypassing the fuel element. With this method of attachment, the fuel element is cantilever-supported from the front tube sheet.

The fuel elements are hexagonal, 1.73 inches across-flats, approximately 33 inches long, and are fastened to the tube sheet on a 1.834-inch triangular pitch. This provides a 0.104-inch gap between fuel elements to accommodate for differential thermal expansion between the fuel element and tube sheet, fuel element growth, and other factors discussed under Design Criteria.

The fuel element is composed of a fueled section, an upper header plate, and a lower header plate. The fueled section consists of a W - $60UO_2$ (vol. %) matrix within a hexagonal metallic cladding. Coolant tubes, through which the coolant gas passes, extend from the upper header plate through the matrix to the lower header plate. The hexagonal cladding, upper header plate, lower header plate, and coolant tubes are fabricated from W - 30Re - 30Mo (at. %). The upper header plate serves as a plenum to distribute the coolant into the coolant tubes. It contains a groove for a metallic "O" ring that provides the seal to the tube sheet, and is

internally threaded to accommodate the threaded fastener. The rear header plate provides an end seal for the matrix and is dimpled to restrain the fuel element laterally.

The fuel element contains 37 coolant channels, with an average diameter of 0.192 inch, located on a triangular pitch of 0.2821 inch. The hydraulic diameter of the coolant channels is the same in any given fuel element; however, the hydraulic diameter of the coolant channels is varied from element to element across the radius of the core to control the radial temperature distribution. The hydraulic diameter in the center fuel element is 0.209 inch and 0.168 inch in the outermost fuel elements. The pitch is decreased slightly on the inner fuel elements, to 0.2793 inch on the center element, to maintain an outer ligament thickness of 0.015 inch in the matrix. This is considered to be the minimum thickness for economical fabrication of the matrix and for stress considerations.

The calculated weight of the completed fuel element is 25.3 pounds.

Assuming the cross-sectional properties are those of the fueled section and are constant along the 33-inch length of the element, the calculated natural frequency of this cantilever-supported fuel element is 33 cps.

ASSESSMENT OF PROBLEMS AND CURRENT STATE-OF-THE-ART

No significant problems can be identified for the fuel element of the reference design evolved during the current study. The current state-of-the-art capability provided by the AEC-funded programs at GE-NMPO is believed to be equal to or greater than that required. Operational modes identified or discussed in other sections of this report, particularly with regard to reactor shutdown and aftercooling, indicate that transient temperature gradients are modest and insignificant.

The use of hydraulic diameter variation for radial temperature control in the present reference design is possible without difficulty except in the centermost fuel elements, where a reduction of the hole pitch is required to avoid ligament thicknesses less than 0.015 inch at the outer boundary. This is a problem only on cores of relatively large size and, consequently, of relatively high porosity. In the present case, only a small volume of the core is affected and the use of reduced UO_2 volume fraction in the affected elements is possible as an attractive alternative method should further study indicate it to be desirable.

The 0.104-inch gap (6% of the across-flats dimension) between fuel elements for preventing contact of the elements during reactor operation is believed to be sufficient for all factors identified by the design criteria (dimensional tolerances, thermal expansion and deflection, and permanent growth of the fuel element). However, to extend the lifetime of the fuel element significantly beyond 1000 hours, use of hydraulic diameter variation within individual fuel elements may be desirable to reduce temperature and power profiles across a single fuel element. Use of varying hole sizes within a fuel element, per se, is no problem for the fabrication process used with the 710 fuel element; further study is required to determine whether any limitation on this approach might arise from the minimum ligament thickness, buth the limitation, if any, is expected to be minor.

The adequacy of the proposed cantilever support for the fuel element should be determined on the basis of a detailed evaluation of the vibration of the reactor structure as affixed to the vehicle, and should be verified by experimental tests. Although the natural frequency of the fuel element can be increased by the use of a rear restraint, the influence of bowing of the fuel elements due to the temperature differences across the elements in operation must be evaluated.

Sheet and plate forms of the W - 30Re - 30Mo (at. %) alloy are readily available in the required sizes for this fuel element. However, tubing is not yet available commercially. Encouraging progress has recently been made in the fabrication of tubing to the necessary quality level in 15-inch lengths. Achieving the 31-inch-long tubing for this fuel element will be an extension of this work. There is no fundamental limit in the process insofar as fabricating lengths required for reactor use.

APPLICABLE WORK UNDERWAY

Current development effort on the 710 Reactor fuel element is guided by the requirements for space power application, and is comparable with the aircraft requirements as summarized below:

	Space Power Application	Aircraft Application
Lifetime, hours	10,000	>1000
Temperature, ^{o}F	<2800	<2500
Power, Mw_t	1.05	250
Power density in fueled core, Mw/ft^3	0.75	49.3
Total average burnup for design life, fissions/cm^3	3.2×10^{19}	1.92×10^{20}
Fuel core material, vol. %	W - $60UO_2$	W - $60UO_2$
Cladding material, at. %	W - 30Mo - 30Re (Ta - 8W - 2Hf, Mo - 50Re)*	W - 30Mo - 30Re

The lifetime and temperature requirements for space power are higher, but the total fission product accumulation is lower.

The scope of the development effort in the 710 Reactor Program had been established from an evaluation of potential causes of fuel element failure, as identified in Figure 5.2.31 for the space powerplant. Because of the need for a rocket boost, some phases of the space application are concerned with vibration and acceleration forces before the reactor is brought to operating conditions. However, those parts of the program under the "Fuel Cartridge Development and Qualification", i.e., non-nuclear and nuclear tests, are directly applicable. The non-nuclear portion involves high-temperature testing (3000°F capability) with thermal cycling in static gas at atmospheric pressure and elevated-pressure (1000 psig capability), and in dynamic gas at elevated pressure. The nuclear portion involves high-temperature testing with thermal cycling in static gas. Figure 5.2.31 shows that such a program covers all potential causes of fuel element failures except for vibration and g-load effects and interference effects should adjacent fuel elements contact each other.

*Alternative Materials.

[redacted]

All non-nuclear test results derived from this program are pertinent and applicable to the present design except for the influence of geometry factors arising from the relatively higher porosity required in the aircraft application. The fuel element design which establishes reference values for the 710 Reactor development program is listed in Table 5.2.2, with the corresponding data for the average element from the present study shown for comparison.

Through 1966, 66,803 hours of non-nuclear specimen test time had been accumulated. This total includes 44,905 hours of 3000°F static tests of multi-channel and single-channel test specimens; 4990 hours of dynamic testing; and 16,908 hours of testing process development specimens of simple geometry at 3000°F.

To some extent, the in-pile work is applicable, i.e., insofar as the results are correlatable with analysis methods which can then be used for predicting capability for the lower-temperature, high-power-density conditions of the aircraft application. In-pile test specimen LT-710-1 has completed 3000 hours of testing in the LITR C-48 facility at a temperature of 2750° to 2800°F. In-pile test specimen LT-710-2 has completed 2130 hours of a scheduled 5000-hour test at a peak calculated temperature of 2800°F in the LITR C-42 facility. Also, as shown in section 3.2, the range of burnup levels achieved in tests under the AEC High-Temperature Materials Program at GE-NMPO have reached those required in the Aircraft Application (Reference Figure 3.2.13).

Substantial support for the 710 Reactor program has come from the High-Temperature Materials Program and is expected to continue in the areas of:

1. Chemical and metallurgical compatibility of 710 Reactor fuel element materials
2. Fission product retention capabilities of fuel element cladding
3. Burnup capabilities of fuel element materials
4. Radiation effects on the properties of fuel element materials
5. A basic understanding of the physical phenomena in containing UO_2
6. The physical and mechanical properties of fuel element materials.

Nevertheless, additional in-pile work for the specific fuel element design and operating conditions is required for proof-tests; such work is outside the scope of any currently or previously underway.

5.2.3 Reactivity Control Conceptual Design and Assessment

DESIGN CRITERIA

1. The reactivity control assembly is to meet the same requirements, where appropriate, as the reactor assembly, specifically with regard to applied loads, lifetime, number of cycles, and exposure to inert gas or water containing a suitable boron compound.

TABLE 5.2.1

PARAMETERS USED IN FISSION GAS GROWTH STUDIES

Specimen Number	Matrix Composition, vol %	Temperature, °F	Burnup Rate, fissions/cm^3-hr	Total Burnup, fissions/cm^3	Diametral Growth, %	
					Measured	Calculated
LTFF-7	W – 60UO_2	3230 (135 hr) 3600 (192 hr) 3900 (293 hr) 3630 (20 hr)	2.03×10^{16}	1.3×10^{19}	0.88 ± 0.06	1.48
LTFF-8	(W + 0.8ThO_2) – (55.4UO_2 – 3.8ThO_2)	3500	1.93×10^{16}	2×10^{19}	0.14 ± 0.06	1.04
LTFF-9	W – (54UO_2 – 6ThO_2)	3630	1.97×10^{16}	2×10^{19}	0.9 ± 0.06	1.59
LTFF-10	Mo – 60UO_2	3200	1.52×10^{16}	1.3×10^{19}	0.2 ± 0.06	1.67
LTFF-11	W – (54UO_2 – 6ThO_2)	3000	1.3×10^{16}	4×10^{19}	0.5[a] ± 0.06	0.86
LTFF-12	Mo – 60UO_2	3270	1.6×10^{16}	1.7×10^{19}	0.73 ± 0.06	3.44
ORRF-1	(W – 25Re) – 60UO_2	2910	8×10^{16}	7×10^{19}	0.42 ± 0.06	0.84
LT-710-1	W – (53.7UO_2 – 6.5ThO_2)	2800	1.33×10^{16}	4×10^{19}	Post-test examination incomplete	0.04

[a]Estimated value. The actual measurement on the outside of the cladding was 0.8 ± 0.06%. However, since the OD cladding was later found to be unbonded with a gap at the interface, it was assumed this gap would be at least as large as the differential thermal expansion between the cladding and the matrix. Therefore, this value (0.3%) was subtracted from the measured value to obtain an estimate of the dimensional growth of the matrix.

TABLE 5.2.2

710 REACTOR FUEL ELEMENT DIMENSIONS

	Space Power Application	Aircraft Application
Matrix (across-flats), in.	1.426	1.73
Number of coolant channels	19	37
Coolant channel hydraulic diameter, in.	0.135	0.192
Coolant channel pitch, in.	0.329	0.282
Coolant channel cladding thickness, in.		
W-Re-Mo	0.010	0.010
Ta – 8W – 2Hf and Mo-Re	0.015	–
Outer cladding thickness, in.		
W-Re-Mo	0.010	0.010
Ta – 8W – 2Hf and Mo-Re	0.015	–
Active fuel length, in.	14.264	30.0

2. Reactivity control is to be by reflector removal if feasible; internal poison control, if not.
3. A radial reflector of molybdenum immersed in borated water is preferred, if feasible, so as to serve the dual function of shield and control system.

It should be noted that no criterion was established for rate of reactivity removal because the reactor with a nonmoderating reflector such as Mo has no identified positive reactivity effects, either instantaneous or delayed, with increase in reactor temperature. Instead, all identified temperature effects are negative with increasing temperature. Should the reflector be moderating, e.g., Be, a delayed positive temperature coefficient would be present, and specification of the rate of reactivity removal by means of the active control system would be required.

ARRANGEMENT STUDIES

The results of studies of various reflector control schemes in previous design applications of the 710 Reactor, e.g., nuclear rocket and space power plant, gave incentive to consider reflector removal control for this application as well, even though the reactor size for the aircraft application is relatively large. Poison control rods in the active core are unattractive because of the length required for operating travel, the inability of the possible poison materials to operate at the desired temperature, and the possible requirement for pressure vessel penetrations. The concept of rotating drums with poison in the reflector was also rejected because of the negative results of previous studies (see section 5.3.3). Consequently, the nuclear feasibility of physical removal of the reflector was determined first as discussed in section 5.3.3 and then, with assurance on this point, several methods for achieving the reflector displacement were investigated. The several methods are illustrated in Figure 5.2.32. The axial displacement concept (a) was discarded because the travel requirements impose severe limitations on duct design and arrangement. The petal concept (c) requires a complex linkage system for actuation. The rotation of reflector segments (e), the feasibility of which has been demonstrated* in a reactor design, was selected.

Arrangement studies were made with the reflector immersed in borated water or in primary coolant gas, as discussed in section 5.2.1. When immersed in gas, the coolant is the primary gas both during operation and in the aftercooling mode. This scheme is adaptable to the concentric duct arrangement for the shield penetrations. During normal operations, however, a problem exists in directing flow to the parts of the reflector having the highest internal heat generation rate, next to the core, since the reflector segments will be rotated close to their innermost position. A special flow path is required if this scheme were adopted. When immersed in borated shield water, the coolant is water; while forced circulation of the shield water becomes necessary specifically for this purpose, the pumping power is much less than if the coolant were gas.

Consideration of the need to maintain aftercooling flow to the reflector led to the concept of including a flow path down the shaft on which the reflector is mounted, with suitable coolant channels bleeding the flow

*PWAC-471 (CRD) "Reactor and Shield Design Status - SNAP-50" Pratt & Whitney Aircraft Division, United Aircraft Corporation.

from the shaft through the reflector. During normal operation, the coolant is recirculated shield water requiring a water-to-air heat exchanger. After the reactor is shut down and the shield water is drained, the coolant must be a gas. The amount of aftercooling required for the reflector and the quantity of gas supply required for this purpose depends upon the temperature levels permissible in the reflector and its support structure while the aircraft is still subjected to normal gust and maneuver loads. The use of Mo as the reflector material will permit higher operating temperatures than would be the case if the reflector were Be. The higher temperature capability will permit radiation to become the predominant heat transfer mechanism much sooner, thereby significantly reducing the quantity of inert coolant gas required.

The shaft on which the reflector rotates is mechanically attached to the reflector segments through suitable flanges eliminating weld connections. The shaft rotates on bearings mounted to support pillars which are attached to the flow divider between core and reflector. The actuator which drives the shaft is mounted to one of the bearing supports to assure alignment. The shaft and bearing supports are located between the inlet and exit ducts.

The stepper motor considered in this study to actuate each reflector element is the Bendix Nutator* motor illustrated in Figure 5.2.33. It consists of a stationary external bevel gear and eight radial segments each consisting of an electromagnetic solenoid. The electrical components, solenoids, and an optional position feedback potentiometer are contained in a hermetically sealed gas environment. Penetrations must be provided through the containment vessel for these connections. The nutating armature and an internal bevel gear are attached to the output shaft by a flexible member which is rigid in torsion. When four adjacent solenoids are energized, the armature pulls the bevel gear into engagement in the sector where the solenoids are located. Energizing solenoids in sequence (always keeping four adjacent solenoids energized) rotates the area of engagement about the stationary gear. A one-tooth differential between the two beveled gears results in advancing the output shaft through an angle subtended by the circular pitch when the solenoids are operated in sequence through one complete revolution. The velocity torque relationship of this motor is shown in Figure 5.2.34 along with the same motor with a 5-to-1 gearing reduction.

The preferred arrangement is for the reflector to operate normally immersed in the shield water. Being Mo, the reflector for the reference design is relatively dense. When the reflector is closed upon the reactor, the drag force caused by the water plus the inertia of the heavy reflector raises a question with regard to the feasibility of the actuator to scram the reactor within a reasonable time. Therefore, an analysis was made to determine the rates that can be achieved with the proposed actuator.

Assumptions for this analysis were:

1. The reflector is divided into 12 circumferential Mo segments, each weighing 735 pounds and with a mass moment of inertia of 69 inch pounds/second^2.

*Registered trade name of the Bendix Corporation.

2. A total reactivity worth of all segments of 5% $\Delta k/k$ was assumed, with a displacement-worth curve as shown in Figure 5.2.35 based partially on published experimental results.*
3. The torque limit of the actuator is 240 in.-lb.

Since the reflector elements operate in a water environment, the scram torque required is defined by the following equation:

$$T = J\ddot{\theta} + C\dot{\theta}^2 \tag{5.1}$$

where T = scram torque
$\ddot{\theta}$ = angular acceleration
$\dot{\theta}$ = angular velocity
J = inertia
C = damping constant

The damping constant was derived from consideration of the dynamic pressure forces caused by rotating the reflector element through water and is estimated to be:

$$C = 3.05 \times 10^{-6} \times L \times W^4 \left\{ 1 + \left[\frac{1}{\frac{ho}{W} + \sin\theta + \frac{t}{W}(1 - \cos\theta)} \right]^2 \right\} \tag{5.2}$$

where L = reflector length, inches
W = reflector width, inches
t = reflector thickness, inches
ho = clearance between core shell and fully closed reflector, inches
θ = angular position of reflector at initiation of scram

Substituting the assumed values of 40 inches for L, 9 inches for W, and 5 inches for t into equation 5.2, the damping equation becomes

$$C = 0.8 \left\{ 1 + \left[\frac{1}{0.028 + \sin\theta + 0.555\,(1 - \cos\theta)} \right]^2 \right\}$$

Using the displacement worth curve, the angular displacement $\Delta\theta$ equivalent to 0.2 percent $\Delta k/k$ at 2.5-degree intervals was derived and a smooth curve describing this relationship is shown in Figure 5.2.36. These angular displacements ($\Delta\theta$) were programmed into a computer program for various scram-time intervals which determined the angular acceleration, velocity, and scram torque for various angular starting positions. A family of torque-velocity data was generated for various reactivity withdrawal rates.

Because a position resolution of 0.001 percent $\Delta k/k$ is desirable, a gear reduction of 5-to-1 was assumed in the analysis:

Total reflector worth, 5% $\Delta k/k$
Reflector motion, 40 degrees
Worth of one reflector element, 0.41667% $\Delta k/k$

---

*NAA-SR-6207 (SRD) "SNAP 8 Reactor Preliminary Design Summary," NAA-SR-6207 (SRD) Atomics International Division, North American Aviation, Inc., edited by H. Rosenburg, June 15, 1961.
PWAC-642 (CRD) "SNAP-50/Spur Program Engineering Progress Report, April 1, 1964, to June 30, 1964," PWAC-642 (CRD), Pratt & Whitney Aircraft Div. United Aircraft Corporation.

One step of motor, 0.45 degree
Equivalent worth of one step, 0.004687% $\Delta k/k$
Worth of one step with 5-to-1 reduction, 0.00093% $\Delta k/k$

Although scram requirements are not explicitly defined, it is desirable to obtain the highest possible scram rate and conserve the scram torque. Results from the analysis indicate the maximum velocity attainable within the torque capabilities of the Nutator motor is 0.2 percent $\Delta k/k$ withdrawal in 0.15 second. The torque velocity relationship of this scram rate is indicated by Figure 5.2.37 and the required torque as a function of starting position in Figure 5.2.38. The analysis shows that the damping term is significant only when the reflectors are very close to the core shell; thereafter, only the torque required to accelerate the reflectors is significant.

If the control system is programmed to develop a scram velocity of 0.65 rad/sec (with a constant acceleration of 4.3439 rad/sec^2) regardless of starting position, the shutdown rate (% $\Delta k/k$ withdrawal) at the smaller starting angles will be considerably higher than the 0.2 percent $\Delta k/k$ per 0.15 second. Consequently, the Nutator motor is conceptually feasible for meeting the control requirements.

DESIGN LAYOUT

The final design layout of the reactor assembly includes the details of the reflector control assembly and support. The actuator design layout has been described under "Arrangement Studies."

ASSESSMENT OF PROBLEMS AND CURRENT STATE-OF-THE-ART

An evaluation of the reflector and drive system show that there are no particular problem areas and that a nominal research and development effort could provide an acceptable control system. The use of Mo as a reflector material does not appear to be a problem because radiation effects would be of minor consequence since the material is not highly stressed. Areas that would require development and test effort would primarily be the actuator and the reflector support bearings. The actuator is not an off-the-shelf item; however, according to the manufacturer, models have been built and operated, and its operating characteristics are reasonably firm. Early procurement and operation of an actuator built to the design requirements would be desirable to firmly establish the drive rate - torque characteristics and evaluate bearing and gear operation using borated water as a lubricant. The actuator was designed to withstand a total neutron dose of 10^{18} nvt. Operation of the actuator - reflector assembly should be conducted in the borated water environment to confirm the predicted torque values particularly at the nearly closed position. Critical experiment data would be required to establish the relationship of displacement to control segment worth from which a design could be generated.

APPLICABLE WORK UNDERWAY

Current reactor design effort of the 710 Reactor Program is concentrated on evaluating axial-displacement-control moderating reflectors; however,

critical experiment measurements have been made with nonmoderating stainless steel and Mo reflectors and these data are being correlated with analytical methods and will be reported in 710 Reactor progress reports.

Current effort on the SNAP 8 reactor involves the use of a rotating leakage control reflector. Some parts of that effort may be applicable and should be evaluated as a guide for future analysis and development work, but the aspect of water immersion is believed to be unique and not under development.

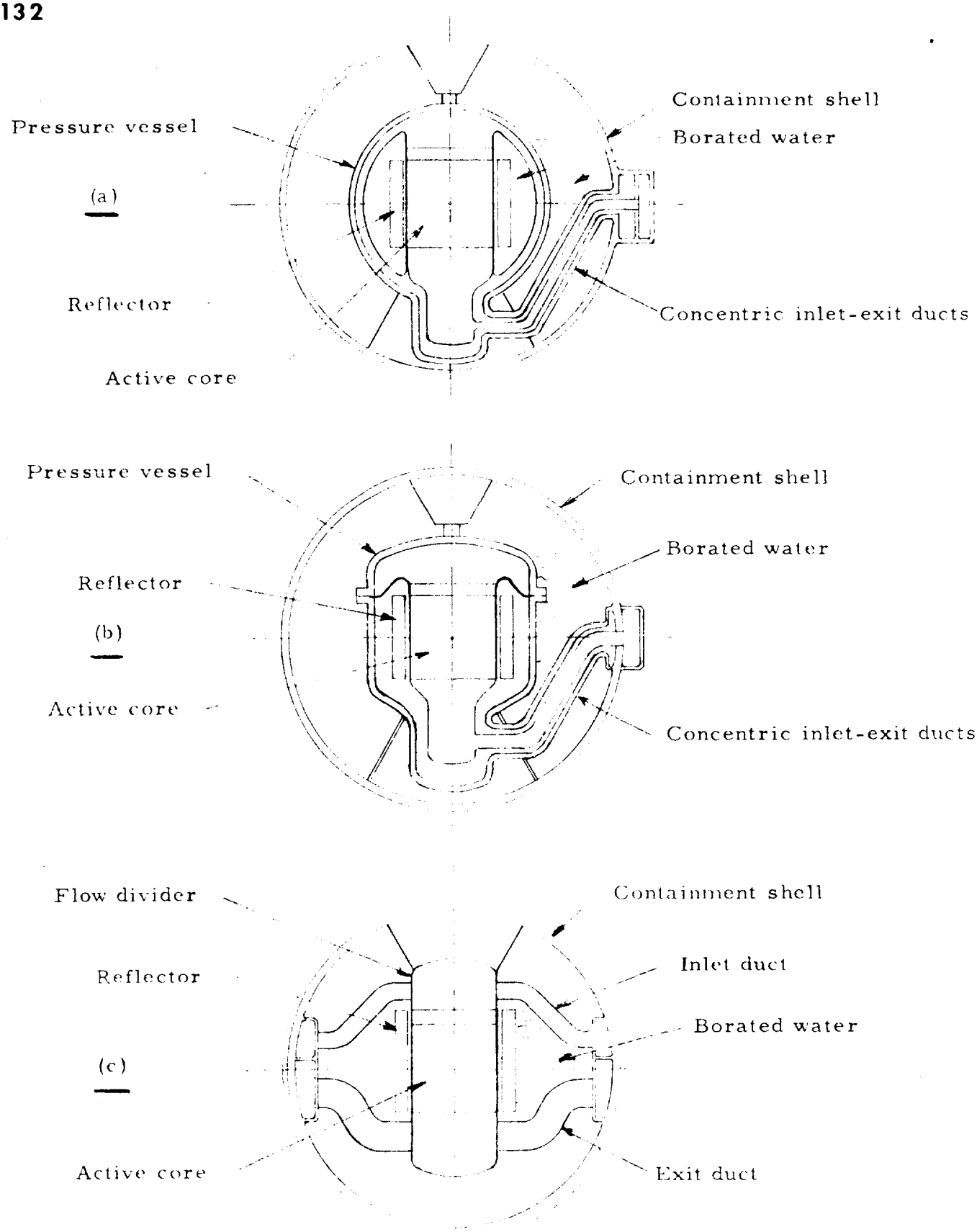

Fig. 5.2.1 - Possible Reactor Arrangements Considered

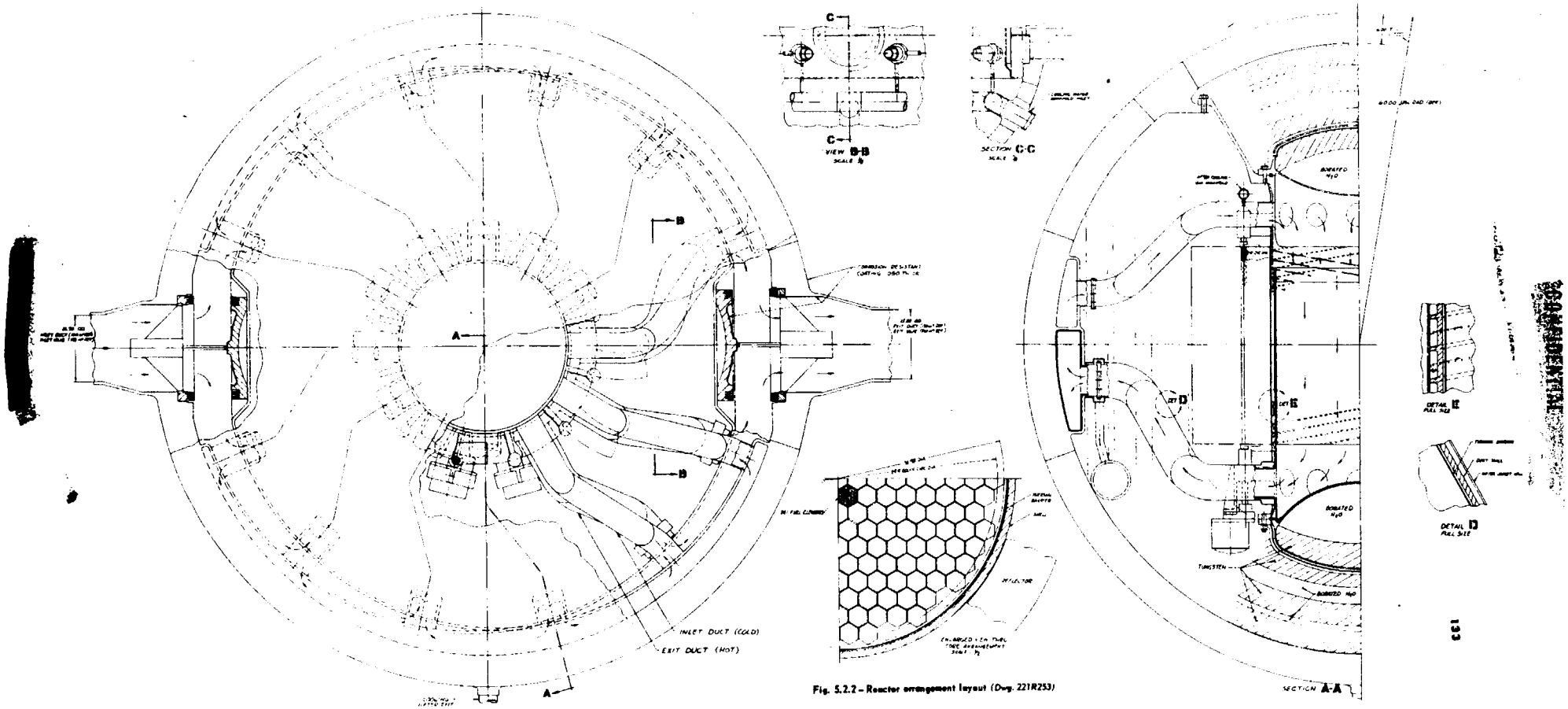

Fig. 5.2.2 – Reactor arrangement layout (Dwg. 221R253)

CONFIDENTIAL

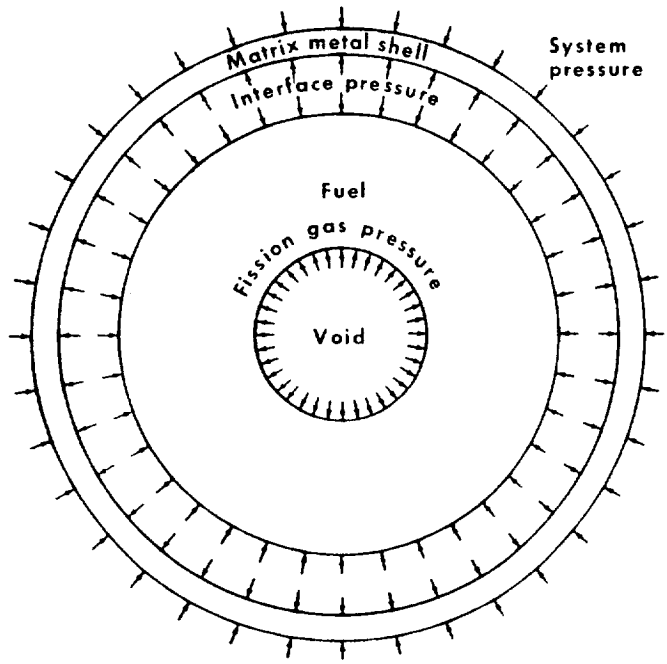

Fig. 5.2.3 – Analytical model for fission gas swelling calculations

CONFIDENTIAL

Reproduced from best available copy.

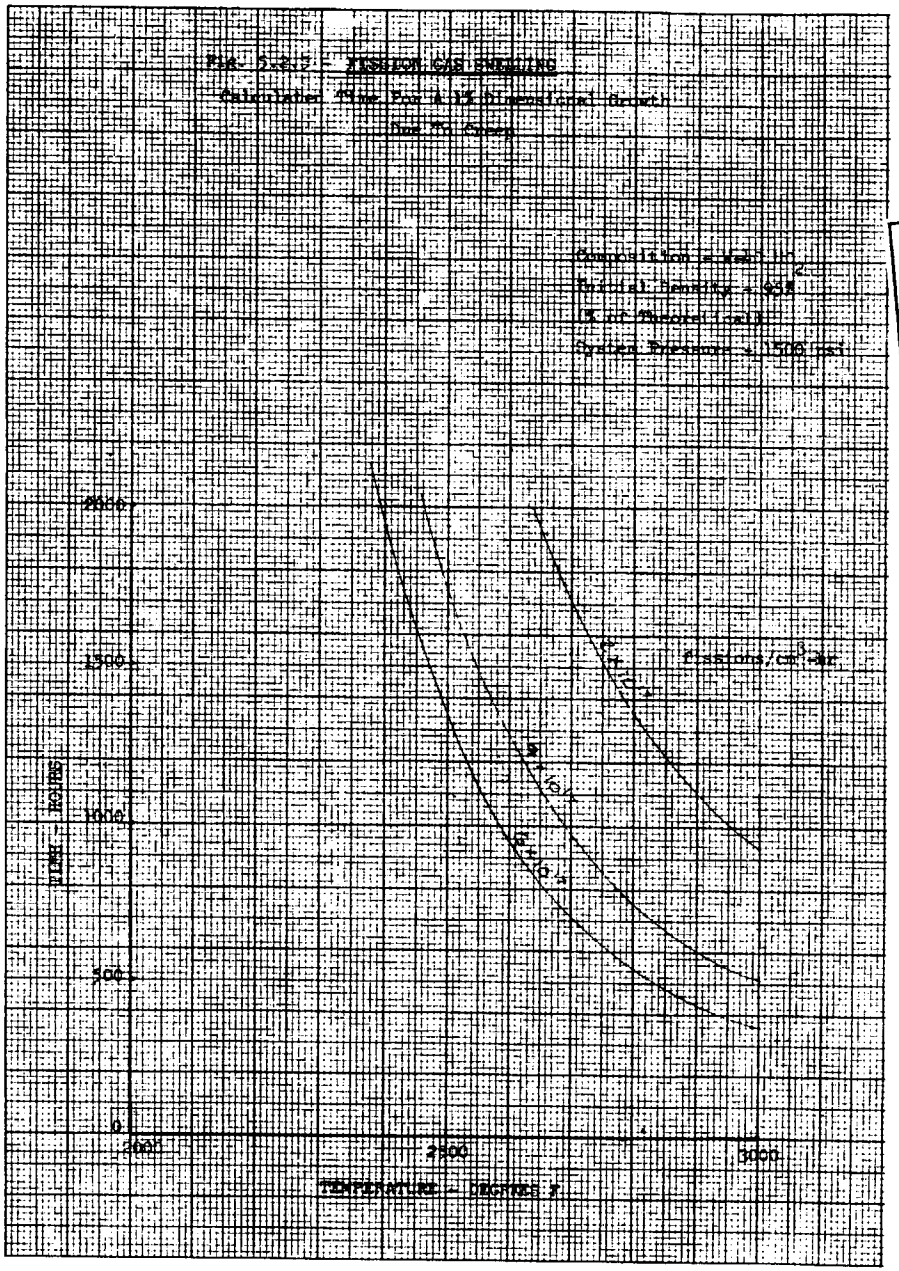

Fig. 5.2.9 - FISSION GAS SWELLING
Calculated Time For A 1% Dimensional Growth Due To Creep

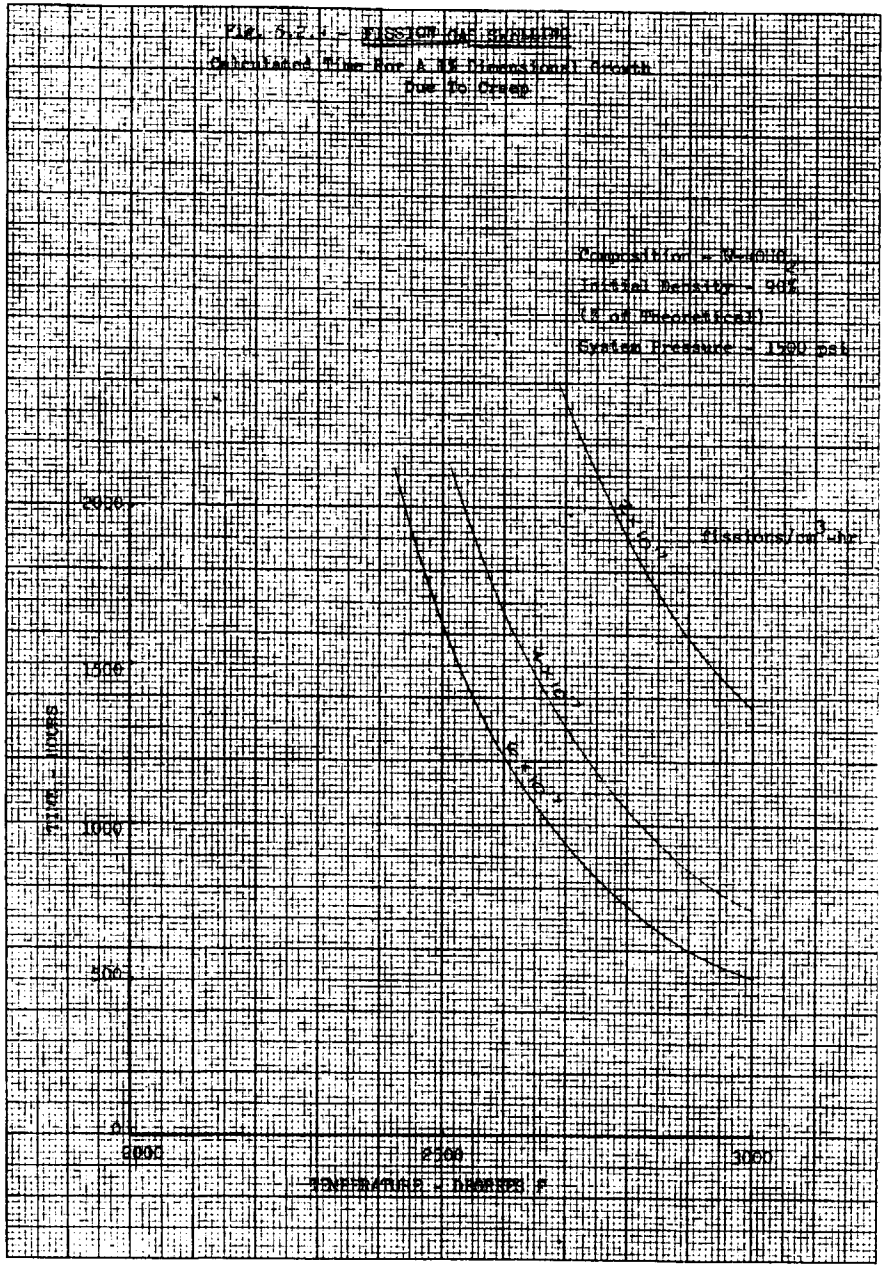

Fig. 5.2.8 - FISSION GAS SWELLING
Calculated Time For A 1% Dimensional Growth Due To Creep

CONFIDENTIAL

FIG. 5.2.7 - FISSION GAS RELEASING
Calculated Time For A 1% Dimensional Growth
Due To Creep

Concentration - 4-50 UO_2
Initial Density - 90%
(% of Theoretical)
Burnup Pressure - 1500 psi

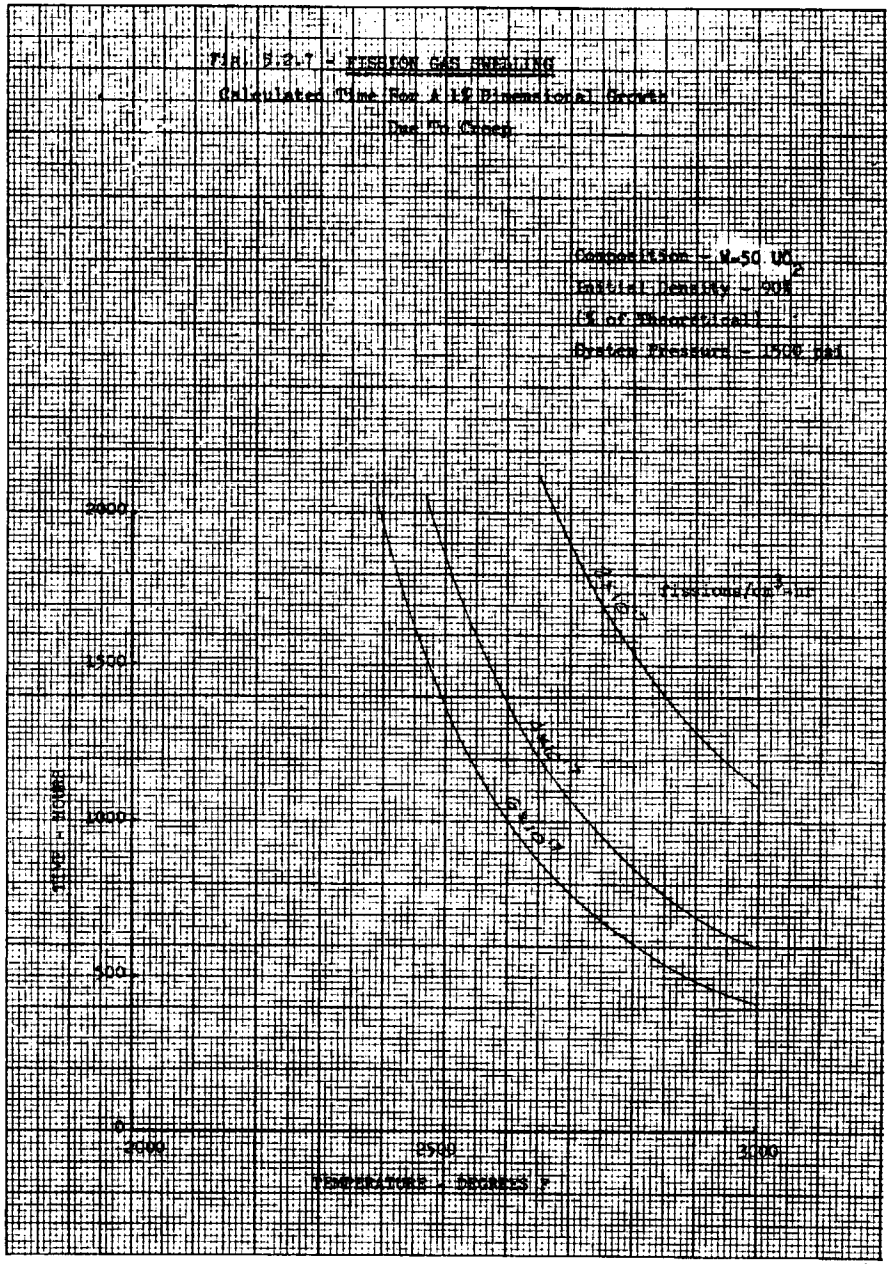

Fission Gas Releasing
Fig. 5.2.8 - Calculated Time For A 1% Dimensional Growth
Due To Creep

Concentration - 4-50 UO_2
Initial Density - 90%
(% of Theoretical)
Burnup Pressure - 1500 psi

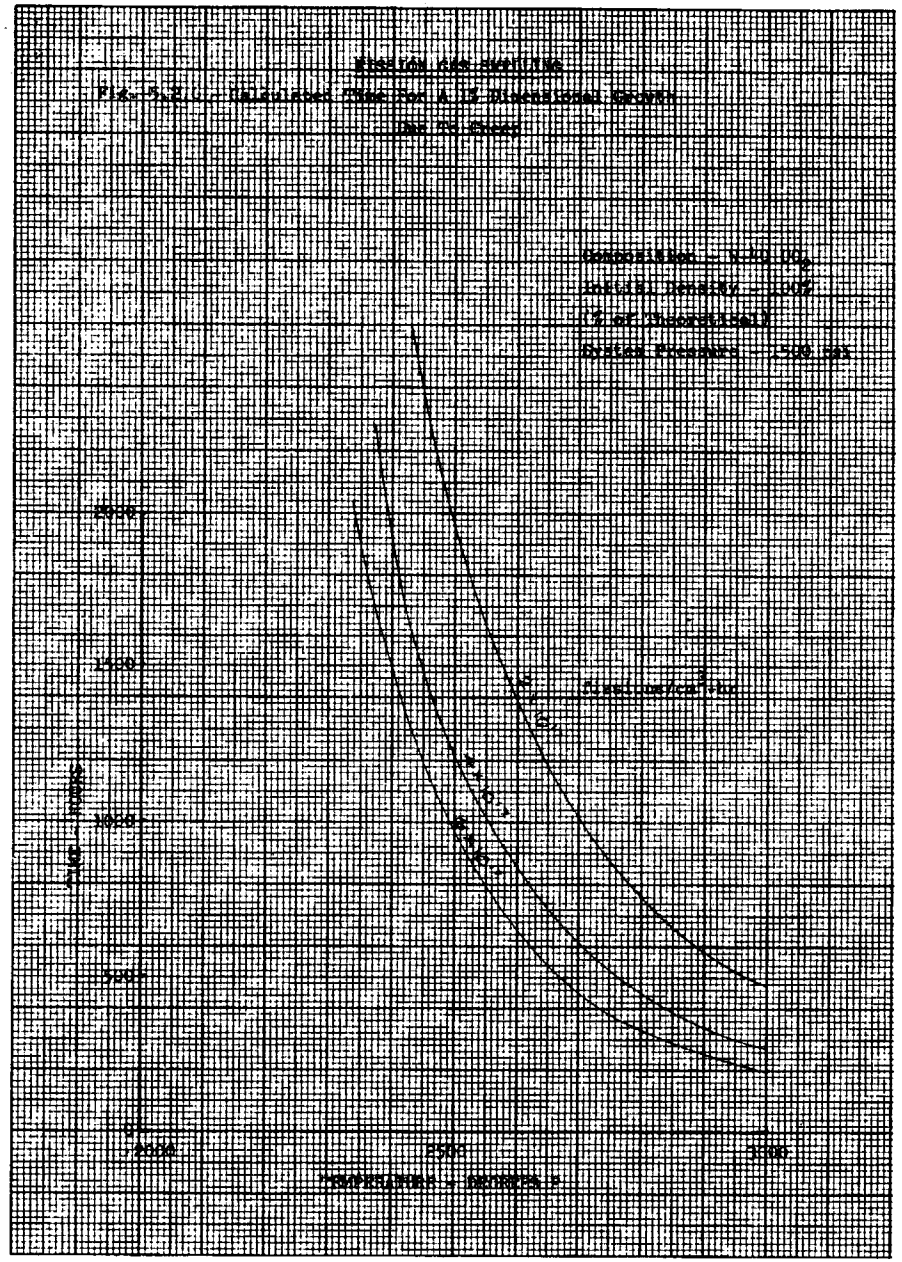

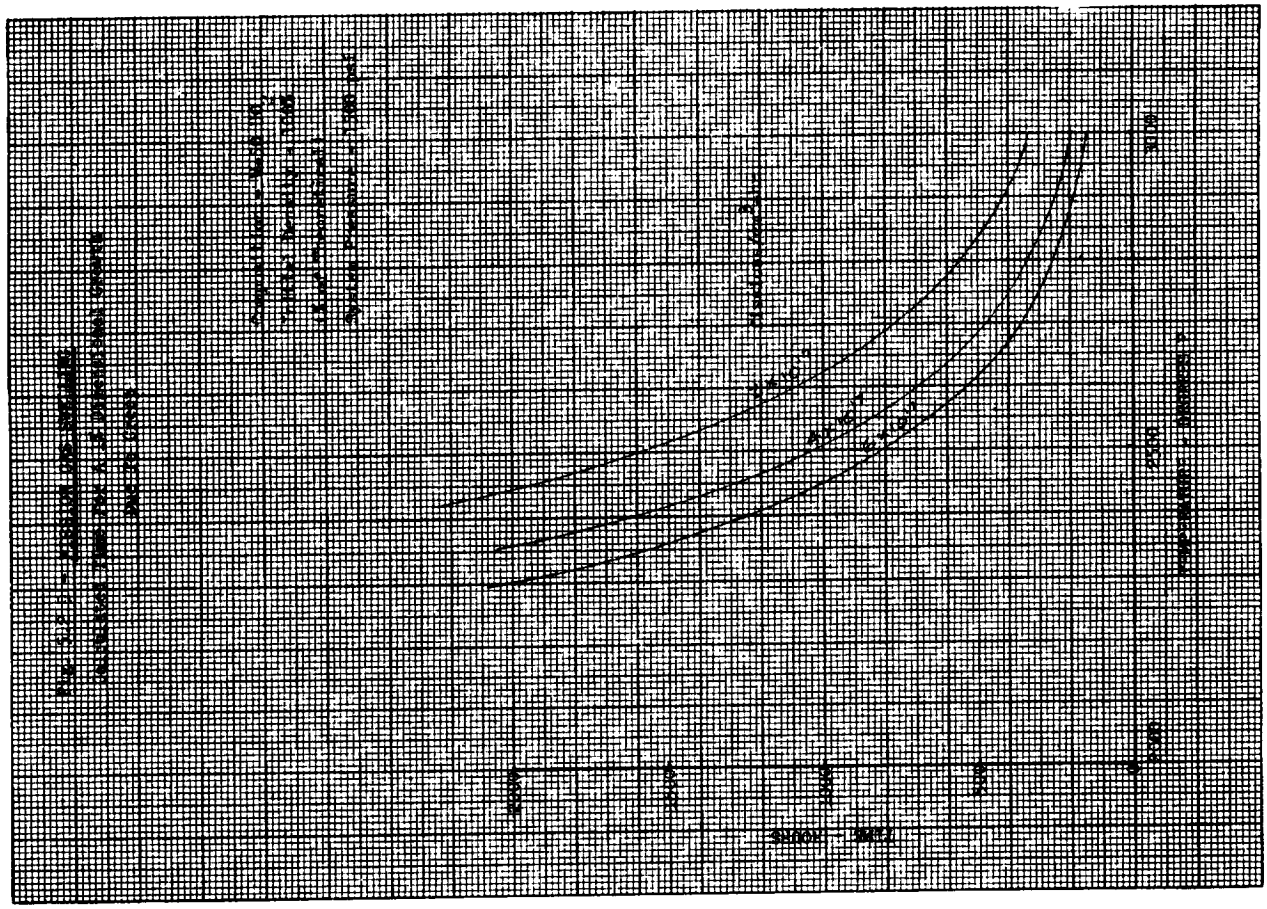

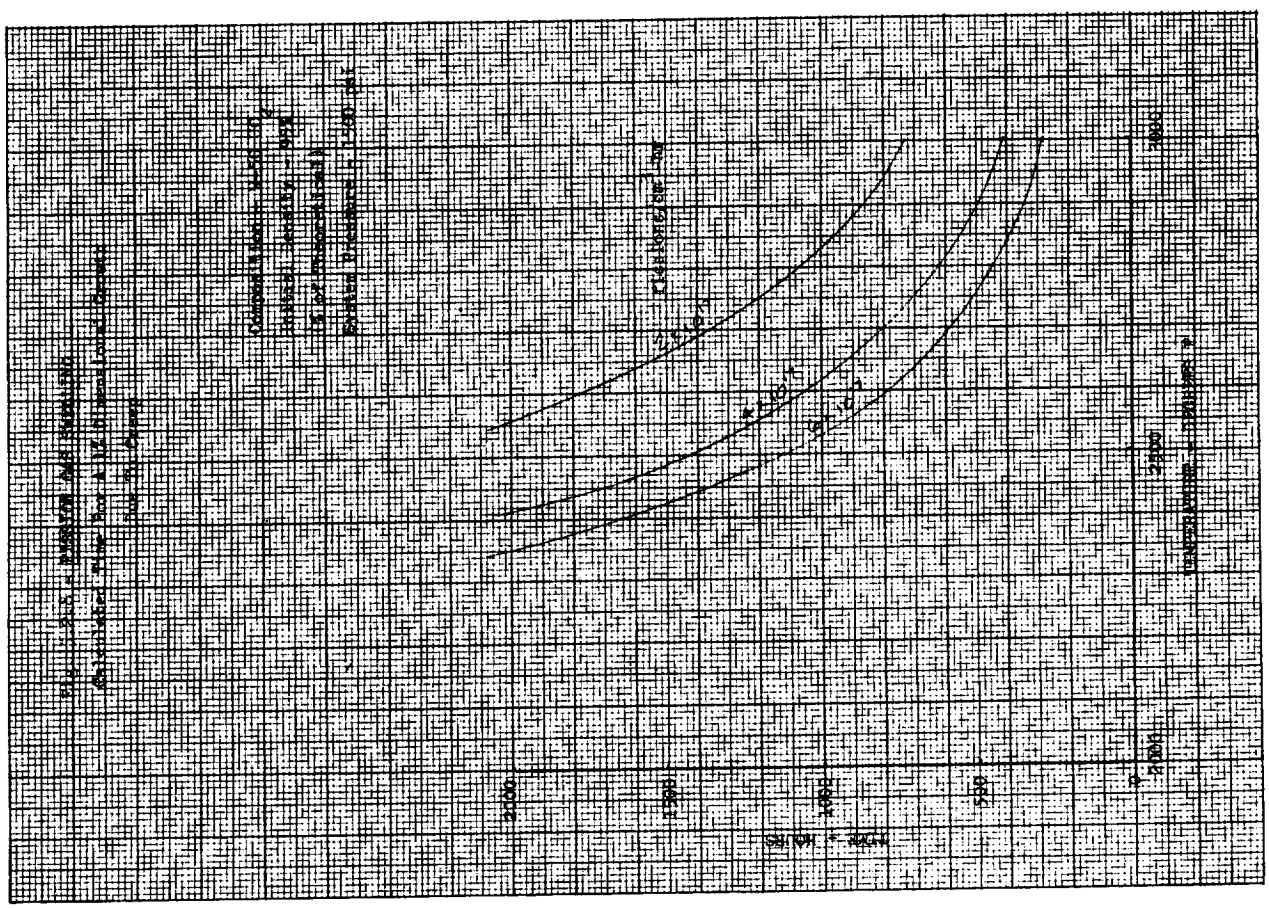

CONFIDENTIAL

FISSION GAS BUBBLING

Fig. 5.2.10 - Calculated Time For A 1% Dimensional Growth Due To Creep

Composition - W-60 UO_2
Initial Density - 90%
(% of Theoretical)
System Pressure - 1500 psi

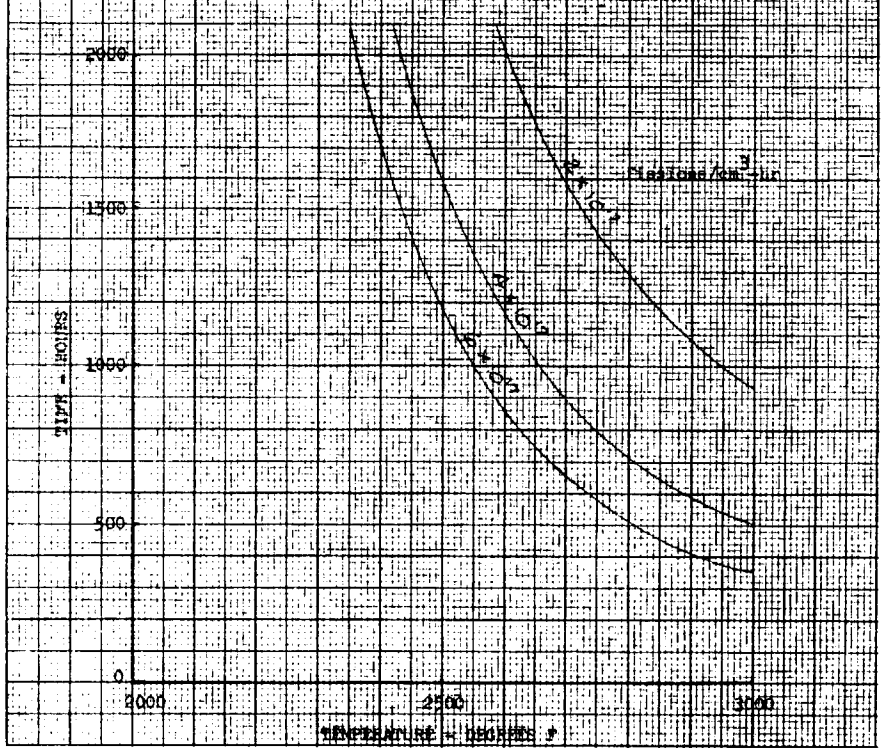

FISSION GAS BUBBLING

Fig. 5.2.11 - Calculated Time For A 1% Dimensional Growth Due To Creep

Composition - W-60 UO_2
Initial Density - 95%
(% of Theoretical)
System Pressure - 1500 psi

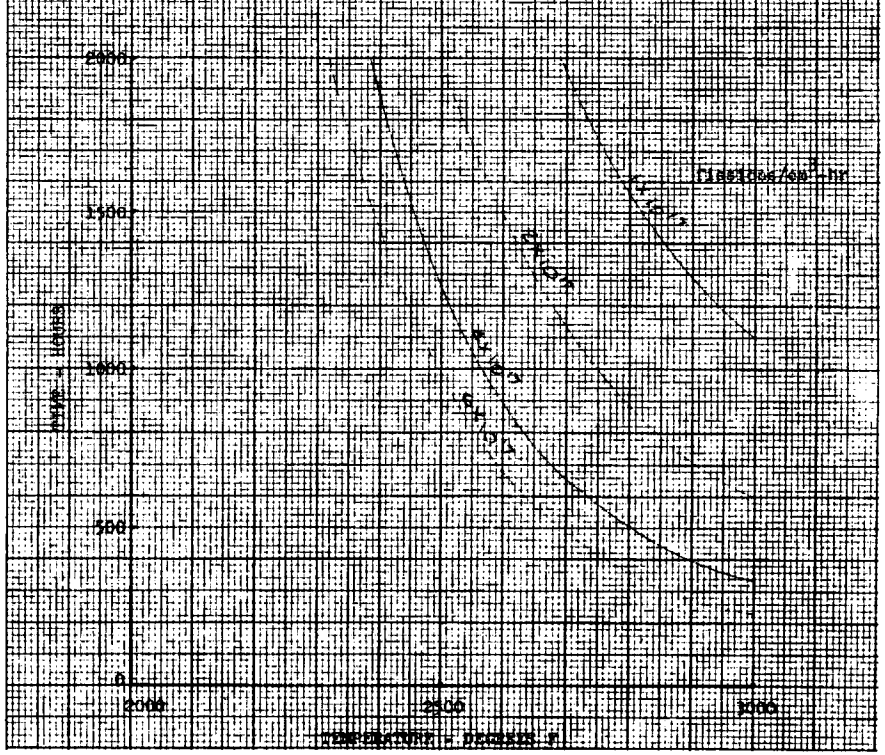

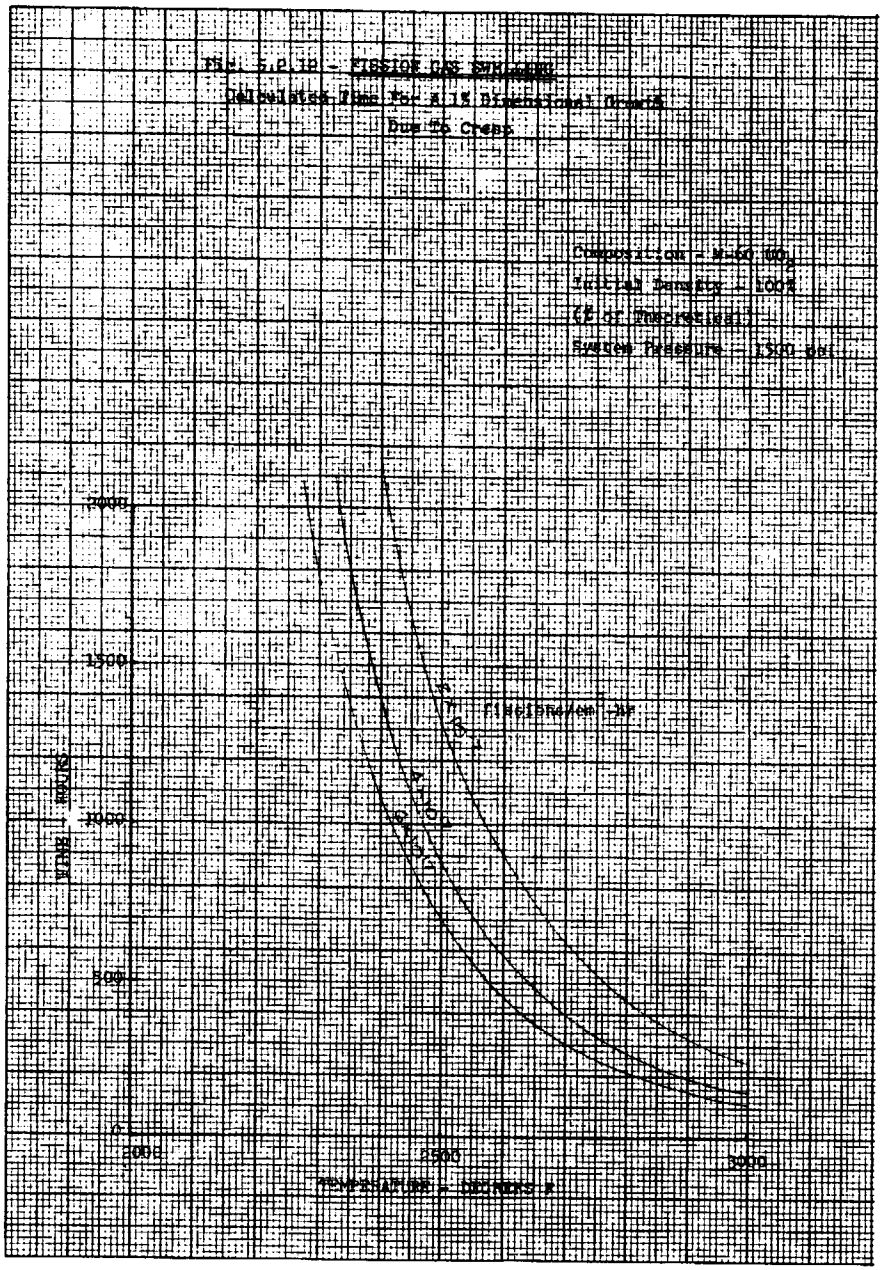

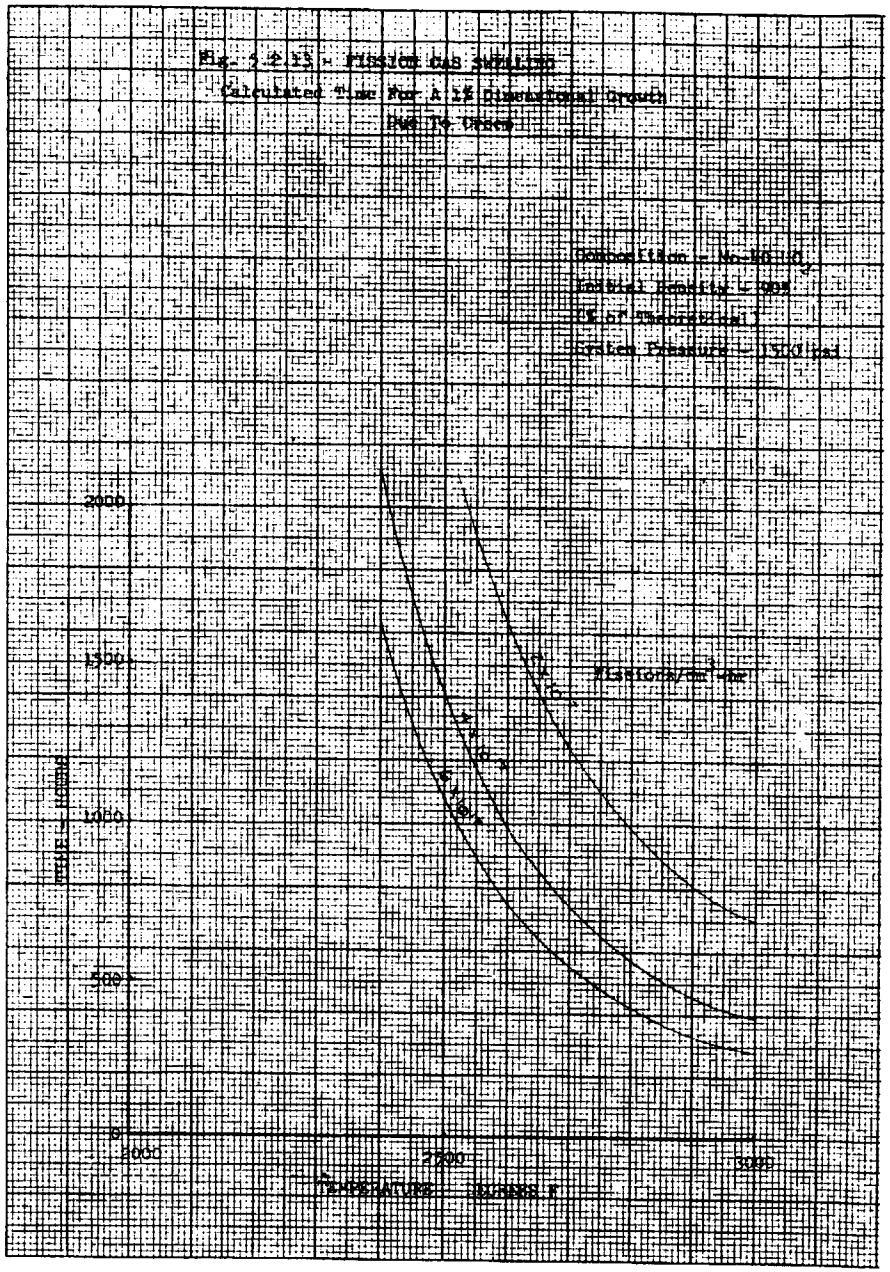

CONFIDENTIAL

CONFIDENTIAL

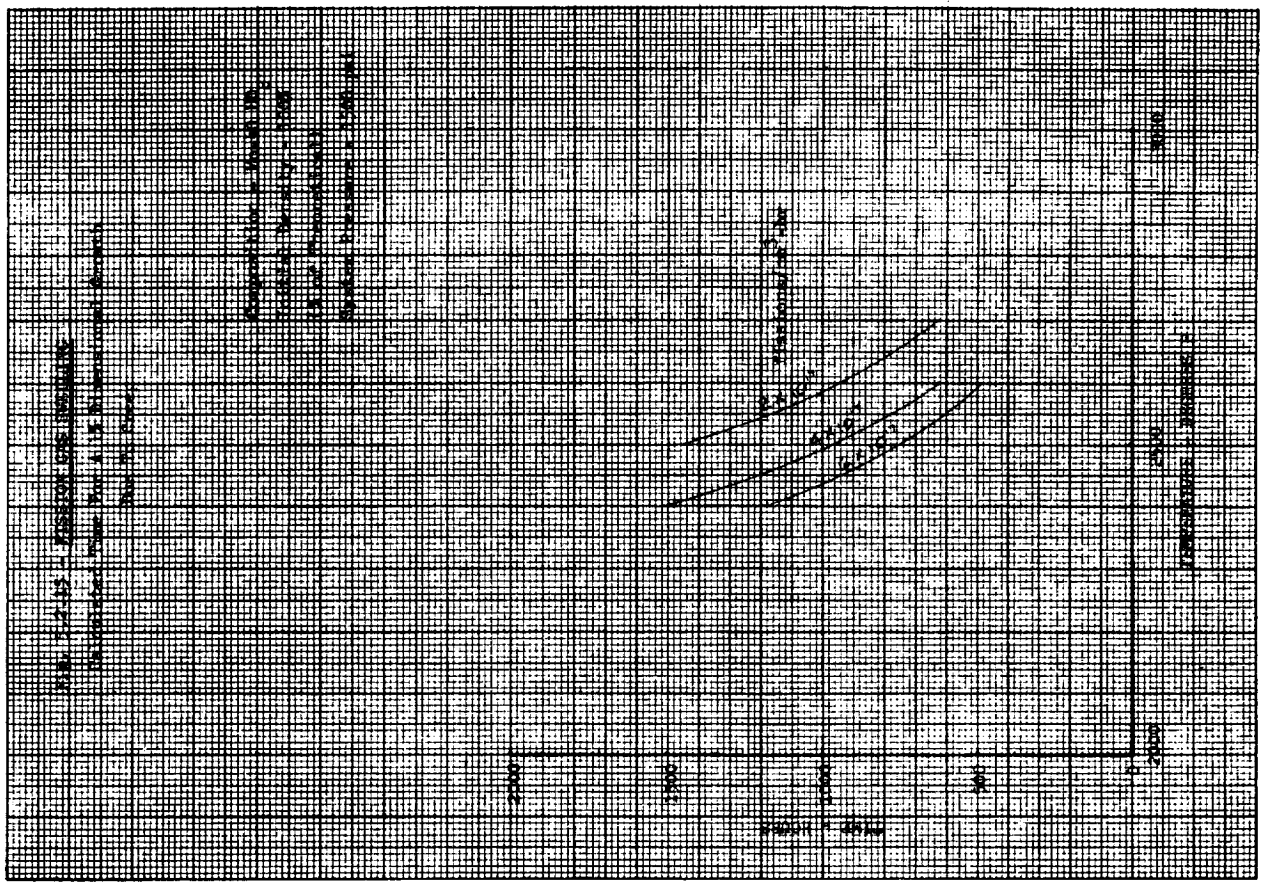

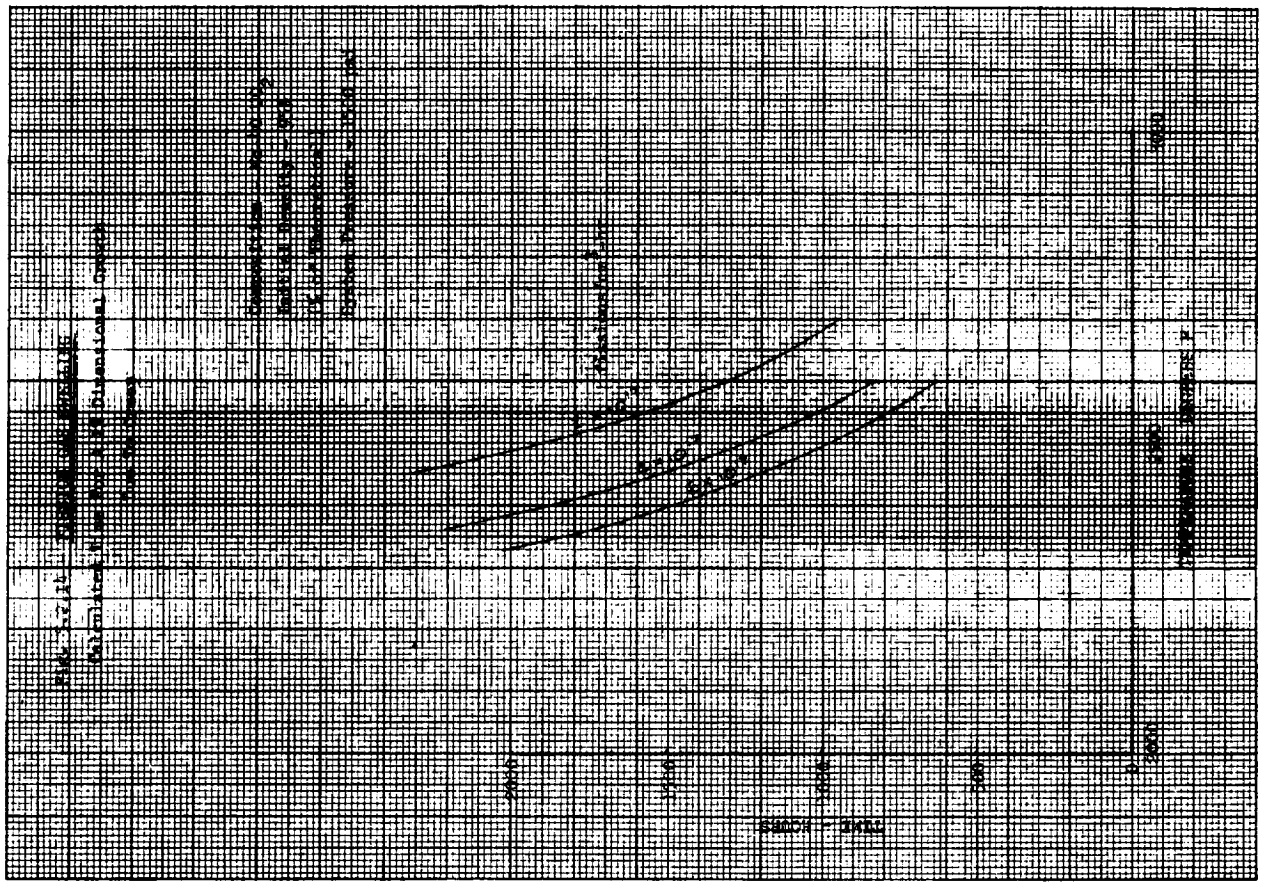

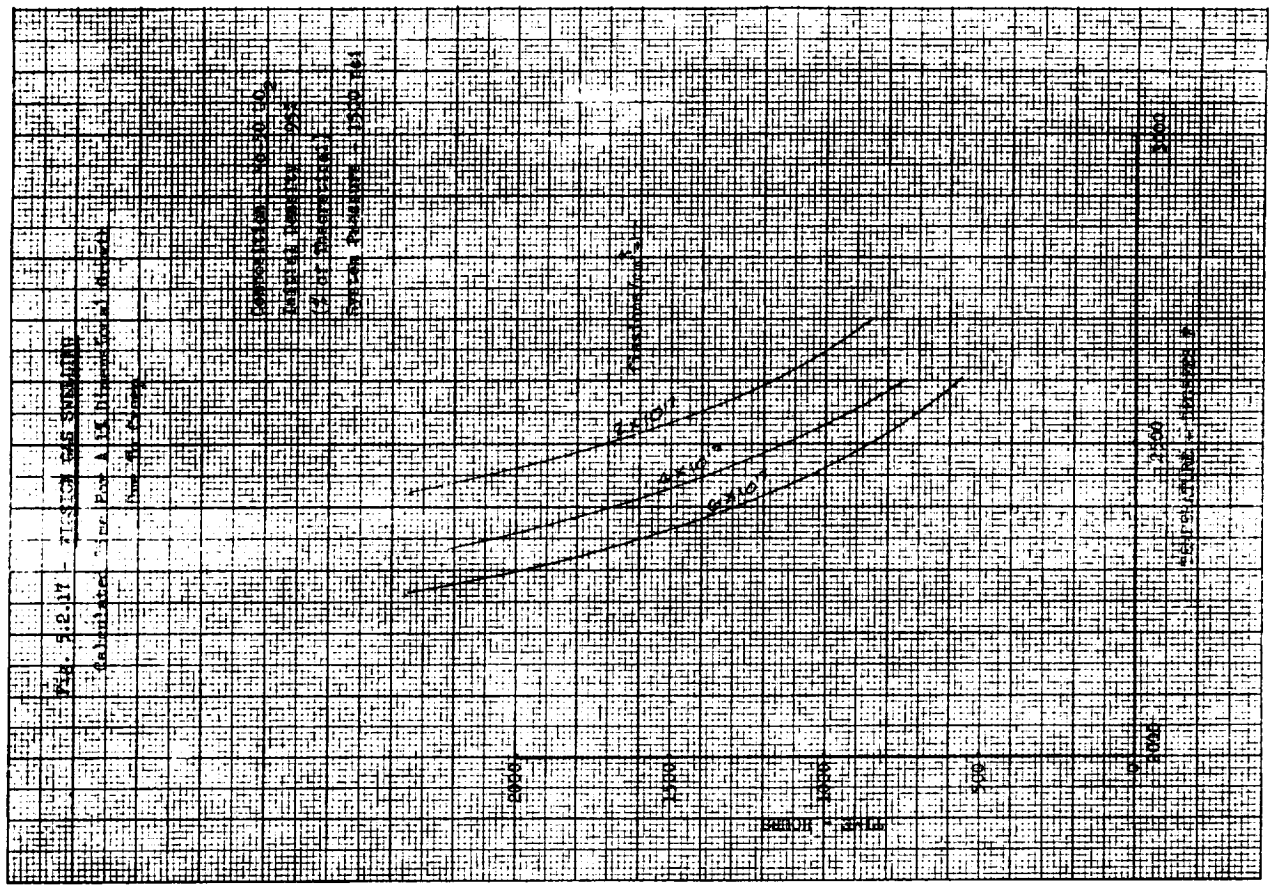
Fig. 5.2.17 - FISSION GAS SWELLING
Calculated Time For A 1% Dimensional Growth
Composition - 40-20 UO_2
Initial Density - 95%
(% of Theoretical)
System Pressure - 1500 psi
Fissions/cm^3
2x10^{17}
4x10^{17}
6x10^{17}
TIME - HOURS
2000
1500
1000
500
0
2000
2500
3000
TEMPERATURE - DEGREES F

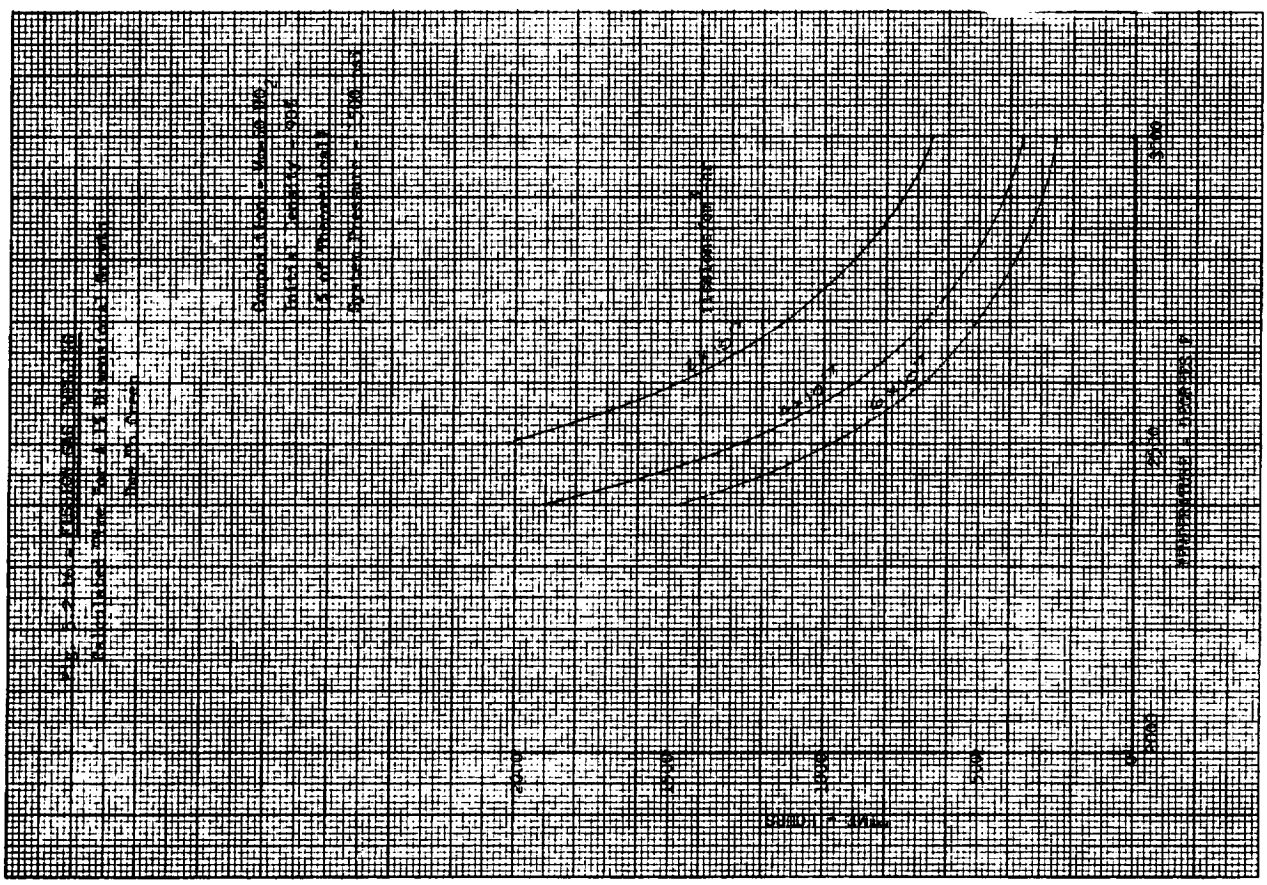
Fig. 5.2.16 - FISSION GAS SWELLING
Calculated Time For A 1% Dimensional Growth
Composition - 40-20 UO_2
Initial Density - 95%
(% of Theoretical)
System Pressure - 1500 psi
Fissions/cm^3
2x10^{17}
4x10^{17}
6x10^{17}
TIME - HOURS
2000
1500
1000
500
0
2000
2500
3000
TEMPERATURE - DEGREES F

CONFIDENTIAL

Fig. 5-2-18 - FISSION GAS SWELLING

Calculated Time For A 1% Dimensional Growth

Due To Gases

Composition - UO_2

Material Density - 100%

(% of Theoretical)

System Pressure - 1500 psi

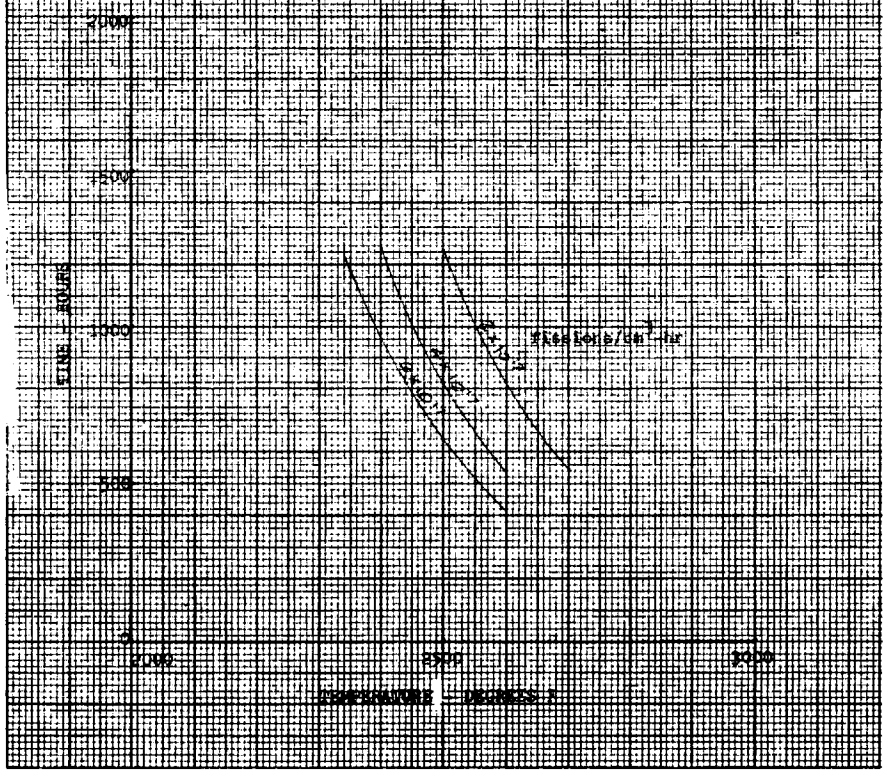

Fig. 5-2-19 - FISSION GAS SWELLING

Calculated Time For A 1% Dimensional Growth

Due To Gases

Composition - UO_2

Material Density - 90%

(% of Theoretical)

System Pressure - 1500 psi

Fig. 5.2.20 - FISSION GAS SWELLING

Calculated Time For A 1% Dimensional Growth Due To Creep

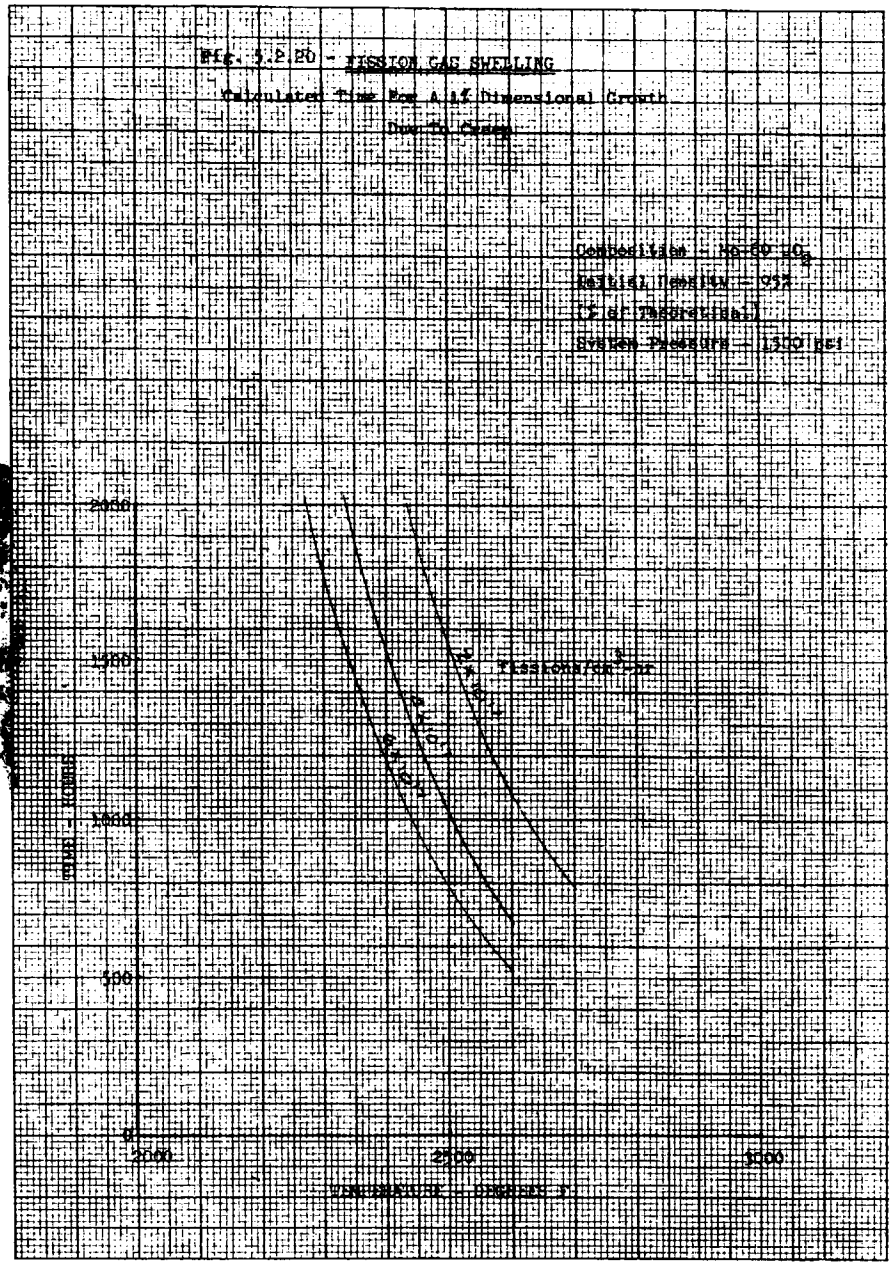

Fig. 5.2.21 - FISSION GAS SWELLING

Calculated Time For A 1% Dimensional Growth Due To Creep

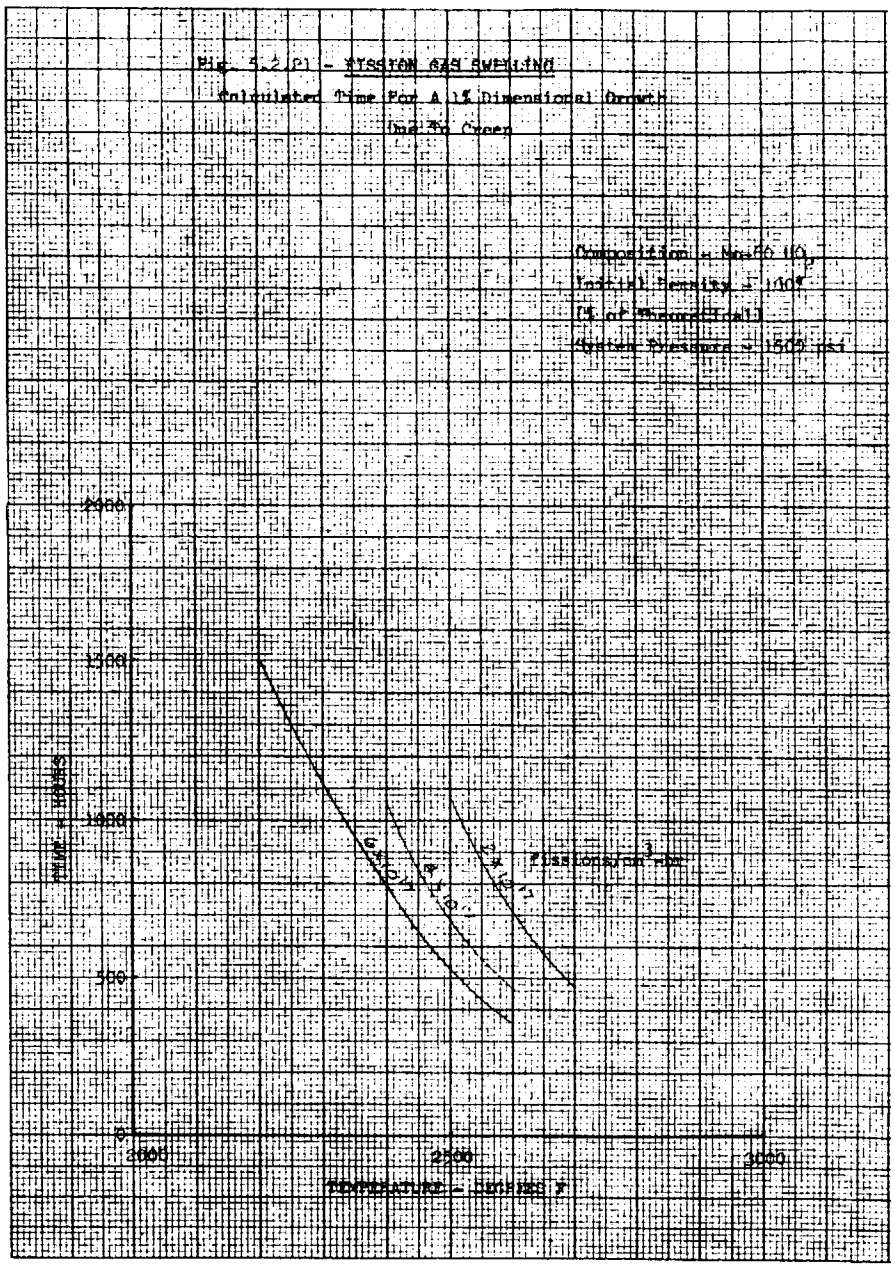

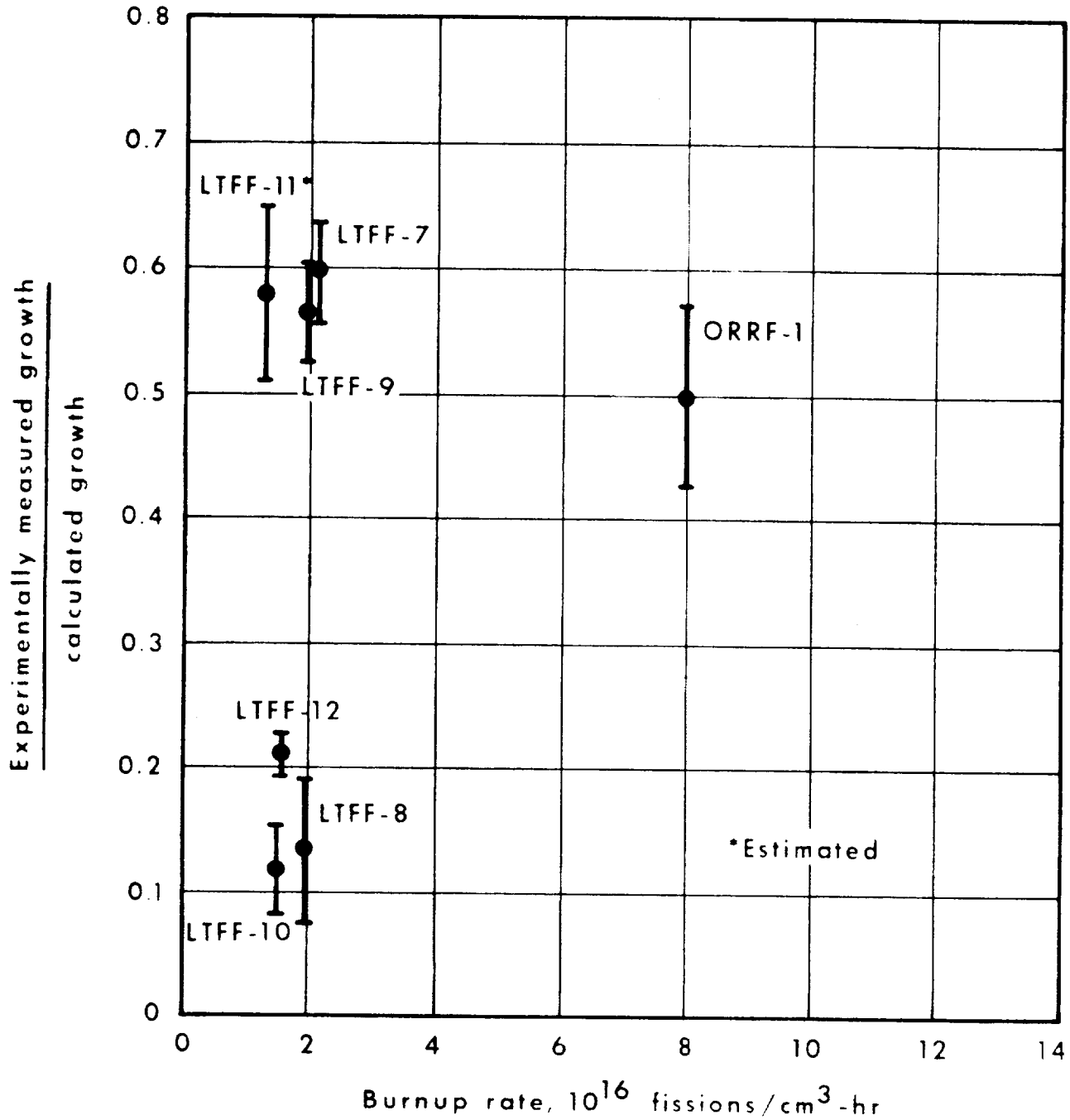

Fig. 5.2.22 – Experimentally measured versus calculated fission gas growth as a function of burnup rate

[redacted]

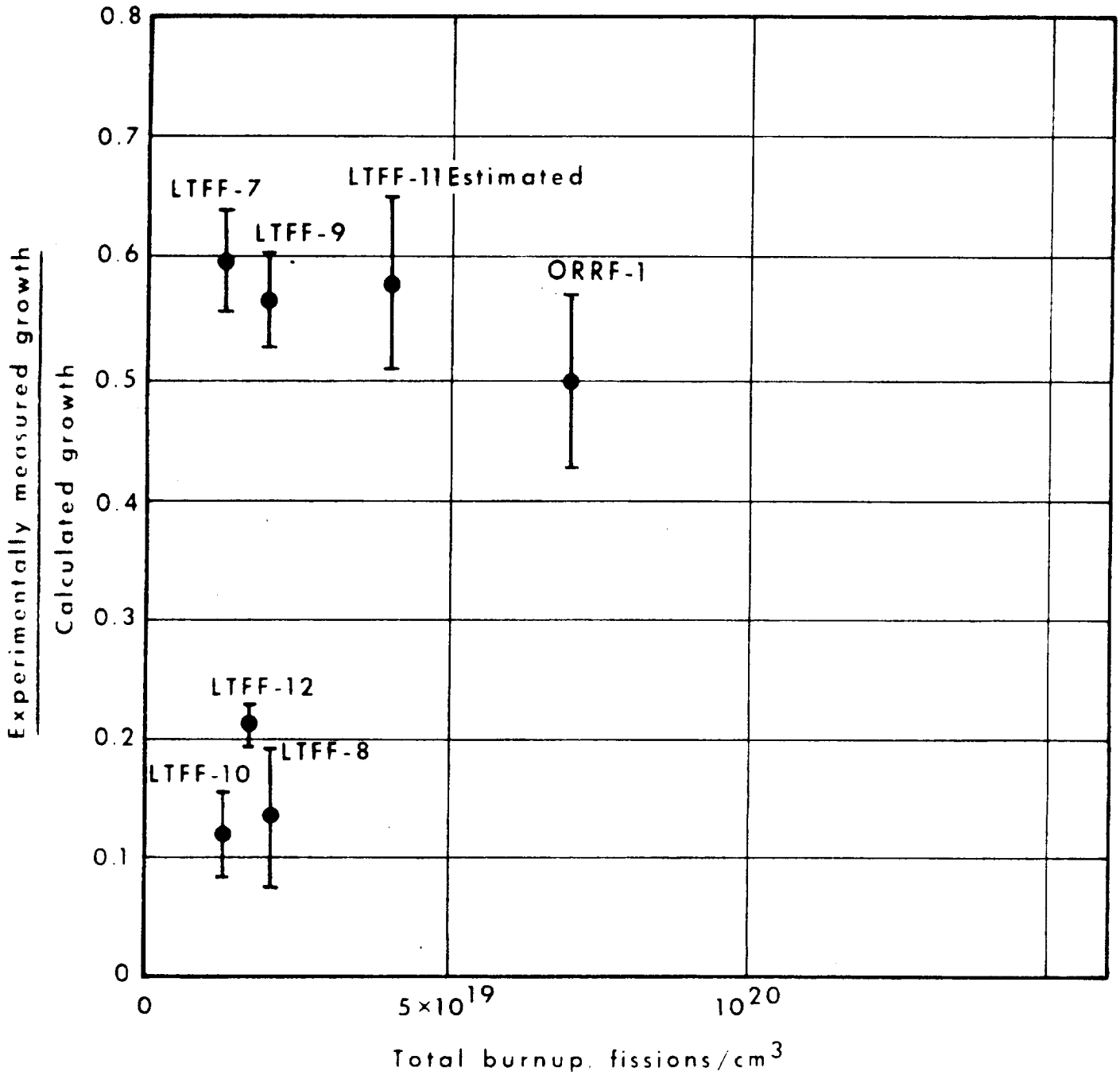

Fig. 5.2.23 – Experimentally measured versus calculated fission gas growth as a function of total burnup

CONFIDENTIAL

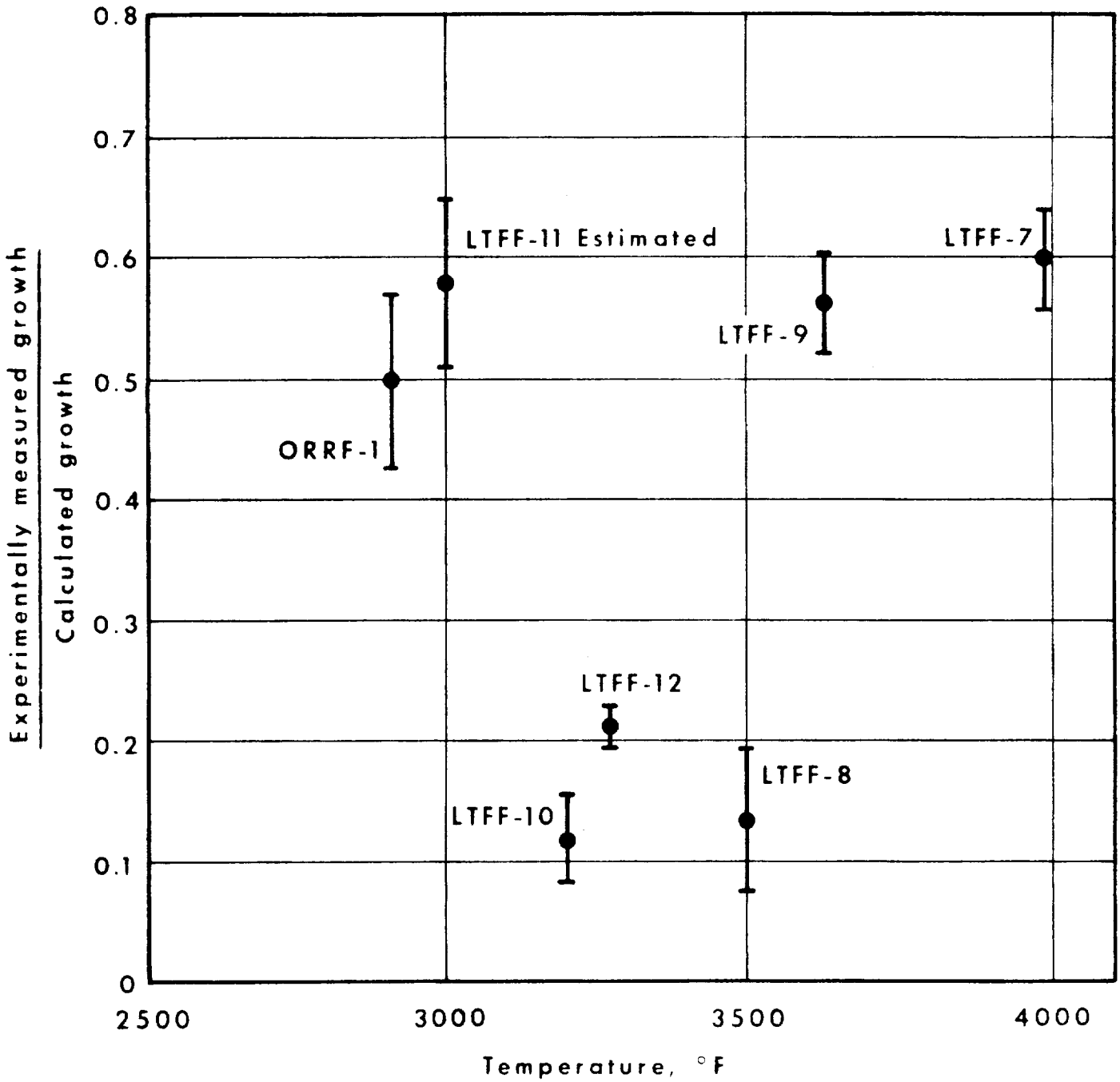

Fig. 5.2.24 – Experimentally measured versus calculated fission gas growth as a function of test temperature

CONFIDENTIAL

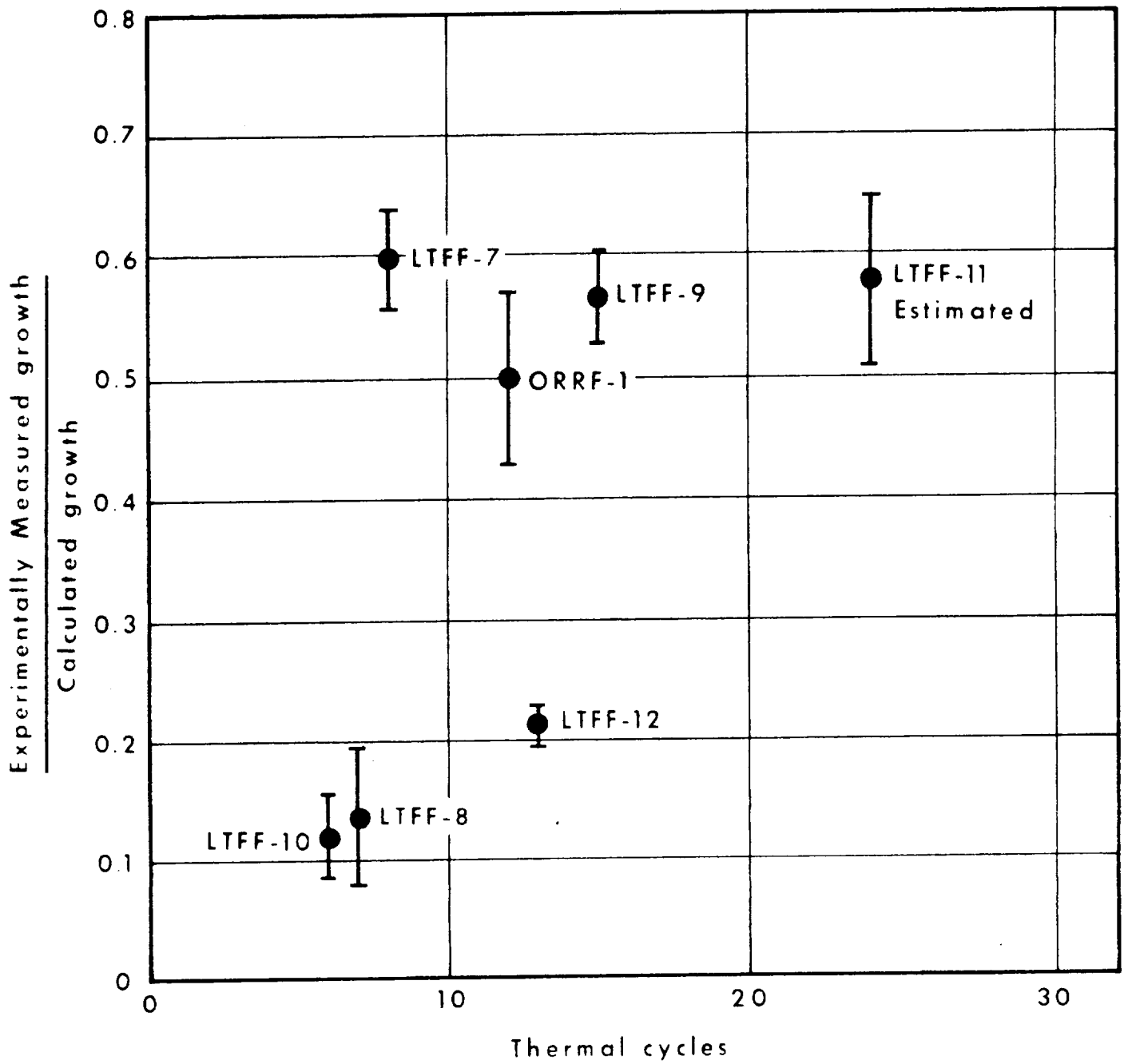

Fig. 5.2.25 – Experimentally measured versus calculated fission gas growth as a function of thermal cycles

CONFIDENTIAL

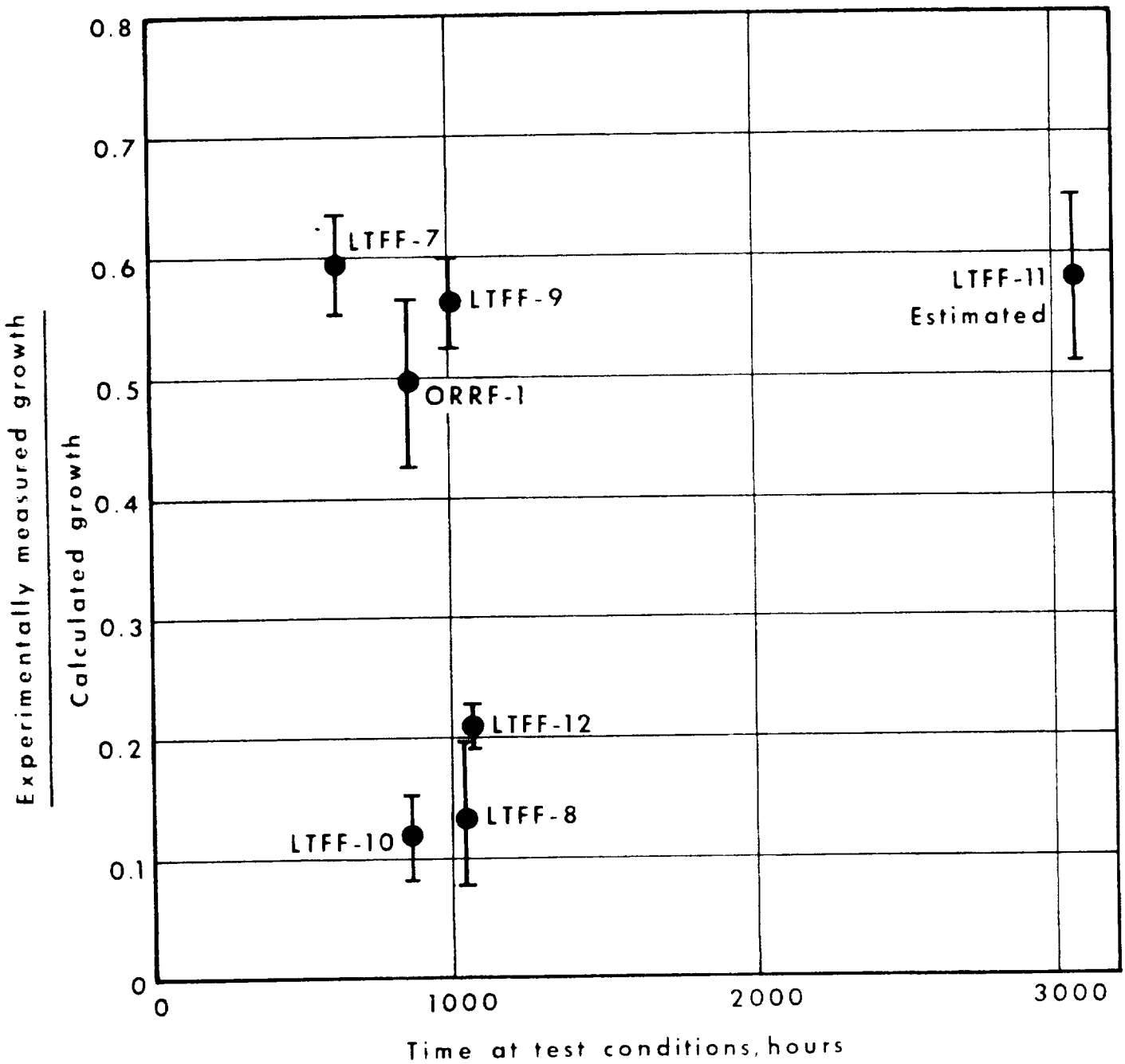

Fig. 5.2.26 – Experimentally measured versus calculated fission gas growth as a function of total time at test conditions

[redacted]

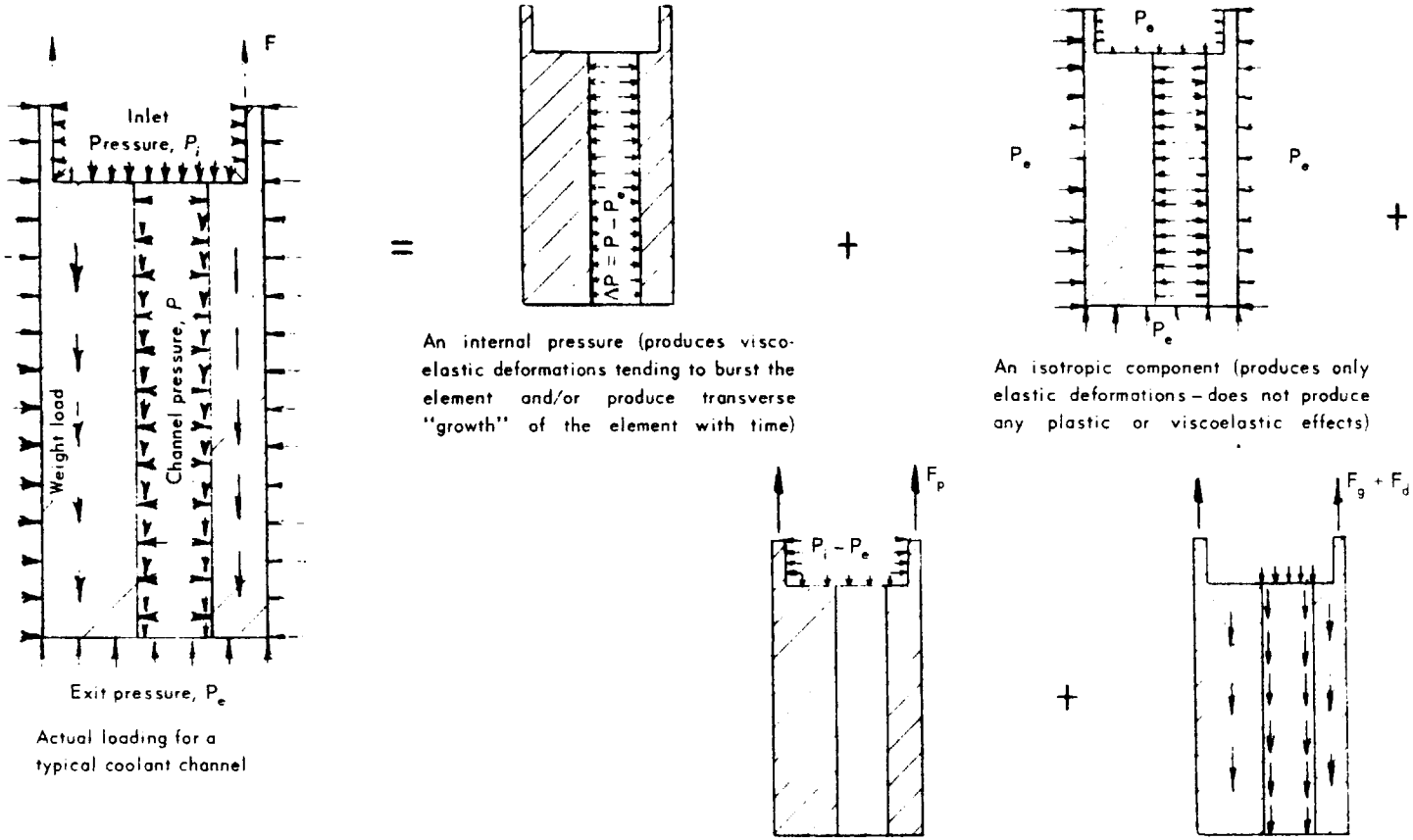

Actual loading for a typical coolant channel

An internal pressure (produces visco-elastic deformations tending to burst the element and/or produce transverse "growth" of the element with time)

An isotropic component (produces only elastic deformations – does not produce any plastic or viscoelastic effects)

Local self-equilibrating set of forces (by St. Venant's principle the corresponding stress field affects only the region within 2–3 "diameters" of the front of the element)

A small drag plus weight load (produces viscoelastic deformations which are small relative to those due to the internal pressure)

F = drag load, F_d + net pressure load, F_p + gravity load, F_g

Fig. 5.2.27 – Breakdown of the fuel element loading to show the effects associated with each of the components

CONFIDENTIAL

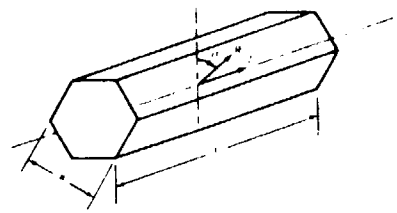

Type Of Stress	Source Of Load	Analytical Model	Method Of Analysis	Planned Evaluation Tests	Required Material Properties
Mechanical	Internal pressure in the coolant channels due to the pressure drop through the core 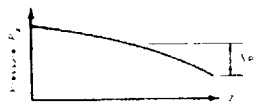	Single equivalent composite tube (on the basis of cross sectional area) 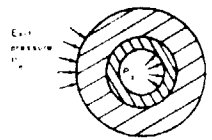	Plane-strain plastic-viscoelastic analysis. Ref: GEMP-288	Pressure rupture tests of partial length fuel elements and single hole test specimens	1. Tensile stress-strain curves 2. Long-time creep data 3. Rupture ductility
	Axial load associated with the pressure drop plus dead-weight load	Same as above 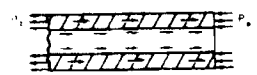	Same as above		
Thermal	Differential thermal expansion between the clad and the matrix	Same as above	Same as above	Isothermal cycling	1. Tensile stress-strain curves 2. Creep curves including first-stage data 3. Matrix-rupture ductility 4. Clad - low cycle fatigue data 5. Thermal expansion 6. Specific heat 7. Thermal conductivity
	Local radial temperature distribution associated with a single coolant channel due to heat removal 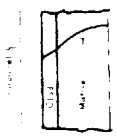	Same as above	Same as above	Single hole test specimen thermal strain test	
	Gross longitudinal temperature distribution 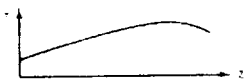	Equivalent homogeneous nonisotropic cylinder $E_R \neq E_\theta \neq E_Z$ 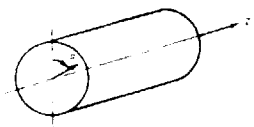	Analysis of Poritsky & Horvay. Ref: 2	None planned	
	Local hot channel 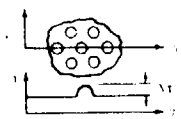	Actual geometry	$\sigma \cong \frac{E \alpha \Delta T}{1-\nu}$	None planned	

Fig. 5.2.28 – 710 fuel element elastic stress analysis summary

Mode	91 Channel Element		37 Channel Element	
	Measured	Calculated	Measured	Calculated
Bending				
1st mode	616*	614	645*	649
2nd mode	1689*	1688	1743*	1784
3rd mode	3096*	3316	3268*	3504
Longitudinal				
1st mode	4571	4770	4000	3950
Torsional				
1st mode	(not	2940	2456	2430
2nd mode	measurable)	5880	4797	4860

*Average of two tests.

Fig. 5.2.29 – Comparison of measured and calculated vibration frequencies (cps)

CONFIDENTIAL

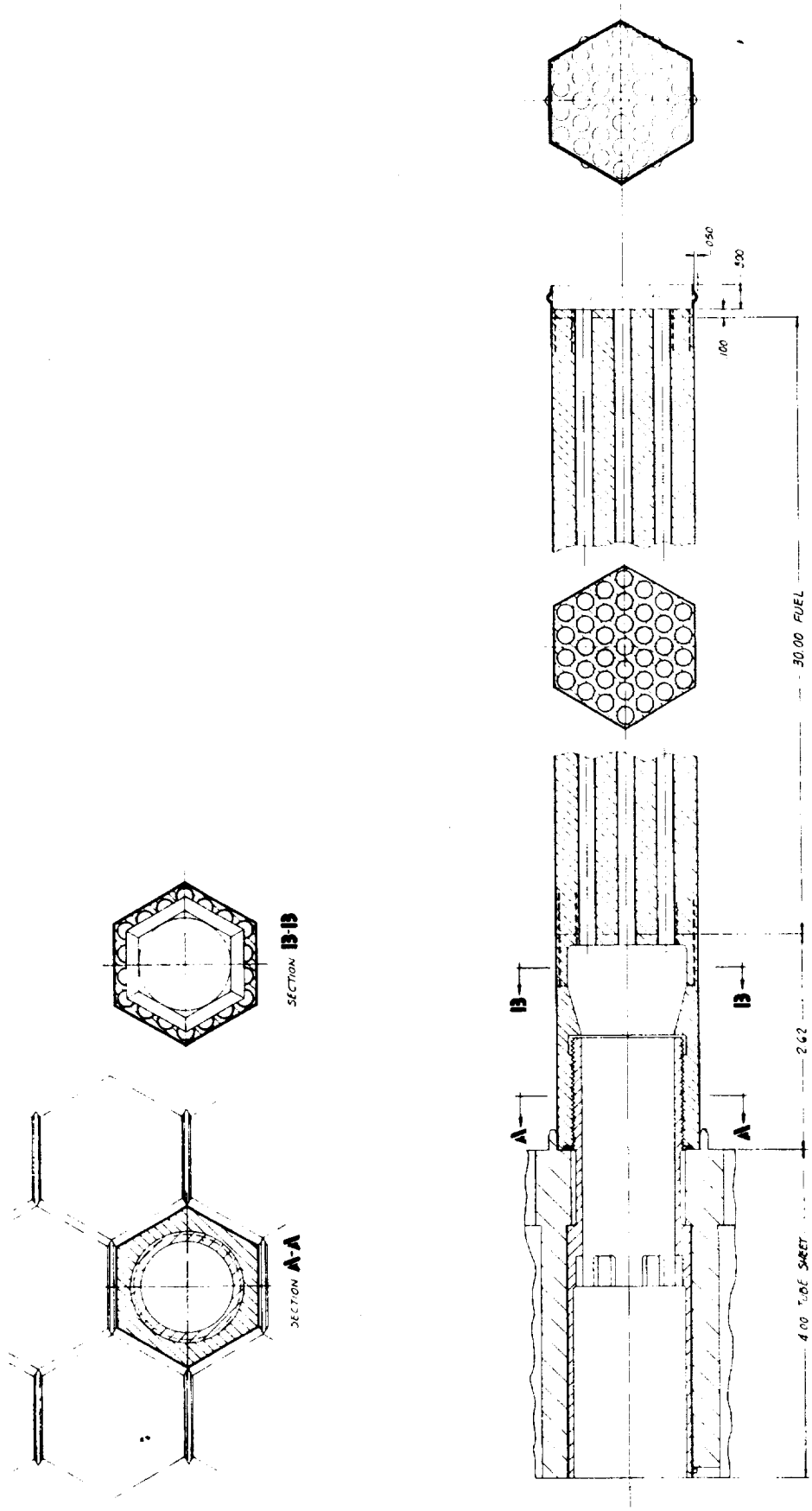

Fig. 5.2.30 – Fuel element – gas-cooled fast reactor (Dwg. 692E795)

[redacted]

Fig. 5.2.31 – Combination of potential causes of failure as related to its operation of space power systems, fuel cartridge development and qualification, and fuel system qualification

	Potential Causes													
	Pre-operational Vibration & Acceleration Forces	Temperature History	Power History	Fission Gas Pressure	Cladding - Core Diffusion	Operational Vibration & Acceleration Forces	Pressure Loads	Gas Stream Impurity Effects	Free Uranium Formation	Radiation Effects on Material Properties	Grain Growth	Interference with Adjacent Elements	Loss of Bond	Unidentified Deficiencies in Specification Limits or Manufactured Product
Space Power System														
Pre-operational (boost) phase	X											X	X	X
Normal operation phase before irradiation effects	X	X	X		X	X	X	X	X		X	X	X	X
Normal operational phase after irradiation effects	X	X	X	X	X	X	X	X	X	X	X	X	X	X
Fuel Cartridge Development and Qualification														
Non-nuclear tests														
Vibration and acceleration	X											X	X	X
Atmospheric static furnace		X			X				X		X		X	X
Pressurized static furnace														
Radiant-heated		X			X		X		X		X		X	X
Resistance-heated		X	X		X		X		X		X		X	X
Dynamic furnace		X	X		X		X	X	X		X		X	X
Nuclear test														
Static in-pile		X	X	X	X		X		X	X	X		X	X
Fuel System Qualification														
Vibration and acceleration	X											X	X	X
Reference Reactor Test		X	X	X	X		X	X	X	X	X	X	X	X

CONFIDENTIAL

CONFIDENTIAL

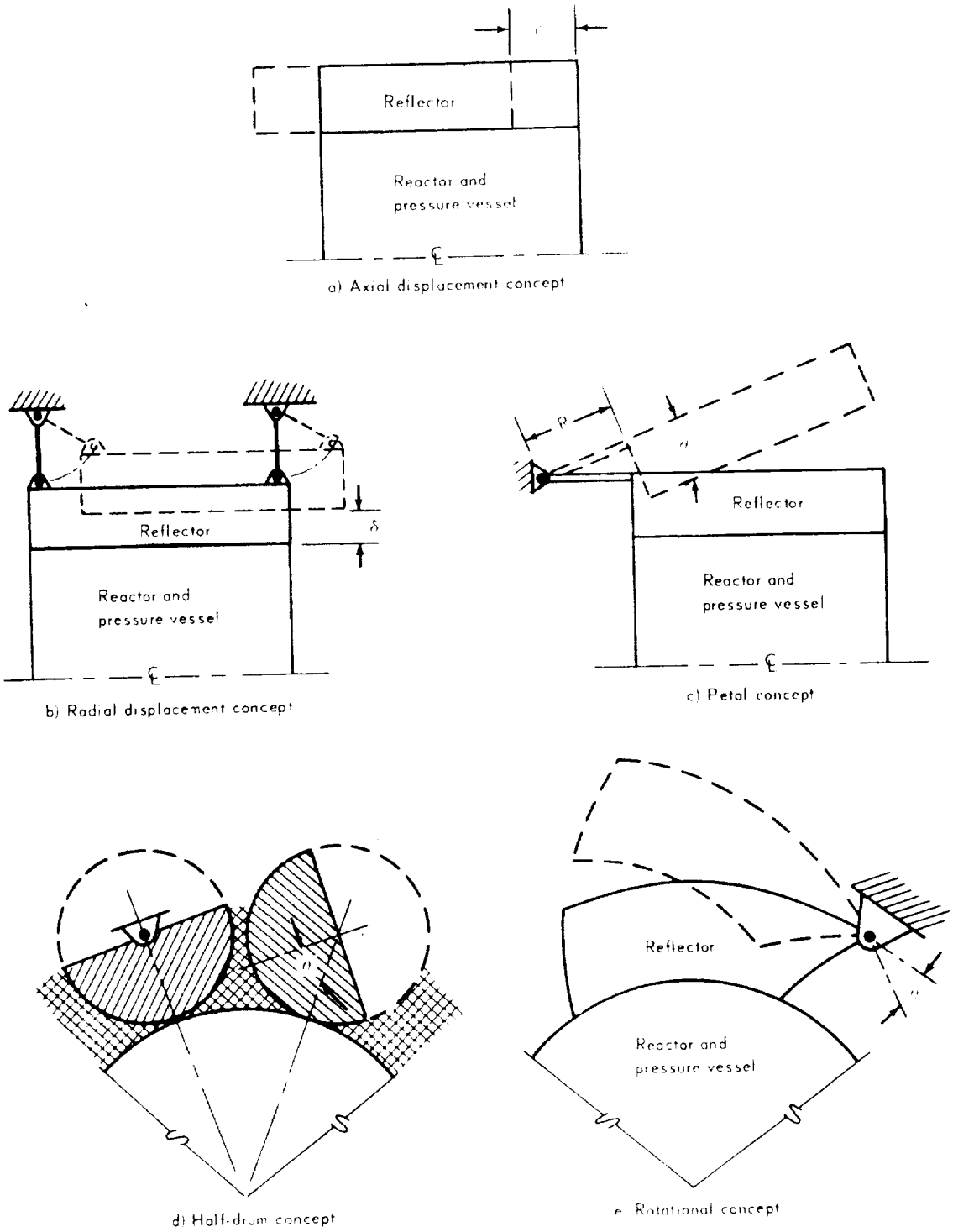

Fig. 5.2.32 – Methods for achieving reflector motion

[redacted]

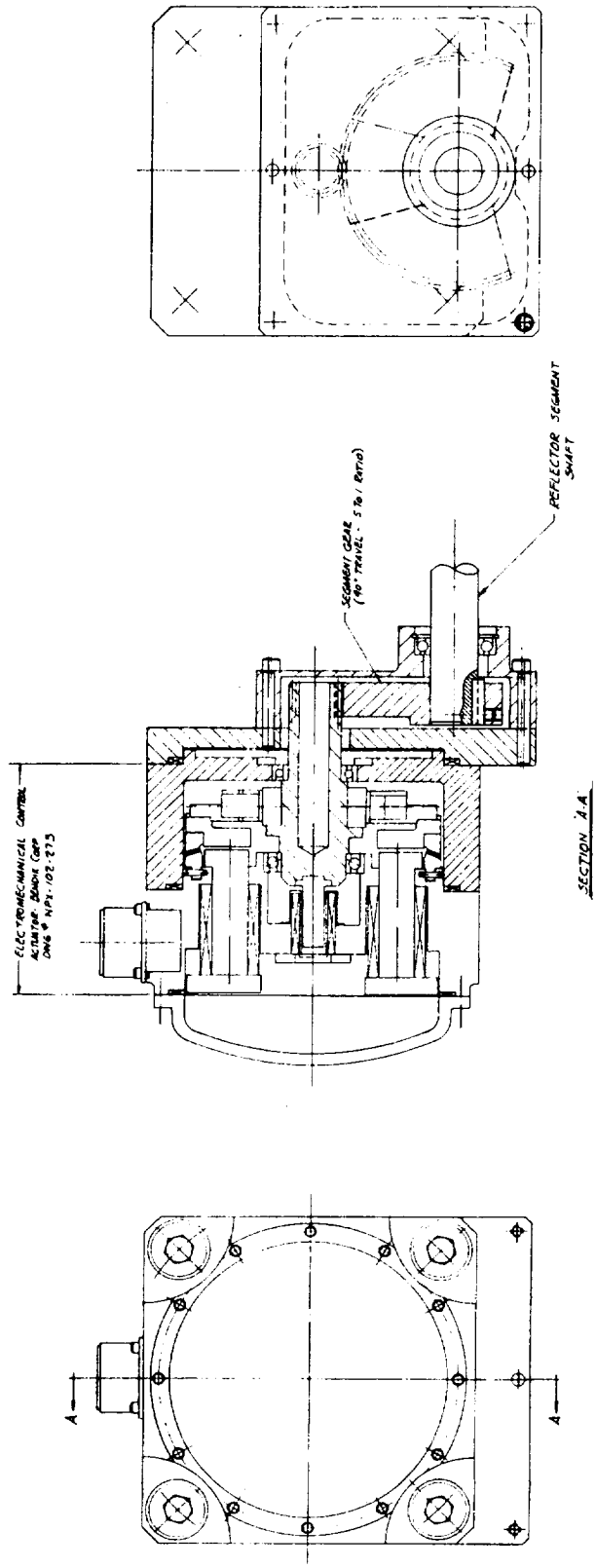

Fig. 5.2.33 – Bendix NUTATOR actuator (Dwg. 692E794)

CONFIDENTIAL

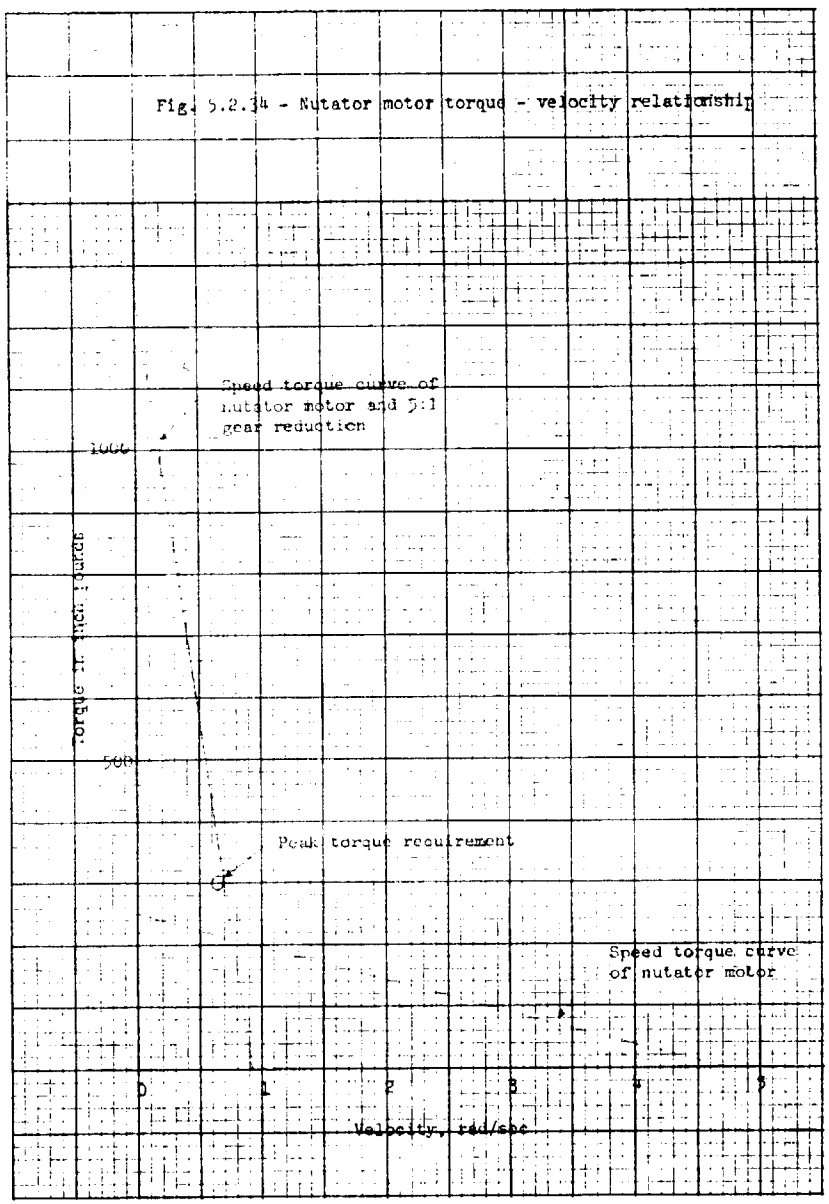

Fig. 5.2.34 - Nutator motor torque - velocity relationship

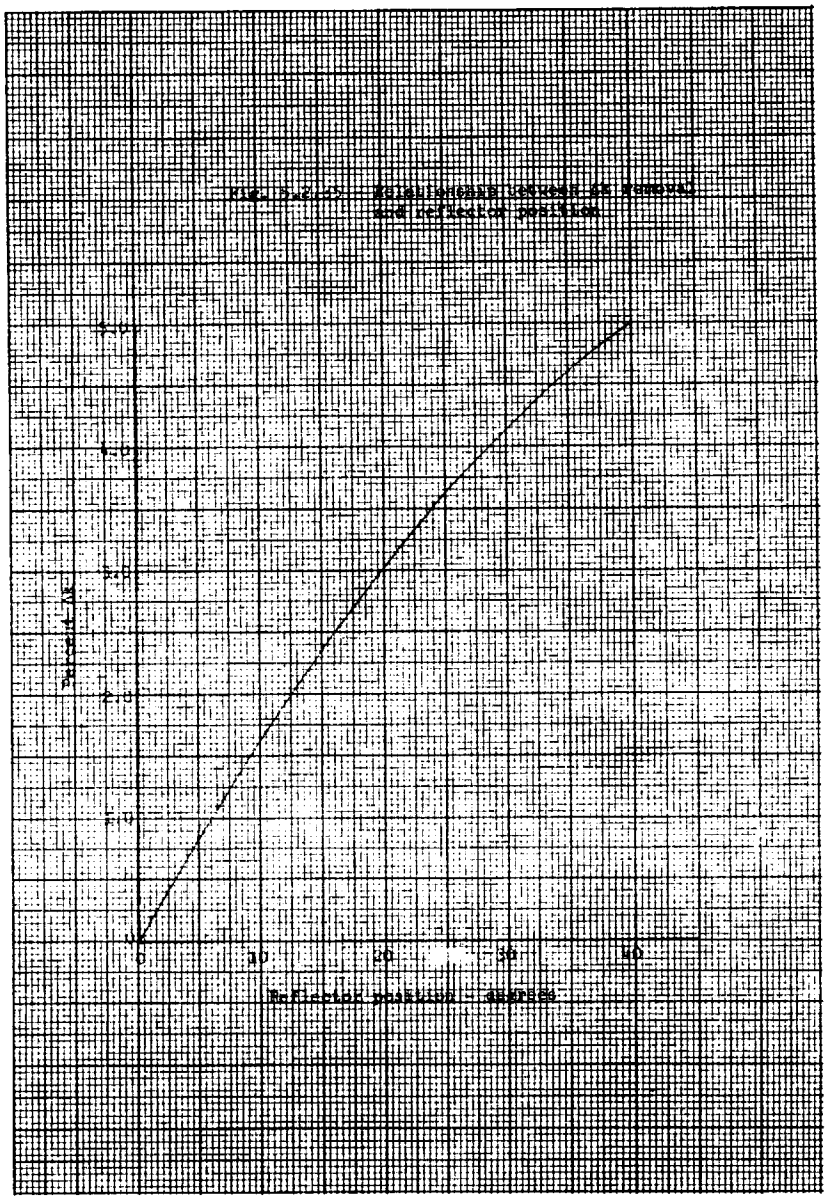

Fig. 5.2.35 - Relationship between Δt removal and reflector position

CONFIDENTIAL

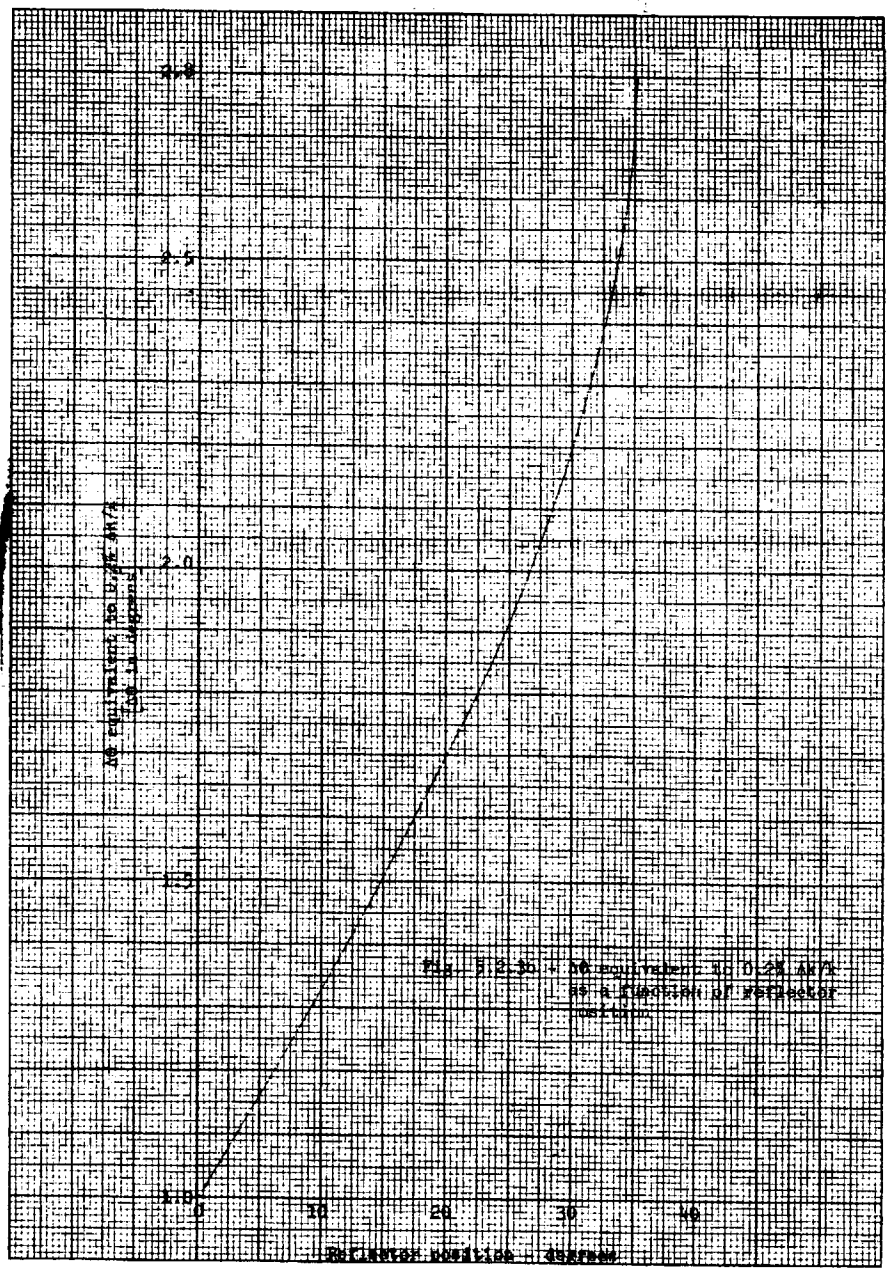

Fig. 5.2.3b - $\Delta\rho$ equivalent to 0.2% $\Delta k/k$ as a function of reflector position.

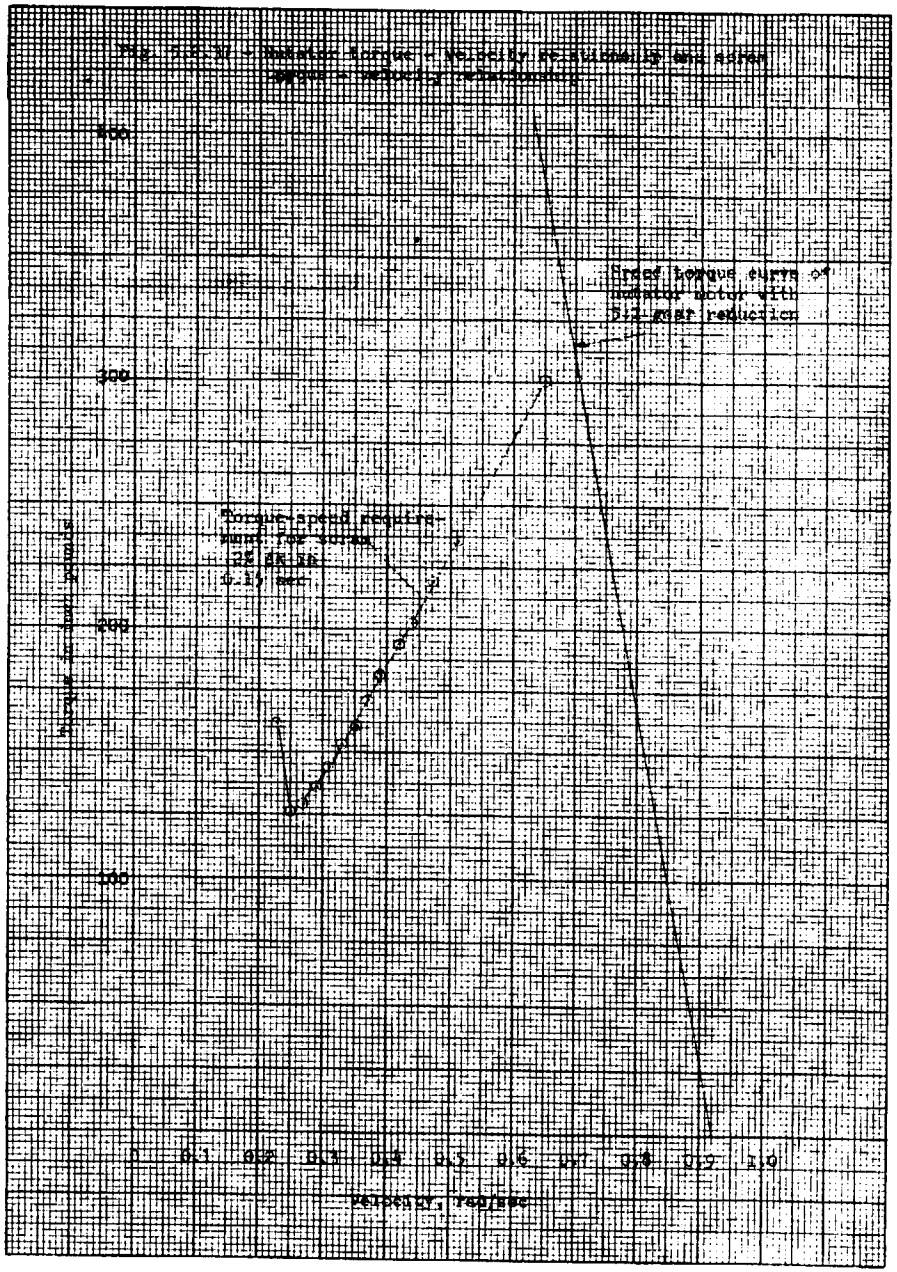

Fig. 5.2.3c - Indicator torque - velocity requirements and screen torque - velocity relationship.

CONFIDENTIAL

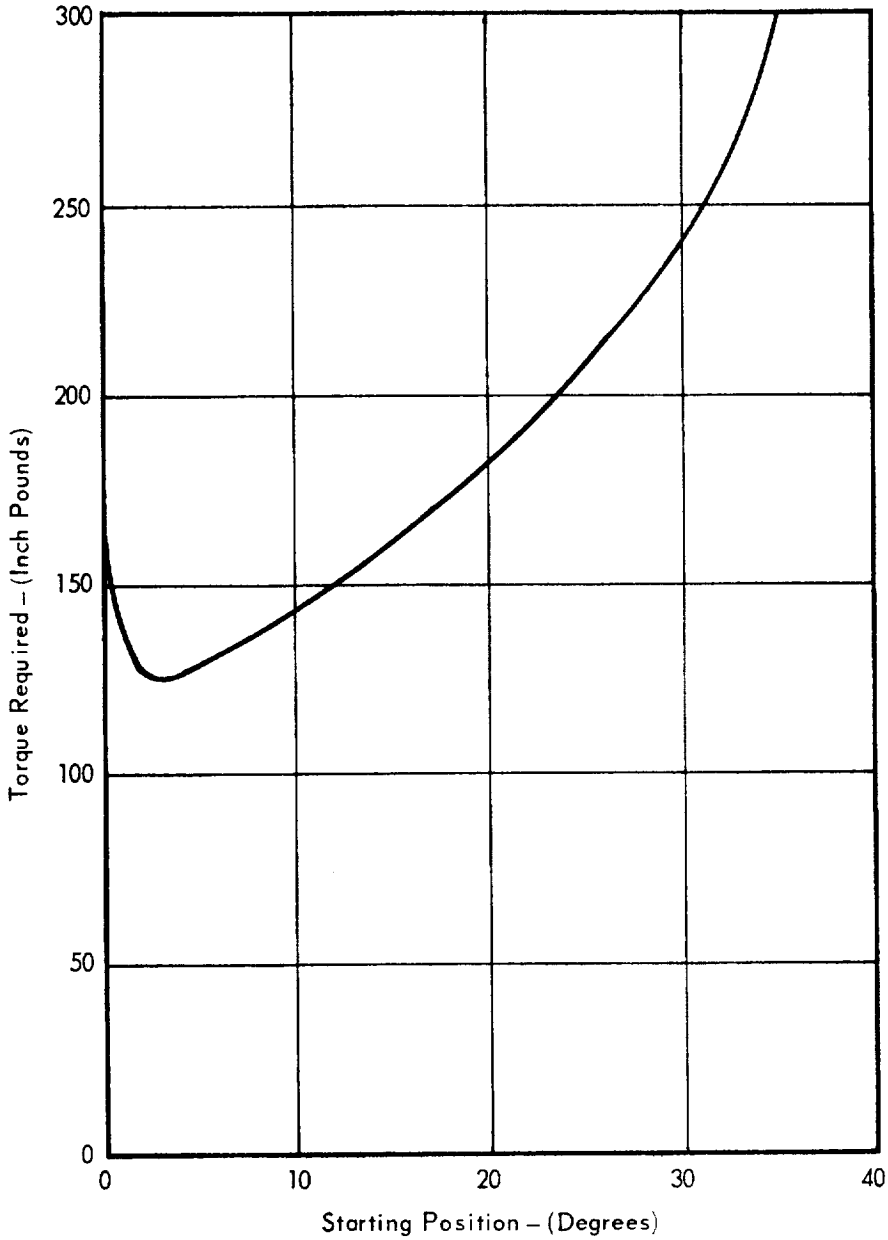

Fig. 5.2.38 – Torque required to remove 1.333% Δk per second

CONFIDENTIAL

5.3 NUCLEAR DESIGN AND ANALYSIS

This section presents the reactor nuclear design information necessary for evaluation in an aircraft application. Included are parametric data for sizing the reactor when variations are made in the flow area, structural material volume fraction, volume percent of UO_2 in the fueled matrix, and length-to-diameter ratio of the core. Data are included for the axial and radial power distribution within the active core for the design configuration selected in this study, for secondary heat and afterheat generation rates, and for fast neutron flux (> 0.9 Mev) levels. Problem areas and required development activities are discussed.

5.3.1 Design Criteria

1. The excess reactivity of the reactor assembly will be sufficient for a minimum of 250,000 Mw-hours, allowing for all short- and long-term effects. The data are presented in Table 5.3.1 which includes the increment required for 500,000 Mw-hours.
2. The reactor will be controlled by regulating neutron leakage through reflector removal. A shutdown margin of at least 2 percent $\Delta k/k$ is required at all times. Table 5.3.2 shows the required control worth.
3. Temperature flattening will be achieved by varying the hydraulic diameter of fuel element coolant channels. The changes in power distribution due to displacement of fuel caused by this variation are accounted for in the power distribution calculations.

5.3.2 Parametric Data

Parametric data were generated for the following range of variables:

Length-to-diameter ratio of core	0.8 to 1.6
UO_2 in fueled matrix, vol %	40 to 60
Void area in core, square feet	0.35 to 6.6
Structure-to-void ratio in core	0.1 to 0.4

The data from this work are presented in a total of 15 graphs, including all combinations of five length-to-diameter ratios (0.8, 1.0, 1.2, 1.4, and 1.6), and three core matrix compositions (40, 50, and 60 volume percent UO_2), by plotting reactor diameter versus void area with the structure-to-void ratio as a parameter. Figure 5.3.1 is a graph of the length-to-diameter ratio and volume percent UO_2 used for the selected design

CONFIDENTIAL

TABLE 5.3.1

REQUIRED EXCESS REACTIVITY

	Required Excess Reactivity, % Δk/k
Fuel burnup[a] – 250,000 Mw-hours (includes nonfission capture in U^{235})	-0.9
Doppler coefficient (68° → 2500° F)	-0.2
Fuel element expansion	-0.3
Total	-1.4

[a]For 500,000 Mw-hours, the fuel burnup would be -1.8% Δk/k, giving a total required excess reactivity of -2.3% Δk/k.

TABLE 5.3.2

REQUIRED CONTROL WORTH

	Reactivity, % Δk/k
Fuel burnup	0.9
Temperature (Doppler and expansion)	0.5
Minimum shutdown margin	2.0
Minimum control system worth[a]	3.4

[a]Preliminary designs should show at least 5% Δk/k control system worth to assure a feasible design.

[redacted]

configuration. The remaining parametric data are presented in Figures 5.3.10 through 5.3.23. The size of any reactor within the limits of the work can be found by interpolation.

Figure 5.3.2 shows the nuclear model used for this study. The thickness of all extra-core gaps was held constant except the clearance gap between the core and core shell, which was proportional to the core radius. The composition of all extra-core regions was also held constant except for the front tube sheet, fuel element nose piece region, and fuel element end plate regions, whose porosity was the same as that of the fuel element. The reactor multiplication factor used for this study was held constant at 1.05. This value includes 2 percent $\Delta k/k$ for observed bias between the analytical and experimental values, approximately 2 percent $\Delta k/k$ for fuel burnup and temperature coefficients (see section 5.3.1), and the rest for design contingencies.

In using these graphs, caution in three areas should be exercised. First, changes from the analytical model used for this study may introduce significant discrepancies. Second, these graphs were generated by an interpolation technique from more exact three-group diffusion calculations. The charts match these more exact calculations to within about ± 0.5 inch over the range of variables specified. Third, the basic methods used in the calculations have been verified by critical experiment measurements only in the reactor size range between 12 inch diameter by 12 inches long and 16.43 inch diameter by 14.7 inches long.

5.3.3 Reactivity, Power Distribution, and Burnup Control

REFLECTOR MATERIAL CHOICE

Nuclear analysis was performed to assess several possible reflector control methods, including two different radial reflector materials, Be and BeO. From a nuclear standpoint, BeO would be essentially equivalent to Be. They also included two different radial reflector environments, with the reflector immersed (1) in borated water and (2) in the same gas as the primary coolant.

The purpose of the analysis was to determine if the control margin available was sufficient in all cases. From a nuclear standpoint, all methods appear feasible. The worth of total reflector removal, shown in Table 5.3.3, is large enough for this application (see section 5.3.1). Beryllium causes a power spike at the core - reflector interface; however, when borated water is used as a coolant between core and reflector, a spike is also present even when the reflector is Mo. Although Mo is a better gamma shield than Be, it is also a source of gamma energy due to neutron capture,* so that there may be no particular advantage of either material relative to one another from a shielding standpoint.

One possible control method is a rotating drum of a moderating material with a thermal poison sector. This method was investigated for the 710 Experimental Reactor, a design concept studied in 1964 and 1965†. Detailed nuclear, mechanical, and thermal analyses were performed, and two critical experiments, Mockups 1A and 1B, were operated. One area which received a large amount of attention was the control worth of rotating poison drums in an engineered configuration. In this method, control is achieved by varying the thermal and epithermal neutron capture in the reflector. In an engineered configuration, the reflector drums or modules must be contained by structural materials. This material, which does not rotate, competes for neutron capture with the rotating poison. In the Experimental Reactor configuration with a core diameter of 16.5 inches, the calculated control worth with fully enriched boron-10 carbide poison segments was between 4 and 8 percent $\Delta k/k$ depending on the structure and configuration chosen. It appears that a maximum of 30 percent of the total removal worth (i.e., complete removal of reflector) of a Be or BeO reflector can be achieved by means of poison rotation. For smaller reactors whose reflectors are worth up to 20 percent $\Delta k/k$, the poison rotation method is feasible. For the selected design configuration, the worth of a Be reflector is about 10 percent $\Delta k/k$. Therefore, it does not appear desirable to use rotating poison control for the present application, especially when reflector removal does appear feasible.

POWER DISTRIBUTIONS FOR THE DESIGN CONFIGURATION

The design configuration was analyzed using a 2DF two-dimensional S_N transport theory code; the code is a direct extension of Carlson's S_N method‡ which was programmed by United Nuclear Corporation and modified by NASA-Lewis Research Center and GE-NMPO. Sixteen energy groups were used, the geometry was cylindrical, and S-4 angular detail was employed.

---

*"710 Reactor Program, Progress Report No. 20," GE-NMPO, GEMP-416, July 1, 1966, p. 34.

†"710 Reactor Program, Progress Report": No. 9, GEMP-301, July 31, 1964; No. 10, GEMP-310, Sept. 30, 1964; No. 11, GEMP-323, Nov. 30, 1964; No. 12, GEMP-333, Jan. 29, 1965; No. 13, GEMP-349, March 31, 1965; No. 14, GEMP-363, June 1, 1965; No. 15, GEMP-373, July 30, 1965; and No. 16, GEMP-385, Oct. 1, 1965.

‡B. G. Carlson, "The Numerical Theory of Nuclear Transport," Methods in Computational Physics, Vol. 1, Statistical Physics, Academic Press, 1963.

CONFIDENTIAL

Figure 5.3.3 shows the nuclear model used. Since the primary item of interest was power distribution, the nuclear model extends outward through only 5 inches of W shield. For this analysis, the control elements were in their closed or most reactive position. Table 5.3.4 lists the non-core zone compositions and Table 5.3.5 lists the various core compositions. (Note the increase in fuel with radial distance from the core center which is due solely to the effect of the hydraulic diameter variation, and does not represent a change in the UO_2-to-tungsten ratio.) The reactor multiplication factor obtained from this 2DF analysis was 1.098; in the three-group diffusion analysis of this configuration, the factor was 1.097.

Figure 5.3.4 shows the axially averaged radial power distribution per unit of fuel matrix volume. Note the small spike at the core - reflector interface due to the borated water in the core shell zone. Figure 5.3.5, 5.3.6, and 5.3.7 show the axial power distribution at the core centerline, at the radial power minimum, and at the core edge. The slight local peak at the rear core edge is caused by the borated water located at the rear of the radial reflector and next to the core shell.

Figures 5.3.8 and 5.3.9 show the fast neutron flux (greater than 0.9 Mev) axially along the core centerline and radially at the axial power peak, respectively.

The power distributions have been reported for one position of the control element. These distributions will change during operation. This effect is discussed in section 5.3.6.

NUCLEAR STABILITY

Although a nuclearly stable reactor system is feasible with some positive-reactivity components, it is virtually assured when all temperature-dependent reactivity coefficients are negative and occur in short time. For this type of reactor, the temperature coefficient of reactivity is short-time without any identified delayed components when using a Mo reflector. The identified reactivity effects are also negative over the entire range from room temperature to the core melting point. The contributions from Doppler broadening (scaled from previous analyses on the 710 Reactor) and from thermal expansion are given below for two temperature levels:

Change in Reactivity From Room Temperature to Operating Temperature (% Δk/k)

	2500°F	5000°F
Doppler broadening	- 0.17	- 0.21
Expansion	- 0.26	- 0.71
Total	- 0.43	- 0.92

The reactor is inherently stable during normal operation because of the short-time negative characteristic. Effects due to the presence of borated water surrounding the reflector and shields are not expected to affect this conclusion for the normal operating procedures of this application; however, thorough analyses are required of malfunctions or possible operator errors to determine if instabilities might arise from these sources.

CONFIDENTIAL

CONFIDENTIAL

TABLE 5.3.3

AVAILABLE CONTROL WORTHS

Reflector Environment	Total Radial Reflector Worth, % Δk	
	Beryllium	Molybdenum
Gas	10.7	13.0
Borated water	9.0	11.2

[redacted]

TABLE 5.3.4

2DF NON-CORE ZONE COMPOSITIONS

Zone Description (See Figure 5.3.3)	Constituents	Amount in Zone[a]
Shield	Tungsten	VF = 0.9
	Borated water	VF = 0.1
Borated water	Water	VF = 1.0
	Boron (as potassium pentaborate, 20.4 grams per 100 grams of solution)	1.609×10^{-3} N/barn-cm
Radial reflector	Molybdenum	VF = 0.9
	Borated water	VF = 0.1
Shell zone (radial and rear)	Inconel 600	VF = 0.346
	Borated water	VF = 0.360
	Nb-752 alloy	VF = 0.059
	Void	VF = 0.235
Shell zone (forward of tube sheet)	Inconel 600	VF = 1.0
End plate	W-Mo-Re alloy	VF = 0.526
Tube sheet	Inconel 600	VF = 0.637

[a]VF means volume fraction.

CONFIDENTIAL

TABLE 5.3.5

CORE COMPOSITION

Core Region in Order of Increasing Radius from Core Center (see Figure 5.3.3)	No. of Cells	Volume Fraction[a]		
		UO_2	W (in Matrix)	W-Mo-Re
1	1	0.1977	0.1318	0.1078
2	6	0.1985	0.1323	0.1077
3	12	0.2006	0.1337	0.1073
4	18	0.2054	0.1370	0.1066
5	24	0.2120	0.1413	0.1056
6	30	0.2227	0.1485	0.1039
7	36	0.2365	0.1577	0.1016
8	42	0.2527	0.1685	0.0989
9	48	0.2722	0.1815	0.0955
10	24	0.2944	0.1963	0.0915
	Total 241	Avg. 0.2428	0.1619	0.1004

[a]Matrix is 40W – 60UO_2 (vol %) at 95% theoretical density. Volume fractions listed are for theoretical density.

[redacted]

Bowing of the fuel elements either due to thermal gradients or to differential growth arising from fission products leads to a zero or negative reactivity coefficient provided there is no rear tube sheet. If a rear fuel element support is used, detailed analysis will be necessary to estimate both the thermal expansion and the permanent growth effects so as to determine if a positive effect could exist.

5.3.4 Secondary Heat Generation Rates

Detailed nuclear heating calculations made on the 710 Reactor* permit the following observations. First, most of the core gamma energy will remain in the core since the core materials are all good gamma ray absorbers. Second, in extra-core components, such as the radial reflectors and structural materials, much of the heating will be due to neutron-capture-induced gamma rays. This fact will require an accurate neutron calculation beyond the core boundaries. Third, the total heat deposited outside the core and core shell will be small. In the 710 Experimental Reactor, approximately 98.5 percent of the total reactor power was deposited in the core, tube sheet, and core shell areas. Most of the rest of the reactor power would be deposited in the reflector and nearby borated water.

5.3.5 Afterheat Generation Rates

The afterheat generation rates were taken from previous analyses of the 710 Reactor. Figure 5.4.8 shows the core heating rate for various times of operation versus time after shutdown.

5.3.6 Assessment of Problem Areas and Current State-of-the-Art

There are several problems in the nuclear design area for which sufficient information for precise design is not available. None of these problems appear to require more than normal experimental or analytical work to resolve. These areas include power distributions, control system worth, power perturbations due to control motion, temperature coefficients, and safety analyses. A critical experiment program would provide much of the needed information and, considering the present state-of-the-art, is an essential part of a preliminary design effort. Besides providing a benchmark for analysis, a critical experiment program would provide power distributions, critical mass, control system worth, power perturbations caused by control element motion, and other static room-temperature data.

Analysis would be necessary to compute temperature coefficients of reactivity and other temperature-dependent effects. The experimental determination of these items in a heated critical assembly represents a matter of economics rather than engineering necessity, since an operating

*"710 Reactor Program, Progress Report No. 14," GE-NMPO, GEMP-363, June 1, 1965, p. 54-55.

reactor test might provide the information as quickly and as cheaply as a heated critical experiment.

Table 5.3.6 shows an example of the possible interplay between experiment and analysis. Note that a reactor built with present knowledge would have to have analytically predicted values for excess reactivity of 4.8 percent $\Delta k/k$ and for control system worth of 12.8 percent $\Delta k/k$ to give reasonable assurance of operating properly. In the final design phase, these numbers might become 2.1 percent $\Delta k/k$ and 5.1 percent $\Delta k/k$, respectively. The maximum reflector worth for the selected design is about 10 percent $\Delta k/k$ which is less than that required using concept phase values. This does not mean that the design is not feasible, but that the uncertainties must be reduced. It is expected that these uncertainties can be reduced by refined analyses, supported with a critical experiment, to the values specified in the last column of Table 5.3.6.

5.3.7 Parametric Data - Figures

This section contains the rest of the parametric graphs described in section 5.3.2, Figures 5.3.10 through 5.3.23. In these figures, VF_{str}/VF_{void} is the ratio of volume fraction of core structural material to the volume fraction of core void, and pertains to the numbers shown on the curves.

5.4 THERMAL DESIGN AND ANALYSIS

This section presents the reactor thermal design information, parametric data on reactor sizing, evaluation of the design, and assessment of problems.

5.4.1 Thermal Design Criteria

1. Maximum temperature for the fuel is set by the limit estimated for 1 percent calculated growth due to gaseous fission product pressure in 1000 hours of full-power operation. This capability is not necessarily fully exploited.
2. Primary control of the radial temperature profile will be by means of hydraulic diameter variation from element to element and, if necessary, within individual elements. Fuel concentration variation may be used to accommodate specific problems unique to their application.

5.4.2 Parametric Data

BLOWER CYCLE

Preliminary phases of the blower cycle study indicated that core diameters of approximately 30 inches were consistent with reactivity requirements and flow areas that would make possible the achievement of core pressure drops as low as 1.5 percent of the coolant pressure level. Coolant channel sizes would yield maximum fuel element surface temperature of 2200°F for the average element in cores of this size. Estimates of potential local fuel element temperature levels were consistent with the requirement of 1000 hours of operation and fuel element growth of 1

TABLE 5.3.6

REACTIVITY AND CONTROL SYSTEM REQUIREMENTS

	Excess Reactivity or Control System Worth, % Δk/k	
	Concept Phase	Final Design
Reactivity Requirements		
Fuel burnup (250,000 Mw-hours)	- (0.9 ± 0.2)	- (0.9 ± 0.1)
Doppler coefficient	- (0.2 ± 0.2)	- (0.2 ± 0.1)
Fuel element expansion	- (0.3 ± 0.3)	- (0.3 ± 0.1)
Total change during operation	- (1.4 ± 0.4)	- (1.4 ± 0.2)
Worst combination expected	- 1.8	- 1.6
Therefore: required excess reactivity (as-built)	1.8	1.6
Accuracy of prediction of excess reactivity (concept phase has no design critical experiment but final design does)	± 3.0	± 0.5
Design excess reactivity must be: (To assure the required amount)	4.8 ± 3.0	2.1 ± 0.5
Control System Worth Requirements		
Reactivity allowance	7.8	2.6
Minimum shutdown worth	2.0	2.0
Total control system worth	9.8	4.6
Accuracy of prediction of control system worth	+ 3.0	+ 0.5
Design control system worth	12.8	5.1

CONFIDENTIAL

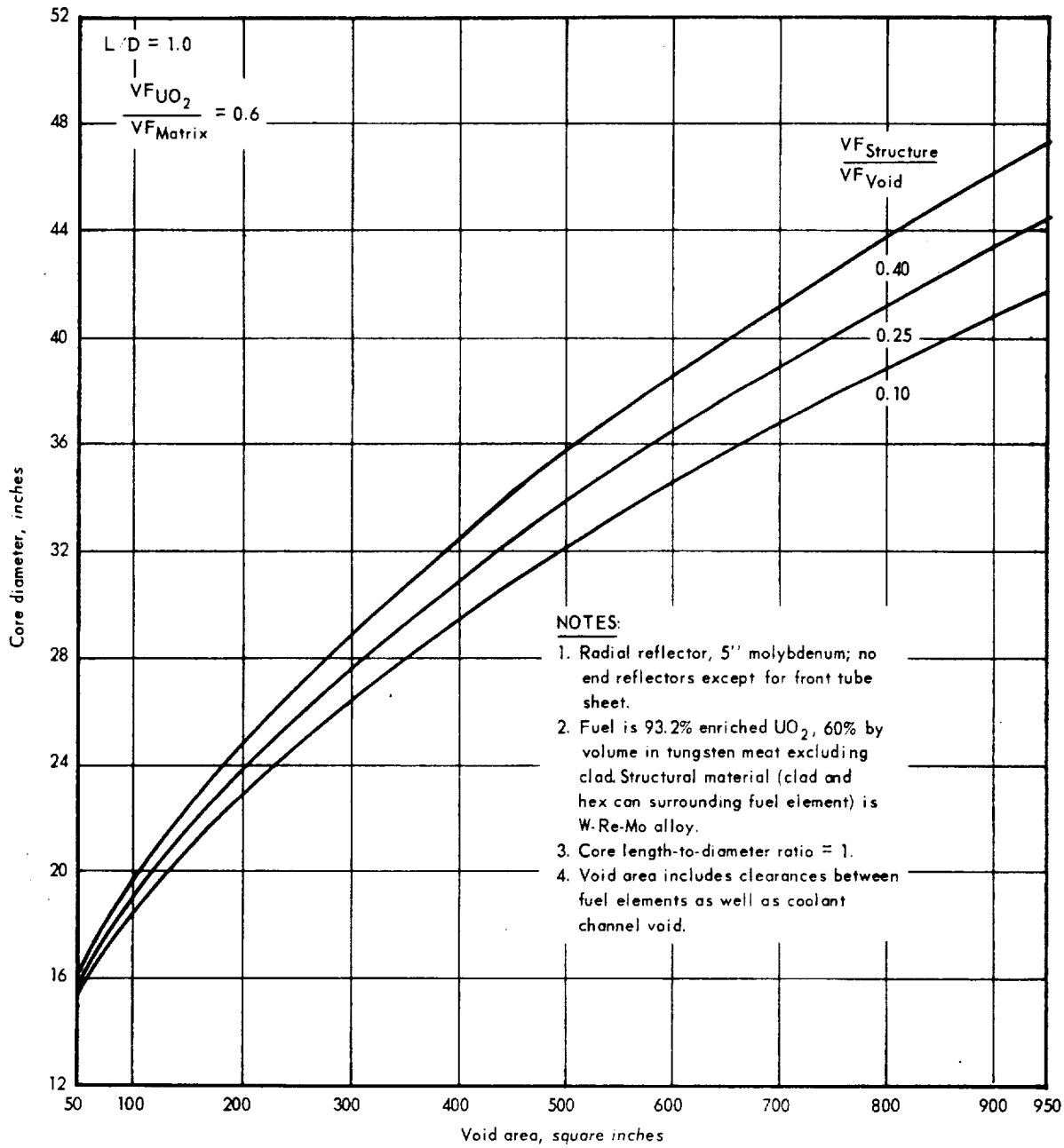

Fig. 5.3.1 – Core diameter versus void area

[redacted]

Figure 5.3.2

Nuclear Model for Parametric Study

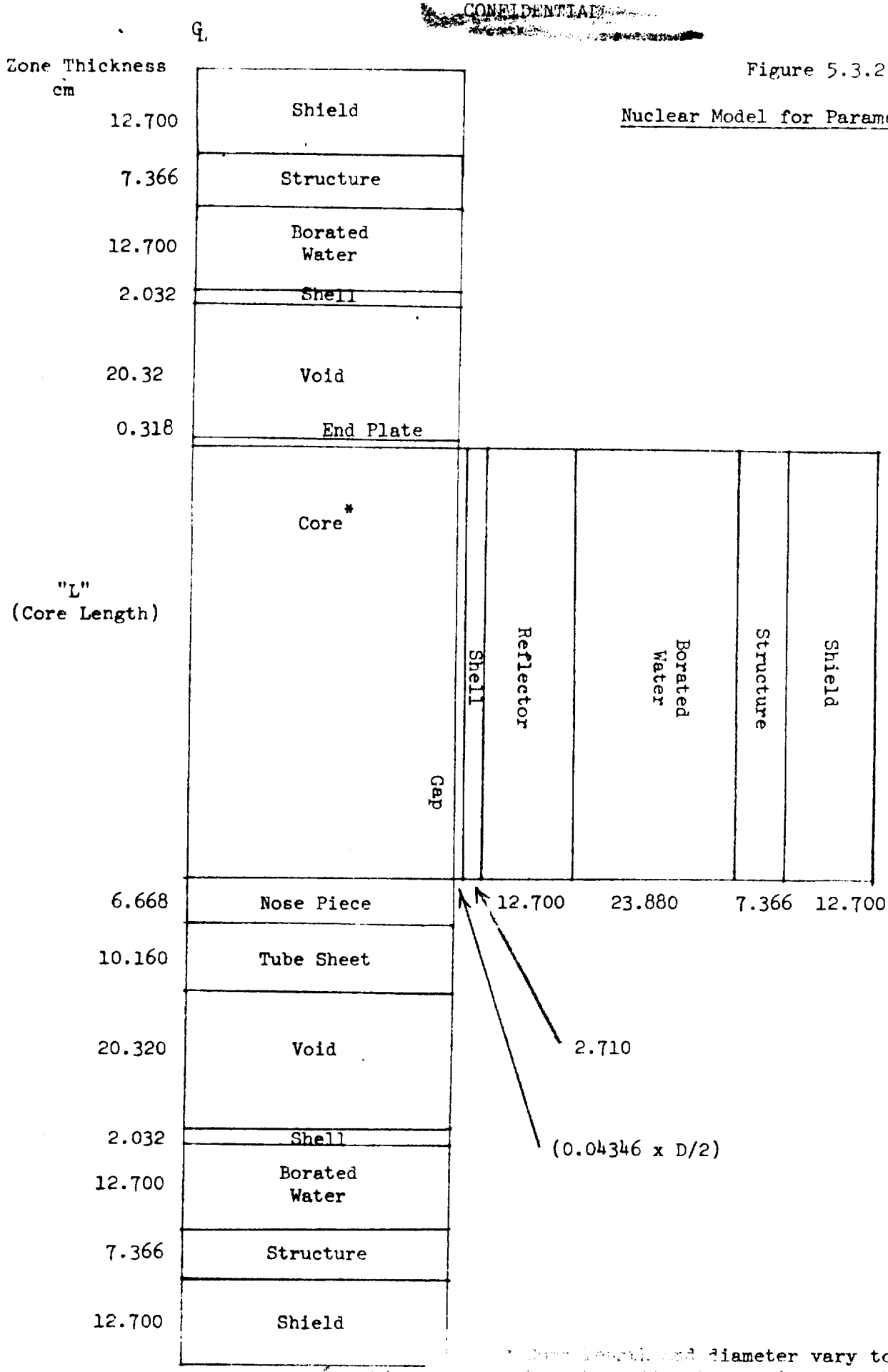

* [illegible] and diameter vary to maintain length-to-diameter ratio and achieve a [illegible] of 1.05

CONFIDENTIAL

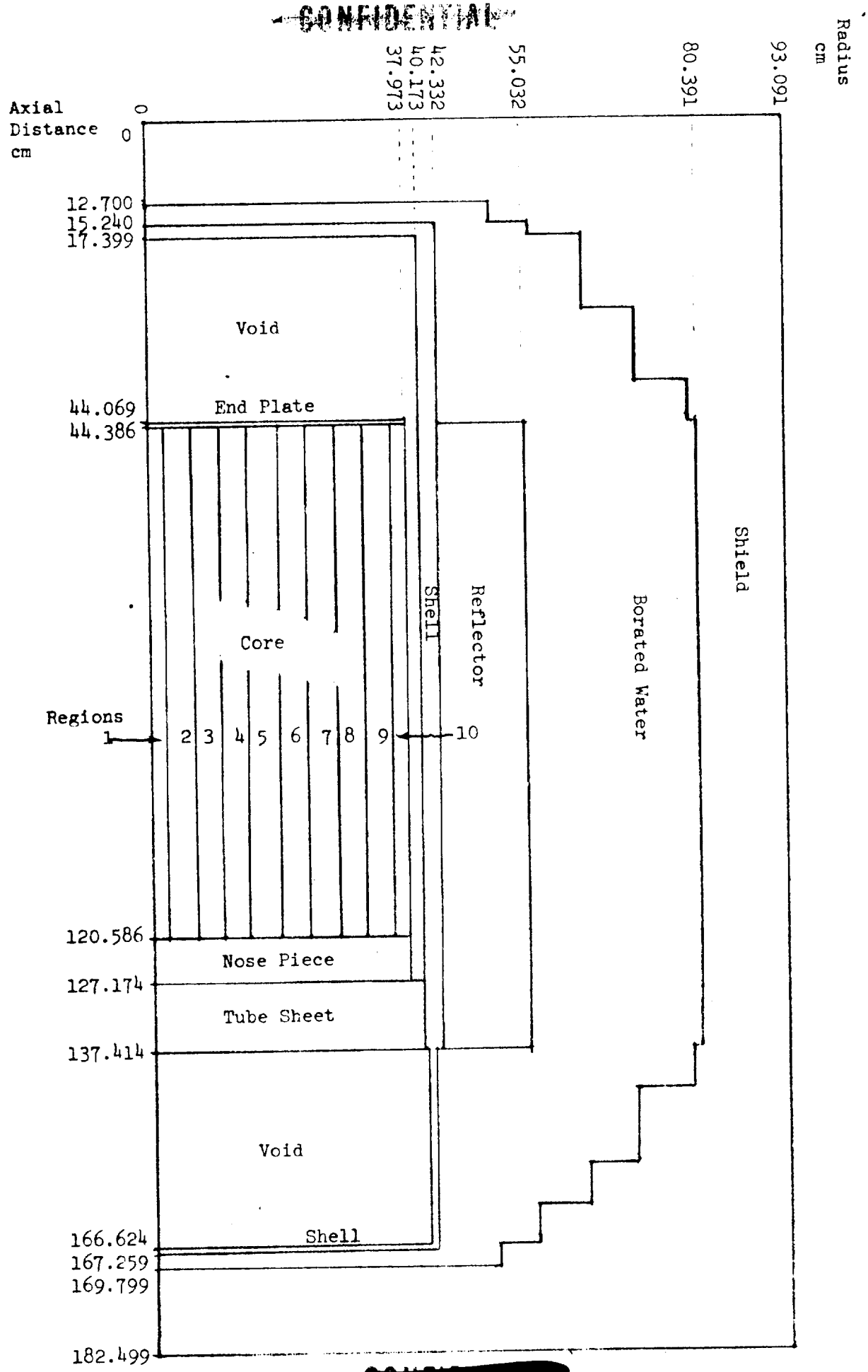

Figure 5.3.3

Nuclear Model for Transport Calculation

[redacted]

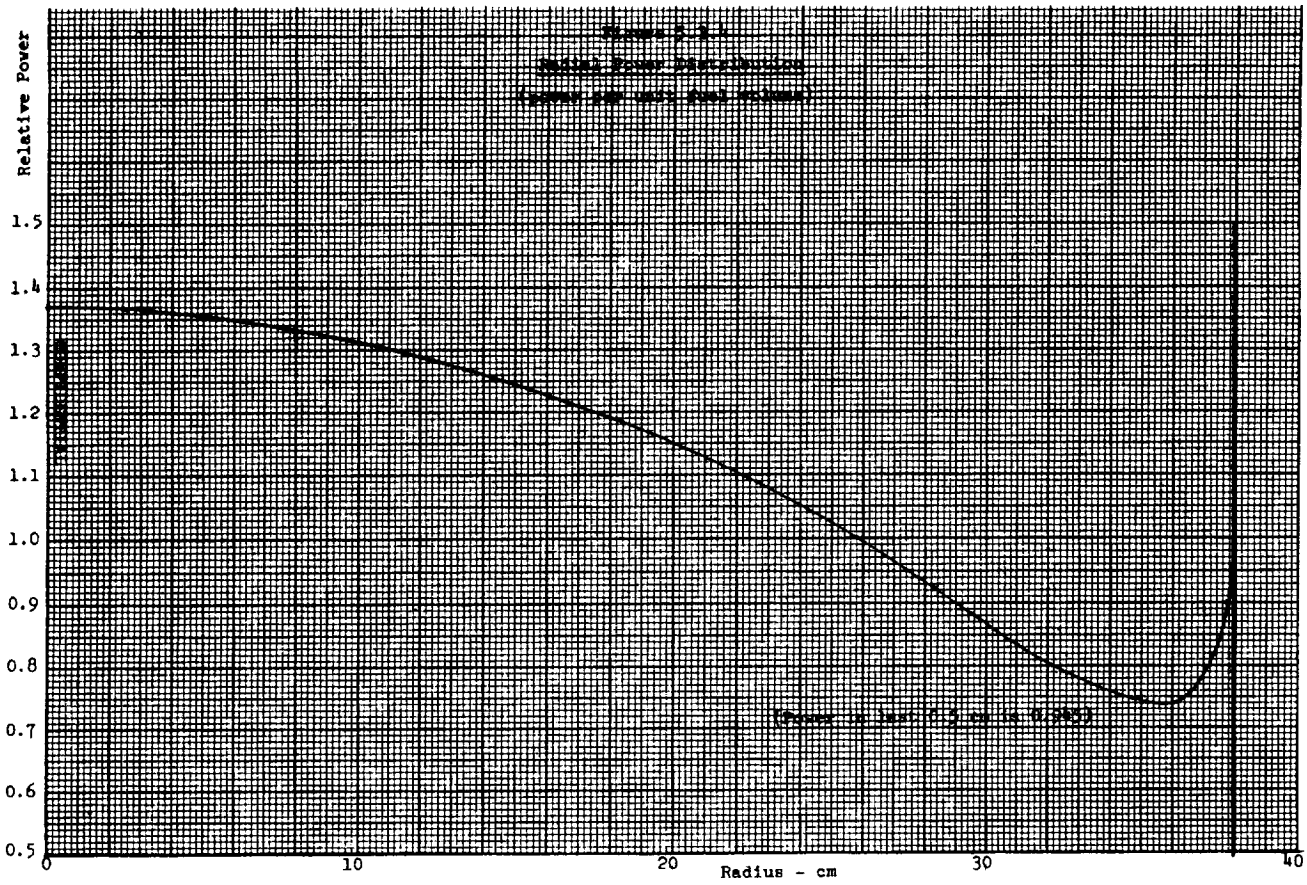
Relative Power
1.5
1.4
1.3
1.2
1.1
1.0
0.9
0.8
0.7
0.6
0.5
0
10
20
30
40
Radius - cm

Figure 5.3.5

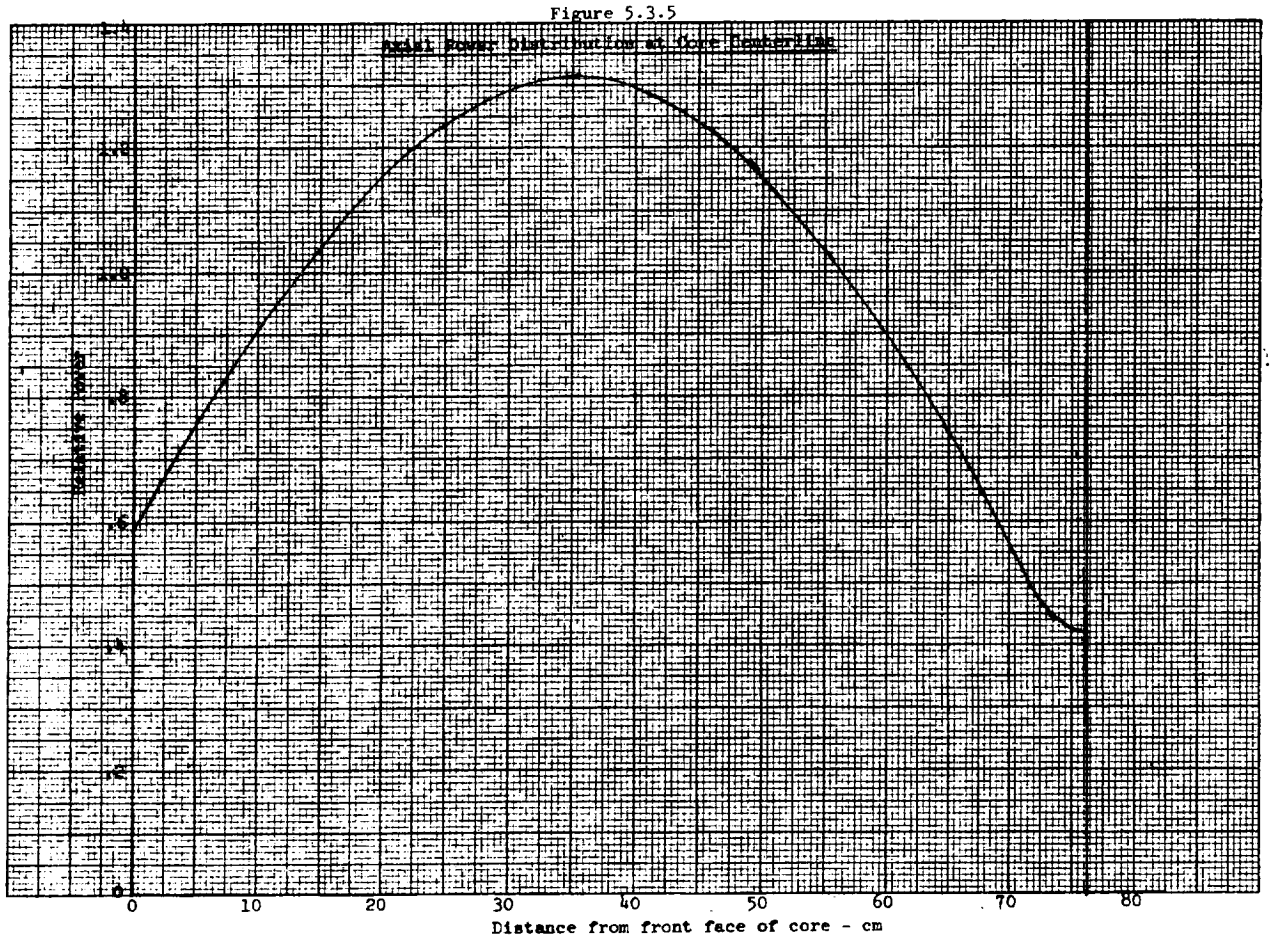
0
10
20
30
40
50
60
70
80
Distance from front face of core - cm

CONFIDENTIAL

Figure 5-2.6

Axial Power Distribution at Reactor Power Maximum

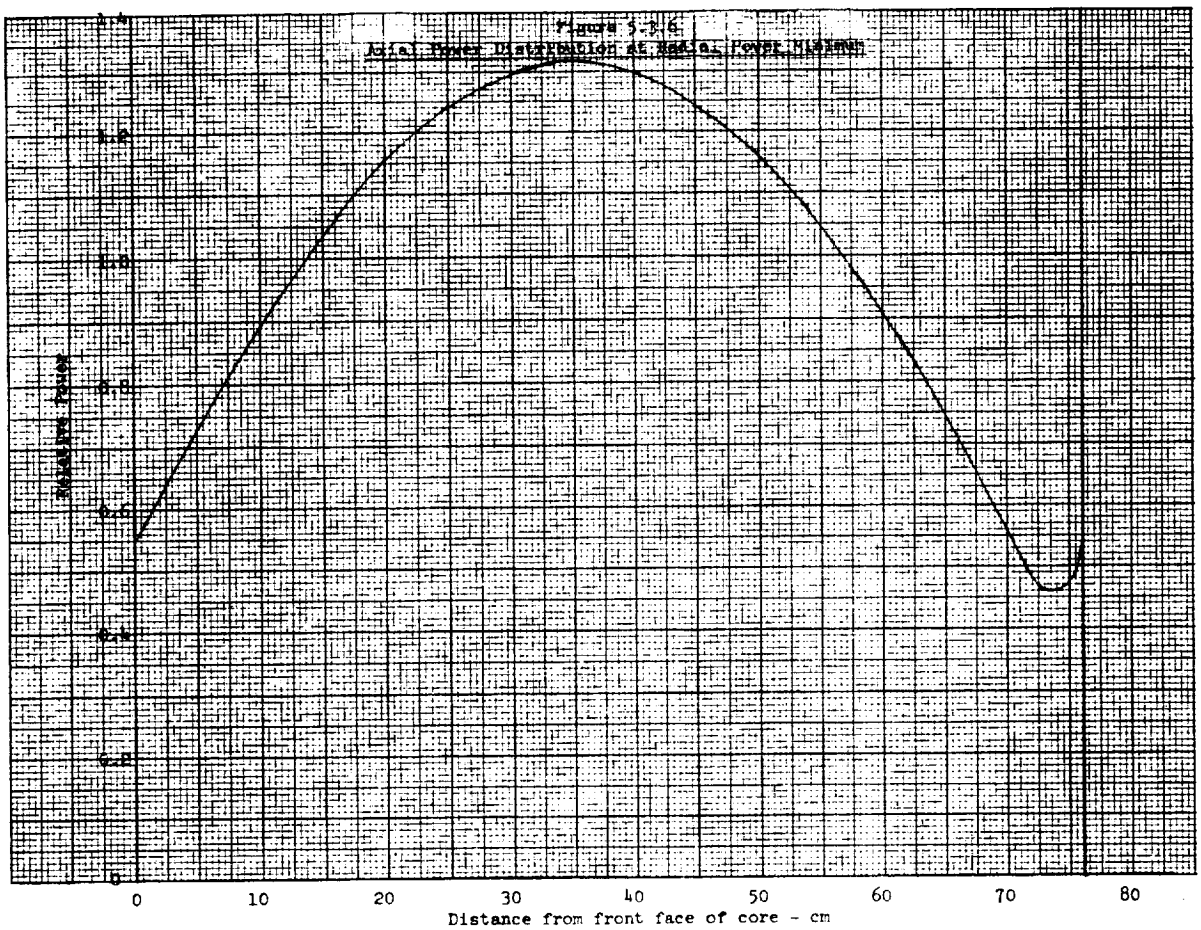

Figure 5-2.7

Axial Power Distribution at Core Edge

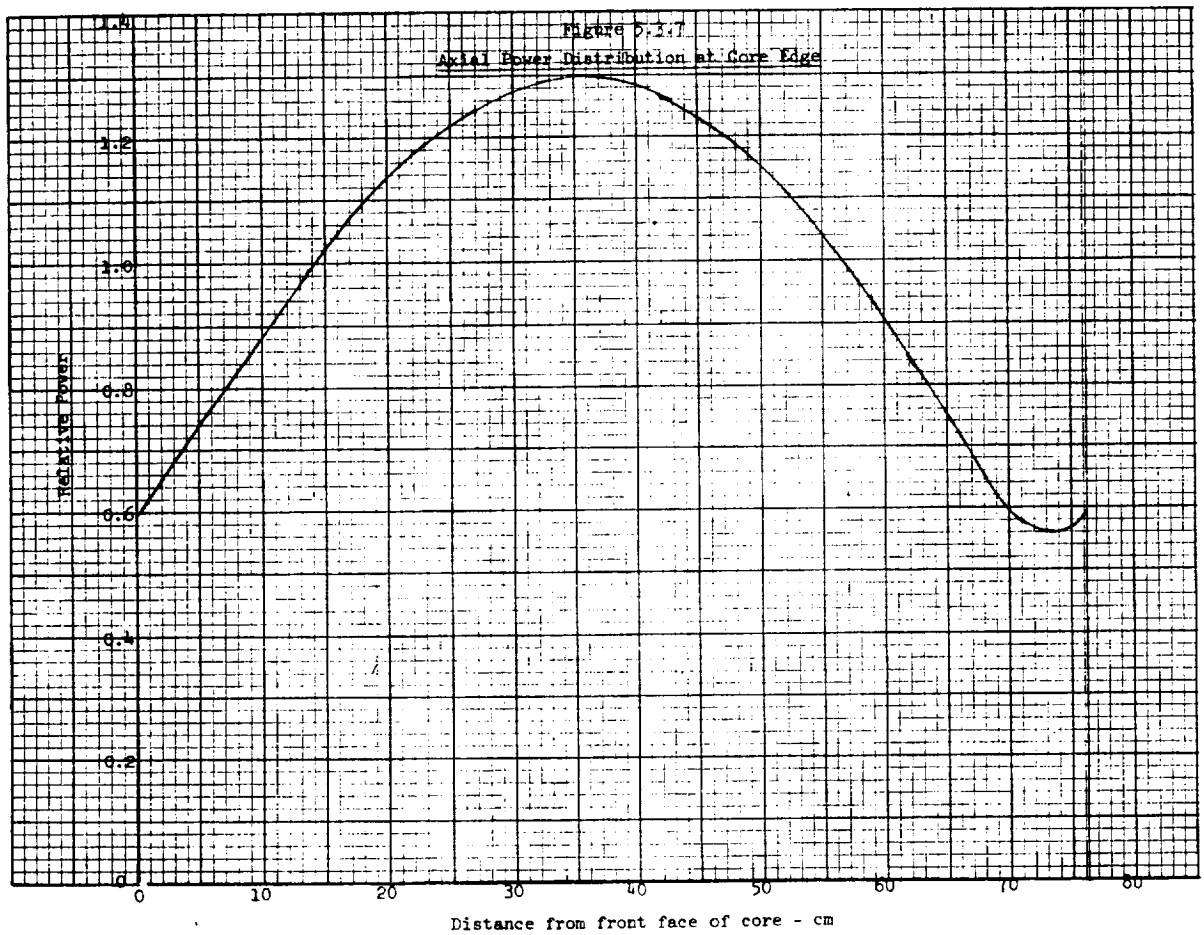

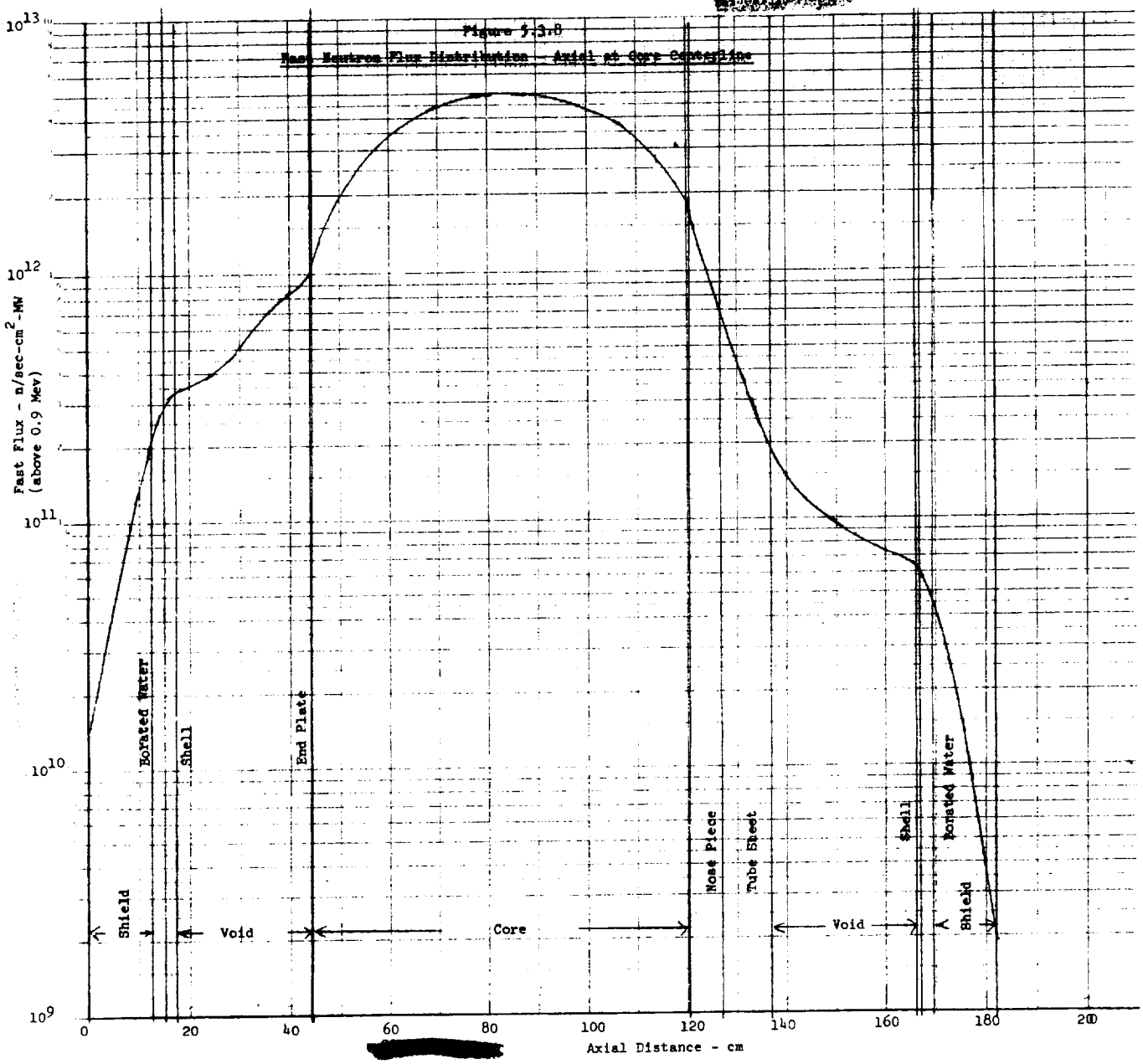

Figure 5.3.8

Fast Neutron Flux Distribution - Axial at Core Centerline

[redacted]

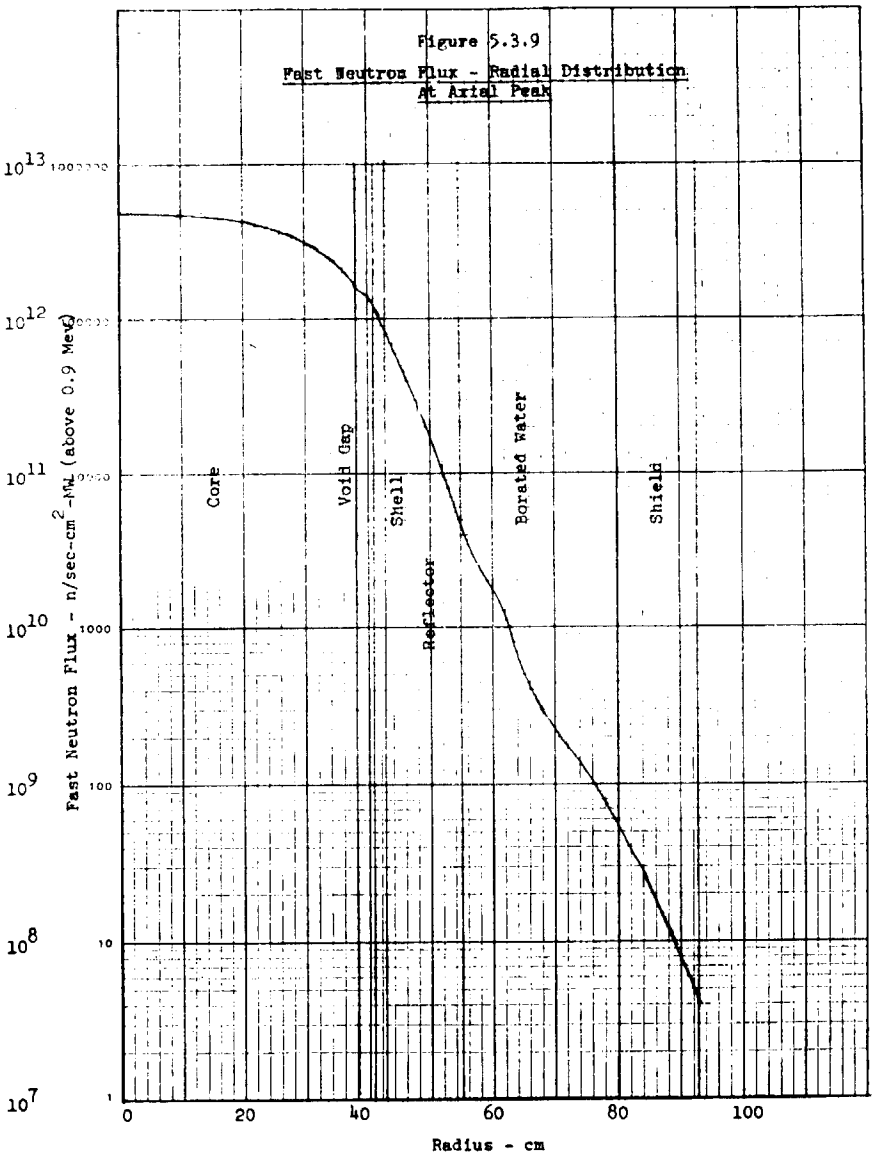

Fig. - 5.3.10 Nuclear Sizing Chart

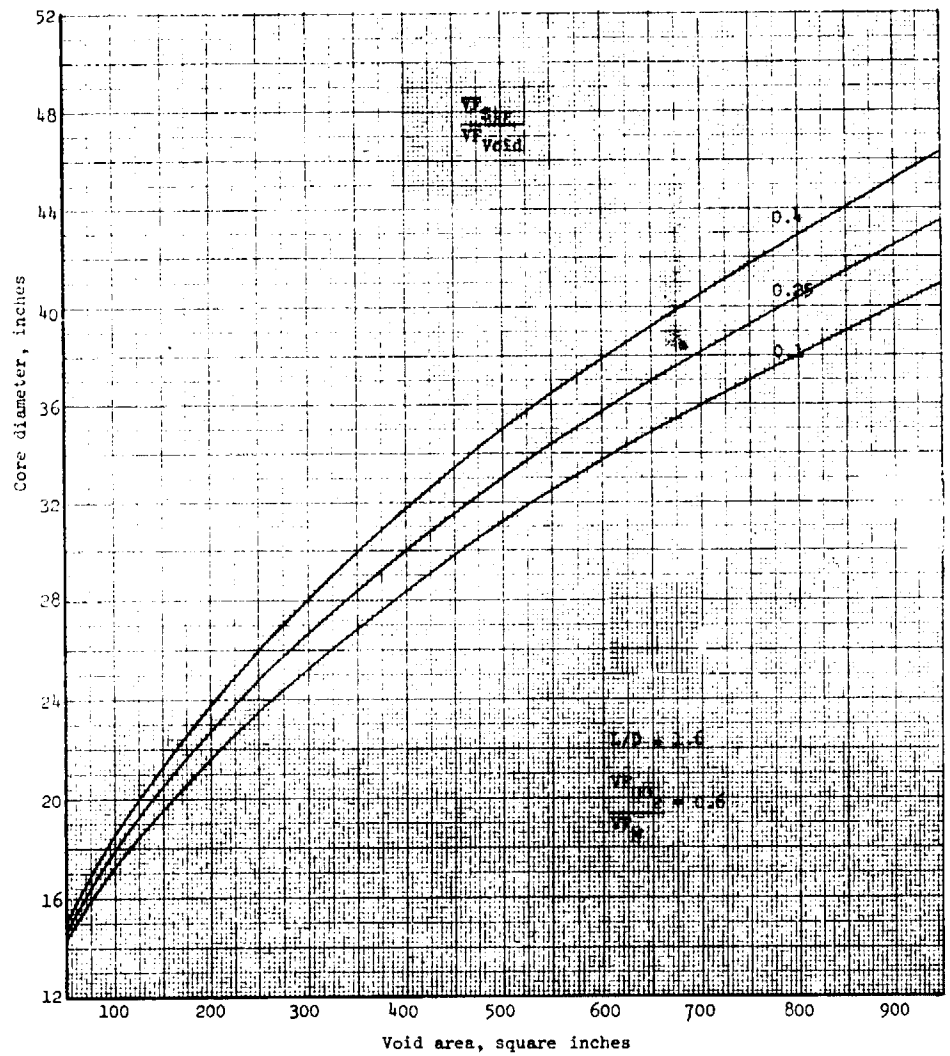

CONFIDENTIAL

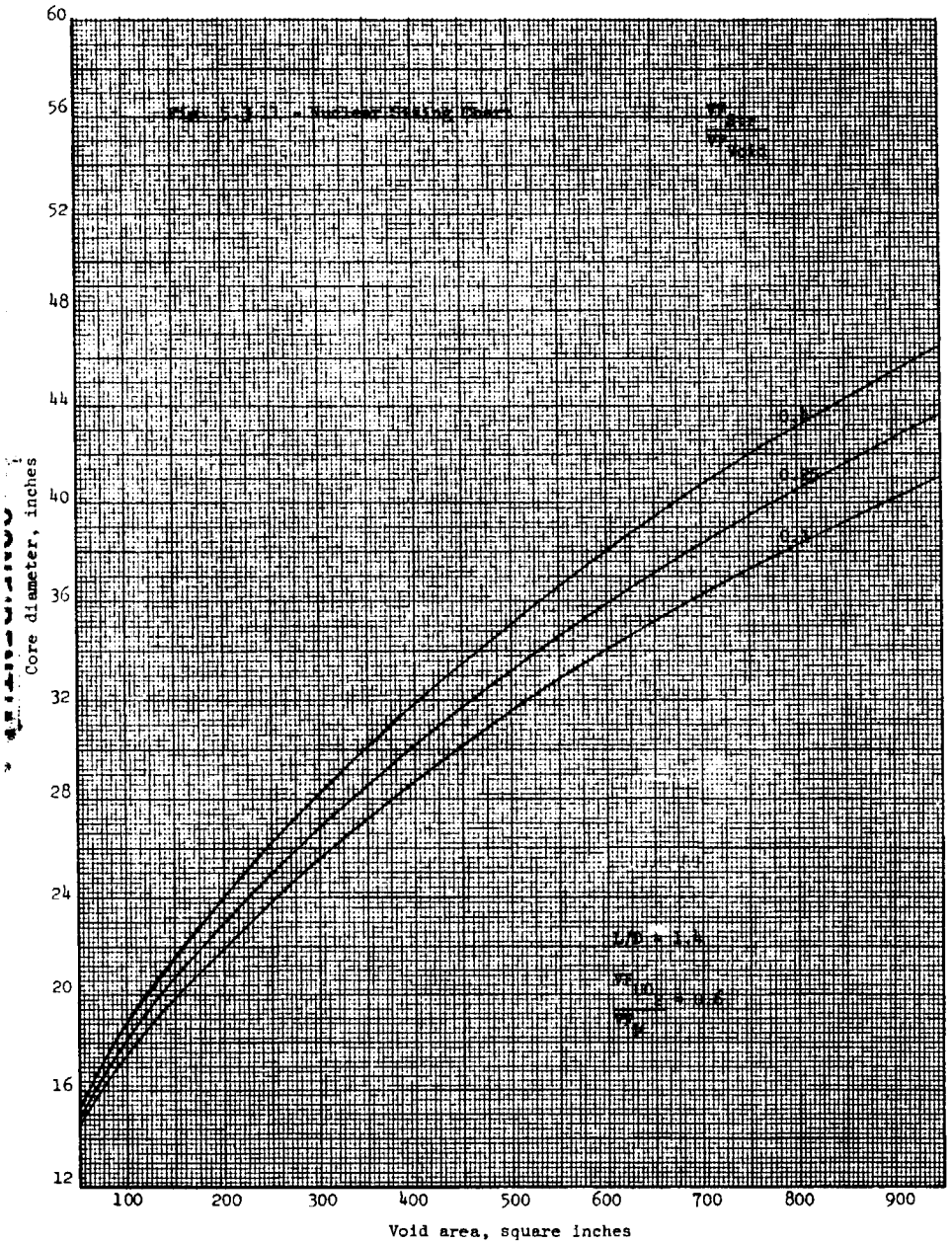
Core diameter, inches
Void area, square inches
60
56
52
48
44
40
36
32
28
24
20
16
12
100
200
300
400
500
600
700
800
900

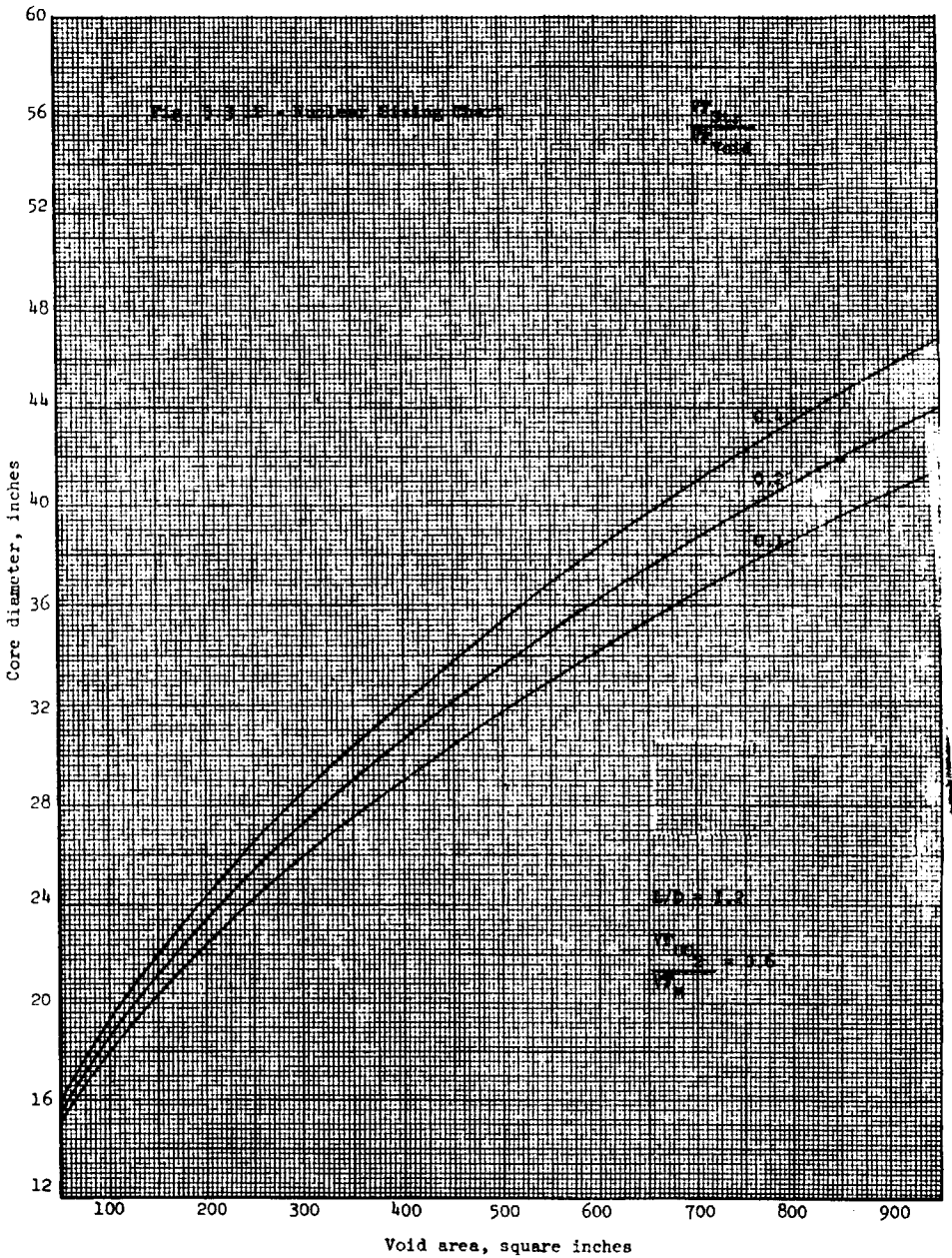
Core diameter, inches
Void area, square inches
60
56
52
48
44
40
36
32
28
24
20
16
12
100
200
300
400
500
600
700
800
900

CONFIDENTIAL

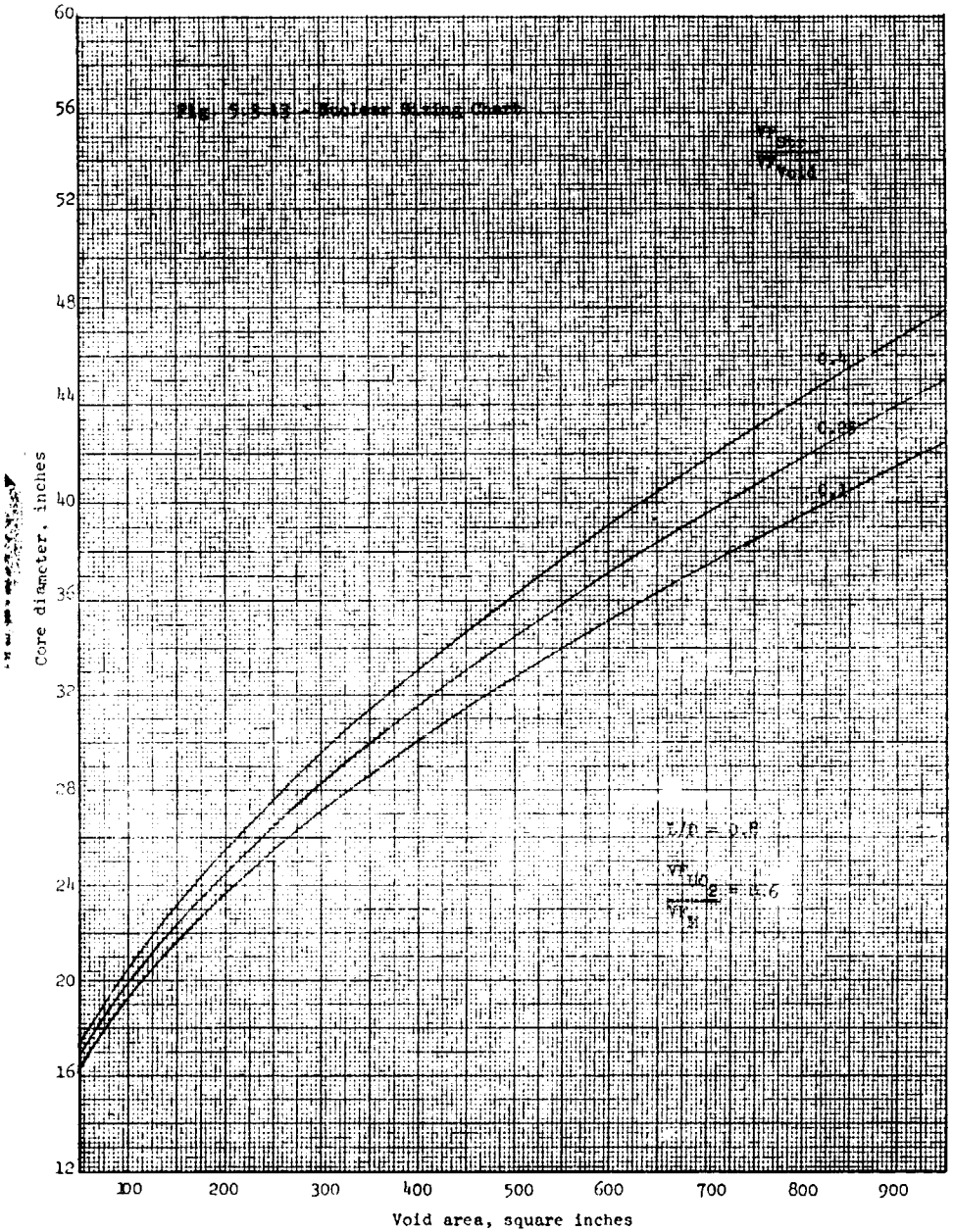

Fig. 5.5.13 - Nuclear Sizing Chart

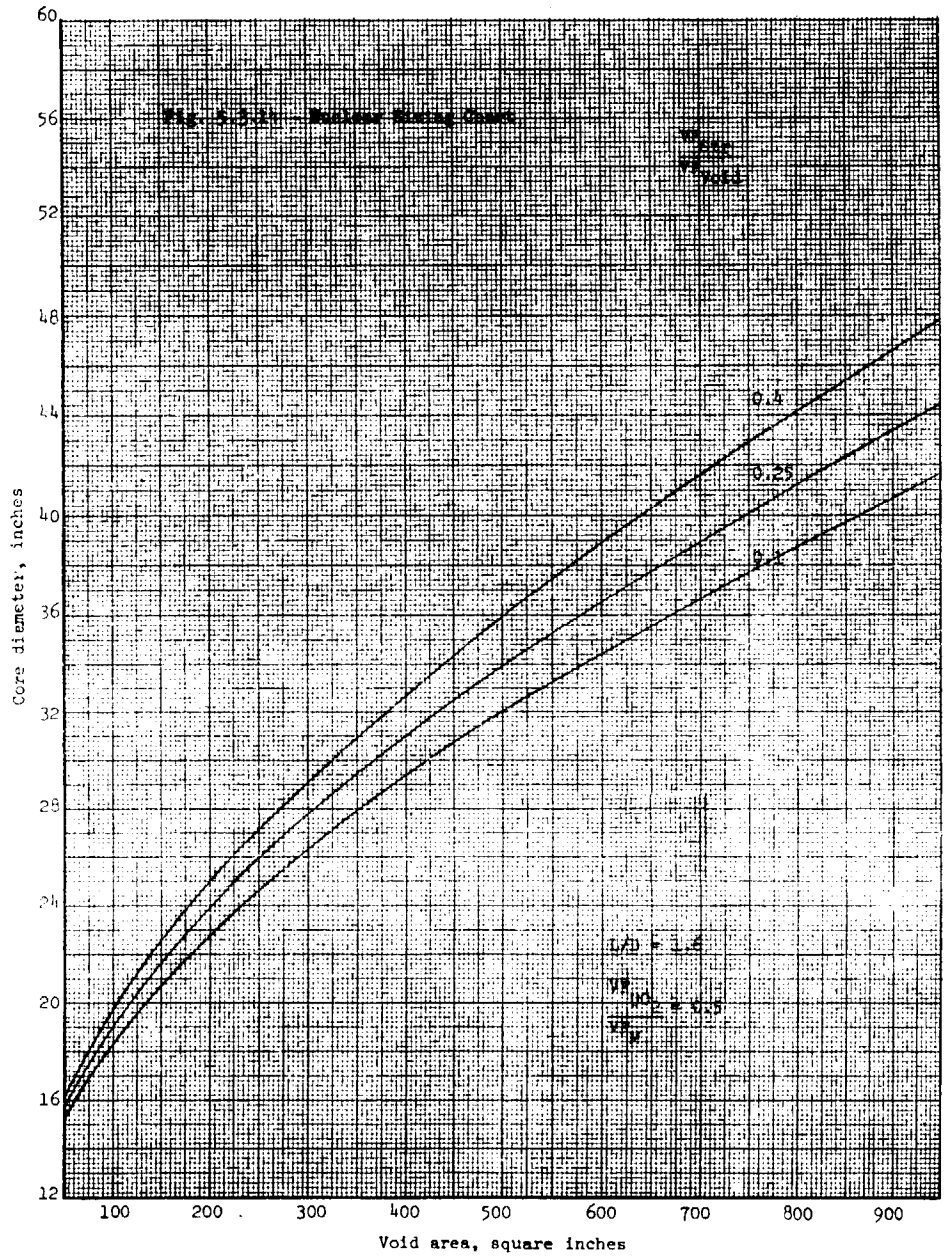

Fig. 5.5.14 - Nuclear Sizing Chart

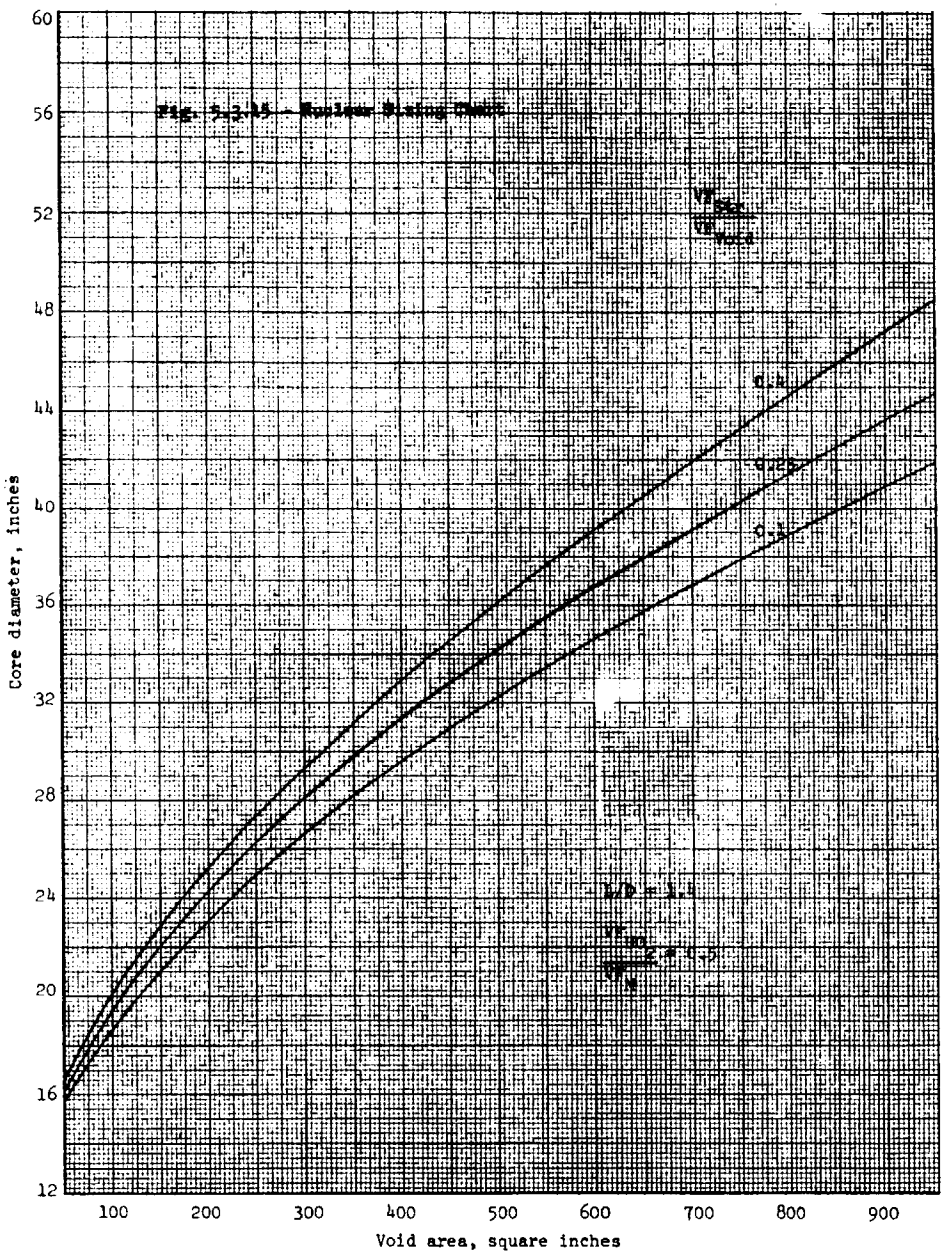

Fig. 5-2-35 - Nuclear Sizing Chart

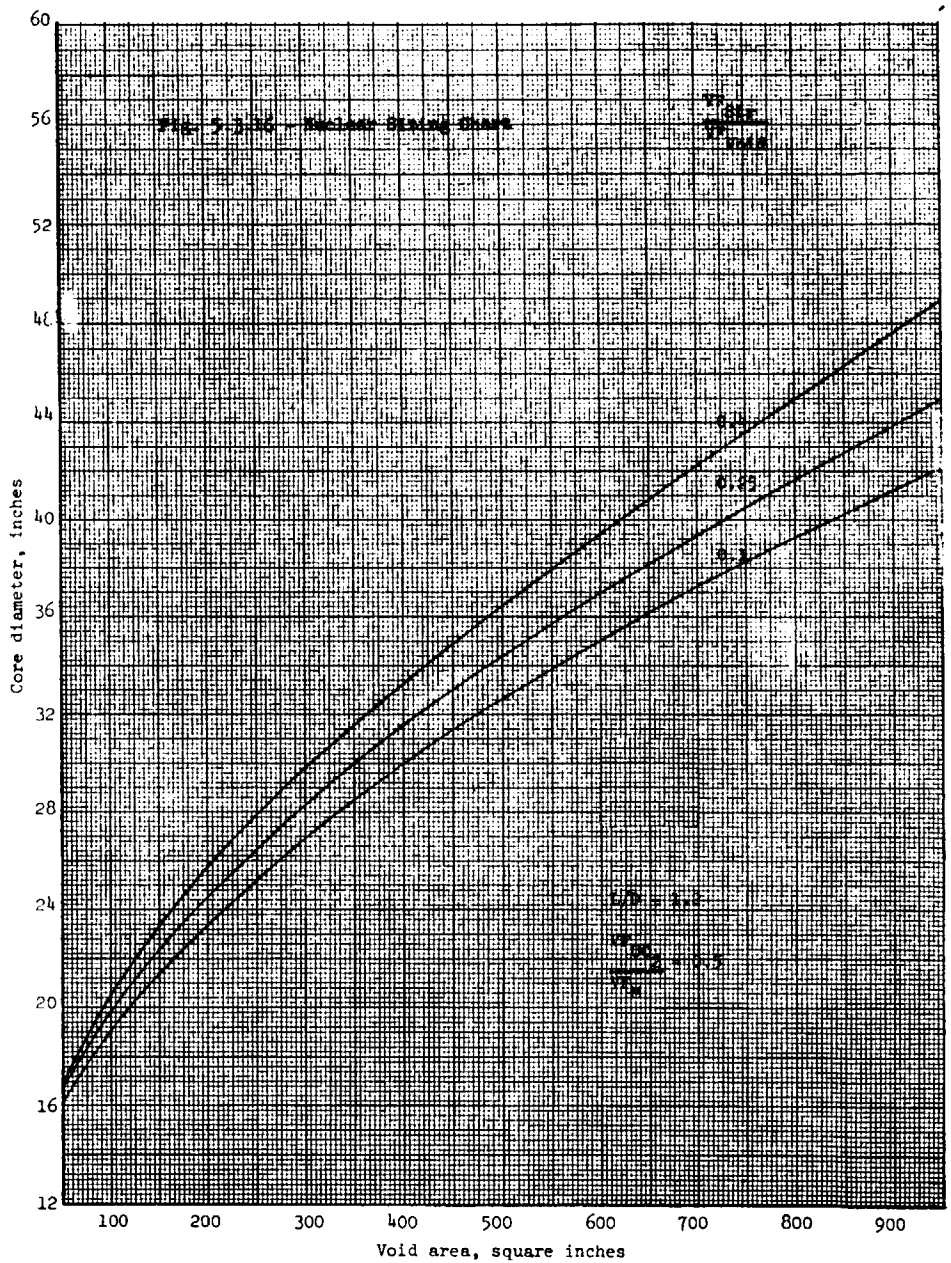

Fig. 5-2-36 - Nuclear Sizing Chart

CONFIDENTIAL

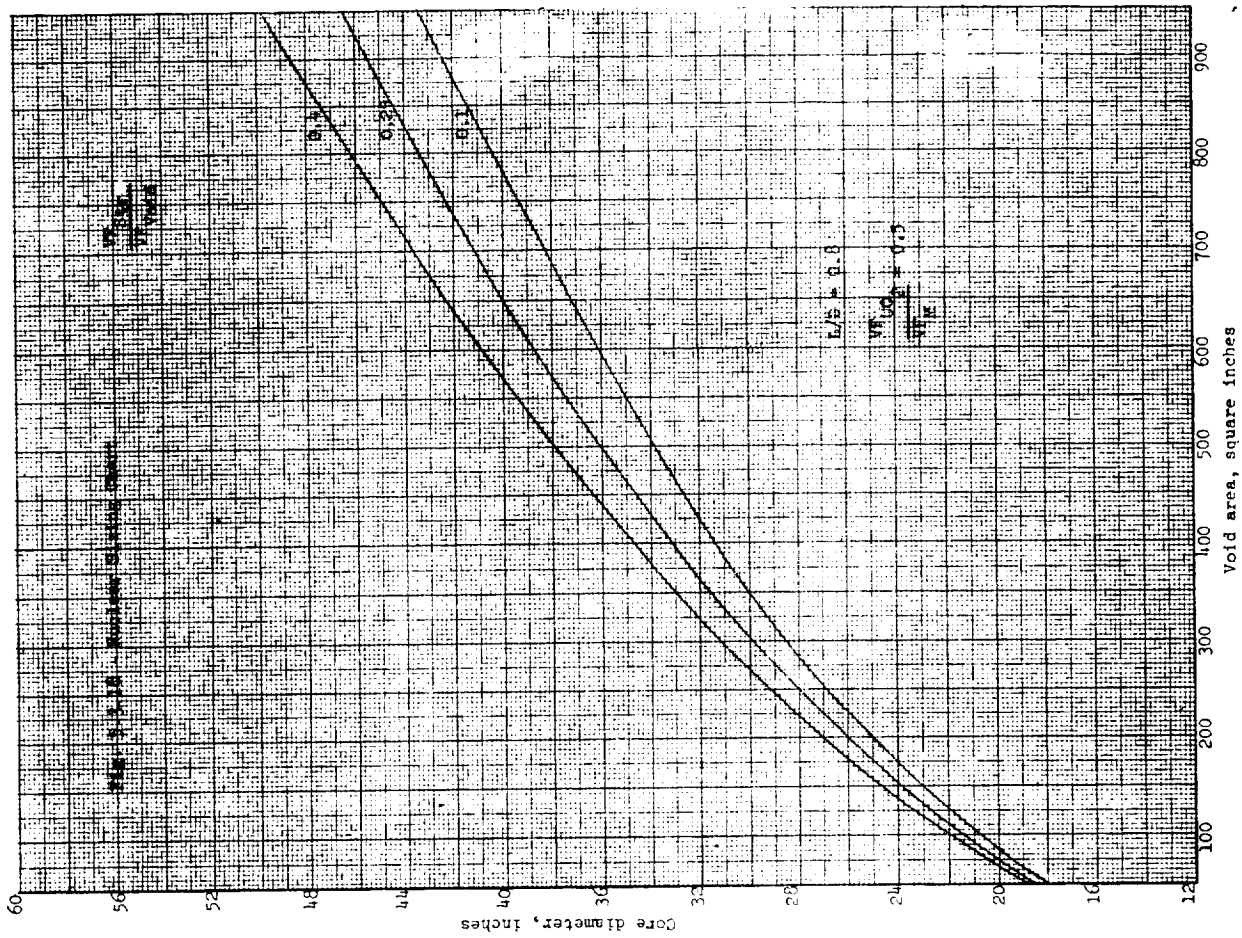

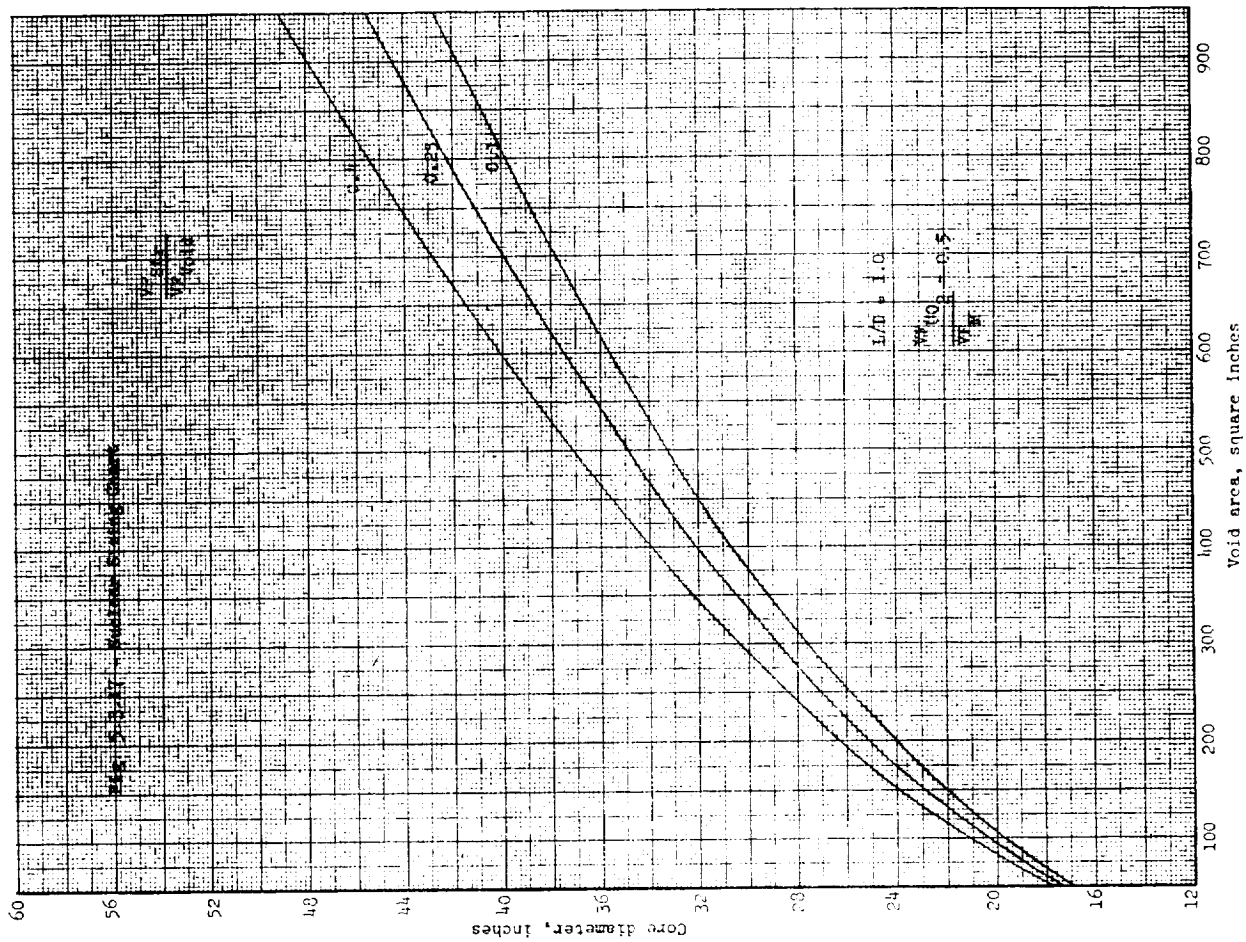

CONFIDENTIAL

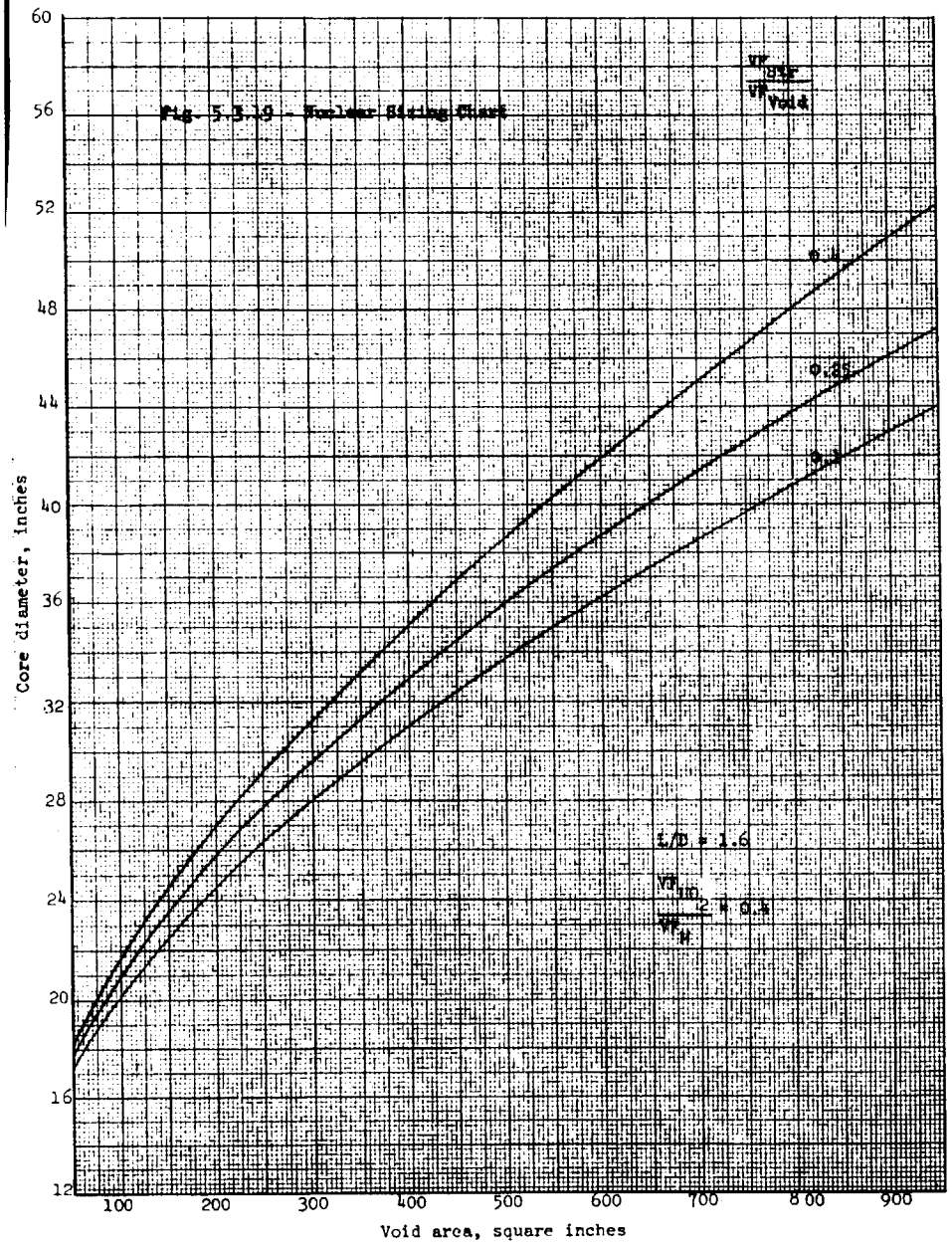

Fig. 5.3.19 - Reactor Sizing Chart

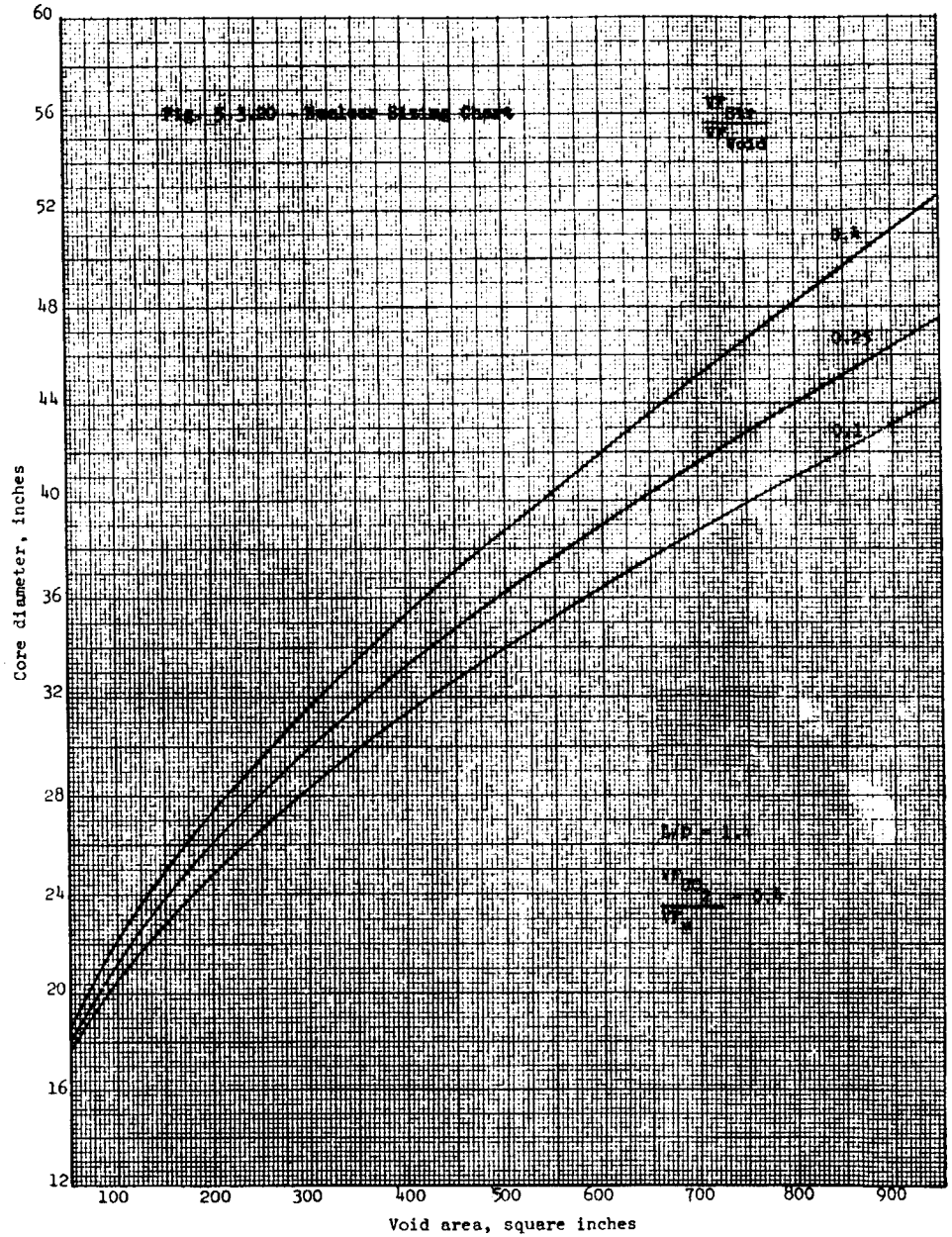

Fig. 5.3.20 - Reactor Sizing Chart

CONFIDENTIAL

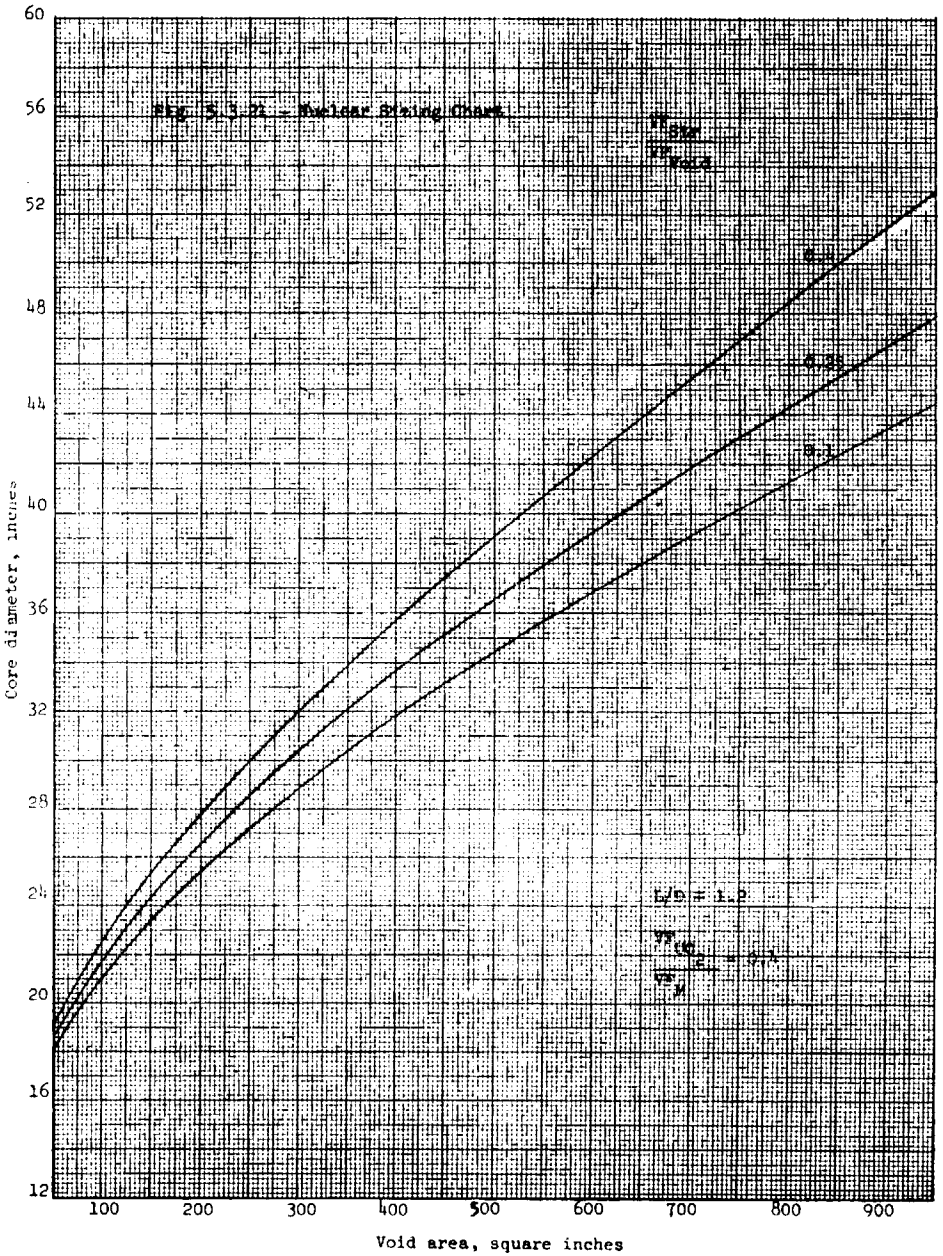

Fig. 5.3.21 - Nuclear Sizing Chart

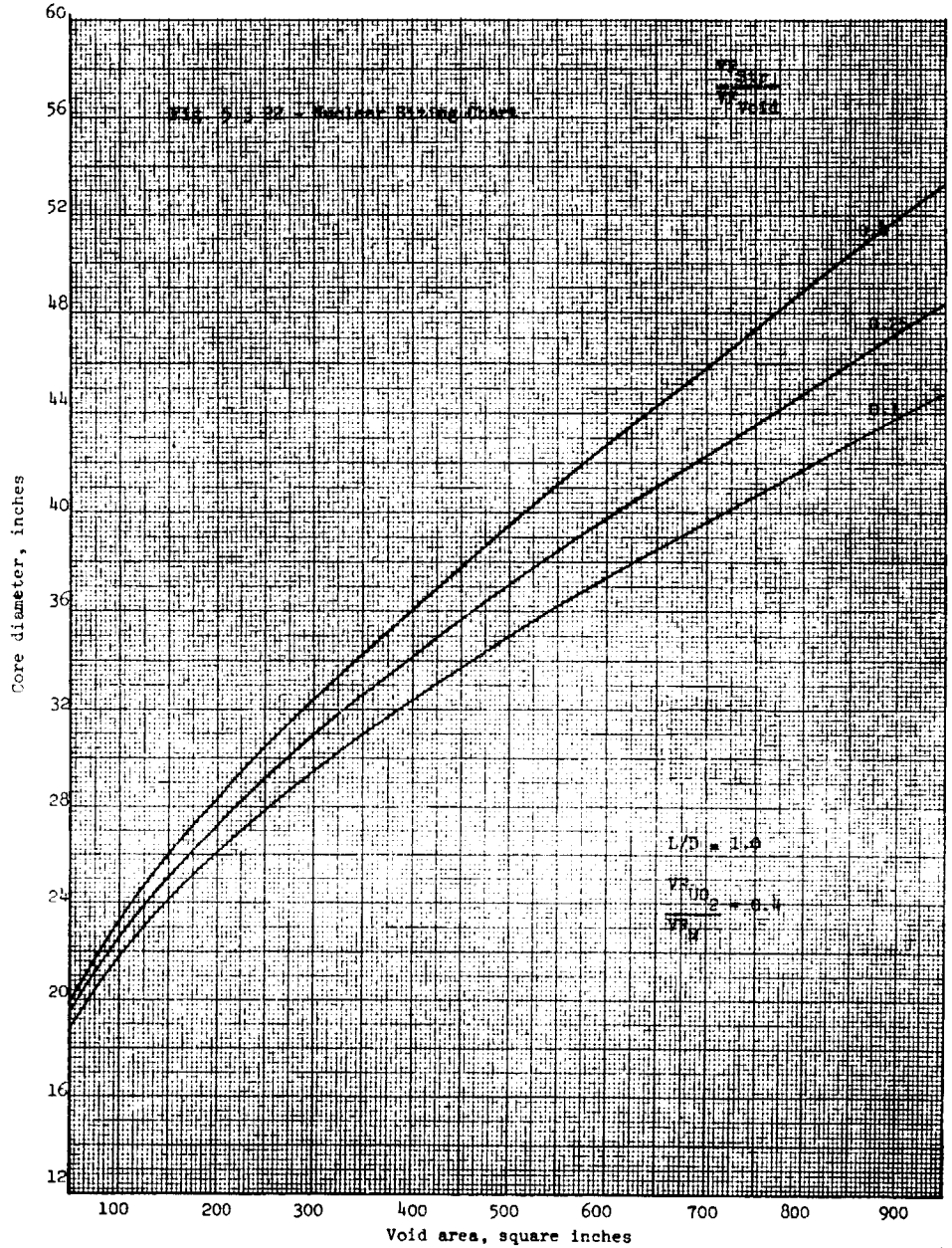

Fig. 5.3.22 - Nuclear Sizing Chart

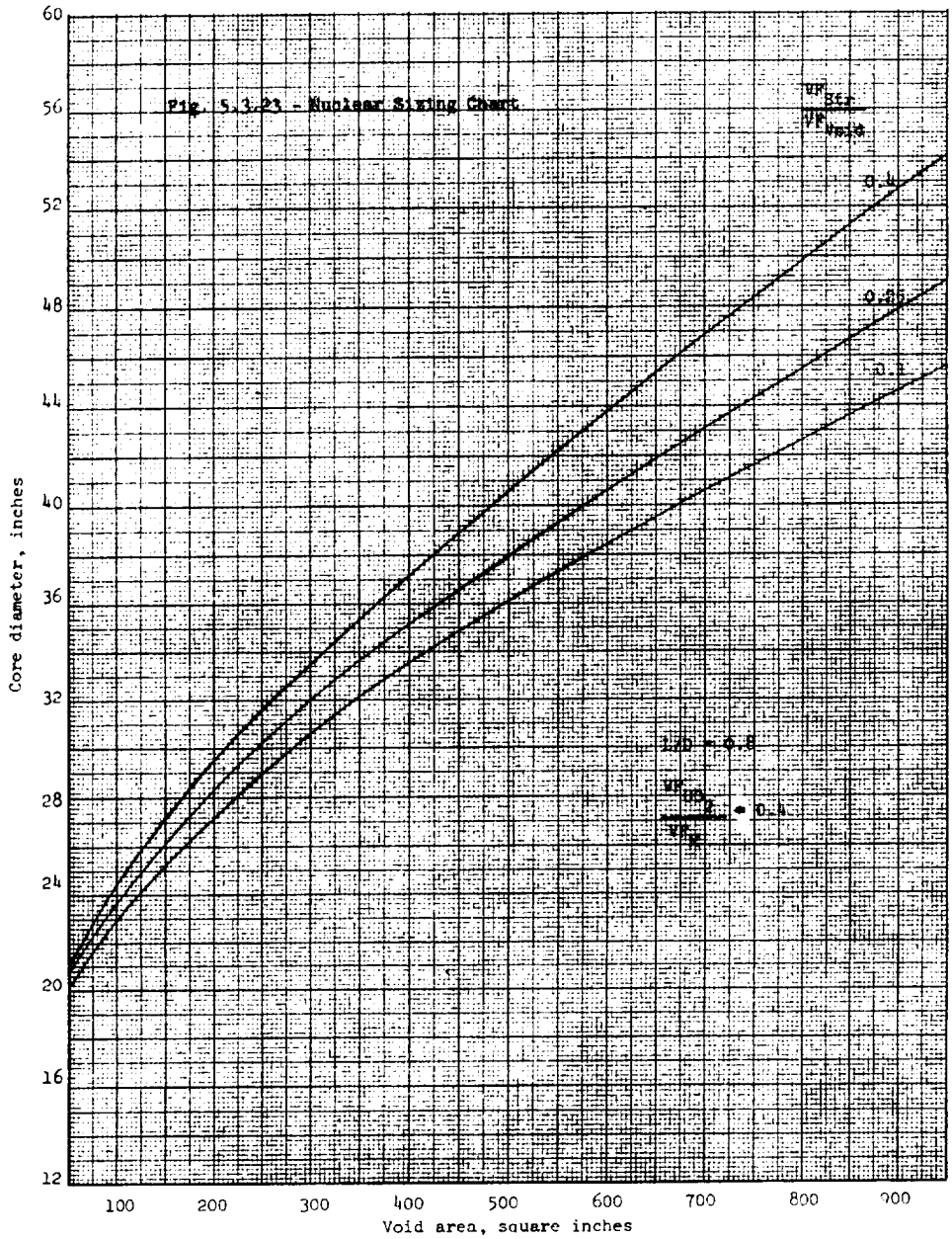

Fig. 5.3.23 - Nuclear Sizing Chart

percent or less. Configuration studies indicated that it would be difficult to fit cores much larger than 30 inches in diameter within cavities of the sizes indicated to be permissible relative to shield requirements. It was further recognized that since the coolant is to be circulated by an external blower, low core pressure drops are highly desirable. Accordingly, parametric data were generated for nominal maximum fuel element temperatures of 2200°F ± 100°F and pressure drops of 1.5 percent and higher.

The relationships of core fractional pressure drop, fuel element surface temperature, and required flow area are shown in Figure 5.4.1. The fuel element surface temperature is the maximum value along the length of an average coolant channel. The reference values used for evaluation in this study are indicated. Geometrical characteristics must be considered in relating the thermal sizing data in Figure 5.4.1 to core size and reactivity, and to mechanical characteristics such as fuel element natural frequency and space utilization. The choice of fuel element surface temperature for the specified coolant temperature rise along the core length (900° to 1800°F) determines a unique value of a parameter involving core length and flow area (for a given mass flow rate) and coolant channel hydraulic diameter. That parameter and the selected value of core fractional pressure drop determine unique sets of values of core flow area and the length-diameter factor, $L/D^{1.2}$, as shown in Figure 5.4.1. For a given core length, each combination of pressure drop and surface temperature corresponds to a required number of coolant channels as illustrated in Figure 5.4.2 where the data of Figure 5.4.1 are repeated at a reduced scale.

Since the number of coolant channels per fuel element is limited to certain values (1, 7, 19, 37, 61, 91, 127, etc.) the number of fuel elements required is also shown in Figure 5.4.2 as a function of number of coolant channels with the number of channels per fuel element as a parameter. For the core sizes of interest, approach to a circular boundary requires that the choice of number of fuel elements be limited to certain values stepped by increments of 12, and in some instances by increments of 6. Of these, a limited number are preferred because lower ratios of core envelope diameter to effective core diameter result.

Finally, the fuel element hexagonal width versus number of fuel elements is shown in Figure 5.4.2 with core effective diameter as a parameter. The fuel element width is of interest as a factor in determining vibrational characteristics and temperature differences across the width of a fuel element.

Volume available within the core for fuel element matrix material is dependent upon both the flow area chosen and the volume occupied by structural materials, i.e., the hexagonal can and coolant channel tubes. Volume fractions of the several core materials are shown in Figure 5.4.3 (for the same thermal conditions as shown in Figure 5.4.1) for a core whose length and diameter are both 30 inches.

GAS GENERATOR CYCLE

Preliminary studies indicated that, for a gas generator cycle with heat exchanger inlet temperature of 1800°F and exit temperature of 900°F,

core inlet temperatures of about 1200°F and exit temperatures of 2100°F are of interest. Diameter and required number of coolant channels, as functions of surface temperature and core pressure drop, are shown by dashed lines in Figure 5.4.2, and composition of 29.9-inch-diameter, 30-inch-long cores are shown in Figure 5.4.4.

DESIGN POINT DATA

Design data consistent with the reference design point shown in Figure 5.4.2 are given in Table 5.4.1. Cladding thickness is 0.010 inch. The overall fuel element across-flats width is 1.730 inch. The nominal cold gap between fuel elements is 0.104 inch.

5.4.3 Evaluation of Design

NORMAL OPERATION

Axial Variations of Core Temperature

The effect of axial power distribution on fuel element axial maximum surface temperature was investigated by computing the maximum temperature corresponding to each of two preliminary axial power distributions shown in Figure 5.4.5, estimated to be the extreme values for all radial positions in the core. The maximum temperatures show a variation of 31°F for a total variation of maximum power of from 1.307 (reference design) to 1.36 times the average. Data shown in section 5.4.2 were generated using the reference design power curve from Figure 5.4.5. These studies indicate that nominal changes in computed or measured axial power distribution relative to these curves may result in levels of performance that differ slightly from those shown in section 5.4.2.

Radial Variations of Core Temperatures

The radial power of cores considered in this study can be 40 percent or more higher at the core axis than the radial average. Since there is a significant shortening of fuel element life with higher temperatures, design control of radial variation of core temperatures is considered to be necessary.

Two approaches are normally considered. Varying the UO_2 fraction within the fuel element matrix versus core radius reduces the average fuel concentration within the core and increases the required core size. The alternative approach proposed for this application utilizes a uniform UO_2 fraction but includes a hydraulic diameter variation with core radius, i.e., larger than average coolant channels are used near the core axis. Because this approach both reduces the volume of heat generating matrix and increases the channel flow capability at the center of the core, it has less effect on core size than varying the fuel concentration.

CONFIDENTIAL

TABLE 5.4.1

THERMAL DESIGN POINT DATA

Reactor pressure loss ($\Delta P/P$)	0.015
Thermal power, Mw	250
Maximum pressure level, psia	1500
Temperatures, °F	
Reactor inlet	900
Reactor outlet	1800
Maximum fuel surface (avg)	2180
Maximum fuel internal (avg)	2298
Maximum internal rise (avg)	127
Helium flow rate, lb/sec	212.4
Active core dimensions, inches	
Envelope diameter	31.2
Equivalent circular diameter	29.9
Length	30.0
Active core volume, in.^{3}	21,068
Core volume fractions	
Structure	0.103
Free flow and voids	0.478
Fueled matrix (95% of theoretical density)	0.419
	1.000
Free flow area (hot), in.^{2}	267.8
Coolant channels per element	37
Elements per reactor	241
Channel diameter (cold), in.	0.192
Burnup in 1000 hours, fissions/cm^3	1.922×10^{20}

[redacted]

In addition to temperature, fuel element life depends upon matrix fission density. Thus, using less than average temperatures in regions of greater than average volumetric heating rates will compensate for the shorter life associated with the higher fission density. This can be thought of as a "life flattening" approach in the sense that it gives a more uniform fuel element life across the core radius.

Although the actual choice of coolant channel sizes versus core radius is dependent in detail upon several final design parameters such as radial variation of power, computations to demonstrate the magnitude of the required variations were completed as a part of this study. The radial power distribution shown in Figure 5.3.4 of section 5.3 was utilized because it is representative of the distribution expected with the side reflectors in the most inward position. Curves of estimated life versus fuel element temperature with fission density as a parameter (section 5.2.2) for W - $60UO_2$ (vol. %, 95% of theoretical density) were used to compute the required radial variation of temperature for uniform lifetime. For the average fuel element, the life curves were entered at a temperature of 2500°F. The difference of 300°F above the previously discussed surface temperature of 2200°F was an arbitrary allowance for difference between surface and matrix maximum temperatures including temperature perturbations. (The hot-spot analysis in this report shows that such a large allowance is not necessarily required.) For that temperature and a preliminary estimate of average fission density, a life of 1760 hours was indicated. The variation of temperature versus relative radial power was obtained by a cross-plot of data taken for a life of 1760 hours, and is shown in Figure 5.4.6.

In addition to the above data and the straight-forward relationships of heat generating volume versus coolant channel diameter, relationships between coolant channel diameter and heat removal capability of the coolant as a function of surface temperature are required to select a radial schedule of coolant channel diameters. For purposes of reactor physics computations, the relationship between hydraulic diameter and channel heat removal was approximated by assuming that channel heat removal was proportional to channel flow area. Rather than having temperatures depressed in the central regions to achieve "life flattening", later appropriate data showed that this simplifying assumption results in a core that is not quite temperature flattened. The core radial variation of hydraulic diameters associated with the simplifying assumption is shown in Table 5.4.2 for the radial regions used in the nuclear computations. The results further indicated that the largest channel size would have to be increased by only a few thousandths of an inch to achieve radial life flattening. The later calculations are those that would be used in a design study and involve the same computational procedures as were used in generating core parametric data (section 5.4.2) except that the same pressure drop from the core inlet plenum to a point at the coolant channel discharge face was used as the potential for determining flow through each channel. Final detailed analysis requires the use of different axial power distributions for different radial regions.

These computations demonstrate the basic flexibility of the channel variation approach in achieving a radially "life flattened" core and

CONFIDENTIAL

TABLE 5.4.2

CORE RADIAL CHARACTERISTICS

Fuel Element Layer	Outer Radius, inches	Number of Fuel Elements Per Layer	Channel Diameter, inches
1 (Core ℄)	0.963	1	0.2089
2	2.548	6	0.2086
3	4.198	12	0.2077
4	5.858	18	0.2059
5	7.521	24	0.2033
6	9.187	30	0.1990
7	10.853	36	0.1934
8	12.519	42	0.1866
9	14.186	48	0.1782
10 (Core edge)	14.950	24	0.1681

[redacted]

indicate the magnitude of channel size variation required. Depending on several parameters such as core porosity, average channel size, and number of channels per element, modifications to this approach may be required, as discussed under "Assessment of Problems" (section 5.4.4).

Fuel Element Hot Spot Temperature

Fuel element temperatures are affected by the factors discussed in the following paragraphs and are summarized at the end of this discussion of hot-spot temperature in Table 5.4.4.

Reactor Core Performance - Initial estimates of reactor core performance as a function of coolant temperature rise and pressure drop are related not only to flow area, hydraulic diameter, channel length, and maximum surface temperature of an average channel but also to the axial power distribution and surface characteristics of heat transfer and friction coefficients. The reference design that evolved from parametric studies was predicted to require an average channel maximum surface temperature of 2180°F.

Reactor Type and Configuration - The 710 Reactor utilizes a matrix cermet pierced by circular coolant channels in a triangular array.

Coolant channels adjacent to the hexagonal outer cladding are bounded by a matrix envelope that is rectangular rather than hexagonal as in the case of inner coolant channels. Conventional design practice in the 710 Program has been to select a channel pitch that provides the same amount of heat generating matrix around all channels (except the six at the corners of the hexagon). For the current reference design, the resulting fueled meat thickness is such that the distance between the hexagonal side of the matrix and the center of the first channel is 0.1221 inch as compared with the normal internal half - pitch of 0.1411 inch. Data have been reported for internal temperature rises within heat generating solids surrounding holes in a square array.[1] Using an equivalent square to approximate the rectangular region, the additional temperature rise over that for a triangular array is 65°F. This value may be less in actual fuel elements because of conduction within the outer hex-can material.

Current design practice is to maintain uniform coolant hole sizes within a fuel element except for peripheral fuel elements having a reflector-produced power spike at the outer boundary. In the reference design considered here, some interior fuel elements experience a radial power variation of ±5 percent. Without accounting for conduction alleviation, the corresponding temperature variation would be ±90°F.

[1] E. M. Sparrow, "Temperature Distribution and Heat-Transfer Results for an Internally Cooled, Heat Generating Solid," Journal of Heat Transfer, Vol. 82, Series C, No. 4, November 1960, pp. 389-392.

Radial power distributions change during the operational lifetime because of change in reflector position and to a small extent because of unequal burnup. The amount of power change during life was not computed during this study. If a change of power of 15 percent were to occur in one radial location, the corresponding change in fuel element temperature would be about 250°F. Simultaneous axial power distribution changes may cause some additional temperature changes.

Design Choice for Nominal Specifications - A major objective of the design activities is to minimize contributions to fuel element temperatures arising from inherent characteristics of the basic reactor type. This can be accomplished in many ways, including hydraulic diameter variation to compensate for core radial power density variations. In concept, temperature penalties associated with some characteristics can be reduced to zero, but may actually only be reduced to small values consistent with realistic degrees of design complexity. Others, such as the radial power swing, cannot be eliminated but resulting temperatures can be caused to vary during operating life in such a manner that an objective "life-flattened" average temperature is achieved.

The objective of this section, then, is to indicate an estimate of temperature effects that remain after an appropriate design is established. The basic assumption is that design values for coolant channel size can be varied within any fuel element.

In high power density regions near the center of the core, internal temperature rises are greater than in regions of average power density. The temperature rise in regions near the hexagonal boundary would also be larger. A modification of the radial life flattening procedure as previously indicated in this report, therefore, may be desirable. Instead of adjusting coolant channel surface temperatures, a characteristic fuel matrix temperature reflecting predictable temperature variations within individual fuel elements can be used to select the schedule of channel diameters. As a guide in estimating a practical goal, a change of 0.001 inch in hydraulic diameter corresponds to less than 25°F in fuel element temperature effect. The uncompensated temperature penalty within a fuel element due to the gradient in radial power density can be as much as 90°F; if channel diameter variation within individual fuel elements is used, that value can be reduced in practice to 25°F without undue difficulty.

Established design procedure to compensate for radial power swings is to radially tailor the design (in this case by channel diameter variation) so that temperatures of fuel elements experiencing the largest power swing are equal to the desired average over the core lifetime. In this manner, the fuel material so affected will operate at higher than average temperature and power density for half the lifetime, but lower than average for the remaining half.

Effects of Fabrication Tolerances - Results of detailed assessment of the potential effect of fabrication tolerances on fuel element temperatures for other operating modes of the same type of reactor core as considered here have been previously reported.[2] A key result of that

[2] "710 Reactor Program, Progress Report No. 9," GE-NMPO, GEMP-301, July 31, 1964, pp. 45-50.

assessment was that tolerances associated with the fabrication of individual segments, i.e., drilled hole diameter and position, fuel concentration, density, and fuel dispersion, tended to produce relatively small contributions to local or "hot-spot" temperatures if actual values varied normally in such a way that statistical averaging over the length of the fuel element was applicable. A second conclusion was that tolerances assumed to apply uniformly over the whole fuel element length, such as for variations in tube wall thickness, were potentially of most concern. Finally, the matrix conductivity relative to the power level was high enough that hot spots would be reduced or alleviated by about 70 percent by conduction of heat to surrounding warm spots, again with the assumption of an effective normal distribution of combination of tolerance effects.

Effects of fabrication tolerances on required fuel element temperatures are shown in Table 5.4.3. The data tabulated were computed using equations and curves from the earlier study cited which, except for some extrapolations, are equally applicable to this study. Basic assumptions included a linearization of temperature perturbation versus causative tolerance and normal distribution of dimensions among 30 fueled segments used to make up the length of one fuel element. Numbers in column "C" of Table 5.4.3 are the products of numbers in columns "A" and "B", and the sums of nominal temperature rises (for this application the components of the sum are coolant: 673°F, surface to coolant: 627°F, and internal: 104°F).

The significance of the data shown in Table 5.4.3 is that a temperature perturbation due to fabrication tolerances is expected to be less than 80°F for the tolerances shown. Thus, a small life-performance penalty can be imposed or tolerances can be increased, if needed, to reduce fabrication costs with small additional penalties. Although not critical with regard to these data, the normal expectation with this number of factors is that the statistical sum will tend to more closely apply than the arithmetic sum. Relative to the previous studies, the effect of alleviation is expected to be reduced because of a higher core porosity and volumetric power density. Hence, alleviation of only a few tens of °F can be anticipated.

Design Uncertainties - Uncertainties in temperature predictions will remain even after the most careful design. These are associated with uncertainties in power distribution measurements and coolant heat removal characteristics. Power distribution measurement accuracy such that axially integrated average power for a given radial location has an uncertainty of ±1 percent is considered achievable. This corresponds to a temperature uncertainty of ±17°F. An additional allowance of 8°F for uncertainty in measurement of local power density requires a total allowance of 25°F for power measurement tolerances. Design compensation for power swings initially requires analytical prediction followed by later measurements in end-of-life cores. An uncertainty allowance for the lifetime average is required. An allowance of 2 percent or 35°F appears to be a reasonable target.

Allowance for uncertainties of 5 to 10 percent in friction factor and heat transfer coefficients are necessary, regardless of the reactor type. Corresponding temperature uncertainties are 40°F to 80°F and 30°F to 60°F, respectively. A coupling between friction factor and heat

CONFIDENTIAL

TABLE 5.4.3

FUEL ELEMENT TEMPERATURE PERTURBATIONS DUE TO FABRICATION TOLERANCES

Parameter	Nominal	Tolerance	(A) Fractional Tolerance	(B) Temperature Coefficient	(C)[a] Temperature Perturbation
% UO_2			± 0.01	0.66	9
Enrichment	93.2%	± 0.3%	± 0.0032	0.66	3
Density	0.95	± 0.01	± 0.0105	0.66	17
Segment hole diameter	0.210	± 0.001 in.	± 0.00476	-1.85	21
Tube wall thickness	0.010	± 0.0005 in.	± 0.05	0.245	17
True position of segment hole	0.281	0.001	0.00356	2.157	11
				Arithmetic sum =	78
				Square root of sum of squares =	35

[a]Product of column (A) x column (B) x ($T_{max} - T_{min} = 1404\,°F$).

transfer coefficient is normally believed to exist; i.e., if the friction factor is high the heat transfer coefficient is also high but by a lesser amount. If there is a statistical distribution among the channels within a fuel element, some alleviation by conduction to adjacent channels will occur. A combined uncertainty allowance of 50°F is believed to be reasonable until experimental data for the specific fuel element is obtained.

Control System Tolerance and Uncertainty - Fuel element temperatures are determined by the operating temperatures of the coolant which, in turn, are determined by the control system. A tolerance would be required for the measurement uncertainty of the sensor, e.g., core exit temperature thermocouple. Realistic tolerances are of the order of ±1 to 2 percent. A control system operational limit of ±1 percent is also required. Hence, a temperature uncertainty allowance of 25°F with a variation of ±20°F throughout normal lifetime is believed to be within current state-of-the-art.

Summary - Statistical combination should be appropriate for tolerances and uncertainties with the following result (arithmetic sum shown for comparison):

Source of Uncertainty	Estimated Effect, °F
Fabrication tolerances	35 (arithmetic 78)
Power uncertainty	25
Power swing design uncertainty	35
Friction and heat transfer	50
Control sensor	35
Statistical sum	82 (arithmetic 223)

An overall summary of all temperature perturbation effects is shown in Table 5.4.4. The data show that, with the average channel maximum matrix temperature of 2298°F, a local hot-spot temperature of 2470°F (2300°F + 170°F) averaged over the operating life can be expected. If the hot spot should be in a region of maximum power swing for the a-priori values presumed, an additional variation of ±150°F could occur, i.e., between 2320°F and 2620°F. The number in parentheses, 450°F, instead of the expected value of 170°F, is a value that could occur if only minimum attention is given to design refinement (i.e., if tolerances and uncertainty effects were not random variations such that they must be summed arithmetically). Hence, the value of 450°F represents a readily achievable system. Reduction from 450°F to 170°F is achievable with careful design and procedures. The design complexity increases as the 170°F figure is approached, and the complexity required to achieve reduction below the 170°F value requires that careful study be made of whether the increased lifetime to be expected is worth the additional fabrication, inspection, and assembly costs that might be required.

TRANSIENTS

Temperatures during transients were not evaluated except for shutdown transients reported in section 5.6. Other transient temperature predictions become meaningful only after the powerplant, control systems, and proposed operating procedures are delineated. All that can be indicated quantitatively, a[illegible]gate and magnitude of

CONFIDENTIAL

TABLE 5.4.4

FUEL ELEMENT HOT SPOT TEMPERATURE FACTORS

Effect	Time Average Temperature Increment, °F	Time Dependent Temperature Increment, °F
Tolerances and uncertainties	82 (223)[a]	
Fuel element hexagonal boundary	35 (65)[b]	
Radial life flattening	25 (75)[b]	
Fuel element power gradient	25 (90)[b]	
Radial power swing		± 125
Control system		± 20
Lifetime physical changes		0
Total	~170 (450)[b]	± 150

[a]Arithmetic sum.

[b]Maximum associated with incomplete design and analysis refinement.

temperature changes following a stepwise power reduction of less than about 70 percent (i.e., to 30 percent of operating power) will be less than indicated in section 5.6 even if the coolant flow rate is not reduced. Qualitatively, it can be noted that the addition of power pulses without increase of flow rate will require computations to determine permissible magnitudes and durations depending on the response of fuel elements near the core axis. Similarly, calculations are required to assess limiting times for coolant flow increase delays relative to step increases in power. In all cases, core temperature distributions must be studied to identify possible excessive fuel element bowing.

AFTERHEAT TEMPERATURES

Afterheat temperatures during an accident situation leading to core meltdown without aftercooling are discussed in section 5.6. For non-accident situations, aftercooling will be needed either continuously or intermittently after shutdown until the afterheat can be transferred by radiation and conduction to surrounding components without exceeding their permissible temperature levels. In a previous study of a core of approximately the same size, it was shown that aftercooling was required until the reactor power had decreased to 67 kw.[3] This corresponds to 0.027 percent of operating power for this application. Afterheat data (Figure 5.4.8) reveal that, if 1000-hour operation were specified, aftercooling by gas circulation would be required for about 2500 hours. Even though detailed calculations for the aircraft system may result in somewhat higher afterheat power levels and shorter times (primarily because of the heat absorption capability of the shield) the problem of supplying coolant flow for long time periods will remain with only reductions in the time required. Natural convection flows may enhance the transport of heat from the reactor core.

Reactor core temperatures were calculated assuming operating pressure and full flow conditions for the first 20 seconds after a 2 percent reactivity insertion following 1000 hours of operation as a part of the accident studies reported in section 5.6. Temperatures were computed at ten axial stations within each of ten radial regions. Flow distribution among the radial regions was assumed to be unchanged from the steady operating distribution. Radial conduction within regions and between adjacent regions was simulated by pseudo values of thermal conductivity to account for effects of the fuel element material composition. Radial variation in thermal storage capacity was represented by using different effective specific heat versus temperature data for each region. A radial matrix heating curve with a peak-to-average value of 1.65 was used. Axially, the heat generation was represented by an approximation to a 2:1 sine curve. Coolant inlet temperature was maintained constant at 900°F.

Temperatures computed are shown in Figure 5.4.7 as a function of radial position in the core with time after shutdown as a parameter. The data in this figure is for an axial fractional distance, X/L, of 0.95.

---

[3] "Design Criteria for a Fast Energy Spectrum Nuclear Rocket Engine, Vol. VI - Controls and Aftercooling Studies," RPL-TDR-64-17, GE-NMPO, GEMP-250, December 1963, p. 27.

Design study assessment using these temperatures or temperatures from more refined computations (i.e., including flow redistribution) will be required to determine whether fuel element clearance is maintained during this time period. Temperature gradients within fuel elements will be less than shown in Figure 5.4.7 if separation is maintained because of temperature discontinuities across the gaps.

It is assumed that system considerations will warrant a minimization of energy required for coolant circulation during aftercooling, which implies a minimization of coolant flow rate. During the 20-second time period studied, the flow rate could have been reduced as the afterheat power level decreased with maintenance of fuel element temperatures at or near design value. Although analysis is required, it is anticipated that fuel element temperatures approximating operating values can be maintained during the initial aftercooling while reducing the flow rate approximately in proportion to the afterheat power level without introducing unacceptable radial variations of core temperature. Continued reduction of flow while maintaining elevated temperatures will result in passing through a mixed flow condition (turbulent inlet flow and laminar exit flow) to an all-laminar operation. This introduces additional considerations because the laws governing flow distribution with laminar flow are different from those for turbulent flow; i.e., for the same coolant exit temperature, relatively more coolant passes through channels with larger than average diameter during laminar flow than during turbulent flow.

As the afterheat power level decreases, the transfer of heat to components adjacent to the core becomes relatively more significant.

Afterheat Power

Afterheat power used in this study is shown in Figure 5.4.8. It was obtained by summation of data generated in a nuclear rocket study.[4] The total fission product power release following 1000 hours of reactor operating time was added to the delayed neutron power release following a negative reactivity insertion of 2 percent.

5.4.4 Assessment of Problems

The following problems have been identified from the thermal analysis study:

1. Minimum ligament thickness limitation introduces a limit on the amount of radial temperature tailoring that can be accomplished by the preferred method of hydraulic diameter variation. This problem is relatively minor in the present case and can be overcome by local reduction in UO_2 volume content in the region affected. This characteristic is inherent in high porosity cores, and would become more restrictive should there be a necessity to use core sizes larger than that for the present design conditions.
2. Adequacy of clearances between fuel elements should be established by further analysis of the bowing of fuel elements to be expected

[4] "Aftercooling Requirements for a Fast Energy Spectrum Nuclear Rocket Engine," Air Force Rocket Propulsion Laboratory, AFRPL-TR-65-196, October 1965, pp. 10, 11, 19, 20.

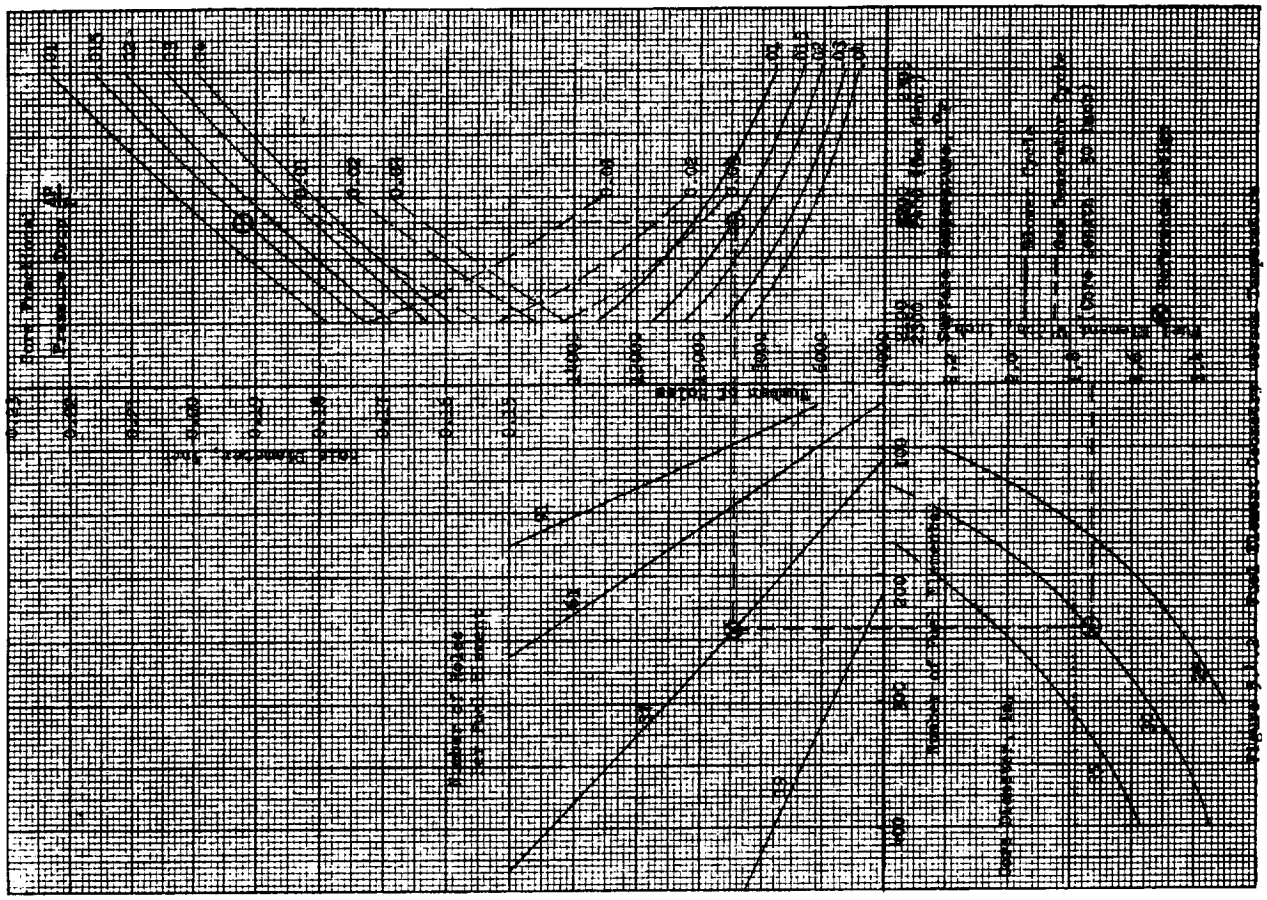

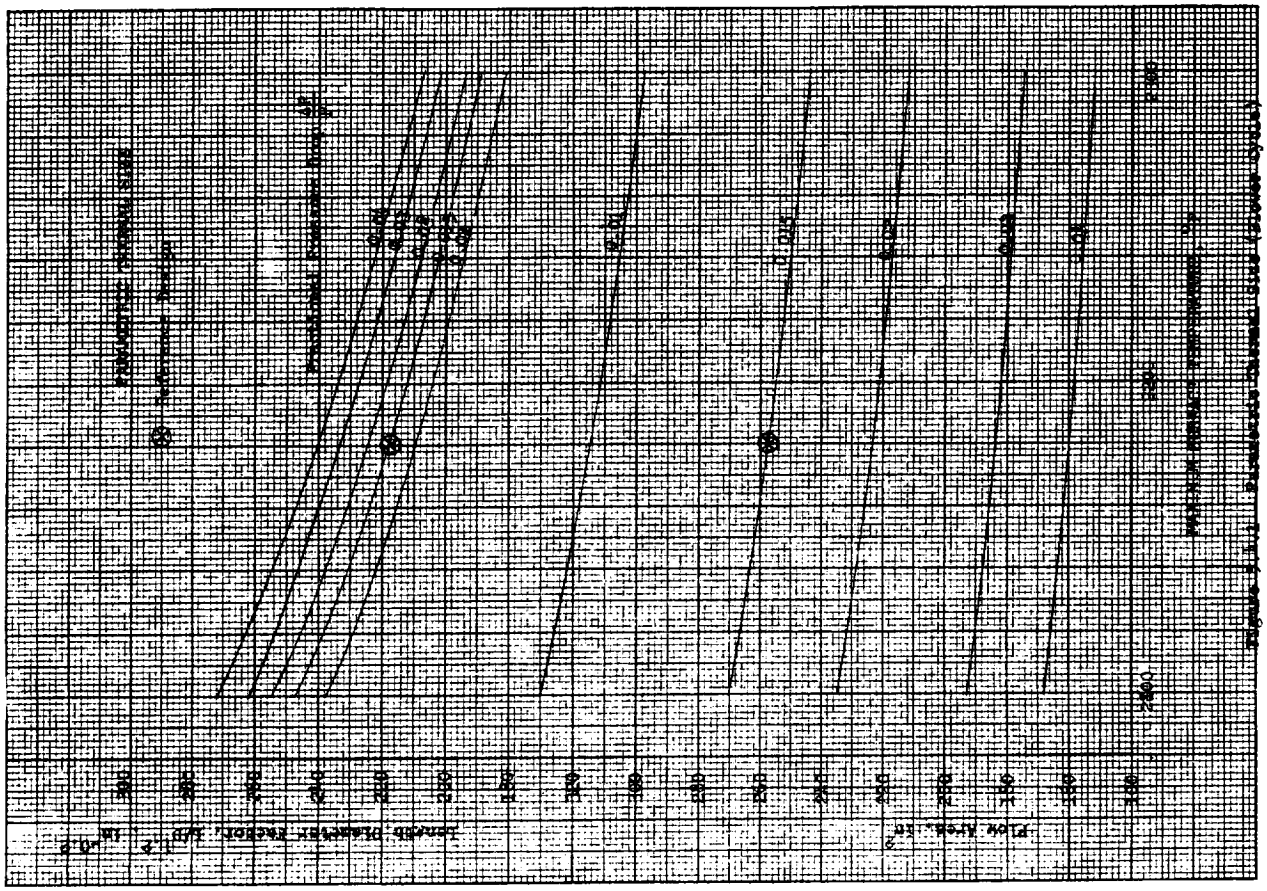

[redacted]

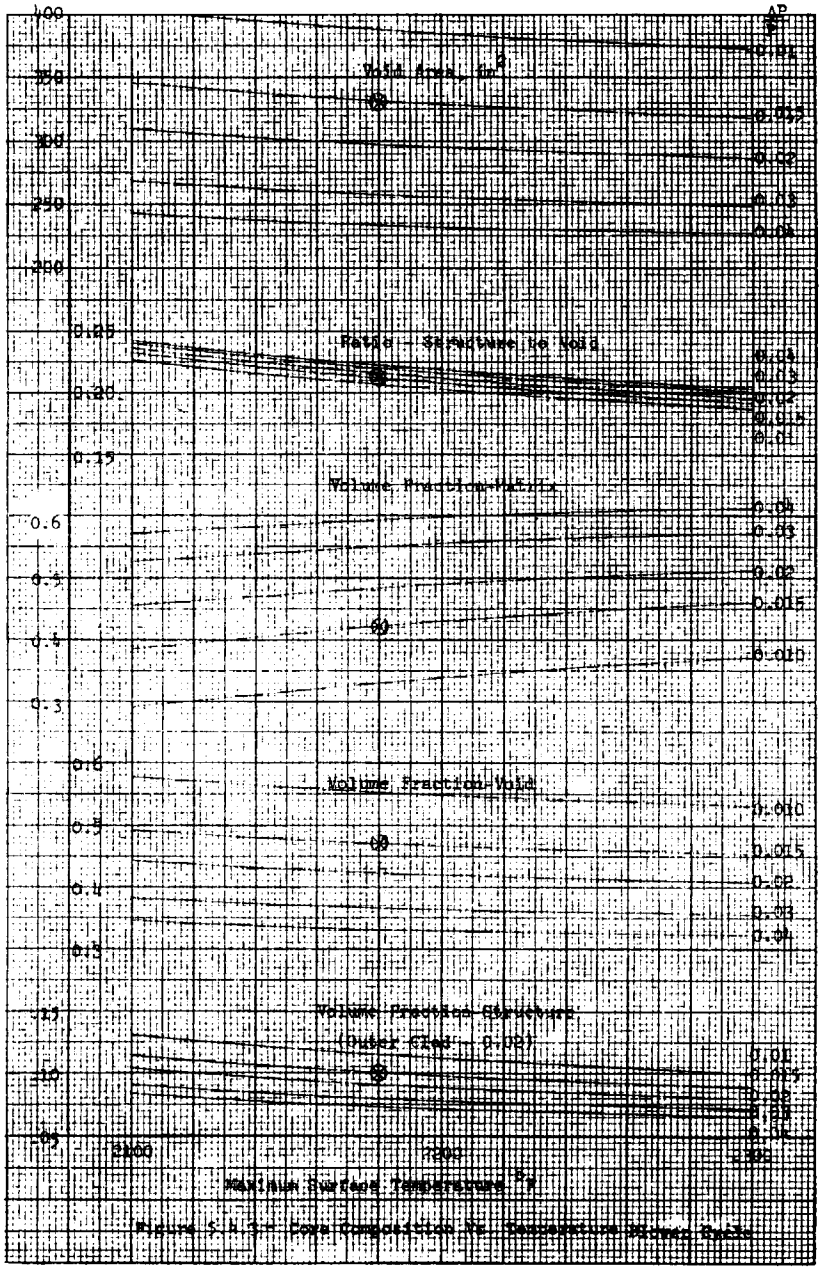

Figure 5.4.3 - Core Composition Vs. Temperature Blower Cycle

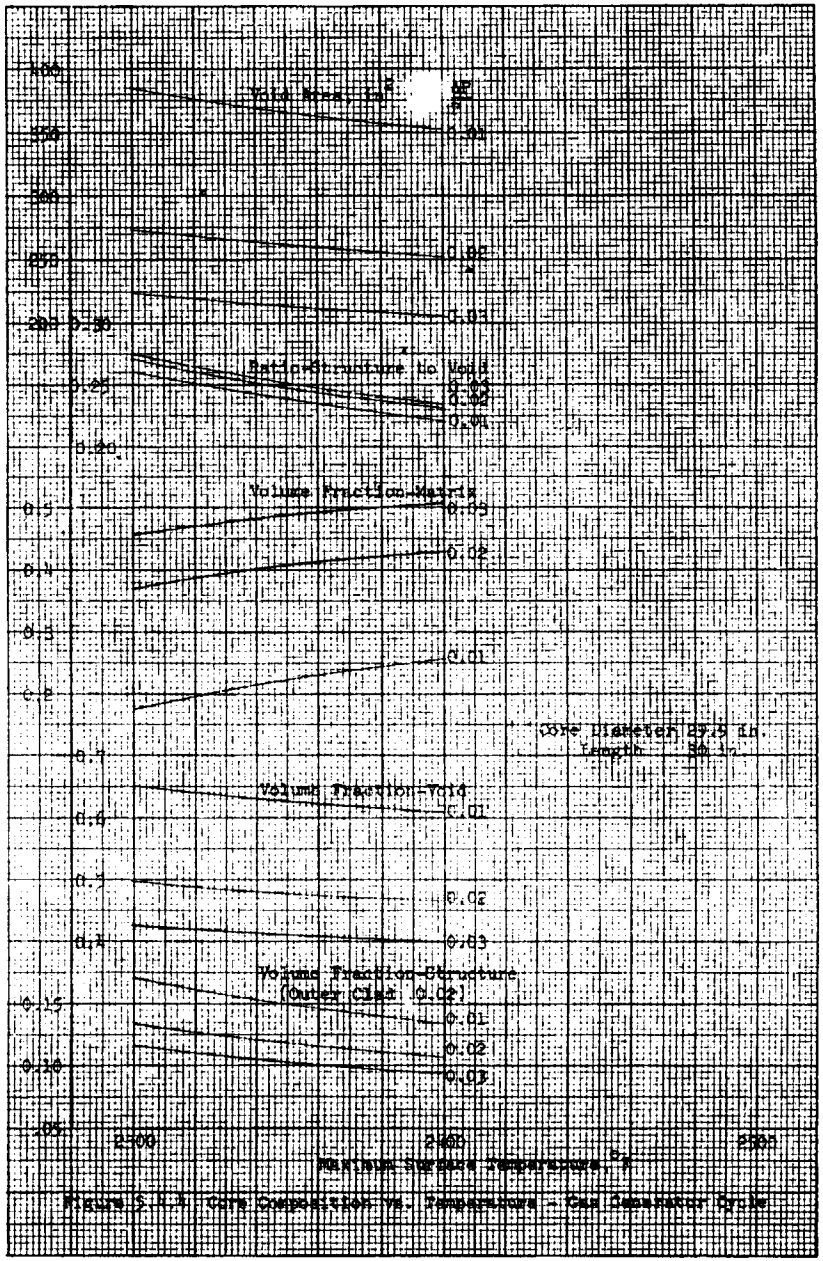

Figure 5.4.4 Core Composition Vs. Temperature - Gas Generator Cycle

CONFIDENTIAL

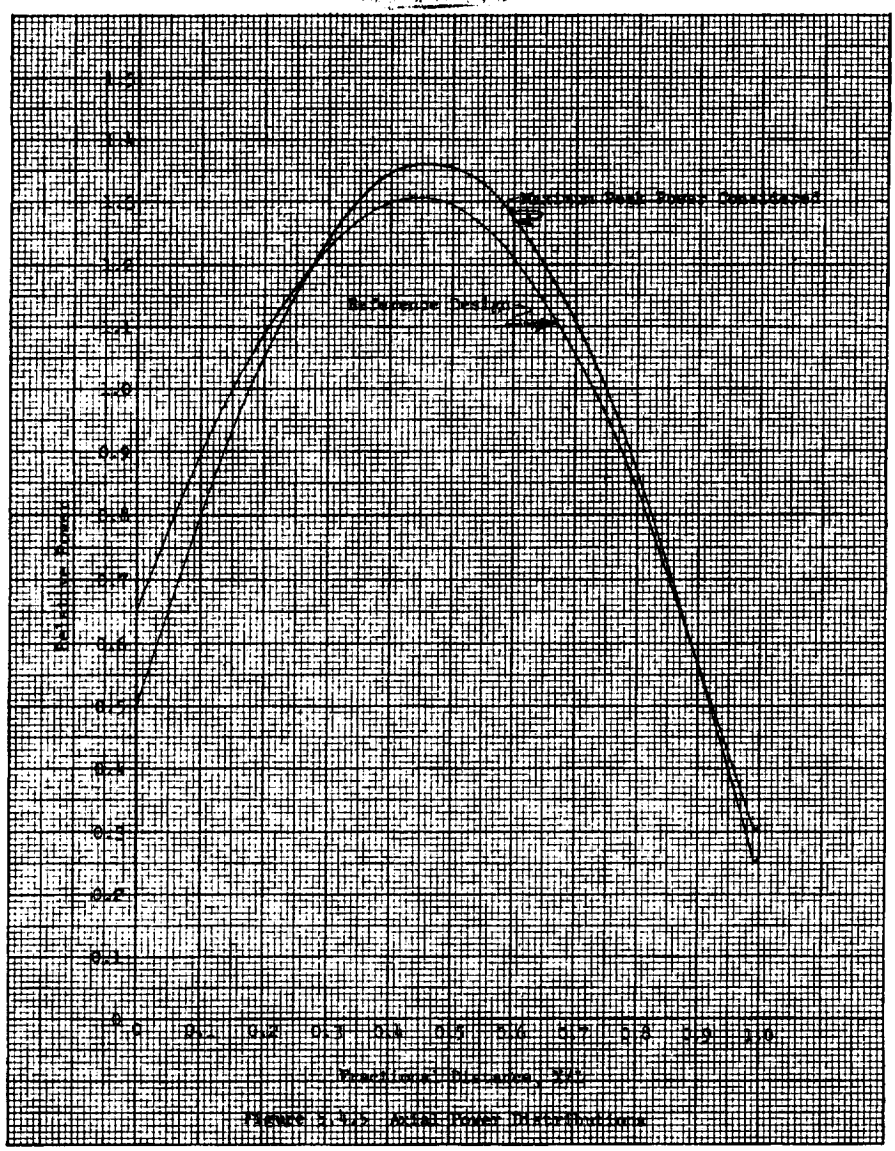

Figure 5.4.5 Axial Power Distributions

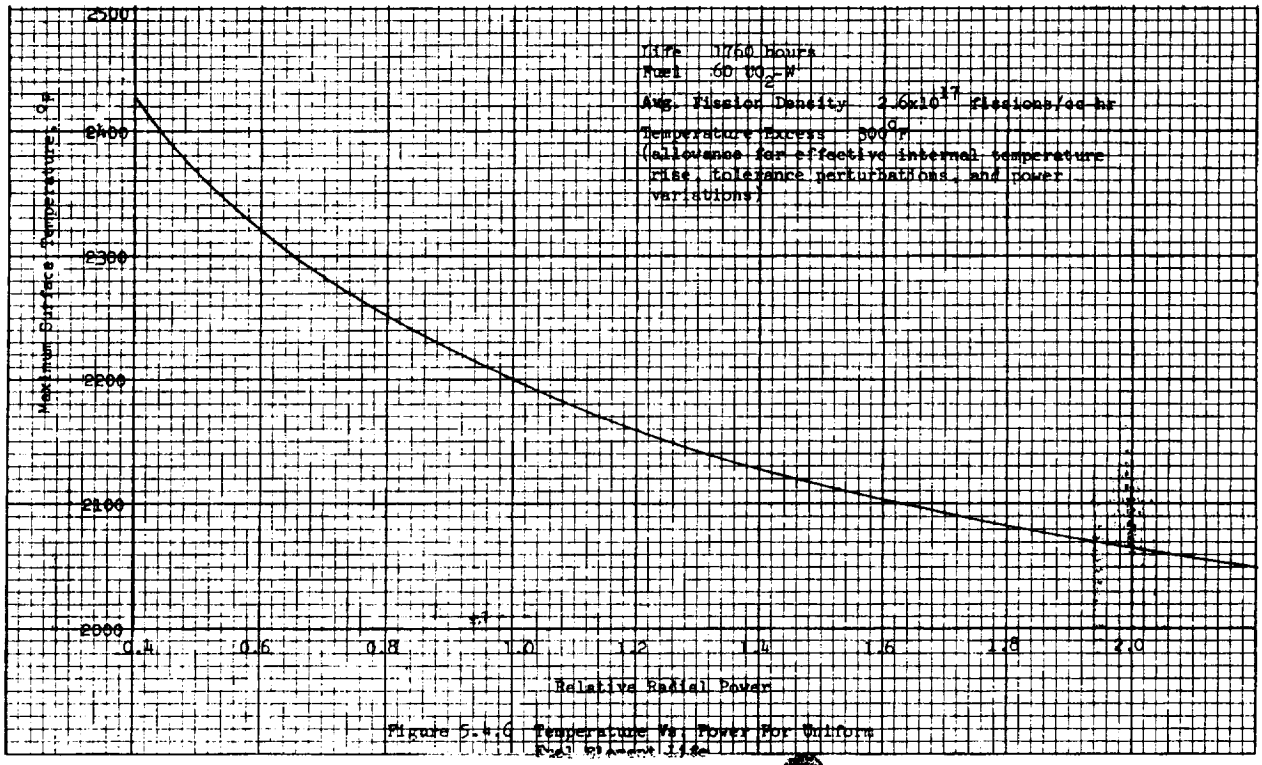

Figure 5.4.6 Temperature Vs. Power For Uniform Fuel Element Size

CONFIDENTIAL

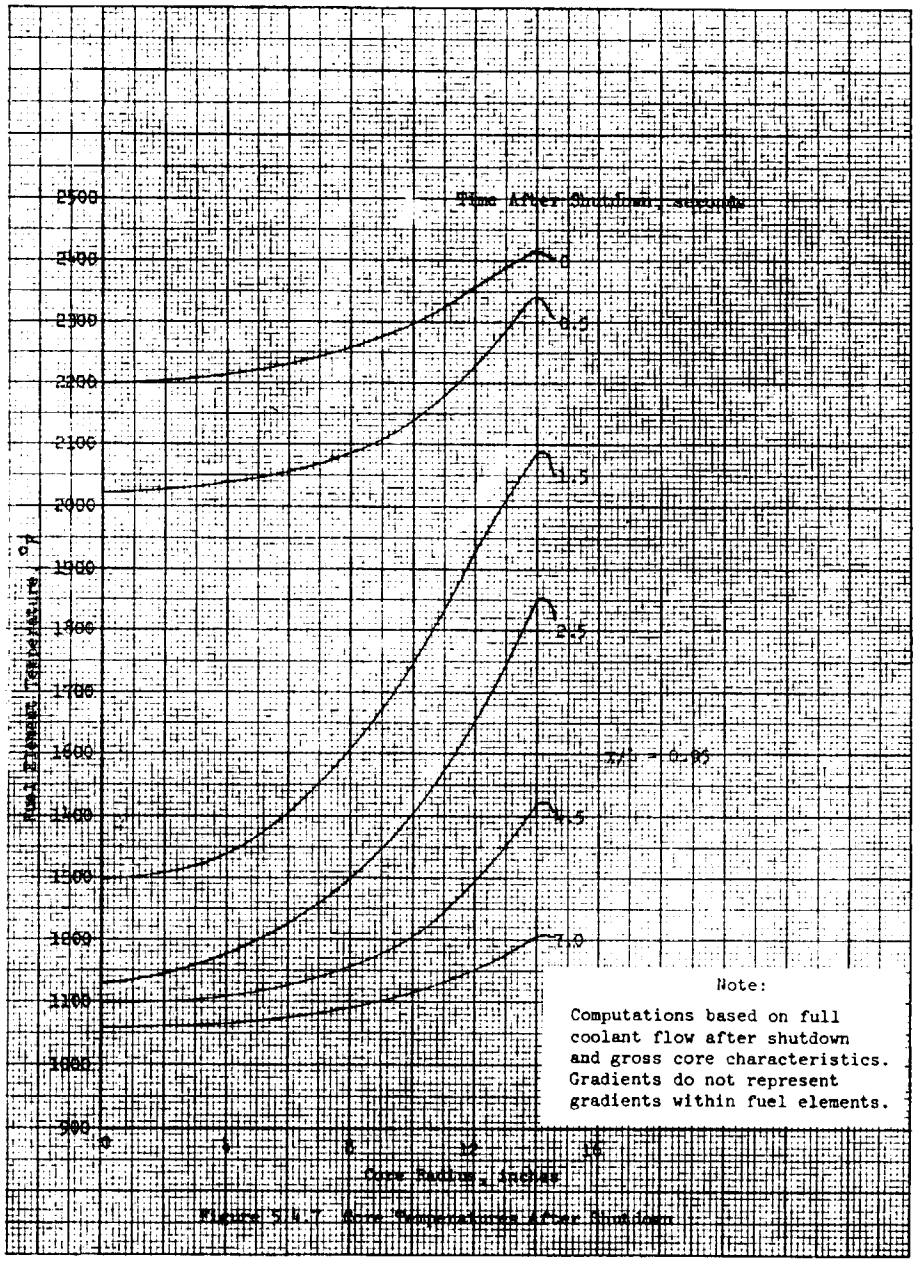

Figure 5.4.7 Core Temperatures After Shutdown

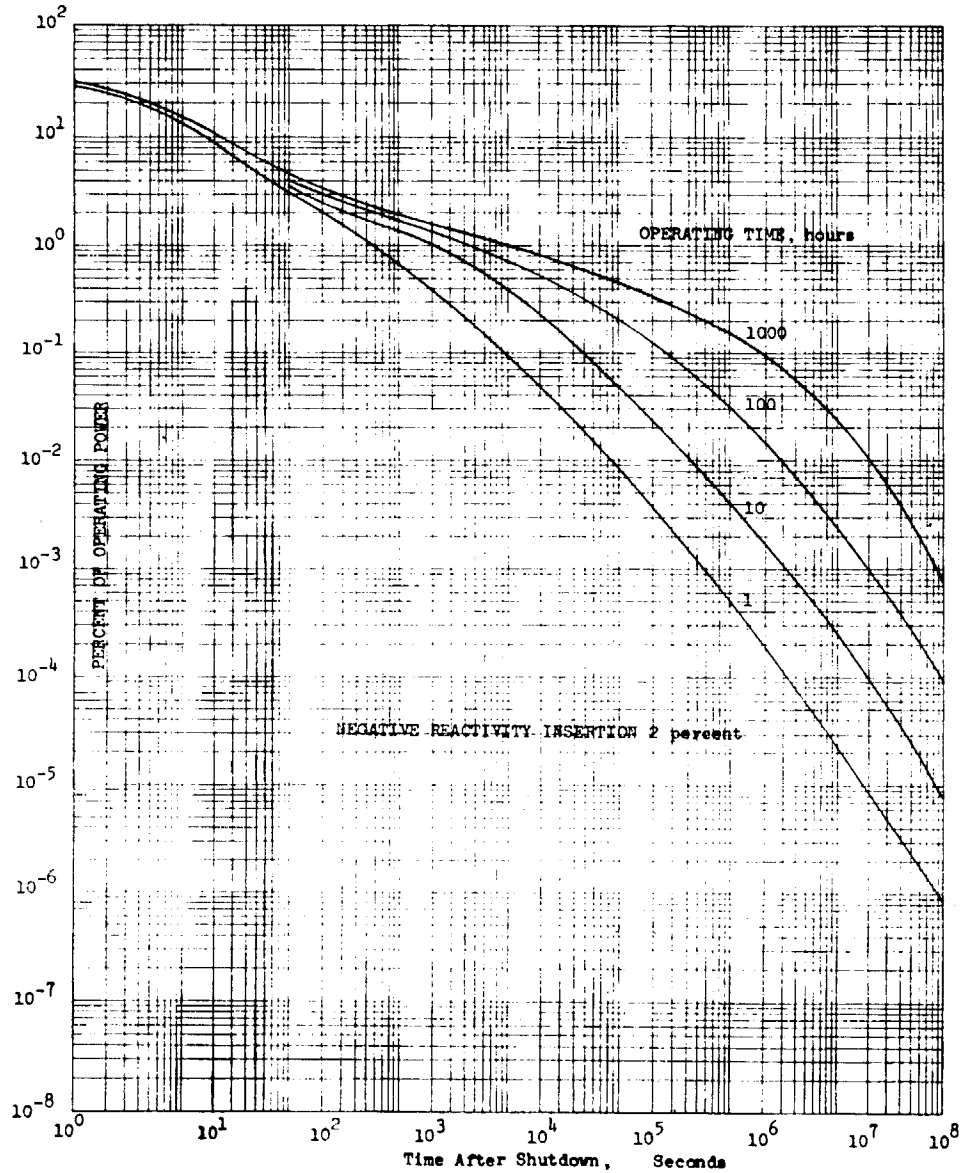

FIGURE 5.4.8 - Afterheat Power

during steady-state operation and during transients. Permanent growth due to accumulation of gaseous fission products must be considered as it affects bowing during steady-state operation. Elimination of any bowing that may be present in normal operation could cause relative movement during transients when aftercooling flow is larger than the afterheat generation rate or, if hydraulic diameter variation within a fuel element is used, from mismatch of cooling and heating rates after shutdown. This evaluation is necessary not only to establish that adjacent fuel elements will not interfere with one another but also to provide the basis for determining the magnitude of reactivity effects to be expected.

3. Aftercooling analyses are required to establish the power requirements and preferred methods of aftercooling through the time period until active aftercooling can be discontinued.

5.5 SUMMARY TABULATION OF REACTOR DATA

A summary of pertinent design values for the reactor assembly is given in Table 5.5.1. The range shown for loop pressure loss represents the uncertainty associated with non-reactor losses; accordingly, the blower horsepower covers a corresponding range. Other values are those either specified by the design requirements or derived during the course of the present study. The value of excess reactivity available in the assembly is not explicitly stated because of the uncertainties that must be considered at this stage of analysis, although the calculated excess of 9.8 percent is believed to be adequate for providing the necessary nuclear lifetime even if most of the uncertainties should be resolved unfavorably.

State-of-the-art values are compared with design values separately in Table 5.5.2 for items of particular interest or which may ultimately establish design criteria. This tabulation shows that the state-of-the-art values are equal to or better than the design values for all items listed except for the system pressure level and for the containment vessel temperature. The state-of-the-art pressure level is shown (in section 4) to be less than 500 psia for blowers which have been or are currently under development. The containment vessel temperature capability is limited by the conditions imposed after a crash in which a pressure of 1500 psi must be contained for 1000 minutes with the vessel at 3000°F and in an oxidizing atmosphere.

The demonstrated fission density in the fueled meat, while equaling the average value imposed in the current application, requires some engineering interpretation by application of refined analysis techniques to account either for shape factors (because of the geometry of the specimen used in the test) or for the trade-off in time versus temperature effects. The only significant uncertainty is the effect of irradiation upon the creep properties and ductility of the W matrix material. Thus, while it is believed that the design value of fission density is well within current state-of-the-art capability, the test results available do not duplicate all the conditions expected in the design and proof testing is required to eliminate the need for any interpretive extensions or interpolations of the available data.

CONFIDENTIAL

TABLE 5.5.1

DESIGN VALUES FOR REACTOR ASSEMBLY

Loop pressure loss ($\Delta P/P$)	0.045 – 0.080
Blower power, hp	11,000 – 20,000
Reactor pressure loss, ($\Delta P/P$)	0.015
Total loss in containment vessel ($\Delta P/P$)	0.030 – 0.038
Thermal power, Mw	250
Maximum pressure level, psia	1500
Temperature, °F	
Helium, reactor inlet	900
reactor outlet	1800
Maximum fuel surface (avg.)	2180
Maximum fuel internal (avg.)	2298
Maximum internal rise (avg.)	127
Helium flow rate, lb/sec	212.4
Active core dimensions, in.	
Envelope diameter	31.2
Equivalent circular diameter	29.9
Length, active core	30.0
Total including front tube sheet	36.7
Radial reflector thickness	5.0
Core volume fractions	
Structure	0.103
Free flow and voids	0.478
Fueled matrix (95% of theor. density)	0.419
Total	1.000
Active core volume, $in.^3$	21,068
Free flow area (hot), $in.^2$	267.8
Coolant channels per element	37
Elements per reactor	241
Fuel element pitch, in.	1.834
Fuel element across-flats width, in.	1.730
Coolant channel pitch, in.	0.2821
Coolant channel diameter (cold), in.	0.192
Fuel cladding thickness, in.	0.010
Average Burnup in 1000 hours, fissions/cm^3	1.922×10^{20}

[redacted]

TABLE 5.5.2

COMPARISON OF STATE-OF-THE-ART AND DESIGN VALUES
(State-Of-The-Art for Individual Items Only)

	State-of-the-Art Value*	Design Value
Circulator discharge pressure level, psia	500[a]	1500
Reactor inlet temperature, °F	~1100[b]	900
Maximum fuel surface temperature (avg.), °F	>3000[c]	2180
Maximum fuel internal temperature (avg.), °F	>2700[d]	2300
Fuel element lifetime, hr	>2000[e]	>1000
Structure lifetime, hr	>2000[f]	2000
Containment vessel temperature, °F	<3000[g]	3000
Equivalent circular diameter of core, in.	30-35[h]	30
Length of fuel element	i	30
UO_2 concentration in cermet, vol %	60[j]	60
Cladding thickness, in.	0.010[k]	0.010
Coolant channel diameter, in.	>0.035 in.[ℓ]	0.168-0.209
Flat width of fuel element, in.	i	1.73
Burnup in 1000 hours (avg.), fissions/cm^3	m	1.922×10^{20}
Number of reactor fuel-power cycles	n	200

*Demonstrated or deduced from related data. Values apply individually, not necessarily in combination.

a. Value from circulating system component limit assuming sealed, oil-lubricated bearing.
b. Based on nonrefractory (Inconel 625) front tube sheet; higher value possible with refractory material.
c. Higher values possible for shorter times. Limit set by metallurgical effects involving the cladding.
d. Set by arbitrary limit of 1% calculated growth due to fission product pressure at design value of power density for 1000 hours.
e. Estimated based upon limit from growth due to fission gas pressure. Presumes good design to limit hot channel effects so that perturbation is less than 200°F.
f. Value subject to details of final design.
g. Conventional oxidation-resistant structural materials melt at temperatures below 3000°F; thickness of shell acting as strength member may be larger than desired in order to meet the specified conditions to be imposed after crash.
h. Feasibility of reflector control uncertain for core sizes above this value. Different control method would significantly affect the structural arrangement and design.
i. Limiting value has not been identified; have been fabricated to 14.77 in. length, 1.426 in. across-flats.
j. Higher concentration (to 70 vol %) may be possible dependent upon ability to maintain continuity of W matrix in the cermet.
k. Thinner claddings may be possible in future designs depending upon quality of available sheet and tube stock.
ℓ. Range demonstrated by actual fabrication and non-nuclear testing.

CONFIDENTIAL

m. Value subject to operating temperature; see Figure 3.2.13 for available test results. These results, being from test samples as part of the NMPO High-Temperature Materials Program, are considered to be indicative of the minimum capability to be expected when the appropriate fuel element geometry and design is used. Effects of temperature and power distribution are such that use of average burnup at maximum temperature (2468°F) is more life-limiting than where maximum burnup at 2360°F occurs.

n. Test results on a similar geometry have demonstrated ability to cycle from 3000°F to 500°F for 50 plus cycles without deleterious results; test is still in progress. Metallurgical samples have been subjected to up to 400 cycles.

[redacted]

5.6 OVERALL ASSESSMENT AND DISCUSSION

This section summarizes the status of the areas of interest with respect to the design requirements for aircraft application, current state-of-the-art, and additional work required.

5.6.1 Materials

FUEL ELEMENT

The temperature levels required for the fuel materials in the proposed design are appreciably lower than the levels of the majority of the research and development work which has been conducted or which is currently in progress at GE-NMPO. Retention of fuel and fission products has been demonstrated at 2900°F for over 3000 hours and at 3600°F for at least 1000 hours, whereas the present design requires a maximum surface temperature of only 2200°F for the average element, with hot channels reaching no more than 2400° to 2600°F, depending upon the degree of design sophistication incorporated to control the magnitude of perturbations.

The burnup level required in the design, an average of about 2×10^{20} fissions/cm^3 in 1000 hours, is greater than that of the current fuel element development program for the space power application of the 710 Reactor, but is in the range of burnup levels obtained successfully in a test under the High-Temperature Materials Program at GE-NMPO. Since higher burnup can be achieved at the lower temperatures of the aircraft application, the data accumulated to date (see section 3.2), together with the analysis of growth of the fueled material due to fission product gases (see section 5.2.2), provide a relatively high degree of assurance of achieving at least 1000 hours' lifetime and, with careful design to restrict the magnitude of temperature perturbations, promise of 2000 hours or more.

The excellent stability of the fuel, as demonstrated by the W-Re-Mo-clad W-UO_2 fuel elements, depends, among other factors, upon maintaining stoichiometric UO_2. Procedures have been developed at GE-NMPO for controlling the stoichiometry of UO_2 during fabrication within the limits of measurement capability, and tests have shown that the diffusion rate of oxygen through claddings of W or Re or their alloys, including Mo, is sufficiently low at high temperatures that stoichiometry can be maintained during operation.

Procedures have been developed at GE-NMPO for fabricating the recommended fuel into the fuel element geometry for this application.

STRUCTURAL MATERIALS

Inconel 625 has been found to meet the design requirements of the structural components of the reactor assembly. Irradiation effects data show that it can withstand the relatively high neutron dosage for the present application, and no problem is expected to stem from its use.

The containment vessel can be of either T-111 or T-222. A thickness of 6 inches is estimated as necessary to meet the post-crash design requirements; the requirement of 3000°F is the most restrictive in establishing the thickness requirement. Fabrication procedures must be developed for such thicknesses. The valve closure for the containment shell

would be made of the same material and would require at least the same thickness. Oxidation-resistant materials for cladding the containment vessel have not been identified in the present study, because all ordinarily used oxidation-resistant cladding materials have melting points below 3000°F. Further work is required to identify the oxidation-resistant material and the method of applying it to the containment vessel.

5.6.2 Reactor Assembly and Reactivity Control

In this study, a concept was evolved of using the containment vessel as the reactor pressure vessel for normal operation; this produces the following advantages:

1. A reflector control based upon neutron leakage variation is possible even for the size of reactor required for aircraft application. This greatly simplifies the mechanical arrangement of the control actuators and avoids any structural complication that would be associated with the use of poison control rods within the active core (e.g., a center island containing a moderating material to make poison control feasible).
2. The reflector control segments can operate while immersed in the borated shield water. Control worth is not significantly penalized even though the shield water has free access to the structural cylinder immediately outside the active core. There is no need for waste void to allow for displacement of the reflector segments.
3. The gas ducts from the containment vessel to the reactor are pressure-balanced; i.e., the external pressure in the shield water is the same as the internal gas pressure. In addition, the structural portions of the ducts can be cooled by the shield water (the design provides forced circulation) so that thermal expansion strains are restricted to a relatively low magnitude. Many small convoluted ducts are possible, therefore, with the result that radiation streaming through the shield because of duct penetrations can be reduced with a relatively large degree of design flexibility.

These advantages are counterbalanced by the need for attention in the following areas:

1. A pressure-balance system is required to maintain shield water pressure equal to gas pressure (within a tolerance of about 200 psia) during normal operation, startup, and shutdown.
2. The need to drain the shield water from the containment vessel removes the cooling water from the ducting. This places a restriction on the gas temperatures that can be permitted during aftercooling, unless a special water cooling circuit is provided specifically for the ducting. Consideration of long-time after-shutdown aftercooling needs indicates the desirability of such an approach in the interest of economy.

Because these concepts are uniquely derived for the present application, there are no specific engineering test results to support the design. Accordingly, while the feasibility is not questioned, component

tests are required to demonstrate that the concepts can be made to perform their required functions. Specific areas requiring work are:

1. Development of the pressure-balancing system to equalize shield-water and gas pressures both for normal operation and for transients required during shutdown of the reactor.
2. Development of the valve for the containment vessel closure, including the actuator and valve seat, for conditions that duplicate those expected when the containment vessel is performing its post-crash function.
3. A critical experiment to determine the reflector control worth as a function of angular displacement and to measure the effect of immersing the radial reflector in borated water.
4. Determination of the mechanical properties and fabrication procedures for the containment vessel material in the thicknesses required.
5. Design and test of the insulation to be used on the gas-side of the ducts that are cooled by shield water.
6. Development of the control actuator for the specific environment (i.e., immersion in the pressurized shield water) and to establish the necessary reliability of operation for the specific design to be used (electrical components, structure, coolant flow passages, and bearings).
7. Evaluation of the need for a rear tube sheet, considering fuel element vibration and bowing effects. Also experimental tests, if necessary, to demonstrate the vibration characteristics of the fuel-element - tube-sheet assembly.

5.6.3 Fuel Elements

The fuel element design for the aircraft application introduces no new features and is a relatively straight-forward application of design concepts that have been evolved during the previous work on the 710 Reactor concept. Suitability of the materials for meeting the aircraft design requirements is discussed in section 5.6.1. Hydraulic diameter variation between fuel elements is required, depending upon the radial position of the element in the reactor, to achieve the lifetime requirement. Because of the relatively high porosity of the average fuel element, those in the central region of the core may require a reduced fuel concentration to augment the hydraulic diameter variation for tailoring the radial temperature profile.

More detailed evaluation of the amount of bowing to be expected is required, considering both the temperature differentials across a single element and the differential permanent growth because of the radial power density gradient. Depending upon the results of this evaluation, use of hydraulic diameter variation within individual fuel elements may be desirable. Fabrication procedures are adaptable without difficulty to accomplish the hydraulic diameter variation in either case.

Since the fuel element materials proposed for the aircraft application may have a lifetime capability significantly greater than the 1000-hour design requirement, in-pile tests of specimens duplicating the geometric characteristics of the fuel element design should be conducted.

5.6.4 Multiplication Constant of Worst Configuration After Crash

The mechanical integrity of the reactor core is presumed to be destroyed in the event of a crash. Under this presumption, it is necessary to determine if the resulting disassembly can take the form of a nuclearly critical mass that would significantly increase the energy that must be contained by the containment vessel. Purely mechanical re-arrangement of the disrupted parts into a critical assembly, while conceivable, is highly unlikely and of less concern than the re-arrangement that can occur if the reactor were to melt. Even melting would be of minimum concern if the amount of material in the molten form did not reach that of a critical mass. Preliminary calculations with simplifying assumptions* indicated that the energy release by afterheat could, in the absence of any energy removal mechanism, melt the core within 40 seconds and vaporize it within 300 seconds. Accordingly, a study was made to determine the amount of the core in the solid, molten, and vaporized state as a function of time after shutdown, and to determine the critical masses of various possible compositions of the molten material.

In the thermal analysis, the effect of using full-flow aftercooling for 0, 10, and 20 seconds after shutdown was evaluated; also, because the fuel matrix power density was estimated to vary within the core from 1 to 4 times the minimum, the effect of power distribution upon local afterheat generation rates was included. The Transient Heat Transfer (THT-C) computer code was used with 100 core and 100 coolant nodes to identify the transient temperature distribution during the flow periods. Flow distribution among the coolant channels was assumed to remain the same as for normal operation. Exploratory computations using the same code after cessation of flow indicated that computational costs would be relatively high. Accordingly, the data contained in that program were used to compute molten and vaporized fractions assuming no heat transfer between nodes; this assumption closely approximates the actual problem soon after shutdown when the afterheat power is high. At later times, the heat transfer problem becomes more complex than the THT-C model used because of vapor and liquid transport. The UO_2 and W-metal matrix were assumed to remain in local contact and at the same temperature until the UO_2 vaporized. The vaporization temperature assumed was the normal boiling point of UO_2 at 1 atmosphere. The cumulated afterheat energy as a function of time after shutdown, derived by integrating the afterheat power generation rates, is shown in Figure 5.6.1.

The results of the analysis are given in Figure 5.6.2. Fuel fraction in the molten and vaporized states is shown as a function of time after the insertion of 2 percent $\Delta k/k$ shutdown margin. The data show that aftercooling with full flow for up to 20 seconds has little effect on the fraction of core which can exist in the molten state: the analysis indicates between 70 and 80 percent. Longer periods will be required to achieve appreciable reduction in the molten fraction, but this would not be possible if the containment vessel valves were closed within the 20-second time limit specified by the design requirement (section 1).

*Involving, among others, adiabatic conditions for the core.

For comparison with the amount of material in the molten state, the critical masses were determined for various possible compositions of the molten material [W - $60UO_2$ (vol %), UO_2, and U metal], assuming spherical geometry without and with a reflector (6 inches of W). The use of the spherical model is for convenience alone and is not intended to represent the condition to be expected, since the actual case will depend upon the geometry of shield material surrounding the active core. The results, given in Table 5.6.1, show that an unreflected sphere of solid W - $60UO_2$ (vol %) is critical with less than 30 percent of the core fuel inventory; when reflected with 6 inches of W, a sphere of about 12 percent of the core mass would be critical. Should the UO_2 and W segregate while in the molten state, the critical masses are appreciably smaller.

These data show that the occurrence of a super-critical mass must be considered credible until a better definition of possible re-arrangement of molten fuel can be established, and until this is done, no conclusion can be reached with regard to whether the possibility can be avoided. It should be noted that the thermal calculations were made using an analytical model in which all the components retain their geometrical form and location; in actuality, the crash loads will probably cause significant disruption, allowing heat flow along paths not yet considered, and the molten fuel will pass from the reactor and collect in various portions of the shield in such a manner that the idealized spherical arrangement is not likely. The shield geometry is very important in this regard; for example, the W can be in the form of spheres (or other preferred geometric shapes yielding the desired shield-water - W volume fractions) so that the molten fuel flows into the interstices and the shield material becomes an effective diluent. Therefore, the results of the present study should be considered as providing a base point from which further studies should be made.

CONFIDENTIAL

TABLE 5.6.1

CRITICAL PARAMETERS FOR VARIOUS GEOMETRIES OF CORE MATERIALS

Case Description	Unreflected Sphere			Sphere Reflected With 6 Inches of Tungsten		
	Radius (cm)	Uranium wt (kg)	% of Total U[a]	Radius (cm)	Uranium wt (kg)	% of Total U[a]
All core materials with no void (imploded, crushed core)	22.71	218	27.6	17.40	98	12.4
All metallic core materials, oxygen in UO_2 driven off	20.05	192.5	24.4	15.05	81.4	10.3
Only UO_2	12.66	82.1	10.4	9.30	32.5	4.1
Uranium metal	8.71[b]	51.9	6.5	6.68[c]	23.4	2.9

[a]Assumed critical mass of uranium metal (93.2% U-235) = 790 kg.
[b]Measured value for LASL Godiva reactor.
[c]Measured value for LASL safety experiment with a 4 inch nickel reflector.

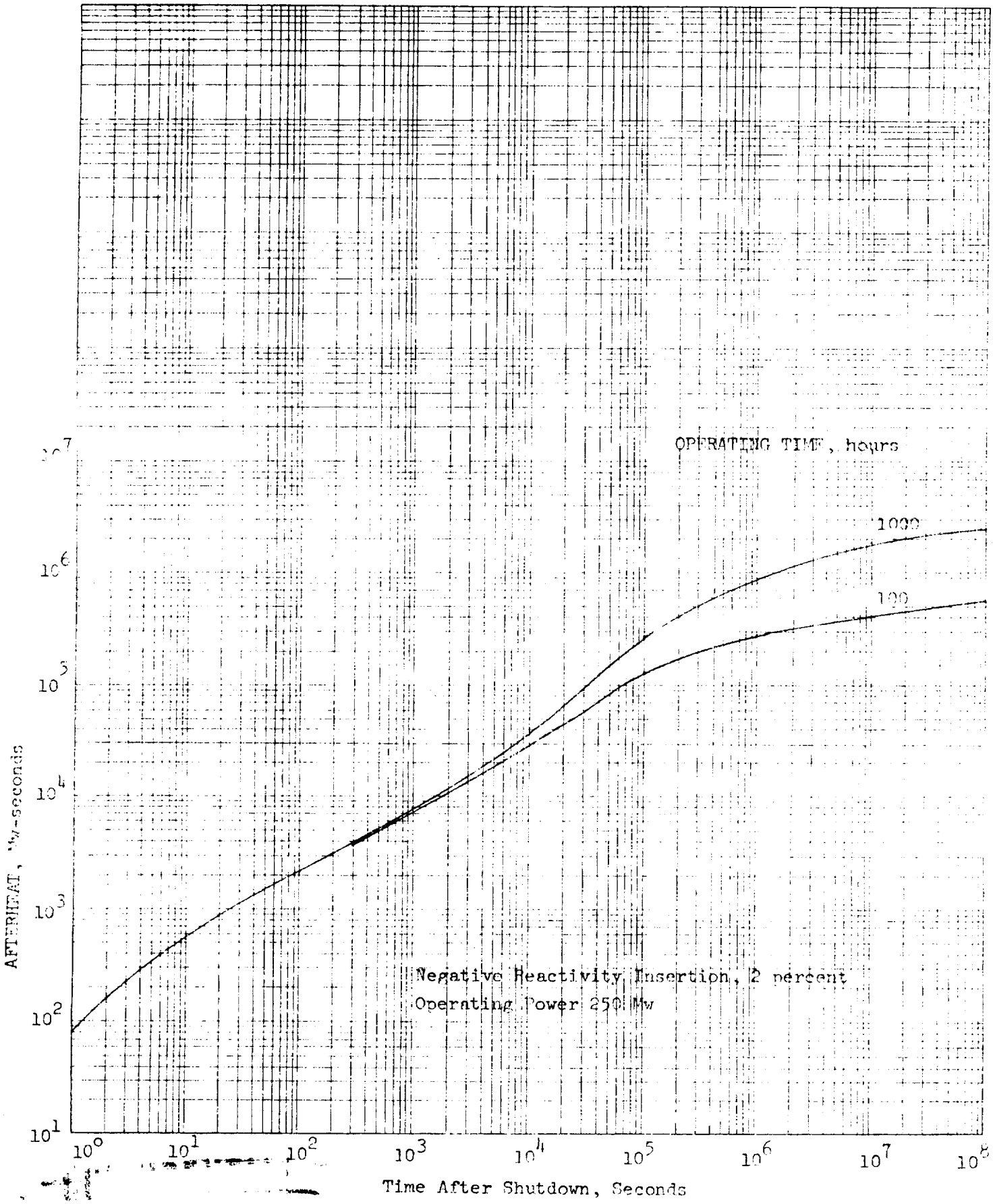

FIGURE 5.6.1 - Afterheat energy as a function of time after shutdown

FIGURE 5.6.2 – Fuel melting and vaporization as a function of time after shutdown

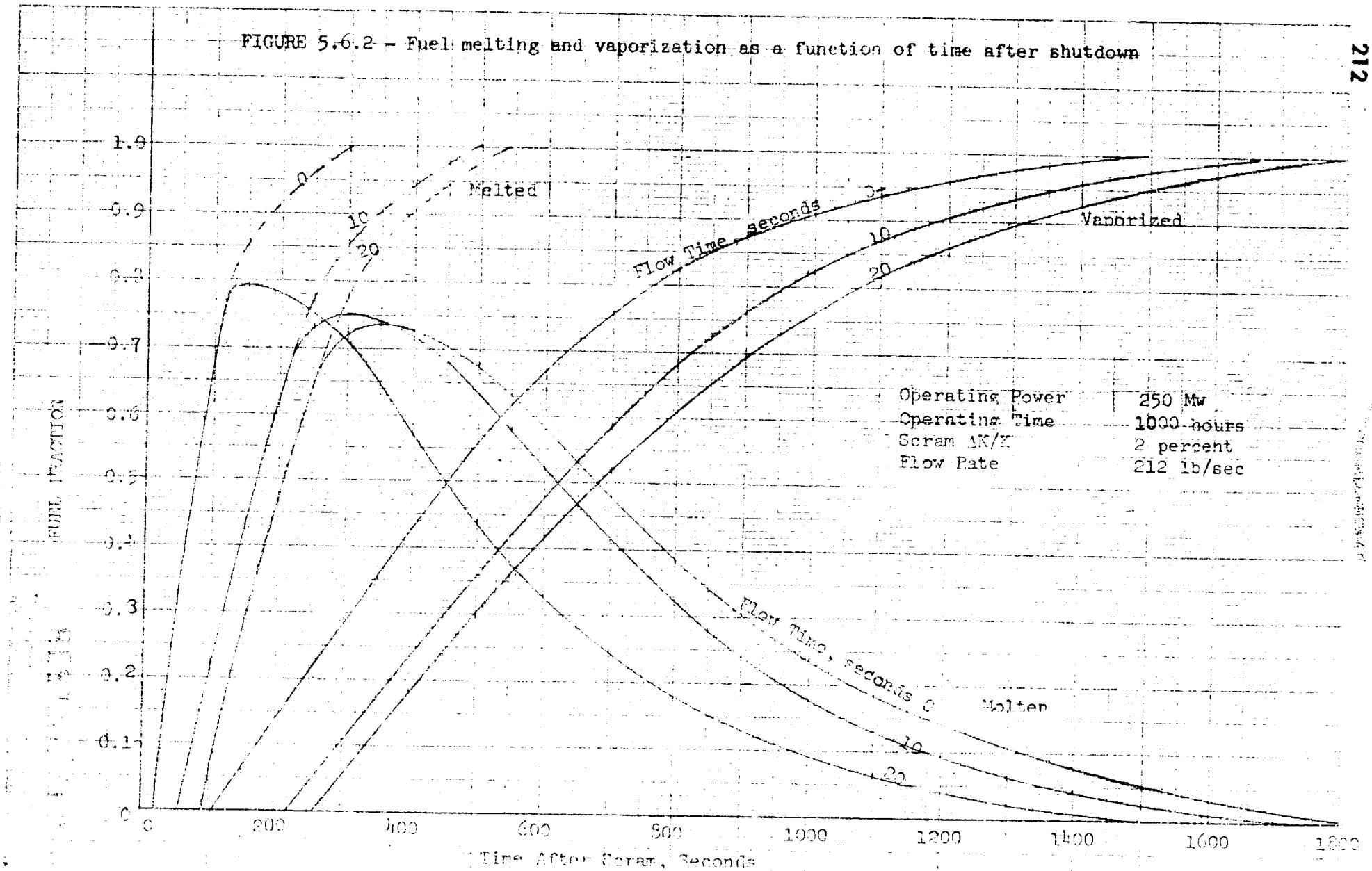

APPENDIX A - COMPILATION OF MATERIALS DATA

This appendix contains supplementary materials data for the candidate materials for the various system components. Although there is considerable variation in literature values of some of the properties, the data contained herein are believed to be reasonably representative and satisfactory for preliminary evaluation purposes. In the case of the mechanical strength properties, however, it should be noted that these properties are normally quite sensitive to prior history (i.e., heat treatment, cold work, etc.), to the form of the product (i.e., sheet, plate, rod, or tube), the thickness, and the source of the material. Consequently, the mechanical properties should be regarded only as a "typical set" of data for the material concerned.

For many of the materials, the Aerospace Structural Metals Handbook* and other references listed in this appendix provide more detailed information.

*ASD-TDR-741, Volumes I and II, and Volume II, Non-Ferrous Alloys, Supplement I.

CONFIDENTIAL

TABLE A1.1

PROPERTIES OF CANDIDATE FUEL ELEMENT MATERIALS

Material	Composition, wt. %	Density, lb/in^3	Melting Range, °F	Reference
Tantalum	99.8 Ta[a]	0.600	5425	b
T-111	Ta – 8W – 2.4Hf	0.604	5400 (est)	b
NMP-256	W – 29.5Re – 18.2Mo	0.608	5252 – 5432	
NMP-306	W – 35.3Re – 18.2Mo	0.616	5072 – 5252	
Mo – 50Re	Mo – 48Re	0.496	4622	c
W – 60UO_2	W – 46UO_2	0.516[d]		
Mo – 60UO_2	Mo – 61.7UO_2	0.385[d]		
W	99.9W[a]	0.697	6170	b
Re	99.9Re[a]	0.759	5788	c
Mo	99.9Mo[a]	0.369	4334 – 4370	b
UO_2		0.396		

[a]Commercial purity

[b]Aerospace Structural Metals Handbook, ASD-TDR-63-741, Volume II

[c]"Chase Rhenium and Rhenium Alloys," Chase Brass and Copper Co., Waterbury, Conn.

CONFIDENTIAL

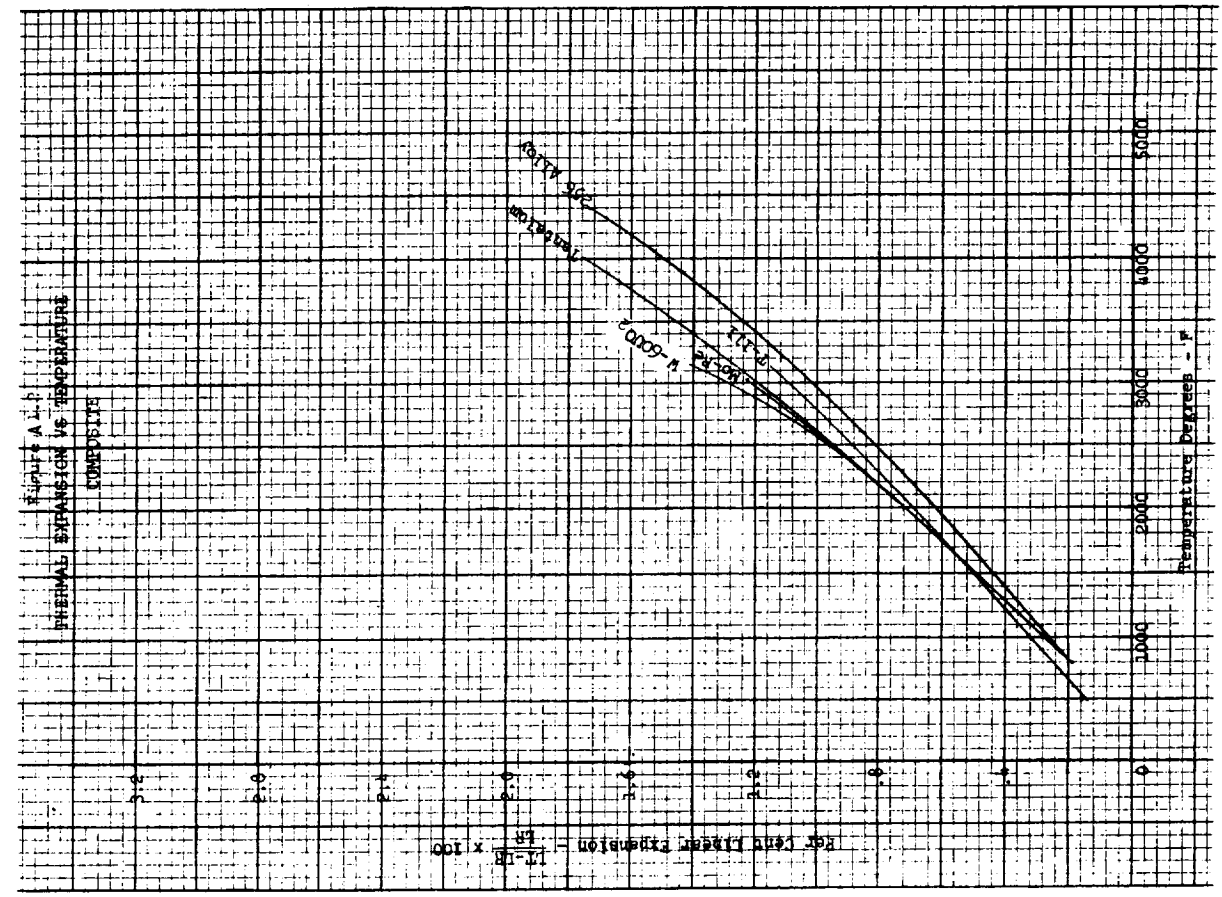
Figure A1.2
THERMAL EXPANSION VS TEMPERATURE
COMPOSITE
Per Cent Linear Expansion
Temperature Degrees - F
Tantalum
Mo-Re
W-60UO2
0
1000
2000
3000
4000
5000
.4
.8
1.2
1.6
2.0
2.4
2.8
3.2

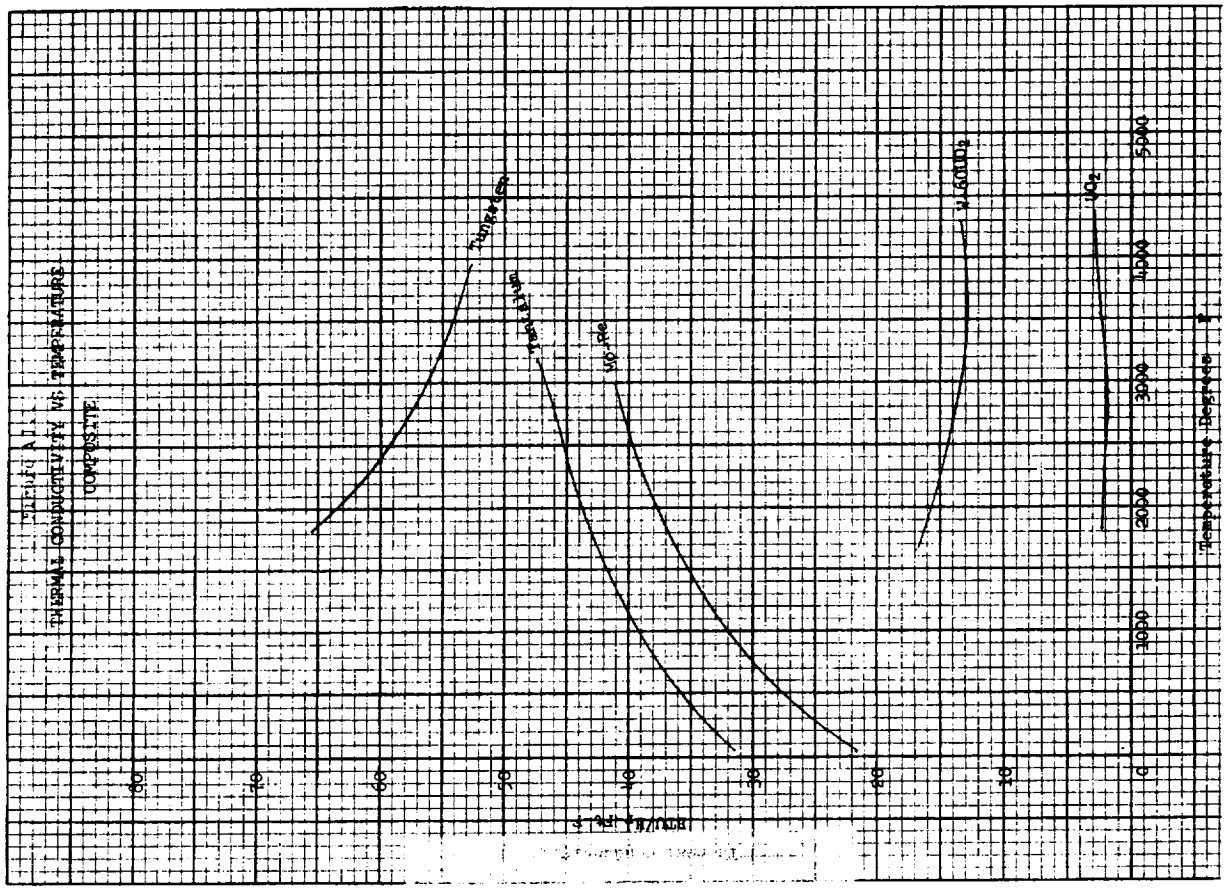
Figure A1.1
THERMAL CONDUCTIVITY VS TEMPERATURE
COMPOSITE
Tungsten
Tantalum
Mo-Re
W-60UO2
UO2
Temperature Degrees - F
0
1000
2000
3000
4000
5000
10
20
30
40
50
60
70
80

[redacted]

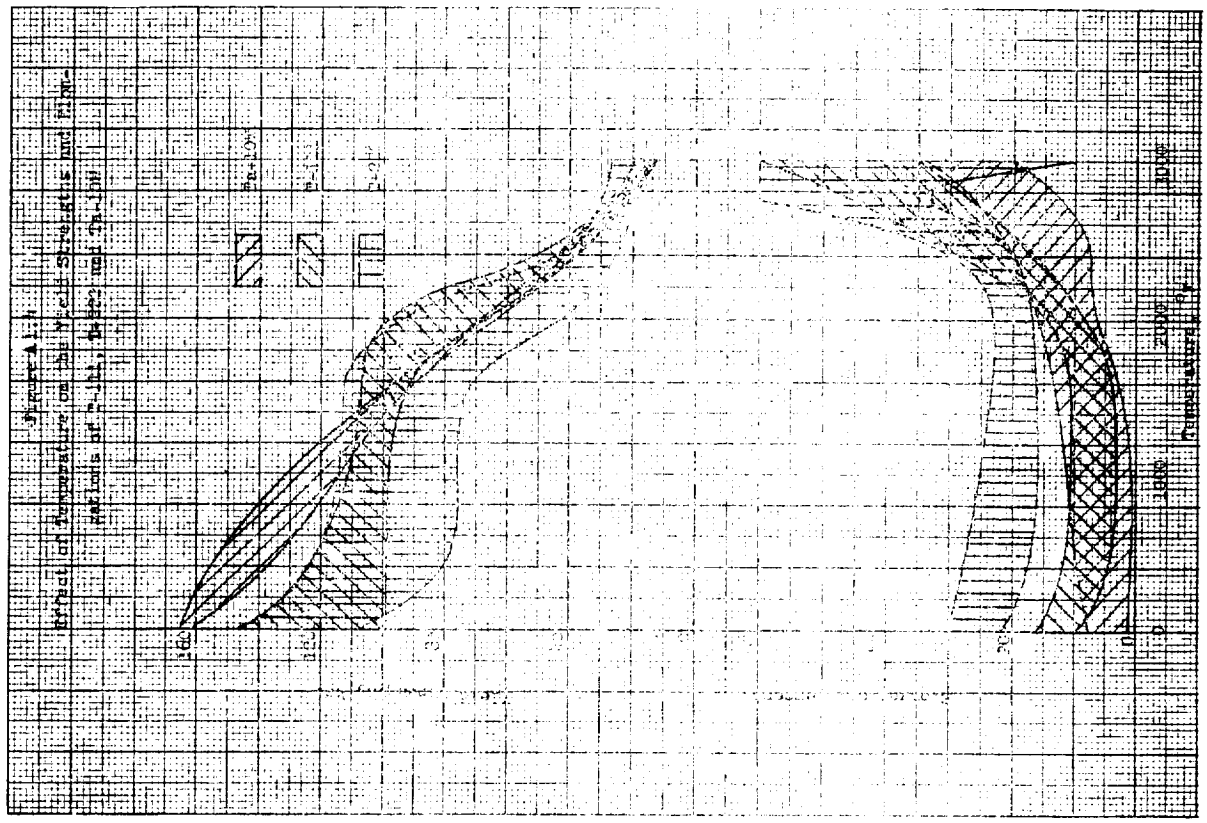

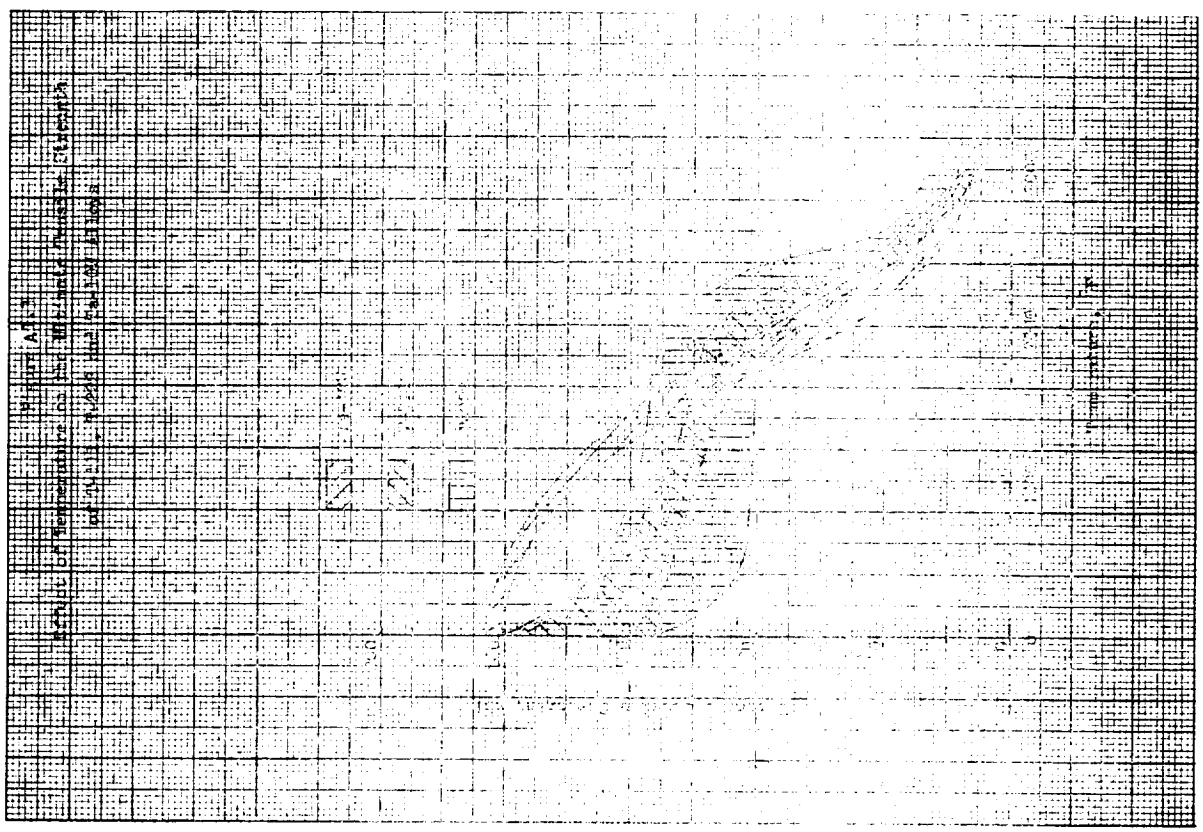

[redacted]

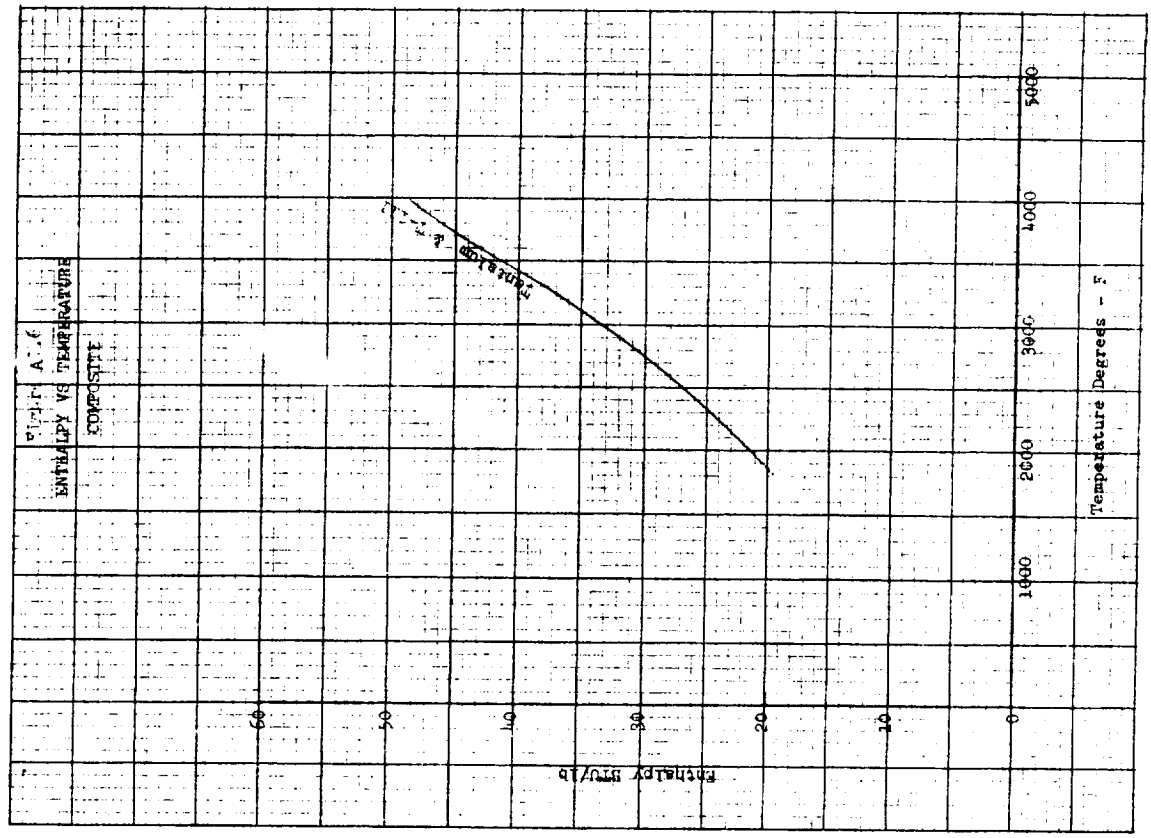

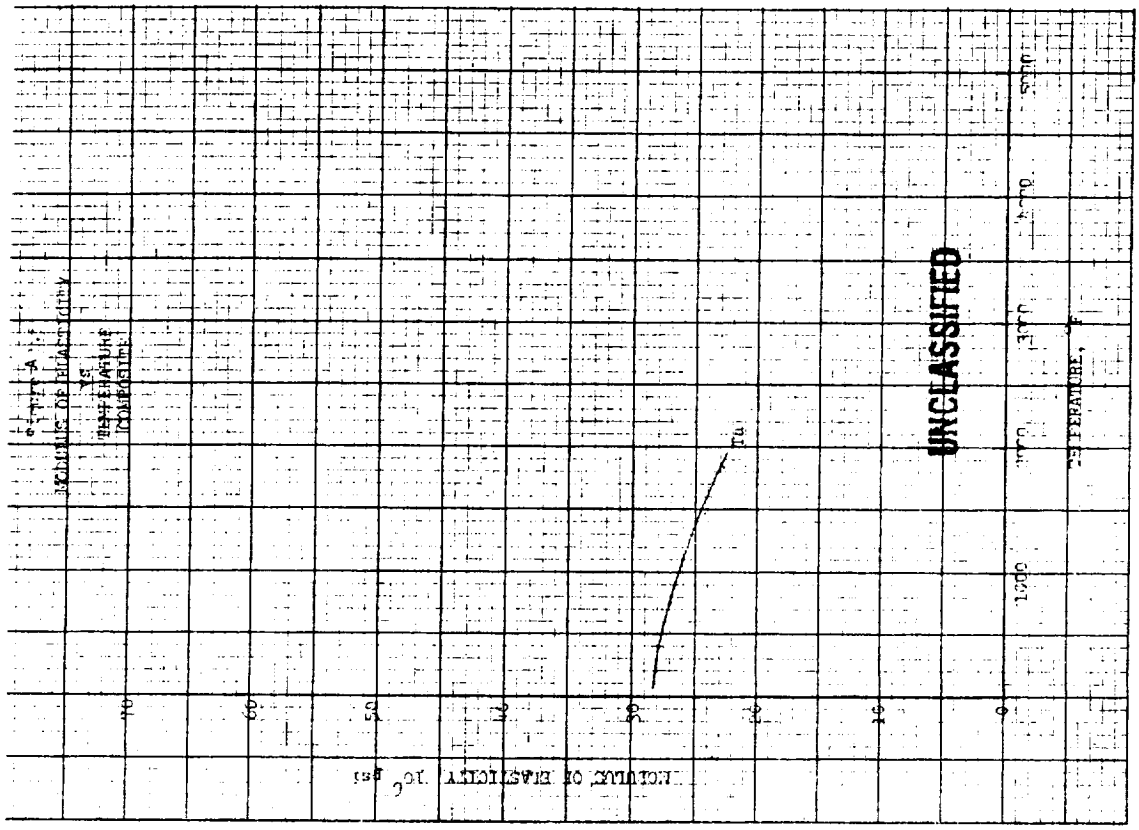

UNCLASSIFIED

[redacted] CONFIDENTIAL

Figure A1.7
ELECTRICAL RESISTIVITY VS TEMPERATURE
COMPOSITE

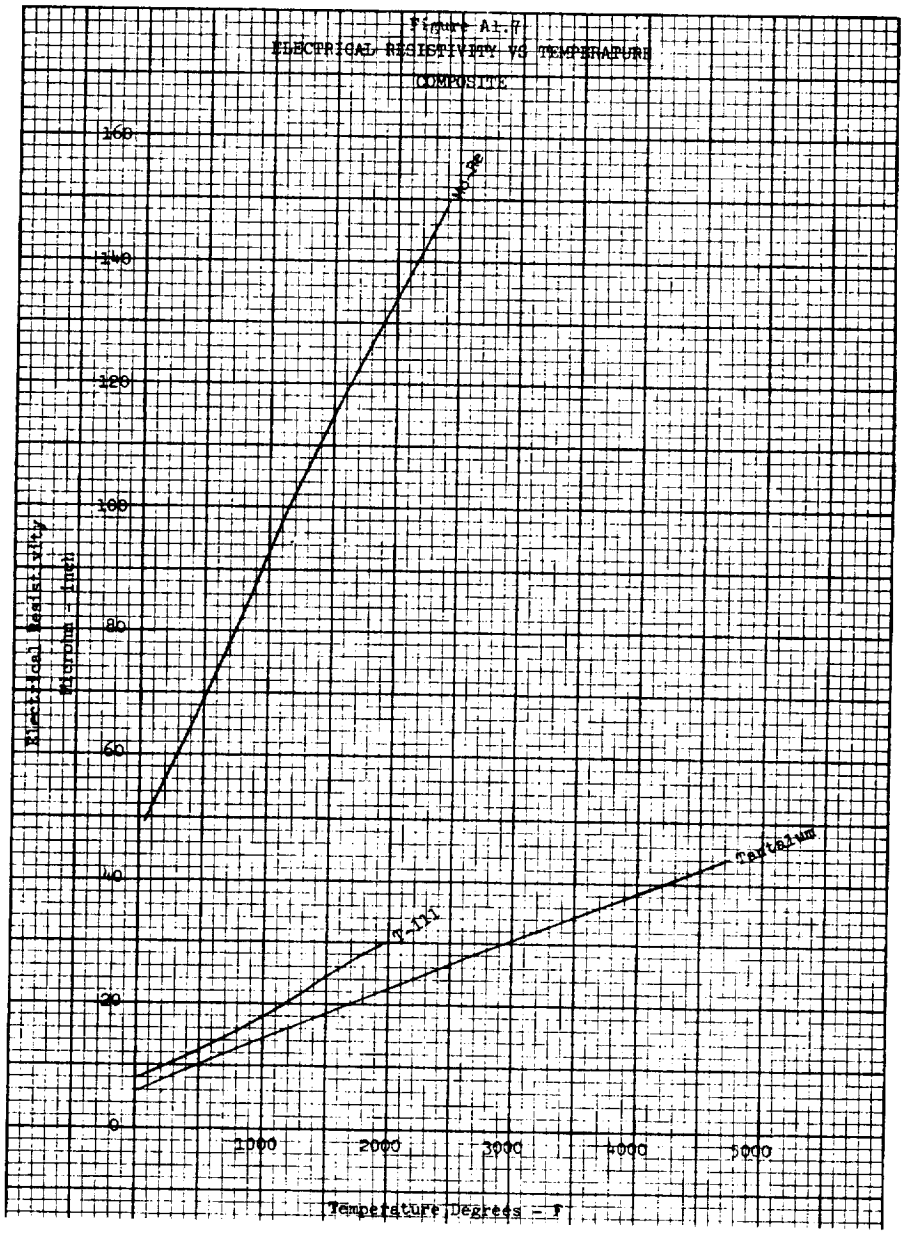

[redacted]

TABLE A2.1

PROPERTIES OF CANDIDATE STRUCTURAL MATERIALS

Material	Composition, wt %	Density, lb/in^3	Melting Range, °F	Reference
304 SS	Fe, < 0.08 C (max), 19Cr, 10Ni	0.287/0.292	2550 – 2650	a
316 SS	Fe, 1.5-3.0Mo, 13Ni	0.288	2500 – 2550	a
347 SS	Fe, 1.5Nb (max), 18Cr, 12Ni	0.287/0.292	2550 – 2650	a
Inconel 600	Ni, 15Cr, 7Fe, 4Nb	0.304	2540 – 2600	b
Inconel 625	Ni, 22Cr, 9Mo, 3Nb	0.305	2500 – 2600	c
Incoloy 800	Fe, 32Ni, 21Cr	0.29	2475 – 2525	d
Hastelloy C	Ni, 16Cr, 16Mo, 5Fe, 4W	0.323	2320 – 2380	e
Hastelloy X	Ni, 22Cr, 18Fe, 9Mo, 1.5Co, 0.5W	0.297	2350	e
Niobium 752	Nb, 10W, 2.5Zr	0.326	≈ 4400	f

[a]Aerospace Structural Metals Handbook, ASD-TDR-63-741, Volume I

[b]Engineering Properties of Inconel Alloy 600, Huntington Alloy Products Division, Technical Bulletin T-7

[c]Preliminary Data of Inconel Alloy 625, Huntington Alloy Products Division, Technical Bulletin S-16

[d]Engineering Properties of Incoloy Alloy 800, Huntington Alloy Products Division, Technical Bulletin T-40

[e]Aerospace Structural Metals Handbook, ASD-TDR-63-741, Volume II

[f]"The Engineering Properties of Columbium and Columbium Alloys," BMI, DMIC Report 188, September 6, 1963

CONFIDENTIAL

Figure A2.1

THERMAL CONDUCTIVITY vs TEMPERATURE

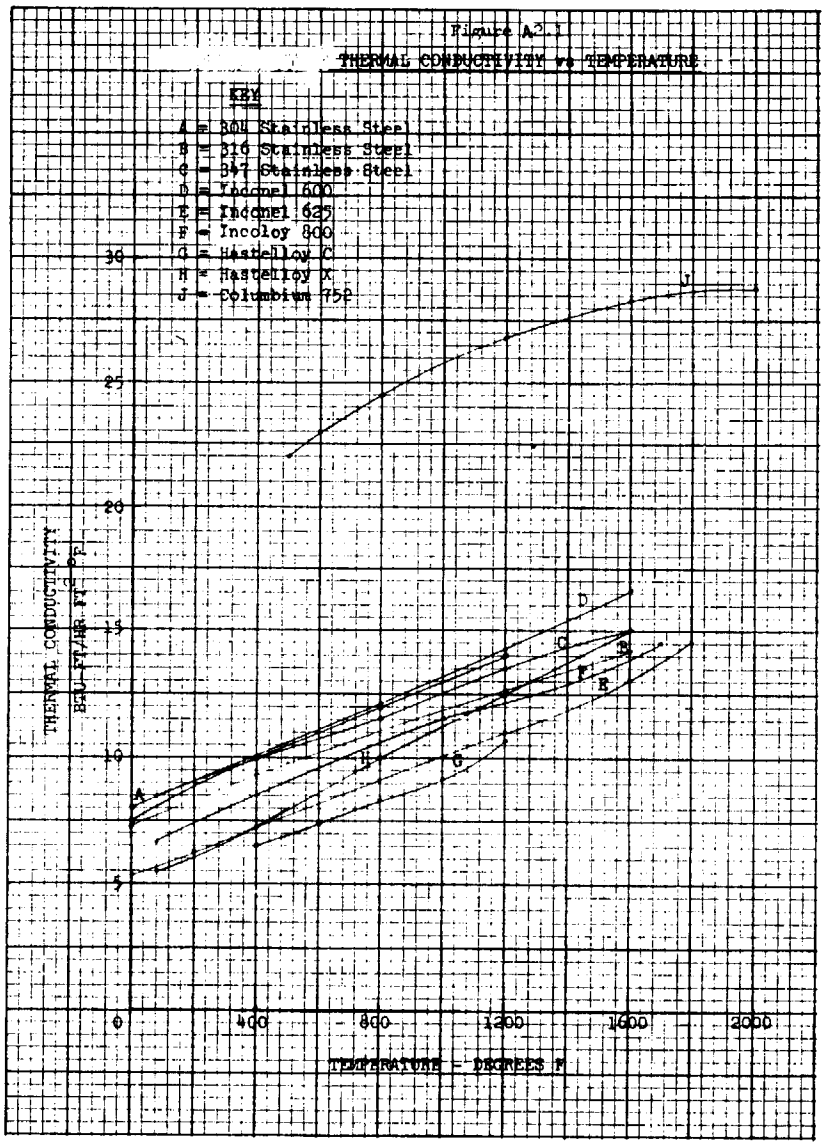

Figure A2.2

MEAN COEFFICIENT OF THERMAL EXPANSION vs TEMPERATURE

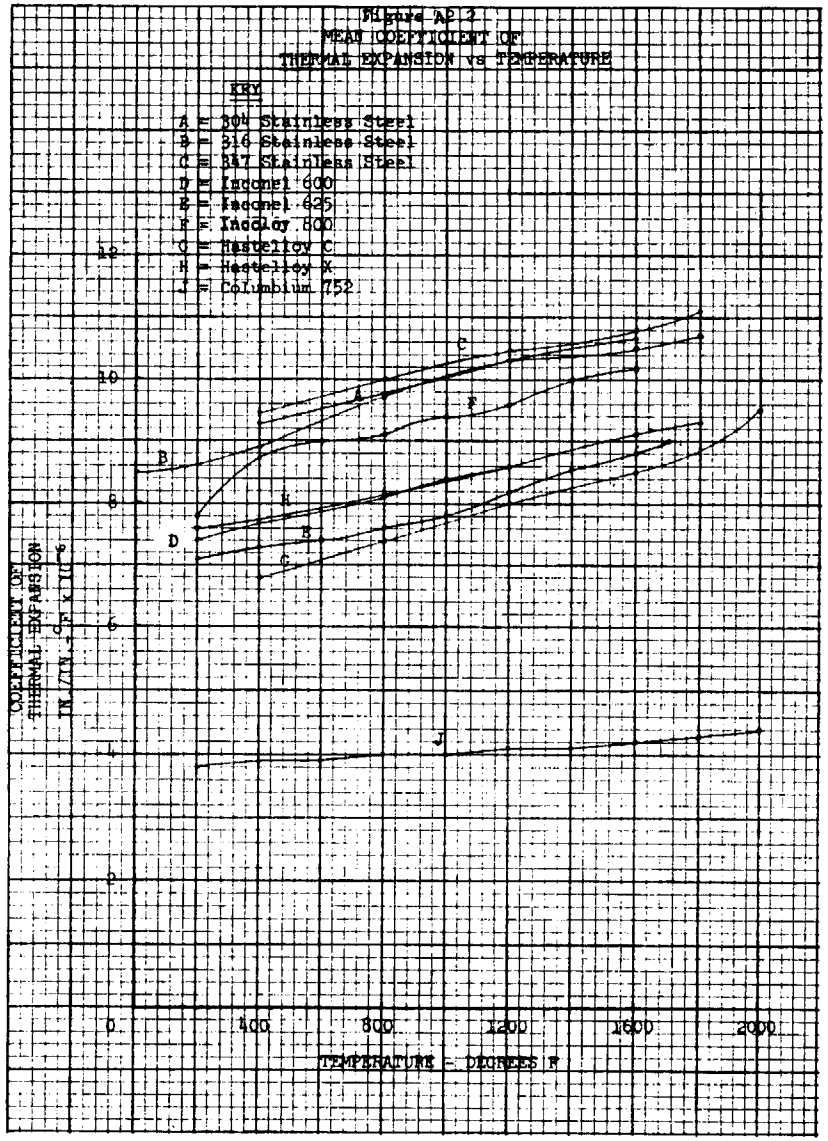

FIGURE A-3

Effect of Temperature on the Ultimate Tensile Strength of the Candidate Structural Materials

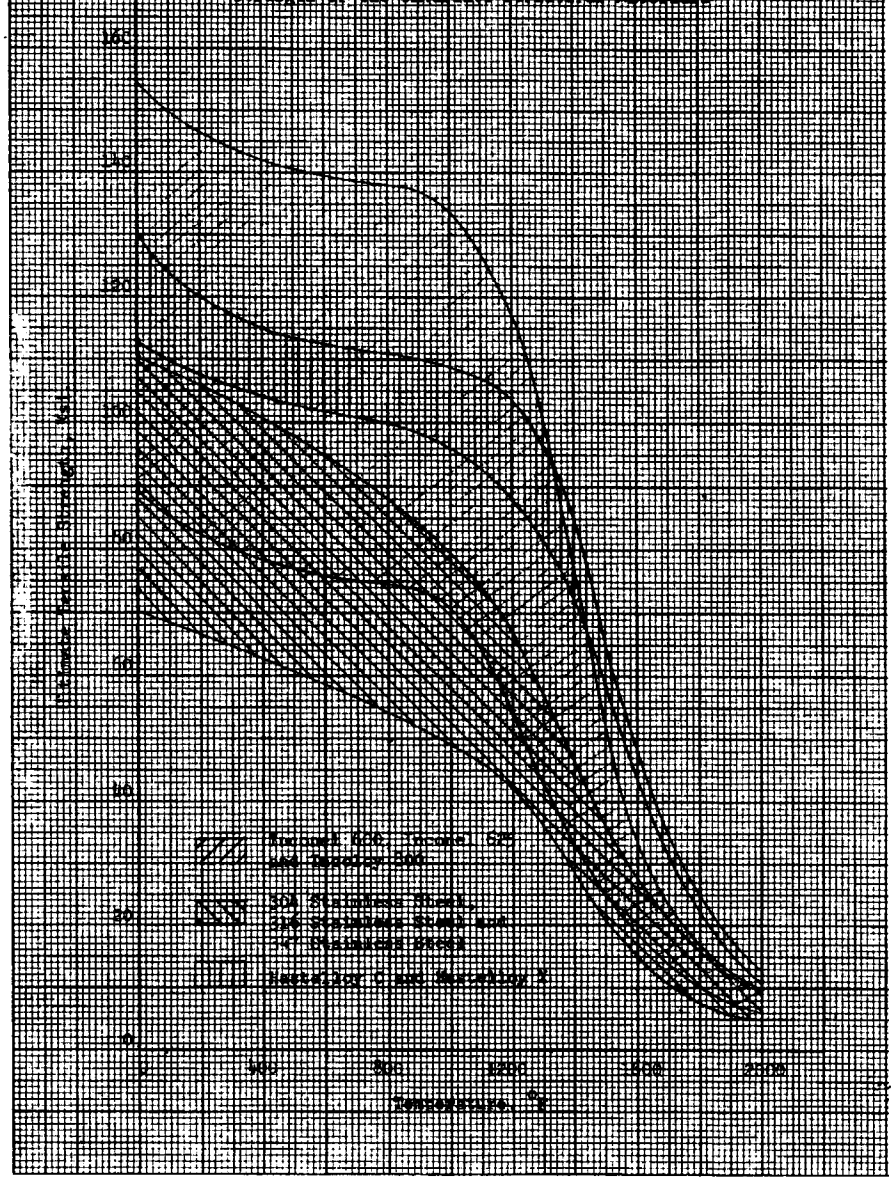

FIGURE A-4

Effect of Temperature on the Yield Strength and Elongation Properties of the Candidate Structural Materials

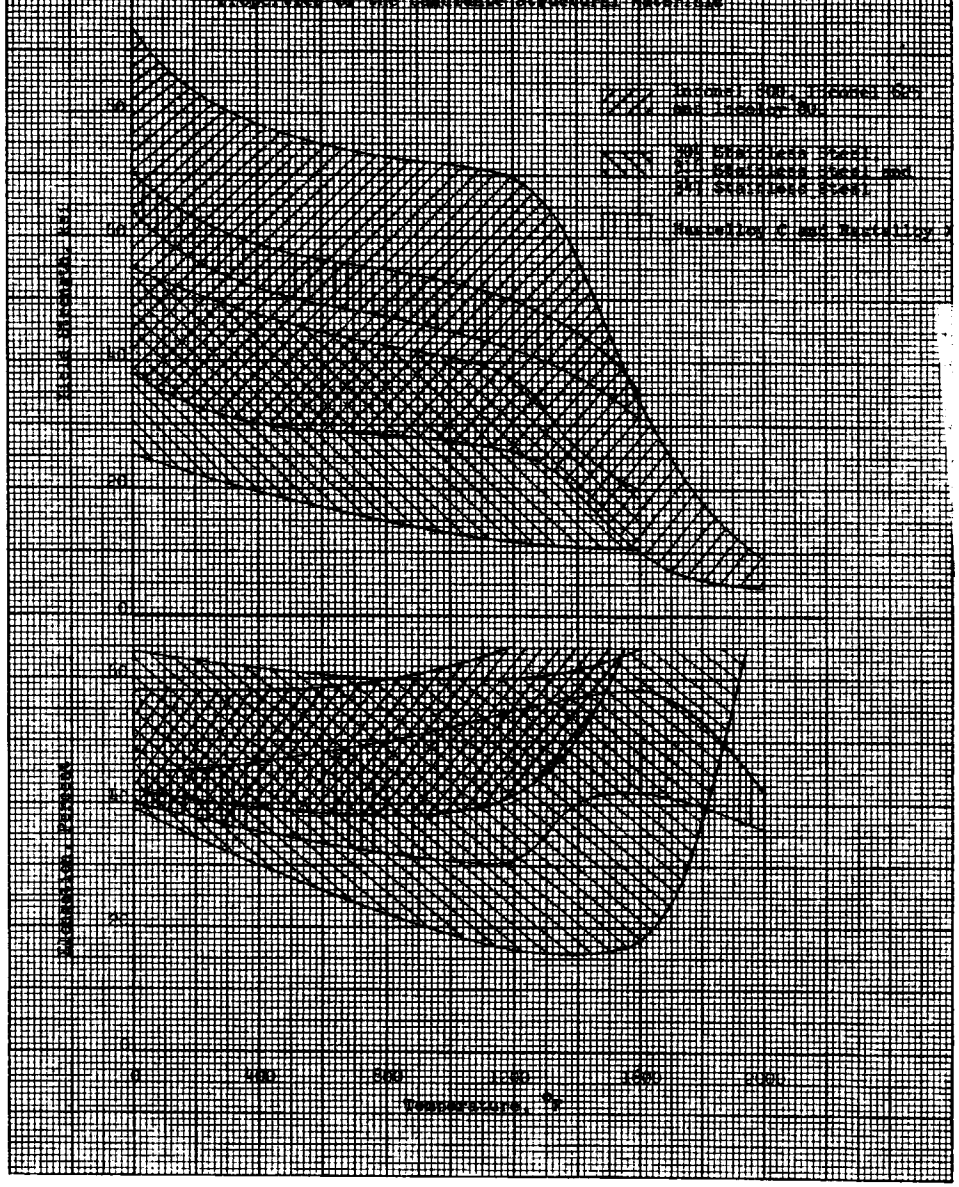

CONFIDENTIAL

Figure A2.5

MODULUS OF ELASTICITY vs TEMPERATURE

KEY

A = 304 Stainless Steel
B = 316 Stainless Steel
C = 347 Stainless Steel
D = Inconel 600
E = Inconel 625
F = Incoloy 800
G = Hastelloy C
H = Hastelloy X
J = Columbium 752

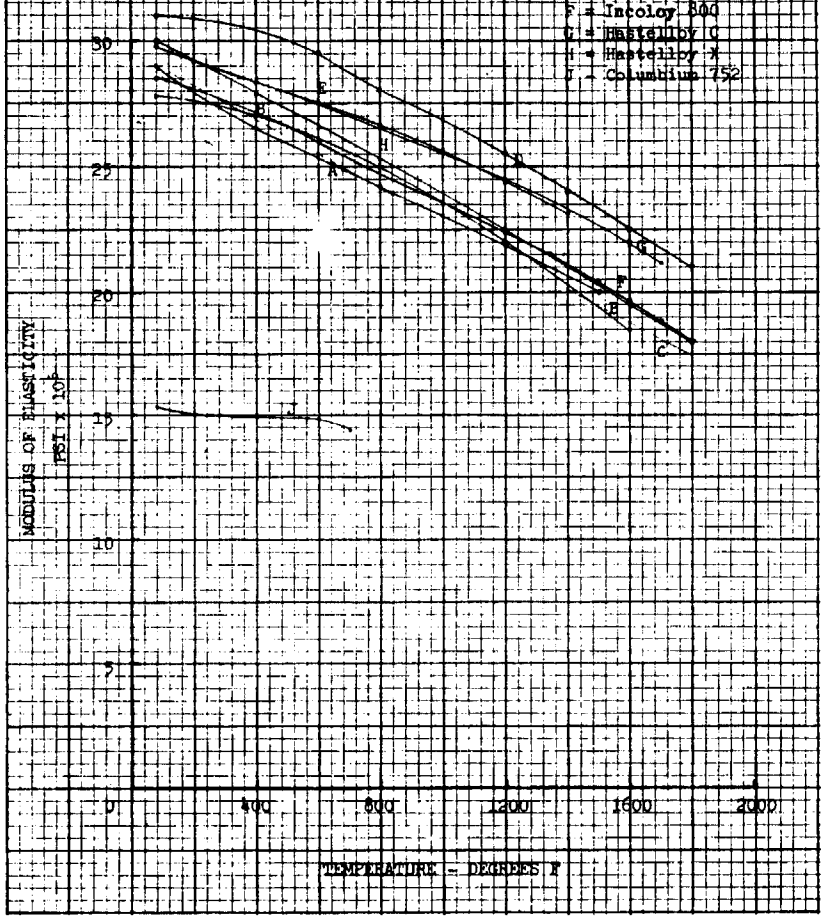

Figure A2.6

1000 HOUR CREEP RUPTURE STRENGTH vs TEMPERATURE

KEY

A = 304 Stainless Steel
B = 316 Stainless Steel
C = 347 Stainless Steel
D = Inconel 600
E = Inconel 625
F = Incoloy 800
G = Hastelloy C
H = Hastelloy X
J = Columbium 752

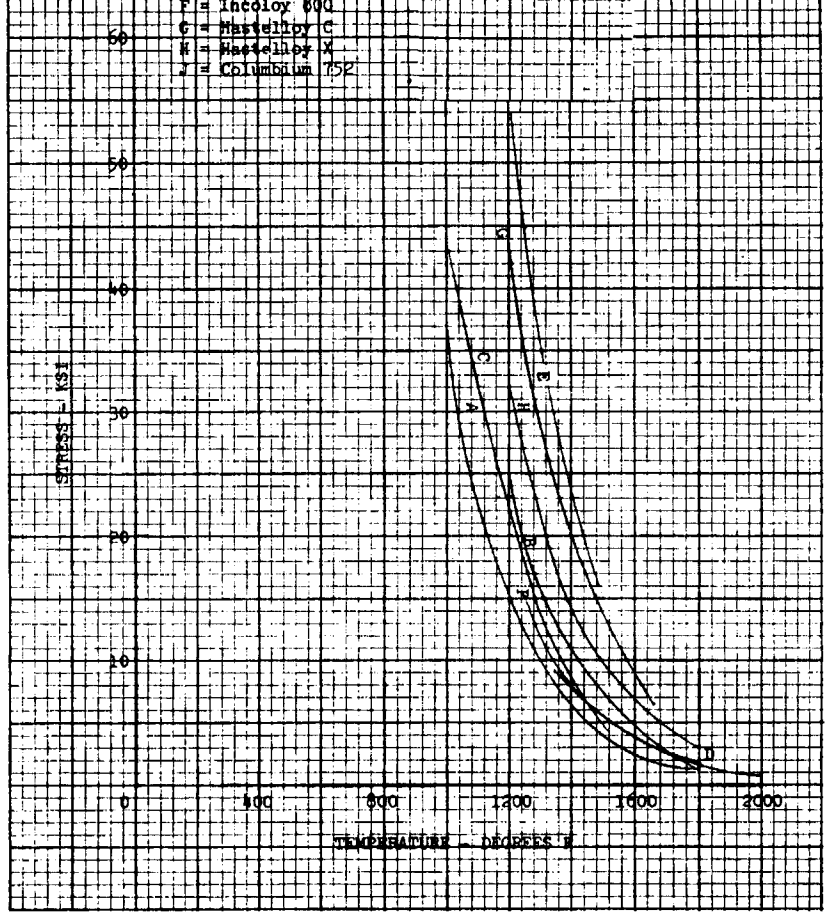

Figure A2.7

SPECIFIC HEAT vs TEMPERATURE

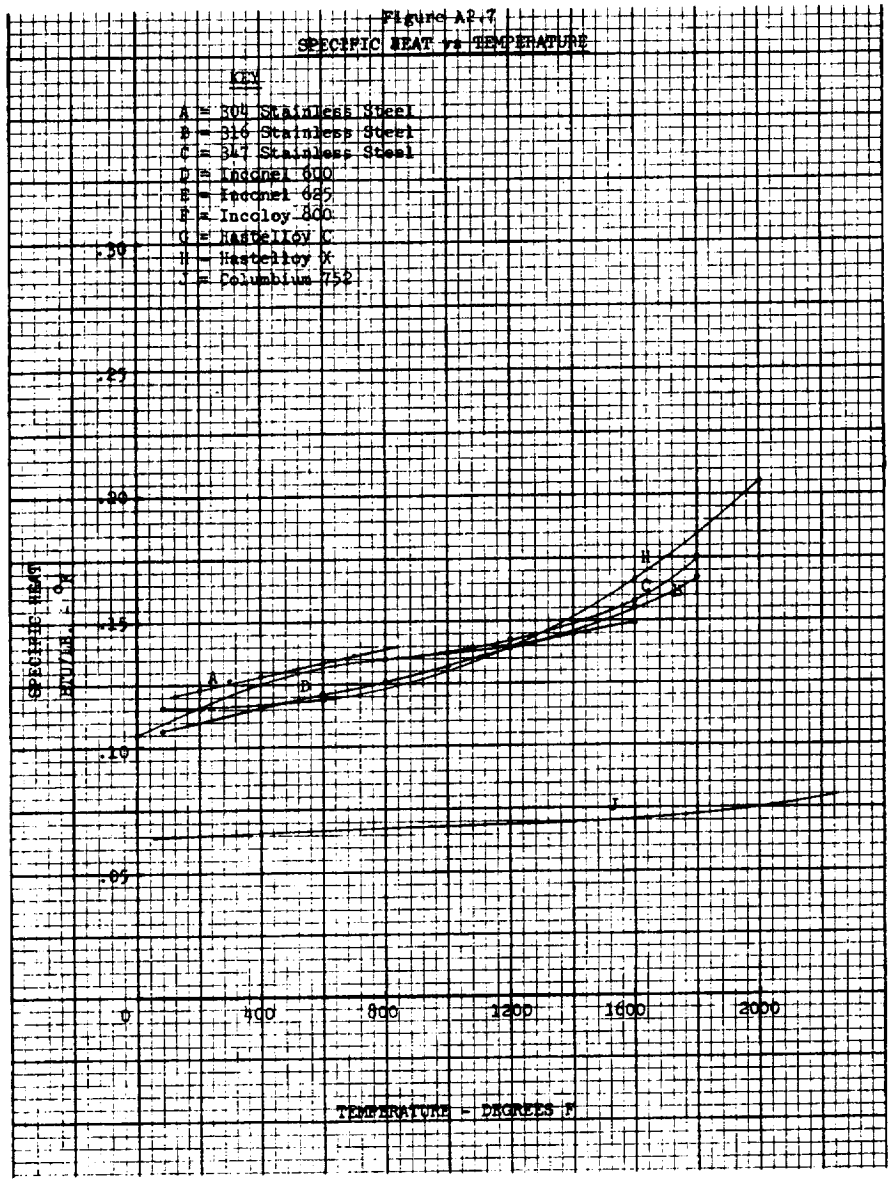

CONFIDENTIAL

TABLE A3.1

PROPERTIES OF CANDIDATE REFLECTOR MATERIALS

Material	Composition,[a] wt %	Density, lb/in^3	Melting Range, °F	Reference
Beryllium	99.8	0.067	2355 – 2365	c
Beryllium Oxide	99.9	0.107[b]	4620	
Molybdenum	99.9	0.369	4334 – 4370	c

[a]Commercial purity

[b]Practical density; theoretical density = 0.109

[c]Aerospace Structural Metals Handbook, ASD-TDR-63-741, Volume II

[redacted]

Figure A3.1

THERMAL CONDUCTIVITY VS TEMPERATURE

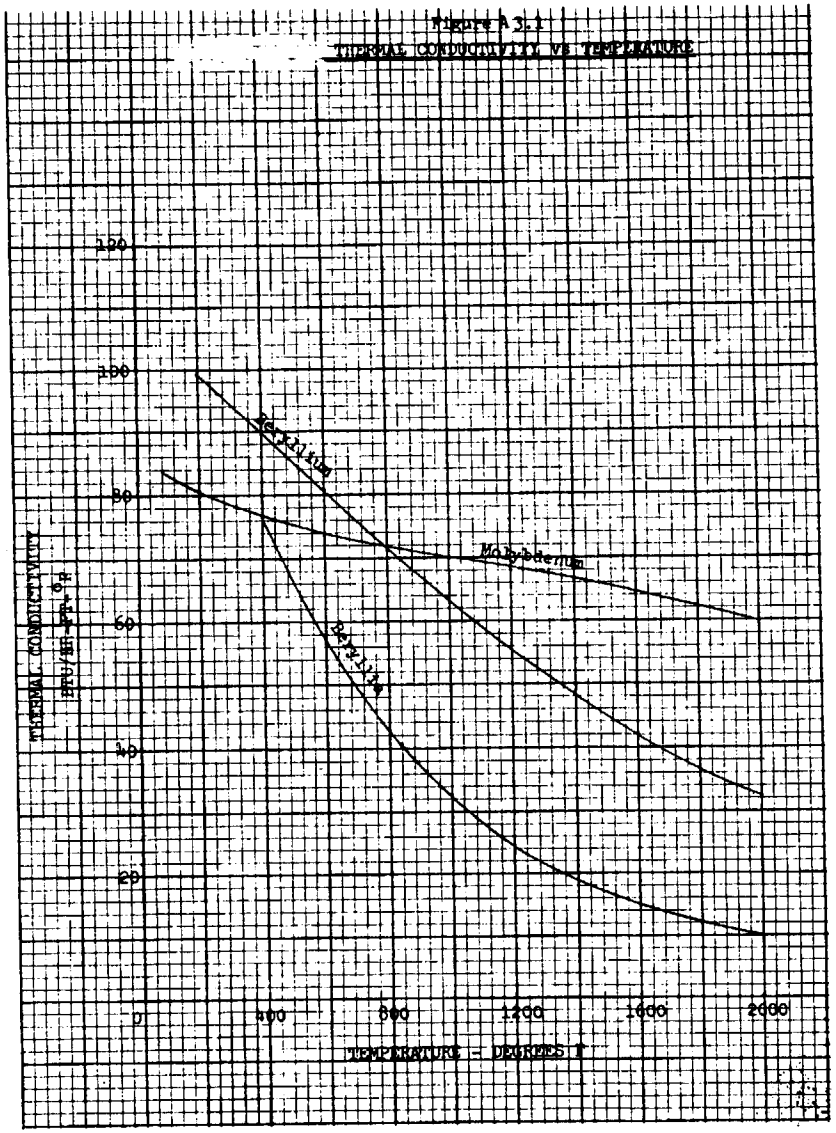

MEAN COEFFICIENT OF THERMAL EXPANSION VS TEMPERATURE

Figure A3.2

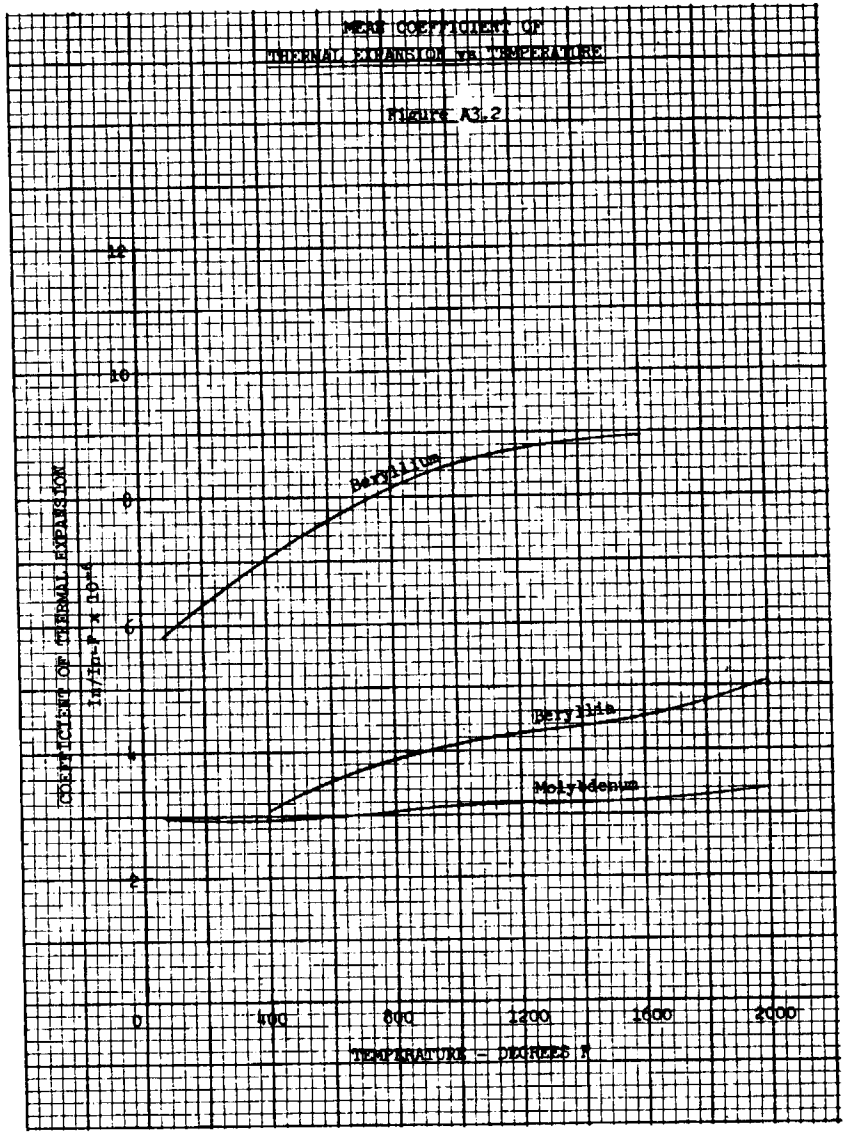

CONFIDENTIAL

CONFIDENTIAL

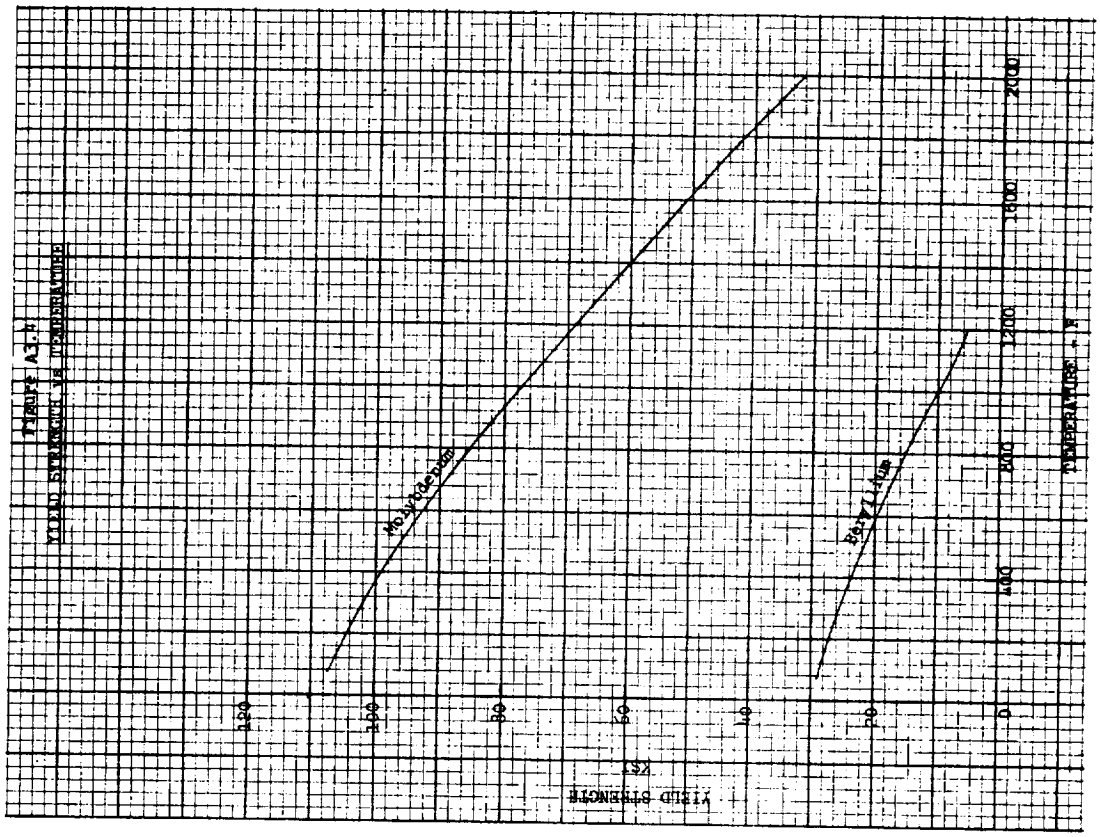

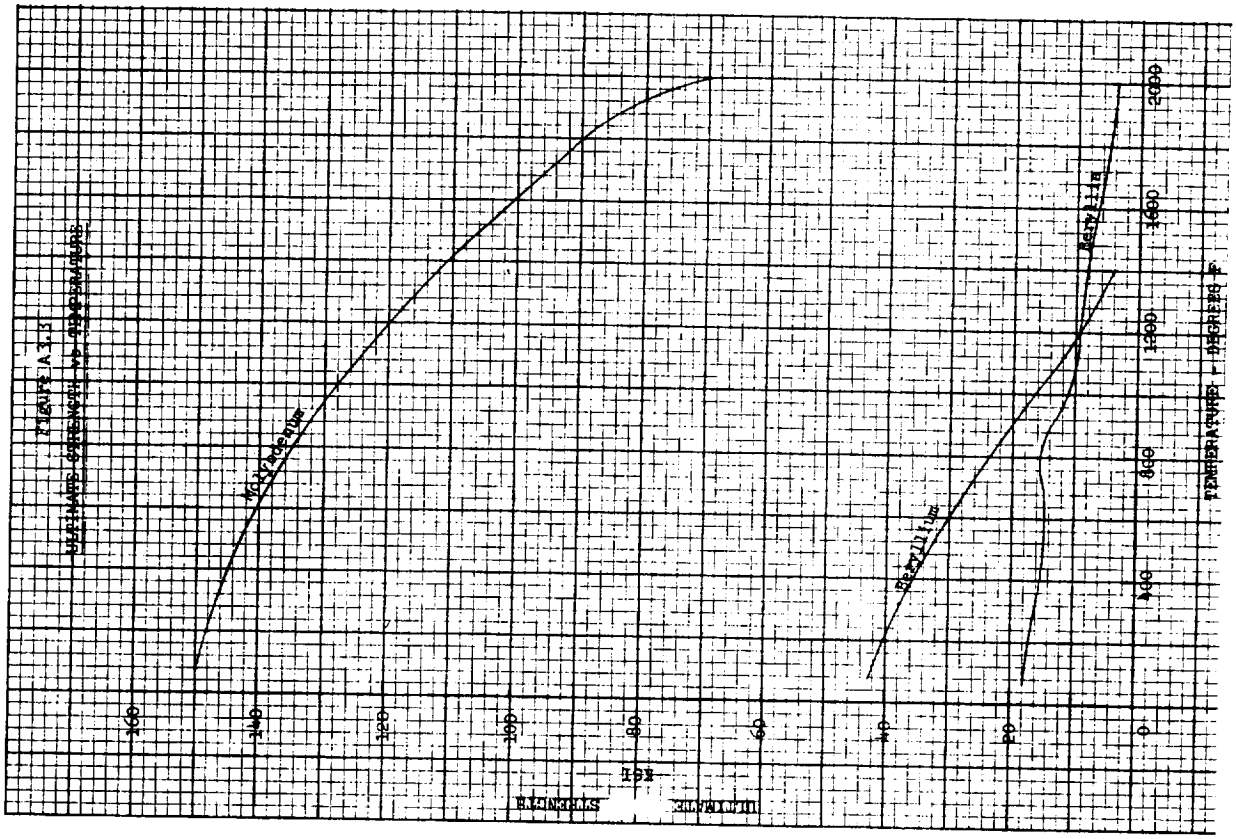

[redacted]

Figure A3.5

Elongation vs. Temperature

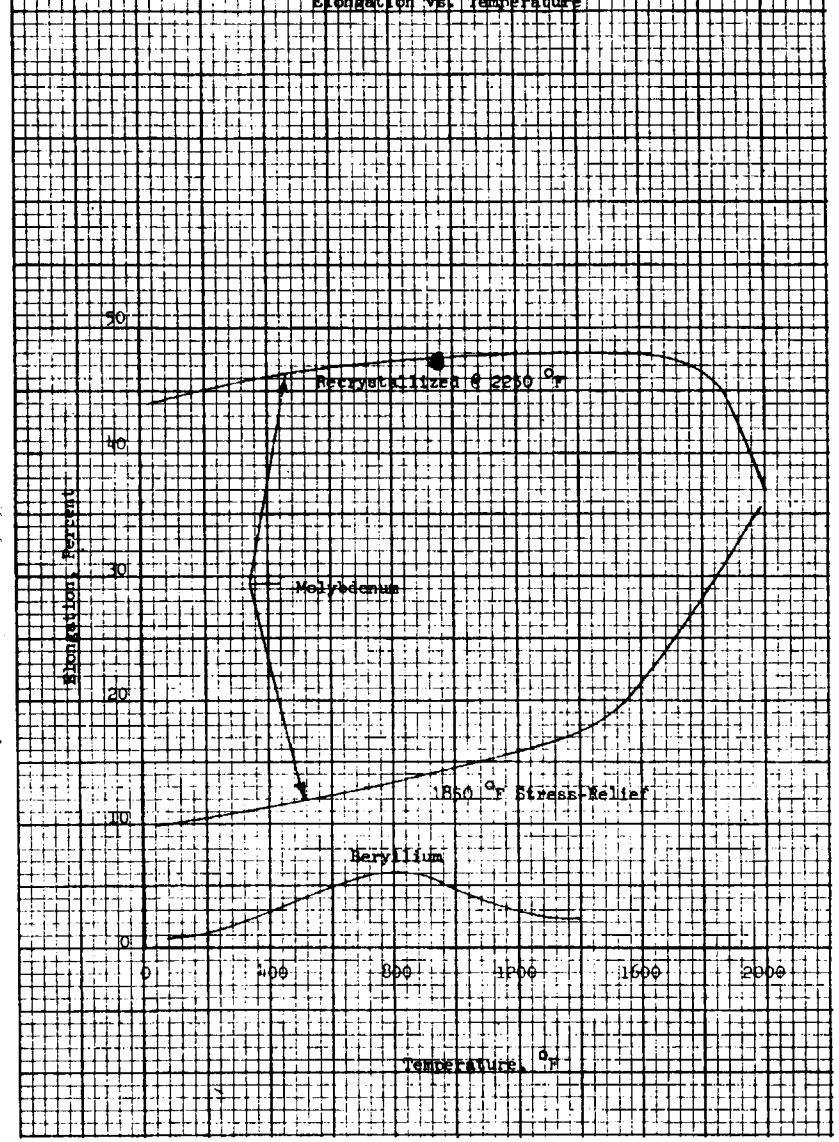

Figure A 3.6

MODULUS OF ELASTICITY vs TEMPERATURE

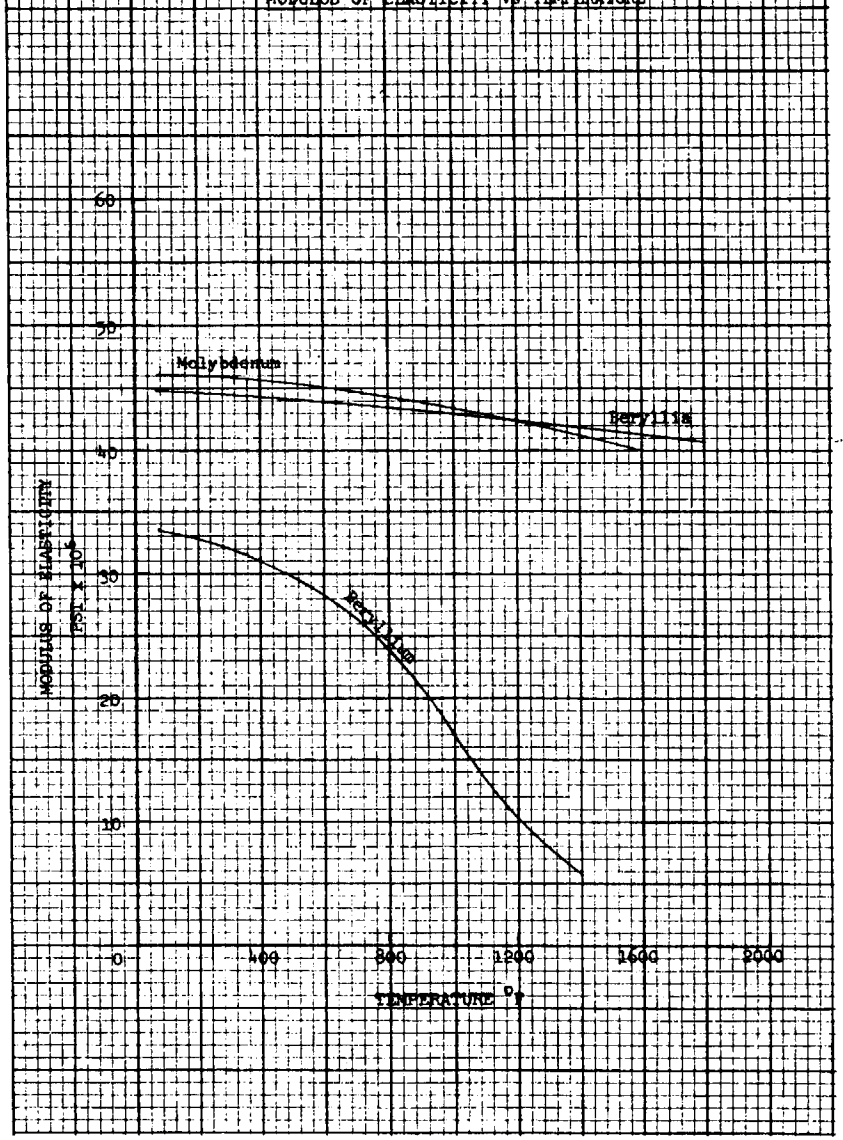

CONFIDENTIAL

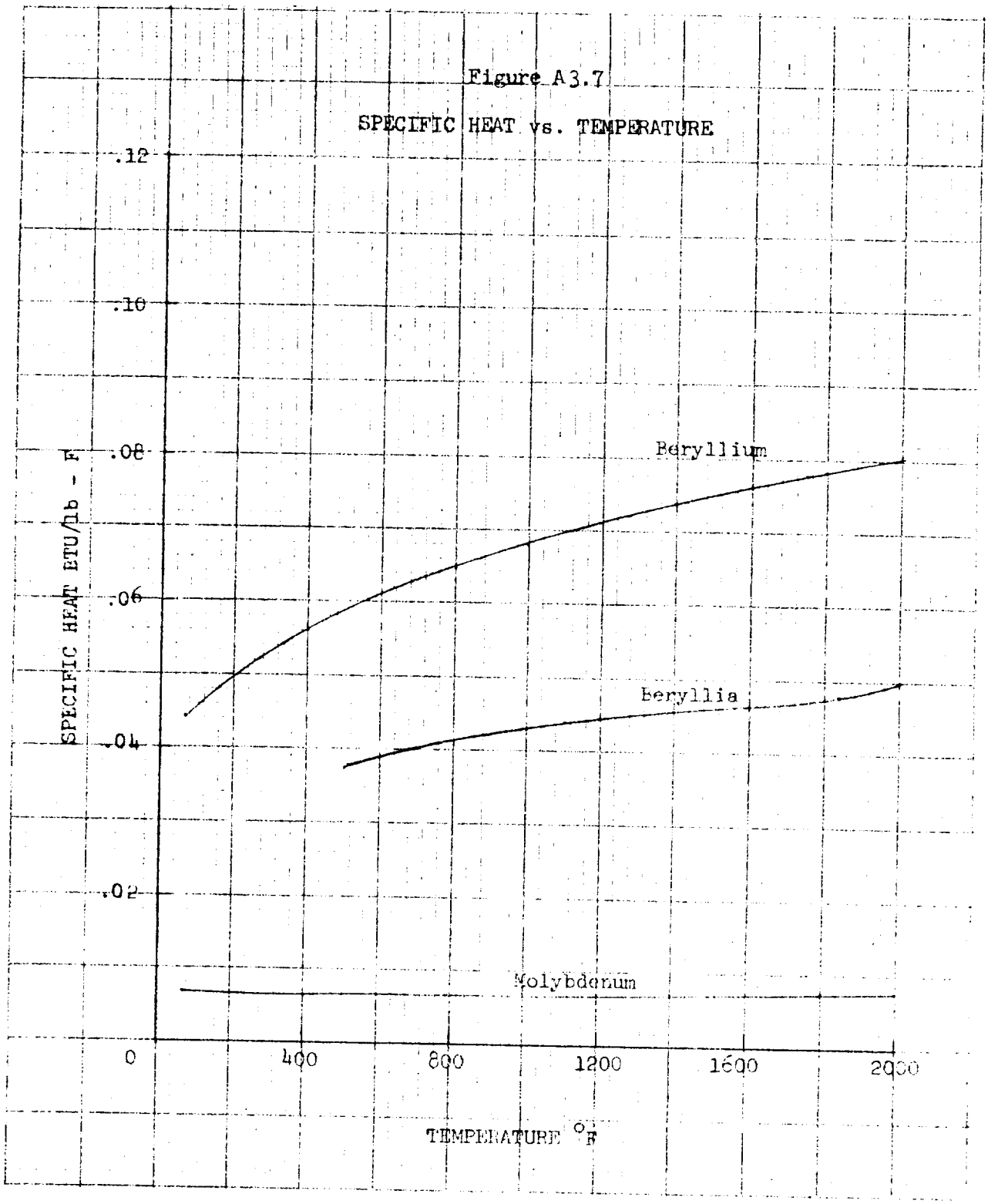

CONFIDENTIAL

CONFIDENTIAL

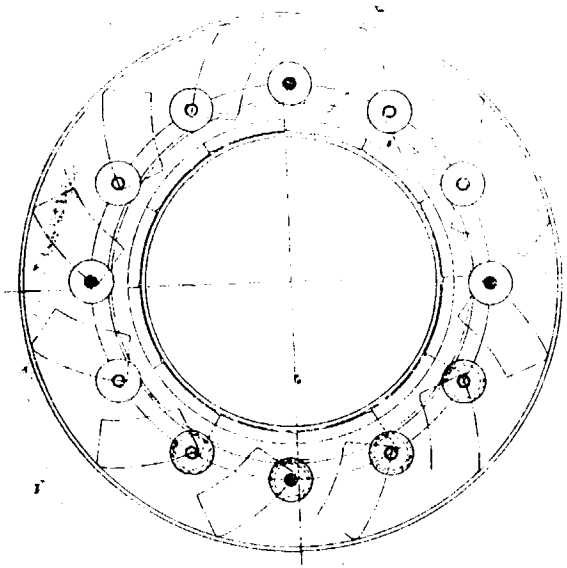

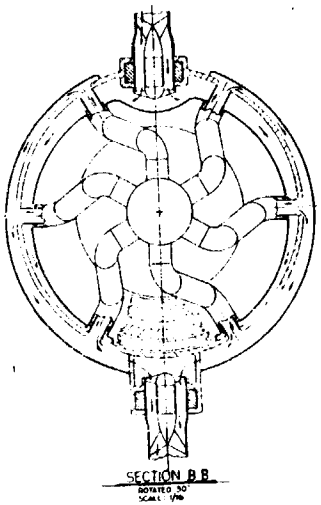

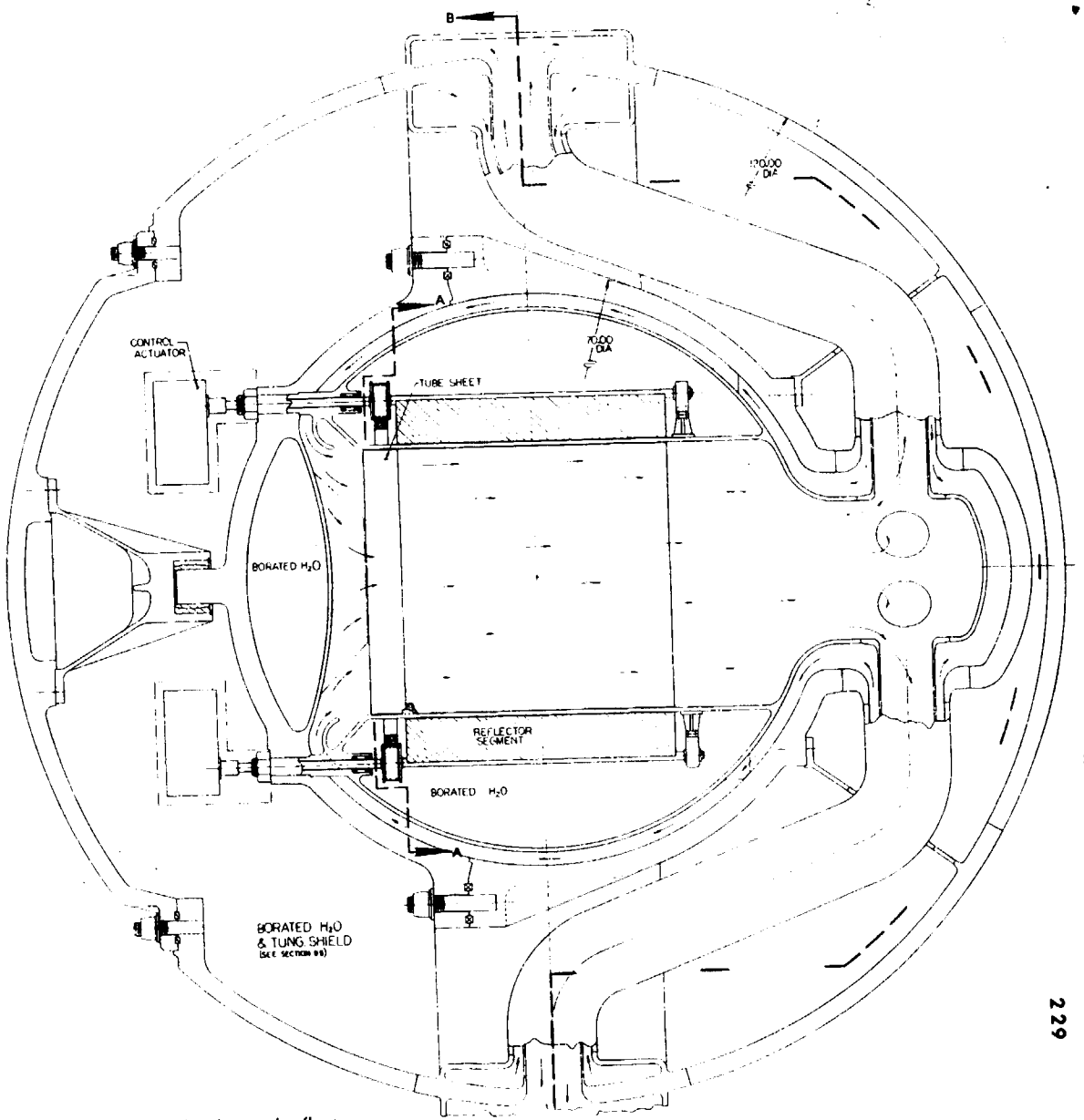

Fig. B-1 -- Arrangement study – inner pressure vessel with submerged reflector
(Dwg. 221R240)

CONFIDENTIAL

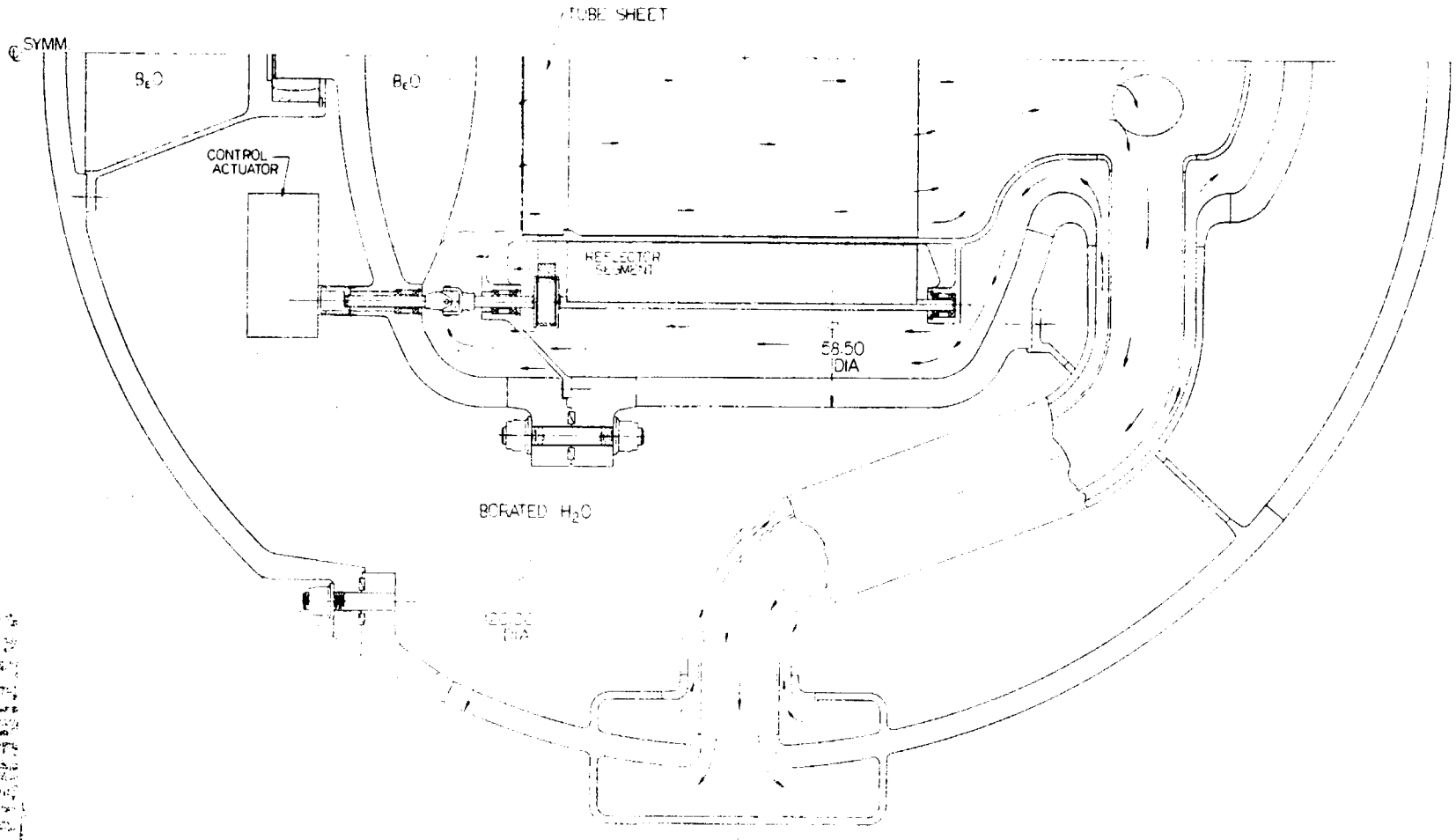

Fig. B-2 – Arrangement study – inner pressure vessel, gas-cooled reflector
(Dwg. 221R239)